

Katholieke Universiteit Leuven
Faculteit Ingenieurswetenschappen
Departement Werktuigkunde
Celestijnenlaan 300A, B-3001 Heverlee

Water-based heating/cooling in residential buildings
Towards optimal heat emission/absorption elements

Promotor

Prof. dr. ir. William D'haeseleer

Proefschrift voorgedragen tot het
behalen van het doctoraat in de
Ingenieurswetenschappen door

Leen Peeters

April 2009

Katholieke Universiteit Leuven
Faculteit Ingenieurswetenschappen
Departement Werktuigkunde
Celestijnenlaan 300A, B-3001 Heverlee

Water-based heating/cooling in residential buildings
Towards optimal heat emission/absorption elements

Jury

Prof. dr. ir. Paul Van Houtte, voorzitter
Prof. dr. ir. William D'haeseleer, promotor
Prof. dr. ir. Hugo Hens
Prof. dr. ir. Lieve Helsen
Prof. ir. Bernard Geeraert
Prof. dr. ir. Dirk Saelens
Prof. dr. ir. Jan Hensen (TU Eindhoven, The
Netherlands)
Prof. dr. ir. Nicolas Kelly (University of Strathclyde,
Glasgow, UK)
Prof. dr. ir. Bjarne Olesen (DTU, Lyngby, Denmark)

Proefschrift voorgedragen tot het
behalen van het doctoraat in de
Ingenieurswetenschappen door

Leen Peeters

April 2009

© Katholieke Universiteit Leuven – Faculteit Ingenieurwetenschappen
Arenbergkasteel, B-3001 Heverlee, België

Alle rechten voorbehouden. Niets uit deze uitgave mag worden verveelvoudigd en/of openbaar gemaakt worden door middel van druk, fotokopie, microfilm, elektronische of op welke andere wijze ook zonder voorafgaande schriftelijke toestemming van de uitgever.

All rights reserved. No part of this publication may be reproduced in any form by print, photo-print, microfilm, or any other means without written permission from the publisher.

Wettelijk depot D/2009/7515/39

UDC 697.1:697.9:728.1

ISBN 978-94-6018-056-9

Voor Janne en Bo

Foreword

The origin of my fascination for buildings

Let's start from the beginning

I was born somewhere in a hospital in a little town in Flanders. After 10 days it was time to move to what was going to be my home for the next 2 years. Then, our whole family moved again to where I would stay for another 16 years. I went to a small village school. After 9 years, I made my little world bigger going to a school in a nearby town.

It wasn't satisfying ... so I again enlarged my little world and started university in Leuven. I moved almost every year, if not to another building, then at least to another room within the building.

The best thing remaining from that period at university is my husband Diederik. We got together looking for 'Sinterklaas' and yes we did find him ...

After graduating, Diederik and I moved. We got married, got a little daughter, Janne, and then the three of us ... moved. I started working at university. And after a year or so we got a little son, Bo. And the four of us ... moved¹.

The department of mechanical engineering being too small, I spent a while at the Technical University of Eindhoven. That being too close to home, I changed to Strathclyde University for a few months.

Having seen and experienced so many different rooms and buildings, it is obvious to be fascinated by them.

¹ This is not a mathematical diverging series.

The inhabitants of the buildings

Limiting the list of people to those who somehow have collaborated to realise this book, it starts with the constants. My mother and father who are responsible for my first housing experiences. Next, the most influencing: my husband Diederik and our kids Janne en Bo. They were supporting throughout the process and especially the last year. Janne and Bo made me put the whole book and everything that had to do with it into perspective. Diederik encouraged me to take the chances I got to go abroad and focus. Meantime, he did a wonderful job in taking care of the kids.

Another constant, from even before day one at the department of Mechanical Engineering is William. I ended up doing research in an area he was definitely interested in, but not very familiar with. And William, as you know, I did appreciate you giving me the chance to build up a broad international network.

I cannot mention all colleagues and friends that meant more than average to me. But there is certainly Jeroen who deserves a special place in this list. Somehow I enjoyed our deadline nightmares. Kathleen as well, needs to receive a special award for always being there for the kids. Caroline, Kristien, Clara, Agnes, Frederik, Bieke, Ingrid and especially Tine know I couldn't have done this without them. They were always there for me, listening to my nonsense and pep-talking to get me out if I had a dip.

Next, consider the variables, mainly linked to the buildings, and who mostly became kind of constants as well.

The 6th floor of the Vertigo building of the Eindhoven University houses the office of a nice set of variables; Jan, Daniel, Mohammed and especially Marija. They helped me discovering the world of *ESP-r*.

At Strathclyde University, I actually first met Nick in 2004 visiting Glasgow for a conference. I forgot the conference name, but both Dries, who joined me on this trip, and I learned to never again forget the details, or at least the name of your hotel when going abroad.

Then I met Nick again as subtask leader in the annex 42. After some mailing on ESP-r, he invited me for a stay at ERSU. I got funding from the FWO and so I took a plane to Glasgow

I shared an office with Georgios, *ESP-r* and movie addicted. But, very patient and helpful. And then there was Tom, for whom a model must be more accurate than reality and kiwis don't need peeling. I also had many fruitful discussions with Jon, Jeremy, Aizas, Paul, Michael, visiting professor Jeff and of course Nick himself. Also the advice and support of Joe should not be forgotten, as well as the flowers of speech in Cameron's letter of recommendation.

Other variables

Alex Ferguson from NRCAN and Ian Beausoleil-Morisson from Carleton University should receive a special award for advising me when I faced another bug. Richard de Dear and Stanley Kurvers have introduced me into the wonderful world of thermal comfort. I appreciate their enthusiasm and their willingness to share their knowledge. Wim and Jo, the 'cluster people' helped me out with so many things, they weren't angry (or did not show it) when I blocked the whole system with my first simulations on it. To the both of them: a big 'thank you'!

Also the jury's efforts have greatly contributed to improving the text.

My contribution in solving the world's carbon emission problem

I use *ESP-r*. I thus use non-existing buildings. As they do not have to be built to be tested, they also do not result in any extra carbon emission. On the other hand, the savings I calculate are not reflected in the real world So it is a zero-effect action.

The only animals I worked with were bugs These are animals with a low carbon emission if they even have an impact. However, I introduced bugs and I did remove bugs, so also that operation is a zero-effect action.

But I did use planes, I actually took 35 planes during the years I worked at the department of mechanical engineering. And that has a major impact. History can not be changed, but the habits for the future can

I learned using *ESP-r*. It can handle all climates and calculate the effects of different ambient conditions on any type of building. It can be used to evaluate the energy performance of different building designs and develop the most efficient installations for realizing comfortable indoor conditions in these buildings. The advantage of using *ESP-r* is that there is actually no longer any need for me to go anywhere ... as the code can predict the performance of any building in any place of the world as long as it has a file of climate data that can be imported in *ESP-r*. Consequently, this knowledge will reduce my airplane trips in the future with a considerable positive impact on my personal footprint.

And yes, there will always be bugs, anywhere in the world. Also for that aspect *ESP-r* gives a reasonable estimation ;-)

Abstract

This dissertation describes the development of a new method for simulating water-based heating/cooling installations in residential buildings and demonstrates how such method could be used to determine optimal heat emission/absorption elements for residential buildings.

The reason to develop this new simulation method was to define optimal heat emission/absorption elements that fulfil the thermal comfort requirements in an energy efficient way. Based on a thorough state-of-the-art study, the thermal comfort requirements for the specific setting of a residential building have been defined. It is shown that 3 different zones can be distinguished: the bathroom, the bedroom and the other zones. Each of these zones requires different temperature settings in order to satisfy the thermal sensation of its occupants. The width of the band of acceptable temperatures around this neutral temperature was determined to be 5 K, asymmetrically distributed around the neutral value.

Besides this steady state thermal comfort, a potential optimal heat emitter/absorber should further cause limited indoor temperature fluctuations. These dynamic thermal conditions are difficult to incorporate in building energy simulation software due to their dependency on the simulation timestep. However, by simulating with a fixed small timestep when optimising different heat emission/absorption elements, a too high cycle frequency of the indoor temperature can be penalised.

The thermal comfort requirements define the boundary conditions a heating/cooling installation should fulfil. An algorithm to verify the thermal comfort requirements and the structure to model heating/cooling installations have been embedded in an existing building energy simulation software to correctly account for the building-installation interactions. The building simulation code used is *ESP-r*. The implicit plant modelling implementation is mainly embedded within the *ESP-r*'s zone/building control level. It contains a heat emission/absorption model with idealised and more realistic controls, a structure for a distribution level and a production device model with different controls and different efficiency calculation routines.

The model for the heat emission/absorption element is based on a formula, commonly encountered in building simulation, to represent different types of water-based heat emission elements. Through an extended theoretical analysis, improvements to this formula have been proposed.

This model requires a limited amount of characterising parameters. To determine the optimal value for each of these parameters, the building simulation code *ESP-r*, extended with the implicit modelling approach, has been coupled with the optimisation tool *GenOpt*. This coupling allows determining the optimal heat emitter/absorber element for a given building model in a specific setting. Through various examples, the possibilities and limitations of this generic methodology have been demonstrated.

Synopsis

Dit werk beschrijft de ontwikkeling van een nieuwe impliciete methode voor de simulatie van verwarming en koeling op waterbasis in woningen. Het toont hoe een dergelijke methodologie kan worden gebruikt om de optimale kenmerken van warmte-emissie en/of -absorptie elementen in woningen te bepalen.

De belangrijkste motivatie om een dergelijke methodologie te ontwikkelen ligt in het zoeken naar een methode om de realisatie van het optimale thermische comfort in woningen zo energiezuinig mogelijk te maken.

Het eerste aspect dat zodoende moet onderzocht worden is het thermisch comfort zelf in een woning. Er wordt aangetoond dat in residentiële gebouwen drie thermisch verschillende zones kunnen worden onderscheiden: de badkamer, de slaapkamers en de andere zones. Elk van die zones heeft een eigen, specifieke comforttemperatuur. Binnen een band van 5 K rondom die comforttemperatuur wordt eenzelfde comfortgevoel ervaren. De band van aanvaardbare temperaturen is asymmetrisch verdeeld rond die comforttemperatuur omdat mensen gevoeliger zijn aan koude dan aan warmte.

Naast de waarde van de temperatuur op zich, wat aangeduid wordt als *steady state comfort*, moet ook het dynamische aspect worden onderzocht. Het fluctueren van de

binnentemperatuur moet beperkt zijn, zowel in grootte als in duur. Het blijkt evenwel moeilijk te zijn een dergelijke beperking op een algemene wijze in een gebouwensimulatiepakket te implementeren. Dat is het gevolg van het gegeven dat de resultaten afhankelijk zijn van de gekozen simulatietijdstap. Een te snelle en daarom onwenselijke verandering van de binnentemperatuur kan echter wél bekeken en vergeleken worden bij simulaties met eenzelfde korte tijdstap. Dat zal dus worden meegenomen worden bij de optimalisatiesimulaties voor deze dissertatie.

Het thermisch comfort bepaalt de randvoorwaarde waaraan een potentieel emissie- en/of absorptie-element moet kunnen voldoen. Om de interactie tussen gebouw en installatie correct te kunnen onderzoeken, werden het thermisch comfortalgoritme en de berekeningsmodule om de verwarmings- en koelingsinstallatie te modelleren als impliciete structuur in een bestaand gebouwensimulatiepakket geïmplementeerd. Daarbij werd gebruik gemaakt van *ESP-r*. De impliciete structuur bevat een model voor het voorstellen van warmte-emissie of -absorptie. Dit model kan zowel toegepast worden voor 'ideale' als voor meer realistische controles. Verder is een module opgenomen voor het inrekenen van distributieverliezen. Tevens kan een ideaal of een veeleer realistisch productiesysteem met dito controles worden gemodelleerd.

Het model voor de bepaling van warmte-emissie en/of -absorptie is gebaseerd op een formule die veelvuldig wordt toegepast in gebouwensimulatie. Door een diepgaande theoretische analyse werd echter aangetoond dat de formule niet zonder meer kan worden gebruikt om het verwarmend resp. koelend effect van om het even welk emissie- en/of absorptie-element correct te berekenen. De formule werd aldus aangepast en in die aangepaste vorm gebruikt als basis voor het generische configuratie- en locatie-onafhankelijke model.

Dit model hanteert slechts een beperkt aantal parameters. Om de optimale waarde van die parameters te bepalen, werd *ESP-r* met de impliciete modelleringstructuur, gekoppeld met het optimalisatieprogramma *GenOpt*. De aldus gecreëerde gekoppelde structuur laat toe om voor een bepaald gebouw in een bepaalde configuratie de optimale emitter/absorber te bepalen. Door middel van een waaier aan voorbeelden worden de mogelijkheden en beperkingen van de gekoppelde structuur gedemonstreerd.

Abbreviations and symbols

Abbreviations

ATL	Adapted Temperature Limits
BES	Building Energy Simulation
CHP	Combined Heat and Power
CFD	Computational Fluid Dynamics
Comf	selected comfort algorithm (-)
DB	Deadband on indoor temperature (K)
ESP-r	Energy Systems Performance, research version
FUR	Fuel Utilisation Ratio (-)
GA	Genetic algorithm
GPS	Generalised pattern search
HVAC	Heating Ventilation and Air Conditioning
MIMO	Multiple input, multiple output
MRT	Mean Radiant Temperature
MRT _i	Mean Radiant Temperature of zone i
MRT _{i,N}	Nominal Mean Radiant Temperature of zone i
NSB	Number of set back periods (-)
PLR	Part Load Ratio (%)
PMV	Predicted Mean Vote
PPD	Predicted Percentage of Dissatisfied

PSO	Particle swarm optimisation
SBT_{\min}	Minimum temperature during set back (K)
SBT_{\max}	Maximum temperature during set back (K)
SISO	Single input, single output
STA_j	Start hour of set back period j (h)
STO_j	Stop hour of set back period j (h)
TAB	Thermally activated building
TR	Throttling range
TRV	Thermostatic radiator valve

Dimensionless numbers

Re	Reynolds number (-)
Pr	Prandtl number (-)
Ra	Rayleigh number (-)
Nu	Nusselt number (-)
Gr	Grashof number (-)

Symbols

a_0	Coefficient of term Energy in objective function (1/Wh)
a_1	Coefficient of term <i>Penalty</i> ₁ in objective function (1/K ² h)
a_2	Coefficient of term <i>Penalty</i> ₂ in objective function (-)
$A_{s_j,ai}$	Contact area for convective heat transfer between solid volume j and air volume i (m ²)

A_r	Surface area for radiation (m^2)
$A_{c,n}$	Surface area for natural convection (m^2)
$A_{c,f}$	Surface area for forced convection (m^2)
$A_{envelope}$	Surface area of building envelope (m^2)
A_{TAB}	Surface area of the thermally activated element (m^2)
A	Surface area (m^2)
b	Power coefficient (-)
b_{min}	Minimum power coefficient (-)
b_{max}	Maximum power coefficient (-)
$c_{p,ai}$	Specific heat capacity at constant pressure for air in zone i (J/kgK)
c_{si}	Specific heat capacity of solid volume of zone i (J/kgK)
c_{pli}	Specific heat capacity of solid enclosure of plant component i (J/kgK)
c_{wi}	Specific heat capacity of water volume of plant component i (J/kgK)
$c_{p,a}$	Specific heat capacity at constant pressure for air (J/kgK)
C_{emit}	Heat capacity of an emission/absorption element (J/kgK)
$C_{emit,i}$	Heat capacity of emission/absorption element i (J/kgK)
C_o	Heat capacity of layer 0 (J/kgK)
C_1	Heat capacity of layer 1 (J/kgK)
Control	Selection of control strategy(-)
DF	Dynamical Factor (-)
D	Diameter (m)
d	Thickness (m)

E_{\min}	Minimum electricity output of cogeneration device (W)
E_{\max}	Maximum electricity output of cogeneration device (W)
E	Electrical output of cogeneration device (W)
F	View factor (-)
$FUR_{10\text{PLR}}$	Fuel utilisation ratio for 10% PLR (%)
$FUR_{30\text{PLR}}$	Fuel utilisation ratio for 30% PLR (%)
$FUR_{100\text{PLR}}$	Fuel utilisation ratio for 100% PLR (%)
$\bar{h}_{s_j,ai}$	Surface averaged heat transfer coefficient for convection between solid j and air volume i (W/m ² K)
\bar{h}_r	Surface averaged radiant heat transfer coefficient (W/m ² K)
$\bar{h}_{c,n}$	Surface averaged heat transfer coefficient for natural convection (W/m ² K)
$\bar{h}_{c,f}$	Surface averaged heat transfer coefficient for forced convection (W/m ² K)
K_1	Weighing factor between 0 and 1 (-)
L	Characteristic length (m)
\dot{m}_j	Mass flow rate between volumes i and j (kg/s)
$\dot{m}_{ak,ai}$	Mass flow rate of air exchanged between volumes k and i (kg/s)

n	Radiator exponent (-)
n_i	Radiator exponent of emitter/absorber element i (-)
n_{\min}	Minimum radiator exponent (-)
n_{\max}	Maximum radiator exponent (-)
n_{ll}	Lower limit for radiator exponent (-)
n_{ul}	Upper limit for radiator exponent (-)
O	Value of the objective function (-)
ΔO	Absolute difference of value of objective function for certain set of parameters compared to value for optimal set of parameters (-)
p_i	Pressure in volume i (Pa)
p_j	Pressure in volume j (Pa)
Δp_{ij}	Pressure difference between volumes i and j (Pa)
p	Vector containing the parameters of the heat emitter/absorber
p^*	Vector containing the parameters of the optimal heat emitter/absorber
P_{ALi}	Thermal permeance per square meter from active layer to zone i (W/m^2K)
P_{ALj}	Thermal permeance per square meter from active layer to zone j (W/m^2K)
P_{01}	Thermal permeance per square meter from layer 0 to layer 1 (W/m^2K)
P_{10i}	Thermal permeance per square meter from layer 1 to zone i (W/m^2K)
P_{emiti}	Thermal permeance per square meter from emitter/absorber element to zone i (W/m^2K)
PP	Input Primary Power (W)
P_{-7}	Performance of device at $-7^\circ C$ ambient temperature (-)
P_2	Performance of device at $2^\circ C$ ambient temperature (-)
P_{10}	Performance of device at $10^\circ C$ ambient temperature (-)

$Q_{si,ai}$	Surface to fluid heat flux (convection) (W)
$Q_{ai,si}$	Fluid to surface heat flux (convection) (W)
$Q_{aj,ai}$	Advective heat transfer from zone j to zone i (W)
$Q_{ext,ai}$	Advective heat transfer from the exterior to zone i (W)
$Q_{cas,i}$	Casual gain in zone i (W)
$Q_{pli,i}$	Heat transfer from plant component i to zone i (W)
$Q_{i,pli}$	Heat transfer from zone i to plant component i (W)
$Q_{si+/-1,si}$	Conductive heat transfer from solid volume i +/- 1 to volume i (W)
$Q_{s',si}$	Radiant heat transfer from surface s' to surface of volume i (W)
$Q_{s',pli}$	Radiant heat transfer from surface s' to surface of plant i (W)
$Q_{si,pli}$	Conductive heat transfer between solid volume of zone i and solid of plant component i (W)
$Q_{si,e}$	Sensible heat gains from sources inside the control volume of water node i (W)
$Q_{solar,i}$	Shortwave solar radiation on solid surface i (W)
$Q_{solar_trans,soli}$	Transmitted solar radiation on solid inner node i (W)
$Q_{soli,e}$	Internal heat gains in solid inner node i (W)
$Q_{si,soli}$	Conduction from solid surface node i to solid inner node i (W)
$Q_{soli+/-1,soli}$	Conduction from solid inner node i +/- 1 to solid inner node i (W)
$Q_{wi,pli}$	Convective heat transfer from plant water node i to plant solid node i (W)
$Q_{pli,wi}$	Convective heat transfer from plant node i to water node i (W)
$Q_{pli+/-1,pli}$	Conductive heat transfer from plant component i +/- 1 to plant component i (W)
$Q_{wi+/-1,wi}$	Conductive heat transfer from plant water node i +/- 1 to plant water node i (W)
$Q_{wi,e}$	Sensible heat gains from sources inside the control volume of water node i (W)

$Q_{sj,ai}$	Convective heat transfer possibly occurring between surrounding or enclosed solid volume j and the air volume of zone i (W)
$Q_{ak,ai}$	Advective heat transfer possibly occurring between all surrounding air volumes k and the air volume of zone i (W)
Q_{pl}	Heat flux injected in an emitter/absorber (W)
Q_{pli}	Heat flux injected in emitter/absorber element i (W)
Q'_{pli}	Heat flux for emitter/absorber element i, passed from production device to distribution system (W)
Q_{prod}	Heat flux to be produced by the production device, as determined by the production device's control (W)
Q''_{pli}	Heat flux requested by control of emitter/absorber element i (W)
Q_r	Radiant heat output (W)
$Q_{c,n}$	Heat output due to natural convection (W)
$Q_{c,f}$	Heat output due to forced convection (W)
$Q_{emit,N}$	Heat output of an emission/absorption element in nominal conditions (W)
$Q_{emit,i,N}$	Heat output of the emission/absorption element i in nominal conditions (W)
$Q_{h_prod,max}$	Maximum heating capacity of production unit (W)
$Q_{h_prod,min}$	Minimum heating capacity of production unit (W)
$Q_{c_prod,max}$	Maximum cooling capacity of production unit (W)
$Q_{c_prod,min}$	Minimum cooling capacity of production unit (W)
$Q_{emit,i}$	Heat output of the emission/absorption element (W)
$Q_{i,j}$	Heat transfer from zone i to zone j (W)
$Q_{AL,j}$	Heat transfer from active layer to zone j (W)
Q_{in}	Injected thermal flux (W)
Q''_{pli_new}	Newly calculated desired flux for TRV output calculations(W)
Q_{ss}	Steady state heat flux as calculated based on EN 12831 (W)

SU	Start Up factor (-)
SD	Shut Down factor (-)
$T_{e,ref}$	Reference external temperature (°C)
T_{today}	Arithmetic average of today's maximum and minimum ambient temperature (°C)
$T_{today-i}$	Arithmetic average of maximum and minimum ambient temperature of 'i' day's ago (°C)
T_{RM}^n	Running mean temperature on day 'n' (°C)
T_{DM}^{n-i}	Mathematical daily average temperature on day 'n-i' (°C)
T_n	Neutral or comfort indoor temperature (°C)
ΔT_{ptp}^x	Peak to peak temperature variation per time-interval (°C/h)
T_{upper}	Upper limit of comfort band (°C)
T_{lower}	Lower limit of comfort band (°C)
T_{ai}	Temperature of air in zone i (K)
$T_{ai,N}$	Nominal temperature of air in zone i (K)
T_{si}	Surface temperature of solid volume of zone i (K)
T_{pli}	Temperature of solid enclosure of plant component i (K)
T_{wi}	Temperature of water node i (K)
T_{sj}	Temperature of solid volume j (K)
T_a	Temperature of air exchanged between two volumes (K)
T_{ak}	Temperature of air in volume k (K)

T_{emit}	Temperature of a heat emission/absorption (K)
$T_{\text{emit},i}$	Temperature of heat emission/absorption element i (K)
$T_{\text{emit},i,N}$	Nominal temperature of heat emission/absorption element i (K)
$T_{\text{emit},i,\text{max}}$	Maximum temperature of heat emission/absorption element i (K)
$T_{\text{emit},i,\text{min}}$	Minimum temperature of heat emission/absorption element i (K)
T_{su}	Water supply temperature (K)
T_{ex}	Water exit temperature (K)
$T_{\text{op},i}$	Operative temperature zone i (K)
$T_{\text{op},j}$	Operative temperature zone j (K)
T_{Al}	Temperature of the active layer (K)
T_0	Temperature of the layer 0 (K)
T_1	Temperature of the layer 1 (K)
$T_{\text{prod,amx}}$	Maximum average temperature of the production unit (K)
$T_{\text{max},i}$	Maximum achievable temperature in zone i (K)
T_i	Zone control temperature (K)
T'_i	Distorted temperature (K)
T_{Comf}	Desired zonal temperature (K)
$T_{\text{surroundings}}$	Surface weighted temperature of surrounding zones or exterior (K)
T_{surface}	Surface temperature (K)
T_{op}	Operative temperature (K)
T_n	Neutral temperature (K)
T_{ll}	Temperature of lower limit of comfortband (K)
T_{ul}	Temperature of upper limit of comfortband (K)
ΔT	Temperature difference between emission/absorption element and zonal temperature (K)

ΔT_N	Temperature difference between nominal emission/absorption element and nominal zonal temperature (K)
ΔT_{lg}	Logarithmic temperature difference (K)
\bar{T}_{water}	Average water temperature (K)
t_{heat_cool}	Production device's minimum time off between heating and cooling (s)
t	Time (s)
Δt	Time difference (s)
t_{lock_out}	Lock out time of production device (s)
U_{ij}	Thermal transmittance from zone i to zone j (W/m^2K)
$U_{average}$	Average thermal transmittance of the building envelope (W/m^2K)
U_{avg}	Thermal transmittance related to the average insulated building (W/m^2K)
U_{good}	Thermal transmittance related to the good insulated building (W/m^2K)
U_{well}	Thermal transmittance related to the well insulated building (W/m^2K)
V_{ai}	Volume of air in zone i (m^3)
V_{si}	Volume of solid of zone i (m^3)
V_{pli}	Volume of solid enclosure of plant component i (m^3)
V_{wi}	Volume of water of plant component i (m^3)
V	Velocity (m/s)
w	Width of comfort band ($^{\circ}C$)
w_{TRV}	Weighing factor for newly calculated flux compared to last timestep's flux (-)

Greek symbols

α	Thermal diffusivity (m^2/s)
α'_i	Fraction of convective over total casual gains for source i (-)
α_i	Fraction of convective over total output for emitter/absorber i (-)
$\alpha_{N, \min}$	Minimum fraction of convective over total output for emitter/absorber i (-)
$\alpha_{N, \max}$	Maximum fraction of convective over total output for emitter/absorber i (-)
$\alpha_{i,N}$	Fraction of convective over total output for emitter/absorber i (-)
β	Indication of type of element, i.e. TAB element or not and specification (-)
γ_N	Nominal fraction of forced over total convective emitter's/absorber's output (-)
ε	Emissivity (-)
λ	Thermal conductivity (W/mK)
μ_∞	Dynamic viscosity of fluid volume (kg/ms)
μ_s	Dynamic viscosity at solid surface (kg/ms)
η	Efficiency characterisation of production unit (-)
$\eta_{\text{distribution}}$	Efficiency of the distribution system (%)
$\eta_{10\text{PLR}}$	Efficiency for 10% PLR (%)
$\eta_{30\text{PLR}}$	Efficiency for 30% PLR (%)
$\eta_{100\text{PLR}}$	Efficiency for 100% PLR (%)

ρ_{ai}	Density of air in zone i (kg/m^3)
ρ_{si}	Density of solid volume of zone i (kg/m^3)
ρ_{pli}	Density of solid enclosure of plant component i (kg/m^3)
ρ_{wi}	Density of water volume of plant component i (kg/m^3)
τ_1	Time constant (s)
τ_2	Time constant (s)
τ_{prod}	Time constant of production device (-)
σ	Stefan Boltzmann constant ($5.67 \times 10^{-8} \text{ W/m}^2\text{K}^4$)
ν	Kinematic viscosity (m^2/s)

Table of contents

Introduction	1
State of the art	2
Methodology and outline of the current work	5
Contributions of the current work	8
1 Thermal comfort in residential buildings	13
1.1 Introduction.....	14
1.2 Conventional model of thermal comfort	15
1.2.1 Fanger's approach.....	15
1.2.2 Remarks on conventional methods.....	17
1.2.3 Standards for thermal comfort.....	18
1.3 Residential buildings.....	19
1.3.1 General considerations.....	19
1.3.2 Ambient temperature characterisation.....	20
1.3.3 Indoor temperature characterization.....	22
1.4 The three different zones.....	23
1.4.1 Bathroom.....	23
1.4.2 Bedrooms	26
1.4.3 Other rooms	29
1.5 Local thermal discomfort	32
1.6 Temperature variations	33
1.7 Acceptable thermal comfort 'regions' for residential buildings.....	34
1.8 Summary and conclusion on thermal comfort	37
References	39
2 Modelling building energy systems.....	43
2.1 Introduction.....	44

2.2	Status of ESP-r at project commencement.....	45
2.2.1	The structure of <i>ESP-r</i>	45
2.2.2	Basic physics in <i>ESP-r</i>	46
2.2.3	Control logic in <i>ESP-r</i>	53
2.2.4	Solution technique within <i>ESP-r</i>	56
2.2.5	Validation of <i>ESP-r</i>	62
2.3	Implicit plant simulation.....	63
2.3.1	The implicit plant structure.....	64
2.3.2	The advantages of the implicit approach.....	74
2.4	Summary and conclusions on modelling building energy systems.....	76
	References.....	77
3	Heat emission/absorption elements.....	81
3.1	Introduction.....	82
3.2	The physics of an emission/absorption element.....	84
3.2.1	The basic processes of heat transfer: Radiation.....	84
3.2.2	The basic processes of heat transfer: Convection.....	85
3.3	An empirically derived formula for the heat output.....	91
3.3.1	Steady-state thermal output.....	91
3.3.2	Cooling.....	93
3.3.3	Thermally activated building elements.....	93
3.3.4	Introducing dynamics.....	93
3.4	Linking the empirically derived formula with theory.....	94
3.4.1	An amount of radiation and an amount of convection.....	94
3.4.2	Extrapolating the correlations.....	96
3.5	Comparing the empirically derived formula with theory.....	101
3.5.1	An amount of convection and an amount of radiation.....	101
3.5.2	The amount of convection compared to the total energy output of the heat emitter/absorber.....	104
3.6	The effect of changes to the empirically derived formula.....	106
3.6.1	Using the average fraction of convection to calculate the room temperature.....	106
3.6.2	Choosing average conditions as nominal conditions.....	107
3.6.3	The overestimated radiant heat emission.....	108

3.6.4	The effect of the three corrections simultaneously	110
3.7	The evaluation of the indoor climate resulting from the heat emission/absorption	112
3.8	The generic emitter model for the implicit approach	113
3.8.1	Overall scheme related to model input data	113
3.8.2	The model parameters.....	114
3.8.3	The steady state model.....	115
3.8.4	Introducing dynamics	118
3.9	Heat emission/absorption of real elements.....	120
3.9.1	Radiators and convectors.....	120
3.9.2	Heated or cooled elements as part of the zonal enclosure	121
3.10	Summary and conclusion on implicit heat emitter/absorber model	121
	References	123
4	Model verification	127
4.1	Theoretical analysis:	128
4.1.1	Uncertainty on the heat transfer coefficients.....	128
4.1.2	Accuracy of the mean radiant temperature calculation.....	131
4.2	Steady state behaviour of the emitter/absorber model	148
4.2.1	Emitter/absorber located in the zone.	148
4.2.2	Emitter/absorber located within the zonal enclosure.	152
4.3	Testing the model's dynamic response	154
4.3.1	Emitter/absorber located in the zone.	154
4.3.2	Dynamical verification of element embedded in the zonal enclosure	158
4.4	Summary and conclusions.....	161
	References	165
5	Producing the hot/cold water	167
5.1	Introduction.....	168
5.2	The generic implicit production model	169
5.2.1	Schematic overview.....	169
5.2.2	The model parameters.....	171
5.2.3	The production system dynamics	176

5.2.4	The overview of the production system algorithm.....	177
5.3	Summary and conclusions.....	178
	References.....	180
6	Controls for heat emission/absorption and heat/cold production systems.....	183
6.1	Introduction.....	183
6.2	Controllers for the emission/absorption of heat	185
6.2.1	Desired indoor temperatures.....	185
6.2.2	The different control strategies.....	186
6.3	Controllers for the production of hot/cold water.....	196
6.3.1	Production controls in general.....	196
6.3.2	The ideal control.....	197
6.3.3	The central room thermostat with modulating production control	199
6.4	Summary and conclusions.....	199
	References.....	200
7	Optimal heat emitter/absorber	203
7.1	Introduction.....	203
7.2	Optimisation process.....	205
7.2.1	The rough mapping technique.....	206
7.2.2	The more refined detailed search technique.....	206
7.2.3	The parameter space considered.....	207
7.3	The objective function	210
7.3.1	The function terms.....	210
7.3.2	The function coefficients.....	212
7.4	The optimum and its neighbourhood	216
7.4.1	The optimum itself.....	216
7.4.2	Interpretation of the optimum and its neighbourhood.....	217
7.5	Summary and conclusions.....	219
	References.....	221

8	Case studies.....	223
8.1	Introduction.....	224
8.2	Description of the simulated building.....	224
8.2.1	The building.....	225
8.2.2	The internal gains.....	226
8.2.3	Simulation details.....	226
8.3	Case studies.....	227
8.3.1	Location of the building.....	227
8.3.2	Heavyweight versus lightweight building structures.....	233
8.3.3	Variations in insulation quality.....	239
8.3.4	Constant indoor temperature versus intermittent heating/cooling.....	243
8.3.5	Limitations to production device: increased lock out time.....	249
8.4	Summary and conclusions.....	253
	References.....	254
9	Conclusions and suggestions for future research.....	257
9.1	Conclusions.....	257
9.2	Suggestions for future research.....	259
	Nederlandstalige samenvatting.....	261
	Appendix A Expressions for mixed convection and for surface temperatures of TAB elements.....	277
A.1	Mixed convection.....	277
A.2	Surface temperatures for TAB elements.....	280
A.2.1	Steady state conditions.....	280
A.2.2	Dynamic conditions.....	282
	Appendix B Coding.....	285
B.1	Relevant routines: state at project commencement.....	285
B.2	Changes to the software structure for the implementation of the implicit plant level.....	287

Appendix C Efficiency calculations for the implicit production device 291

C.1	Input parameters.....	291
C.1.1	Efficiency of an ideal production device.....	292
C.1.2	Efficiency related to ambient temperature	293
C.1.3	Efficiency related to part load ratio	293
C.1.4	Efficiency calculation for CHP devices	293

Appendix D Non-ideal implicit emission/absorption and production controls 295

D.1	Emitter/absorber controls.....	295
D.1.1	The on/off room thermostat.....	295
D.1.2	The modulating room thermostat	297
D.1.3	The thermostatic radiator valve	298
D.2	Production controls	300
D.2.1	The central room thermostat.....	300

Appendix E Building model description..... 303

E.1	Dimensions of the building	303
E.2	Thermo-physical properties	304
E.2.1	Heavyweight construction	304
E.2.2	Lightweight construction	306
E.2.3	Additional capacity.....	307
E.3	Ventilation/infiltration	307
E.4	Internal gains.....	307

Water-based heating/cooling in residential buildings
Towards optimal heat emission/absorption elements

INTRODUCTION

Occupants of any building expect a thermally comfortable and healthy indoor environment to perform their daily tasks and actions. Focusing on heating and cooling in residential buildings, this means that each zone in the building should have a thermal condition that meets the standards for the specific but diverse activities conducted within it.

A wide variety of parameters influences this comfort; the climate the dwelling is built in, the thermal performance of the building envelope and the HVAC-installation are just some of them. In an ideal case, they deliver the required power to decrease or increase the indoor temperature to within the comfort range. But, by introducing these installations, a sometimes large energy consumer is installed in the dwelling. Reducing the heating and/or cooling energy consumption is therefore an important aspect that has to be taken into account from the design stage of the building on.

This dissertation will focus on one particular aspect of reducing the energy for heating/cooling in a residential building, namely the optimal water based heat emission/absorption element in a building zone.

Although in climates with moderate summer conditions as in Belgium, the cooling demand can and should be limited or even avoided from the design stage of the building on, the model set up in the framework of the current dissertation is applicable for both heating and heating and cooling cases. The cooling strategy proposed, however, is only to avoid extreme indoor temperatures.

State of the art

Reducing the energy demand in buildings is a hot topic. As any other aspect in real life, also for buildings, the financial resources are usually limited. So, choices must be made. Several authors have therefore defined priority lists, stating which energy demand reducing measures should be taken first, based on their impact and cost-effectiveness. Balaras et al. [1], as well as Verbeeck and Hens [2] mention the importance of improvements to the building envelope as the top priority when it comes to reducing the energy demand. Also Hastings [3] lists the main breakthrough barriers for houses without active heating system as being building-envelope related.

The impact of building-envelope improvements has been investigated considerably ([4] to [10]). Most of these studies investigate the energy-demand reduction of adding a certain amount of insulation. Kaynakli [6], however, uses a life cycle analysing (LCA) approach to define the optimal insulation thickness. Such an LCA is also conducted by Verbeeck [11], evaluating a wide range of energy related aspects of a residential building. It should be noted though, that besides thermal insulation, the thermal performance of the building envelope and how the building structure influences the indoor environment is also determined by parameters such as air tightness and ventilation, compactness, (accessible) thermal mass, shading and orientation [12], [13].

Whilst not at all being complete, the above overview shows that building-envelope design has been quite thoroughly examined. The effect of it is obvious. However, this does not diminish the importance of carefully designing the other energy-related aspects of the building. The lists of Balaras [1] and Verbeeck and Hens [2] both

indicate improvement of the heating/cooling installation as the next most important potential energy-saving measure.

The most obvious heating/cooling installation¹ component to be considered is the production unit. As its efficiency has a large impact on the energy consumption, it has been investigated and discussed widely. Zogou and Stamatelos [14] discuss the simulation results of a performance study on different types of heat pumps. Ozgener and Hepbasli [15] describe both simulation results and experimentally achieved performances of ground source heat pumps. Kuhn et al. [16] as well as Possidente et al. [17] discuss measurement results for different micro-CHP technologies. Van der Veken and Hens [18] describe simulation results comparing a high efficiency and a condensing gas-fired boiler. Wider ranges of production devices are compared in various studies, for example [19] to [21].

The production device reacts to a control signal and consequently influences the action of a possible storage, distribution and heat emission/absorption system. None of the above listed publications, however, takes into account the interaction with these installation components. Tanton et al. [22] consider the effect of variations in capacity by adding a storage tank and determine the impact of different radiator sizes. They however do not discuss the effect of the boiler or indoor temperature control. That the control has a non-negligible impact has been shown by amongst others Peacock and Newborough [23]. They take into account the control aspect when comparing the potential savings of micro-cogeneration devices and conventional boilers, but they do not consider the heat emission elements. Also Yan et al. [24] discuss savings due to changing the control of the given heating and cooling installation. The effect of controls has also been shown by the current author in [25] where simulation results are described showing the impact of different residential heating/cooling control strategies on energy consumption and thermal comfort for radiators combined with a range of boiler types.

The impact of the combined effect of both control and installation design is well described by Van der Veken and Hens [18] and by Crommelin and Ham [26] for boilers. For the development of an exergy indicator, Favrat et al. [27] determined the

¹ The water-based heating/cooling installation comprises all 'hardware' components of the central heating/cooling system: the production device (boiler, heat pump, CHP, etc.), the distribution system, and the heat emitting/absorbing elements (radiators, floor heating, etc.).

exergetic efficiency of different plant components for a range of installation combinations and a variety of control-related settings.

All of these publications use existing installation components² in their analyses. The list of discussions on especially improvements of, or new developments for, the zonal emission elements in a water-based heating/cooling installation is limited. Beck et al. [29] try reducing the cost and efficiency decrease of a finned panel radiator used for heating only. Kilkis [30], [31] starts from an existing production device and designs a composite radiant panel useable for both heating and cooling. The effects of changes to radiator coating or floor covering in case of floor heating systems are described by Hollingsworth et al. [32] and by Chen and Athienitis [33], respectively. While Arslanturk and Ozgnuc [34] as well as Kowalski [35] discuss optimal dimensions of existing radiators, Roy and Avanic [36] apply the use of phase-changing materials to a radiator model to provide for large fluctuations in the heat demand.

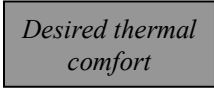
The above listed authors report efficiency decreases in the range of 10% for not correctly designed emitter configurations [29], [31]. It is thus clear that heat emission/absorption elements can have a substantial impact on the overall heating/cooling energy consumption. However, the optimal set of characteristics a certain heat emission/absorption element should have in a given context has not been defined so far. Moreover, only when this aspect is covered for all zones in a building, is it possible to identify the requirements for a suitable production device.

Such optimisation analysis enables ranking existing installation components and defining tendencies for future developments in the area of water-based heating/cooling installation components. In the framework of the current dissertation, a tool has been set up that allows determining the optimal emission/absorption characteristics for a zone in a given building. The so defined optima can be used as guidelines for future product developments.

² Emission efficiencies of existing heat emission elements can be found in EN 15316 [28].

Methodology and outline of the current work

To define the optimal characteristics of the heat emitters/absorbers, it is necessary to first define what indoor climate has to be achieved. The thermal comfort can thus be considered as the ‘boundary condition’, and not achieving should thus negatively influence the performance analysis of the given heat emission/absorption element. But what is thermal comfort for residential buildings? Whilst standards for offices and commercial buildings are widely available [37], [38] and [39] well-founded guidelines for domestic settings are not yet defined. Therefore, in chapter 1, thermal comfort relations for different zones in a residential building are set up (Figure 0.1).



*Desired thermal
comfort*

Figure 0.1: The ‘boundary condition’ defined.

The thermal condition in a zone is influenced by a wide range of parameters; solar radiation, infiltration and ventilation as well as transmission losses through the building are just a few of the possible impact variables. The heating/cooling equipment should, despite these sometimes unpredictable influences, maintain or achieve the desired comfort. When simulating any heating/cooling installation in a variable setting as a residential building, it thus is a necessity to incorporate the effect of these unpredictable parameters. Different building simulation programs are currently available to do so. Therefore, the residential building with its heating/cooling installation is modelled within an existing building energy simulation program, as elaborated in chapter 2.

The thermal comfort settings in this residential building indirectly define the requested output of the emission/absorption element. To determine the required energy input for this element, a model logic must be set up that can represent any kind of water-based heat emitter/absorber. Such a generic model is developed in chapter 3, and validated in chapter 4. Figure 0.2 shows the emitter/absorber model, indicated in italic, and its position in the structure described so far.

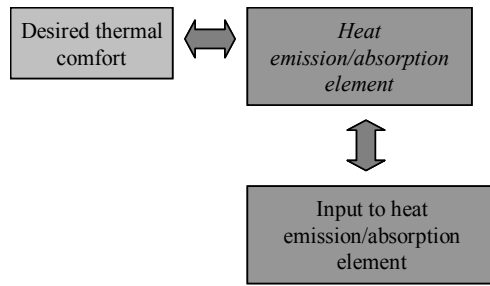


Figure 0.2: The emitter/absorber element's input defined by the element's model acting to fulfil the boundary condition set by the thermal comfort. The 'position' of the emitter/absorber model is indicated in italic.

The emission/absorption element gets the energy through the distribution system (indicated in italic in the scheme of Figure 0.3). In this dissertation, the distribution system is simplified by assuming that the loss equals a fixed percentage of the energy transported. The value has been defined based on simulations performed by amongst others the current author, as described in [40].

The input of the distribution system equals the output of a particular production device. As with the emitter/absorber element, also for the production device a generic model has been set up so as to determine its required energy input (Figure 0.4). Once the optimal emitter/absorber has been determined, it is thus possible to define the characteristics of an ideal production device.

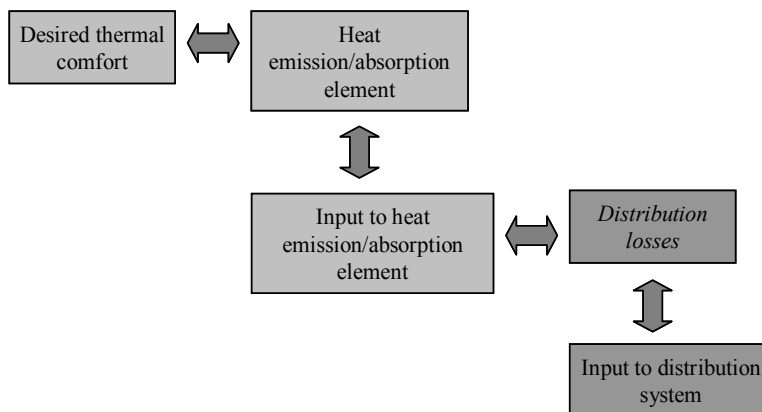


Figure 0.3: The required input to the distribution system (model indicated in italic) as a consequence of losses in the delivery to the heat emitters/absorbers.

However, this production model is not as detailed as the emitter/absorber model. The main reason is that the focus in this dissertation is on the effect of possible limitations of the production device on the optimal heat emitter/absorber more than on optimising the production device itself.

The model of the production device and how it can be used to represent existing production units is explained in chapter 5. Chapter 6 discusses ideal and more realistic controls for both the heat emission/absorption elements and the production elements.

Once the heating/cooling installation model is set up, it can be used to determine the characteristics of an optimal heat emitter/absorber for a given building. To do so, the building simulation software configured with the plant³ model as described in this dissertation is coupled with an optimisation program. Chapter 7 discusses which optimisation algorithms are selected and briefly describes the mechanisms these algorithms use to ensure convergence to the minimum. In chapter 8 the generic model is applied to a range of case studies. These case studies focus on the optimisation of the heat emitter/absorber of a specific zone in a multi-zone building; both the case of the emitter/absorber as single installation component and the case where the emitter/absorber is coupled with a production device. The case studies show what information can be extracted from the results and how it can be interpreted.

³ The term ‘installation’ is used for the heating/cooling equipment in a real-life context. The term ‘plant’ indicates the same in a model-related context.

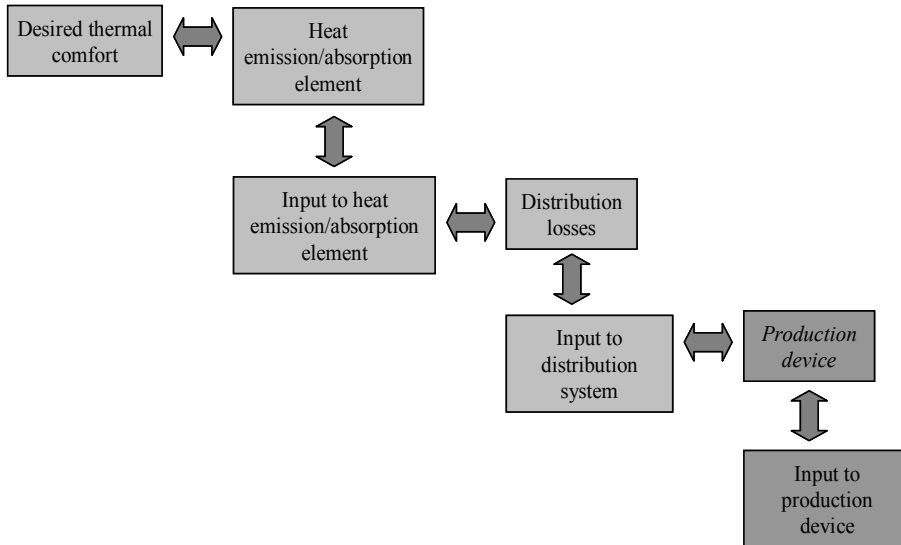


Figure 0.4: The required input to the production device (model indicated in *italic*) in order to achieve the required thermal comfort.

Finally, Chapter 9 summarises the major conclusions and indicates potential areas for future research.

Contributions of the current work

This dissertation provides a critical view on heating/cooling developments for residential buildings. A first important contribution to the field of thermal comfort is the determination of residential thermal comfort curves and comfort bands. Secondly, the implicit plant modelling structure, implemented in the framework of the current dissertation, is a useful tool to get a general idea on the performance of a certain installation, without setting up a detailed model. The generic formula for heat emitter/absorber elements enables to easily evaluate different emission/absorption types, changing no more than just a few commonly available parameters. Finally, the optima, as can be determined by the coupling of the implicit plant modelling structure with the existing optimisation software *GenOpt*, provide useful directions for future emitter/absorber product design.

The aim of the research was to develop a generic tool and to show its usefulness, more than generating generic results.

References

- [1] C. Balaras, A. Gaglia, E. Georgopoulou, S. Mirasgedis, Y. Sarafidis, D. Lalas, 2007, European residential buildings and empirical assessment of the Hellenic building stock, energy consumption, emissions and potential savings, *Building and Environment*, vol. 42, pp. 1298-1314
- [2] G. Verbeeck, H. Hens, 2005, Energy savings in retrofitted dwellings: economically viable?, *Energy and Buildings*, vol. 37, pp. 747-754
- [3] S. Hastings, 2004, Breaking the "heating barrier". Learning from the first houses without conventional heating, *Energy and Buildings*, vol. 36, pp. 373-380
- [4] M. Mohsen, B. Akash, 2001, Some prospects of energy savings in buildings, *Energy Conversion and Management*, vol. 42, pp. 1307-1315
- [5] B. Rolfman, 2002, CO2 emission consequences of energy measures in buildings, *Building and Environment*, vol. 37, pp. 1421-12430
- [6] O. Kaynakli, 2008, A study on residential heating energy requirement and optimum insulation thickness, *Renewable Energy*, vol. 33, pp. 1164-1172
- [7] G. Saha, J. Stephenson, 1979, An analysis of residential space heating in New Zealand, *Energy and Buildings*, vol. 2, pp. 297-307
- [8] E. Kossecka, J. Kosny, 2002, Influence of insulation configuration on heating and cooling loads in a continuously used building, *Energy and Buildings*, vol. 34, pp. 321-331
- [9] M. Wetter, 2000, Design optimization with GenOpt, *Building Energy Simulation User News*, vol. 21, pp. 19-28
- [10] S. Kalogirou, G. Florides, S. Tassou, 2002, Energy analysis of buildings employing thermal mass in Cyprus, *Renewable Energy*, vol. 27, pp. 353-368
- [11] G. Verbeeck, 2007, Optimisation of extremely low energy residential buildings, PhD dissertation, University of Leuven (KULeuven), Belgium
- [12] M. Wetter, 2000, Design optimisation with GenOpt, *Building Energy Simulation, user News*, Lawrence Berkeley National Laboratory, vol. 21
- [13] M. Wetter, J. Wright, 2003, Comparison of a generalized pattern search and a genetic algorithm optimization method, *Proceedings of the 8th Ibpa Conference*, Eindhoven, the Netherlands, pp. 1401-1408
- [14] O. Zogou, A. Stamatelos, 1998, Effect of climatic conditions on the design optimization of heat pump systems for space heating and cooling, *Energy Conversion and Management*, vol. 39, pp. 609-622
- [15] O. Ozgener, A. Hepbasli, 2007, Modelling and performance evaluation of ground source (geothermal) heat pump systems, *Energy and Buildings*, vol. 39, pp. 66-75
- [16] V. Kuhn, J. Klemes, I. Bulatov, 2008, MicroCHP: Overview of selected technologies, products and field test results, *Applied Thermal Engineering*, vol. 28, pp. 2039-2048
- [17] R. Possidente, C. Roselli, M. Sasso, S. Sibilio, 2006, Experimental analysis of micro-cogeneration units based on reciprocating internal combustion engine, *Energy and Buildings*, vol. 28, pp. 1417-1422

-
- [18] J. Van der Veken, H. Hens, 2005, How efficient are residential heating systems, Proceedings of Clima 2005, 8th REHVA World Congress, Lausanne, Switzerland, October 9-12
- [19] V. Ugursal, A. Fung, 1998, Residential carbon dioxide emissions in Canada; Impact of efficiency improvements and fuel substitution, Global Environmental Change, vol. 8, pp. 263-273
- [20] Y. Tonooka, J. Liu, Y. Kondou, Y. Ning, O. Fukasawa, 2006, A survey on energy consumption in rural households in the fringes of Xian city, Energy and Buildings, vol. 38, pp. 1335-1342
- [21] G. Schaumann, 2007, The efficiency of the rational use of energy, Applied Energy, vol. 84, pp. 719-728
- [22] D. Tanton, R. Cohen, S. Probert, 1987, Improving effectiveness of a domestic central-heating boiler by the use of heat storage, Applied Energy, vol.27, pp. 53-82
- [23] A. Peacock, M. Newborough, 2008, Effect of heat-saving measures on the CO₂ savings attributable to micro-combined heat and power (µCHP) systems in UK dwellings, Energy, vol. 33, pp. 601-612
- [24] Y. Yan, J. Zhou, Y. Lin, W. Yang, P. Wang, G. Zhang, 2008, Adaptive optimal control model for building cooling and heating sources, Energy and Buildings, vol. 40, pp. 1394-1401
- [25] L. Peeters, J. Van der Veken, H. Hens, L. Helsen, W. D'haeseleer, 2008, Control of heating systems in residential buildings: Current practice, Energy and Buildings, vol. 40, pp. 1446-1455
- [26] R. Crommelin, P. Ham, 1987, The influence of modifications in a central heating system of a dwelling on the energy consumption, calculated with a dynamic model, Energy and Buildings, vol. 10, pp. 1-17
- [27] D. Favrat, F. Marechal, O. Epelly, 2008, The challenge of introducing an exergy indicator in a local law on energy, Energy, vol. 33, pp. 130-136
- [28] European Committee for Standardization, 2007, EN15316-2-1: Heating systems in buildings, method for calculation of system energy requirements and system efficiencies, part 2-1 space heating emission systems, Brussels, Belgium
- [29] S. Beck, S. Grinsted, S. Blakey, K. Worden, 2004, A novel design for panel radiators, Applied Thermal Engineering, vol. 24, pp. 1291-1300
- [30] B. Kilkis, 2006, Cost optimization of a hybrid HVAC system with composite radiant wall panels, Applied Thermal Engineering, vol. 26, pp. 10-17
- [31] B. Kilkis, 2006, From floor heating to hybrid HVAC panel: A trail of exergy-efficient innovations, ASHRAE Transactions 2006, part 1, pp. 343-349
- [32] D. Hollingsworth, L. Witte, J. Hinke, K. Hurlbert, 2006, Reduction in emittance of thermal radiator coatings caused by the accumulation of a Martian dust stimulant, Applied Thermal Engineering, vol. 26, pp. 2383-2392
- [33] Y. Chen, A. Athienitis, 1995, A three-dimensional numerical investigation of the effect of cover materials on heat transfer in floor heating systems, ASHRAE Transactions 1995, part 2, pp. 1350-1355
- [34] C. Arslanturk, A. Ozguc, 2006, Optimization of a central heating radiator, Applied Energy, vol. 83, pp. 1190-1197

- [35] J. Kowalski, 1995, Triple objective optimum design of a two-column radiator of central heating, *International Communications in Heat and Mass Transfer*, vol. 22, pp. 401-409
- [36] S. Roy, B. Avanic, 2006, Optimization of a space radiator with energy storage, *International Communications in Heat and Mass Transfer*, vol. 33, pp. 544-551
- [37] ANSI/ASHRAE 55-2004, Thermal Environmental Conditions for human occupancy, American Society of Heating, Refrigerating and Air-conditioning Engineers, Inc. Atlanta, USA
- [38] ISO 7730, 2005, Ergonomics of the thermal environment-Analytical determination and interpretation of thermal comfort using the PMV and PPD indices and local thermal comfort criteria, International Organization for standardization, Switzerland
- [39] A. Vanderlinden, A. Boerstra, A. Raue, S. Kurvers, R. De Dear, 2006, Adaptive temperature limits: A new guideline in the Netherlands. A new approach for the assessment of building performance with respect to thermal indoor climate, *Energy and Buildings*, vol. 38, pp. 8-17
- [40] J. Van der Veken, H. Hens, L. Peeters, L. Helsen, W. D'haeseleer, 2006, Economy, energy and ecology based comparison of heating systems in dwellings. *Proceedings of the 3th International Building Physics Conference*, Montreal, August 27-31

1 THERMAL COMFORT IN RESIDENTIAL BUILDINGS¹

Comfort values and scales for building energy simulation

Building Energy Simulation (BES) programs often have conventional thermal comfort theories built in as evaluation tool for the indoor thermal environment. These theories are based on the evaluation of the heat exchanges between a human body and the thermal environment it occupies. Based on such research rationally-based theories as the well-known theory of Fanger [2] have been developed. Besides these studies, there has been a continuous parallel stream of thermal comfort field studies [3]. The comfort temperatures observed during various field studies vary one from another and are often difficult to harmonize with the more rationally-derived values. Humphreys and Nicol [4] describe that these phenomena led to viewing

¹ A slightly modified version of this chapter has been published in Applied Energy [1]

thermal comfort as part of a self-regulating system of the human body. The effect is generally referred to as adaptation².

In this chapter, a brief overview of the conventional rationally-based theory of Fanger will be given, followed by a discussion on the effects of adaptation. Based on theories specifically mentioned as applicable for residential buildings, combined with measurements described in the literature, temperature guidelines for residential buildings will be extracted. They will here be defined in an algorithmic way, easily implementable in any BES code. The focus is on comfortable temperature levels in the room, more than on the detailed temperature distribution within that room.

As stated in the introduction, this thermal comfort algorithm is the first step towards the development of a tool for optimisation of residential heat emission/absorption elements.

1.1 Introduction

When comparing the effect of changes to buildings, be it changes to the building structure, the materials used or the installations, an important boundary condition is that the thermal comfort must, in all cases, be maintained. BES software often uses conventional methods to determine the achieved comfort level: common programs as *ESP-r* [5], *TRNSYS* [6] and *IDA Ice* [7] use the ISO 7730 assessment method. This thermal comfort standard is based on Fanger's conventional approach. However, when determining general comfort temperature guidelines for residential buildings a broad variation of activities and multiple ways to adapt to the existing thermal environment are available. Comfort temperatures as well as acceptable temperature variations can be influenced by parameters not considered by the conventional methods. Thermal comfort guidelines specifically developed for the different zones of a residential building, as well as for the estimation of the thermal sensation of the building occupants in these zones, will improve the resemblance with reality. These guidelines, presented in an algorithmic format, must take into

² The first publications on adaptive thermal comfort indicated an immense range of adaptive options, sometimes not all as realistic for residential buildings. Later publications show a more nuanced approach.

account the knowledge of the traditional methods as well as recent findings in the field of thermal comfort with a focus on residential buildings.

1.2 Conventional model of thermal comfort

1.2.1 Fanger's approach

In order to develop mathematical models to predict people's responses on the thermal quality of an environment, researchers have been exploring the thermal, physiological and psychological response of people in varying circumstances. 'Thermal comfort' is defined as "that condition of mind which expresses satisfaction with the thermal environment" [8]. Thermal comfort is a result of a combination/adaptation of parameters of both the environment and the human body itself. Fanger [2], who developed the first heat balance thermal comfort model, stated that the condition for thermal comfort is thus that skin temperature and sweat secretion lie within narrow limits. For his comfort equation, Fanger obtained data from climate chamber experiments, during which sweat rate and skin temperature were measured on people who judged their thermal sensation as comfortable. He then defined an estimation of skin temperature and sweat secretion as a function of metabolic rate by regression analyses of the measured data. This way, an expression for optimal thermal comfort was deduced from the metabolic rate, clothing insulation and environmental conditions. His assumption for this was that the sensation experienced by a person is a function of the physiological strain imposed on him by the environment. The thermal environment is taken into account by the air temperature, the mean radiant temperature, the partial pressure of water vapour in ambient air and the air velocity.

Satisfying the comfort equation is a condition for optimal thermal comfort. However, it only gives information on the possible combination of the variables to achieve thermal comfort. Additionally, Fanger proposed a method to predict the actual thermal sensation of persons in an arbitrary climate where the variables might not satisfy the equation: the Predicted Mean Vote (PMV). This, he defined as "the difference between the internal heat production and the heat loss to the actual environment for a person kept at the comfort values for skin temperature and sweat production at the actual activity level". Following Fanger then, the sensation of thermal comfort is quantified by an adapted ASHRAE 7-point psycho-physical scale with values ranging from -3, indicating cold, over 0, indicating neutral, to +3,

indicating hot. With experiments in a constant well controlled, environment, Fanger obtained a reasonable statistical basis for the quantification of his PMV-index. The method allows to predict what comfort vote would arise from a large group of individuals for a given set of environmental conditions for a given clothing insulation and metabolic rate.

It nevertheless might be more meaningful to state what percentage of persons can be expected to be dissatisfied, because that indicates the number of potential complainers. The dissatisfied are defined as those voting outside the range of -1 (slightly cool) to +1 (slightly warm). Through steady state experiments, Fanger determined the relationship between the PMV-index and the Predicted Percentage of Dissatisfied (PPD), as shown in Figure 1.1. This figure shows a PPD of 5% for a PMV equal to 0. That indicates the impossibility to satisfy all persons in a large group sharing a collective climate. Complaints cannot be avoided, but should be kept to the minimum as shown by this figure.

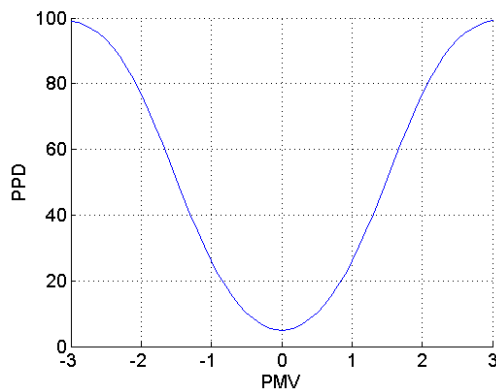


Figure 1.1: Predicted Percentage of Dissatisfied (PPD) as a function of Predicted Mean Vote (PMV).

The curve of Figure 1.1 shows an equal amount of complaints on the 'warm' side as on the 'cold' side: the curve is symmetric around the PMV of 0. At the optimal condition, there is thus a balance between those sensing uncomfortably warm and those sensing uncomfortably cold. However, a deviation from 0 would not only mean a greater percentage of dissatisfied, but also an asymmetric distribution between those experiencing warmth and those experiencing cold. Therefore, based

on the conventional comfort theories, this deviation is expected to result in a demand for a unilateral change.

Figure 1.1 further shows that a PPD of 0% is never achieved. That is inherent to individual differences that are not incorporated in the equations of Fanger. However Fanger did test the validity of his equations for a range of test groups, he showed none of the tested variations (such as male-female, origin and age) causing significant differences in the evaluation of the thermal environment. Nevertheless he emphasizes that the PMV shows the average meaning of a group of people, which is not equal to the opinion of the individual occupants. That effect is thus shown in a minimum PPD of 5%.

1.2.2 Remarks on conventional methods

The PMV and PPD concepts were derived based on laboratory experiments, with in most cases test persons wearing standardised clothing executing sedentary activities. Numerous publications assess this uniform approach as a limitation ([9], [10], [11], [12]). Another often mentioned limitation has to do with the accurate data on the insulation of the clothing garments or ensembles ([9], [13]) and the sensitivity of the PMV equation to this [12].

The majority of comments are on PMV or PPD disregarding the effect of adaptation. Adaptation in this context is the changing evaluation of the thermal environment because of changing perceptions. Different forms of adaptation³ can be distinguished, which are connected and will influence one another ([13], [14]).

Psychological adaptation depends on experiences, habituations and expectations of the indoor environment ([15], [16], [17]).

Physiological adaptation can be broken down into two major subcategories: genetic adaptation and acclimatisation. The former deals with effects

³ It should be mentioned that adaptation is limited in buildings that have a fully equipped heating and cooling system allowing an almost constant indoor temperature. In this study, it is assumed that cooling is only applicable to reduce peak indoor temperatures. The neutral temperatures in case of fully equipped cooling systems will differ from the values proposed here.

on timescales beyond that of an individual's lifetime. The latter comprehends changes in the settings of the physiological thermoregulation system over a period of a few days or weeks. It is the response to sustained exposure to one or more thermal environmental stressors [13].

Behavioural thermoregulation, or adjustment, includes all modifications a person might consciously or unconsciously make, which in turn modify heat and mass fluxes governing the body's thermal balance [13]: personal adjustment ([12], [18], [19]), technological or environmental adjustment [8] and cultural adjustment.

It should be noted though, that Fanger [20] formulated an extension to his PMV-model to account for the effect of expectation. He emphasizes the importance of the factors as the clothing value and metabolic rate, but widens the range of comfort values as calculated by the conventional PMV-formula so as to account for the phenomenon of psychological adaptation. The proposed corrections mentioned in that paper are for non-air-conditioned buildings in warm climates. Furthermore, one could argue that more 'adaptation' is incorporated in the conventional theory of Fanger: changes in clothing and activity level to account for variations in indoor temperature can be seen as behavioural adaptation as well.

1.2.3 Standards for thermal comfort

The International Standard ISO 7730 [21] uses these PMV and PPD indices to predict the thermal sensation of people exposed to moderate thermal environments, as well as to specify acceptable thermal environmental conditions for comfort. Local discomfort and draught are taken into account by additional conditions. As it is not known whether or how the number of dissatisfied due to local discomfort can be added to those dissatisfied due to general thermal discomfort, or whether the percentage of the total dissatisfied equals the sum of the dissatisfied per individual discomfort criterion, the ISO 7730 proposes to specify different levels of comfort [22]. The optimal temperature is the same for the different comfort classes, but the acceptable temperature range will vary as the allowed percentage of dissatisfied changes. The limits of validity for different variables, whether included in the equations or not, are listed for each comfort level. It is stated that the standard applies to indoor environments where steady state thermal comfort or moderate deviations from comfort occur. When considering thermal environments in which occupants have many possibilities to adapt themselves or the environment to achieve

a more agreeable thermal sensation, the ISO standard suggests using a wider PMV range.

The standard 55-2004 set up by ASHRAE [8] is a revision of the former ASHRAE 55-1992. As the ISO 7730, also the ASHRAE 55 is valid for healthy, adult people. The activities they perform, the clothes they wear and the thermal environment they occupy, all are determined by variable values within given limits. Besides the recommended PPD and PMV ranges, this standard increases the percentage of persons dissatisfied with 10 percent points, to incorporate the effect of local thermal discomfort, e.g. draft and temperature asymmetry. It also determines the values of acceptable temperature changes per given time interval. Thereby partly accounting for the dynamic effects ignored both by Fanger [2] and in ISO 7730 [21].

The adaptive temperature limits, ATL, is another standard for thermal comfort. It is set up by Van der Linden et al. [23] on request of the Dutch government. It is based on the ASHRAE measurement databases and attempts to incorporate the possible effects of adaptation in the guidelines for design temperatures. Two building types are introduced: alpha and beta. The latter category holds the buildings which have a sealed façade, and a heating installation as well as an active cooling system. This active cooling installation can be a forced air system or a cooled ceiling that is not part of the building structure [23], [24]. The operation of the cooling installation in these beta-buildings is all but individually adjustable. The category of the alpha-buildings holds the naturally ventilated offices and dwellings. They can have operable windows, or easy controllable cooling installations and the clothing can be adapted according to the outdoor conditions. For both building types, alpha and beta, the ATL defines indoor temperatures that are related to the ambient temperature.

1.3 Residential buildings

1.3.1 General considerations

Focusing on residential buildings, conditions are not quite comparable to those during the experiments for calibration of the PMV and PPD equations. The domestic

scene is far from steady state: both the activity level⁴ and the clothing value⁵ can vary within small timescales, fluctuating internal and external gains can rapidly affect the indoor temperature and the variation in occupancy will influence, amongst others, the required ventilation rate. Nearly all forms of adaptation apply to the case of residential buildings: changing activity, clothing, opening windows, drinking cold or warm drinks, expected temperatures in summer, siestas, etc. The acceptable temperature range might even be wider as occupants of residential buildings generally have to pay for their energy consumption themselves [25], [26] and hence accept a larger deviation from the neutral temperature⁶.

Calculation of the neutral indoor temperature, being the most important environmental parameter [27] of a residential building, thus should incorporate the effects of adaptation. Based on the above gathered knowledge, some common methods are compared and discussed, focusing on residential buildings.

In this dissertation, **3 thermal zones** are distinguished in residential buildings: bathroom, bedroom and others. In bathrooms, a wet naked body has special thermal comfort requirements, while in a bedroom especially overheating requires attention. Other zones include mainly kitchen, living room and office, in which mostly the activity levels are rather low (0.7 met for reclining to 1.6 met for cooking [2], [8]) and the clothing is in accordance with seasonal conditions.

1.3.2 Ambient temperature characterisation

The outdoor climate influences more than just the clothing ([4],[19],[28],[29]). Therefore, the outdoor temperature must be characterised by a value that includes

⁴ The activity level indicates the intensity of the physical action of a person. The dimension *met* is used to express the consequently generated energy inside the body. 1 met equals 58.2 W/m², the energy produced per surface area of an average person at rest.

⁵ The clothing factor is the total thermal resistance from the skin to the outer surface of the clothed body. It is common to indicate it in *clo*, where 1 clo equals 0.155m²K/W.

⁶ When considering the effect of adaptation, one could argue that some of the adaptive possibilities are invoked only when the current thermal condition does not meet the desired condition. Therefore, it might be more meaningful to consider neutral or likely indoor temperatures, instead of comfort temperatures.

the required amount of detail. It is clear that the effect of the detailed course of the external temperature will partly be flattened out by the time constants of the building. When averaging information over a long period, however, some effects risk to be neglected. Some methods use monthly averaged external temperature values, while amongst others Humphreys et al. [4] suggest that most adaptation is within a week or so. Morgan and de Dear [30] demonstrate that besides today's weather also the weather of yesterday and that of the past few days influence clothing and perception of comfort temperature. An appropriate measure for the incorporation of the outdoor temperature is therefore required, so that it can respond to the day to day weather variations.

In Van der Linden et al. [23], the adaptive temperature limits (ATL) method is defined, using $T_{e,ref}$:

$$T_{e,ref} = \frac{(T_{today} + 0.8T_{today-1} + 0.4T_{today-2} + 0.2T_{today-3})}{2.4} \quad (1.1)$$

where $T_{e,ref}$ = reference external temperature (in °C)

T_{today} = arithmetic average of today's maximum and minimum external temperature (°C)

$T_{today-1}$ = arithmetic average of yesterday's maximum and minimum external temperature (°C)

$T_{today-2}$ = arithmetic average of maximum and minimum external temperature of 2 days ago (°C)

$T_{today-3}$ = arithmetic average of maximum and minimum external temperature of 3 days ago (°C).

That method has been set up for use in different building types. However, it must be interpreted with care when the focus is on special zones such as bathrooms and bedrooms. In case of rooms with office-like activity levels and clothing values varying from 0.5 to 2.0 clo (including added values to account for the effect of chairs or sofas) it can be used for a residential context as well. Also Nicol and McCartney [31] have set up a short term relationship for activity levels and clothing values in the same range. In task 3 of their SCATS project, they developed an adaptive algorithm for comfort temperatures as a function of outdoor temperature. It resulted in the following equation for incorporating the outdoor temperature [32]:

$$T_{RM}^n = cT_{RM}^{n-1} + (1-c)T_{DM}^{n-1} \quad (1.2)$$

where T_{RM}^n = running mean external temperature on day 'n' (°C)
 T_{RM}^{n-1} = running mean external temperature on day 'n-1' (°C)
 T_{DM}^{n-1} = mathematical daily average external temperature on day 'n-1'
(°C)
 c = a constant.

The constant was derived from empirical field study data in offices and public buildings in different European countries, resulting in a value of 0.8. The format of Eq. (1.2) does express a short term relation with the external conditions.

In the ATL method, more emphasis is given on more recent weather data, as can be seen by comparing Eq. (1.1) with the elaborated equation of T_{RM}^n , given by Eq. (1.3):

$$T_{RM}^n = 0.2T_{DM}^{n-1} + 0.16T_{DM}^{n-2} + 0.128T_{DM}^{n-3} + 0.1024T_{DM}^{n-4} + \dots \quad (1.3)$$

As the literature shows that also the current outdoor condition is of importance ([33], [34]), the ATL-calculation, $T_{e,ref}$, is preferred. The difference will, however, be small in cases of moderate climates. The ease of implementation in a particular BES program might therefore be decisive.

1.3.3 Indoor temperature characterization

The indoor temperature that characterizes the thermal sensation of the occupants is the operative temperature. Operative temperature is defined as the uniform temperature of a radiantly black enclosure with standard air velocity in which an occupant would exchange the same amount of heat by radiation and convection as in an actual non-uniform environment.

For indoor activities in dwellings, an average 30% of the metabolic heat is emitted through sweat secretion, breathing and perspiration [35]. In order to achieve a body in thermal equilibrium, the remaining 70% should be emitted by convective heat

exchange with the zonal air and radiant exchange with the surroundings. Based on the body's heat balance, the operative temperature can thus be defined as a sum of a certain percentage of air temperature and percentage of surface temperature⁷ of the enclosure.

Different percentages can be found in the literature, Marret determines the percentage of air temperature to be 41% [36], while Hens mentions 55% [35]. The former being closer to the findings of Kurazumi et al. [37] based on the results of their extended measurements. It should be noted though, that the percentages depend on factors as how the body is positioned, which body parts can exchange heat, as well as on the parameters in the heat balance equation, i.e. parameters such as air velocity, relative humidity and activity. Based on engineering judgement, a 50/50 split will be used in the current analysis.

1.4 The three different zones

1.4.1 Bathroom

The bathroom has a critical lower limit defined as the coldest temperature that is acceptable to a nude, wet body. However, once dry and dressed the person must still feel comfortable. A similar wide range of wet, nude and dressed persons in the same zone can be found in a swimming pool. Lammers [38] describes this situation, indicating three groups of occupants: the drying swimmers (persons with skin wetness of 20%), the superintendant and the spectators. Seven male persons showering and drying afterwards were tested on skin temperature and evaporative losses. Lammers then applies a heat balance method to end up with comfort operative temperatures between 23°C and 30°C for the dry swimmer and 27°C to 35°C for the wet swimmer.

Temperatures in the same range as the above mentioned 23°C to 30°C range, can be found in Tochihara et al. [39] and Zingano [40] both especially focussing on bathrooms. The former tested 12 male students in Japan ending up with values

⁷ The sensed surface temperature depends on the position and orientation of the person compared to the specific surface as well as on material properties of that surface. This is expressed by the viewfactor [2].

between 23°C and 30°C. They compared their test results with the values they found in various literature sources. The latter provided 20 families in Malawi with mercury-in-glass thermometers leading to 275 data points, with a neutral temperature of 24.6°C. However, the measurements are not coupled to comfort judgements and thus do not necessarily reflect the comfort temperatures.

As the condition of being wet and uncovered is limited in time, in most cases the body will either be covered, or uncovered but dry. For the latter condition both above mentioned comfort studies of Lammers [38] and Toshihara et al. [39] indicate a comfort range of 23°C to 30°C as is shown by the semi-transparent grey zone in Figure 1.2. Toshihara et al. [39] mention 26°C to be comfortable for a bathwater-temperature of 40°C.

Bathrooms are used for more than bathing: activities such as hair styling, teeth brushing and putting on make-up are generally carried out once dressed. So the bathroom comfort temperature will be influenced by the seasonal dependent clothing (either nightwear, either daywear) and the metabolic rate of the performed tasks. Therefore, the here suggested bathroom neutral temperature is a consensus between the comfort range for the naked and the dressed occupants.

For the comfort range of the dressed occupants, the ATL-methodology [23] is used. Figure 1.2 shows these comfort ranges for a variation of PPD-values.

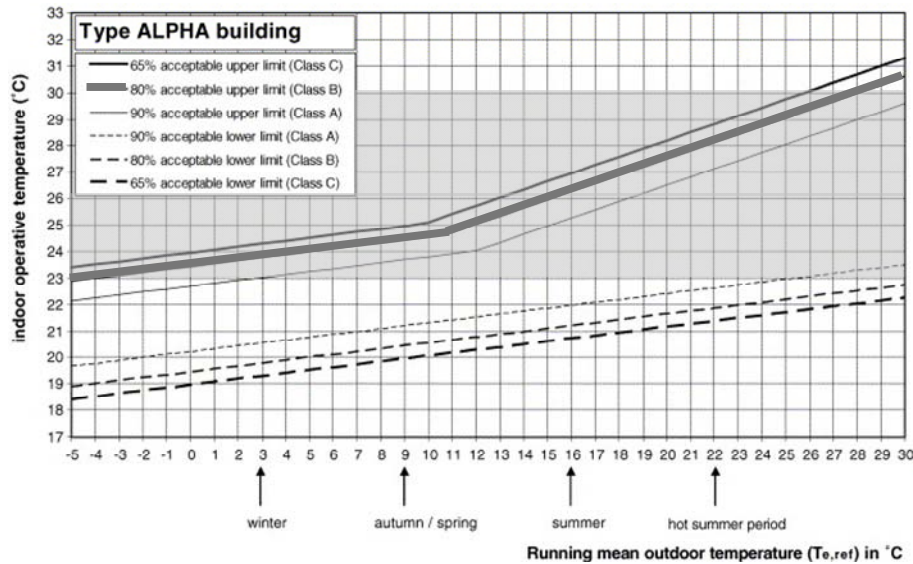


Figure 1.2: Temperature limits as a function of the outdoor temperature $T_{e,ref}$ (Eq. (1.1)) for different levels of acceptability (10% PPD defines a class A, 20% PPD a class B and 35% a class C) for an alpha building. This is for the general case of persons dressed according to the season and performing office-like activities. The semi-transparent grey box indicates the comfort range for the dry naked occupants according to Lammers [38] and Toshihara et al. [39]. The thick grey line indicates the bathroom comfort temperature as determined in the current dissertation. Adapted from [22].

The upper-value of the 80% acceptability range for the dressed case, indicated by the thick grey line in Figure 1.2 results in a bathroom temperature that is within the comfort range for the undressed occupants for all but severe winterdays and extreme summerdays. As the tests of Lammers and Toshihara et al. were not performed for such conditions, a minor deviation from the comfort zone they determined is here accepted. Therefore, the neutral temperature for the bathroom is here defined as the above mentioned 80% PPD curve of the ATL-method. More experimental data for non-average ambient conditions might result in a further refinement of the proposed neutral temperatures.

The resulting equations for the bathroom neutral temperatures T_n (°C) are given by:

$$T_n = 0.20 \cdot T_{e,ref} + 22.65^\circ\text{C} \quad \text{for} \quad T_{e,ref} < 11^\circ\text{C} \quad (1.4)$$

$$T_n = 0.31 \cdot T_{e,ref} + 21.44^\circ\text{C} \quad \text{for} \quad T_{e,ref} \geq 11^\circ\text{C} \quad (1.5)$$

1.4.2 Bedrooms

The theoretical analysis of Maeyens et al. [41] describes the effect of a decreasing body temperature and metabolism on *summer* comfort temperatures in bedrooms. Considering the calculation of the neutral or comfort temperature with any heat balance model, this would result in higher comfort temperatures. The authors however, mention the absence, also described in other works, of adaptation to low or high temperatures in bedrooms. According to Maeyens et al., the explanation offered by Parmeggiani is that physiological and behavioural adaptation is limited during sleep.

Maeyens et al. suggest using the comfort equation of Fanger, referred to above, to calculate the comfort or neutral temperature and define the input parameters as:

- Metabolic rate of sleeping: 0.7 met
- Clothing index (sleepwear, sheets, mattress and pillow): 0.8 clo
- Relative humidity: 55%
- Air speed: 0.05 to 1 m/s

That the Fanger equation cannot be applied in all cases has been clearly explained above. Therefore, the validity of this equation is checked comparing the above stated parameter values with the results of the parametric analyses as given in [10]. This last publication mentions for each variable a range of application, more restricted than what is given in ISO 7730. It turns out that all parameter estimates of Maeyens et al. [41] meet even the 90% acceptability requirements, except for the metabolic rate. The latter is just outside the range considered in that publication.

Applying the Fanger equation with these assumptions results in a summer comfort temperature estimate of 26.4°C, with a maximum of 27.5°C (PMV +0.5). This is close to the maximum temperature of 26°C suggested by CIBSE [42]. CIBSE shows the results of data collected in the UK by Humphreys [43], indicating the quality of

sleep as a function of the bedroom temperature. A steep drop in quality can be seen for bedroom temperatures above 24°C. Both this CIBSE Guide A, as well as the ASHRAE 55-2004 indicate that higher bedroom temperatures can be accepted if a fan is used: ASHRAE indicates an acceptable increase of up to 3°C.

Figure 1.3 shows the bedroom temperatures in a recent monitoring campaign in 39 Belgian houses, where monitoring periods varied from 6 months to 2 years ([44], [45]). The daily mean bedroom temperature is shown as a function of $T_{e,ref}$ (as introduced in Eq. (1.1) above). The aim of the research was not to investigate thermal comfort, but to gather data on the actual situation in Belgian dwellings. Therefore, it should be interpreted with care.

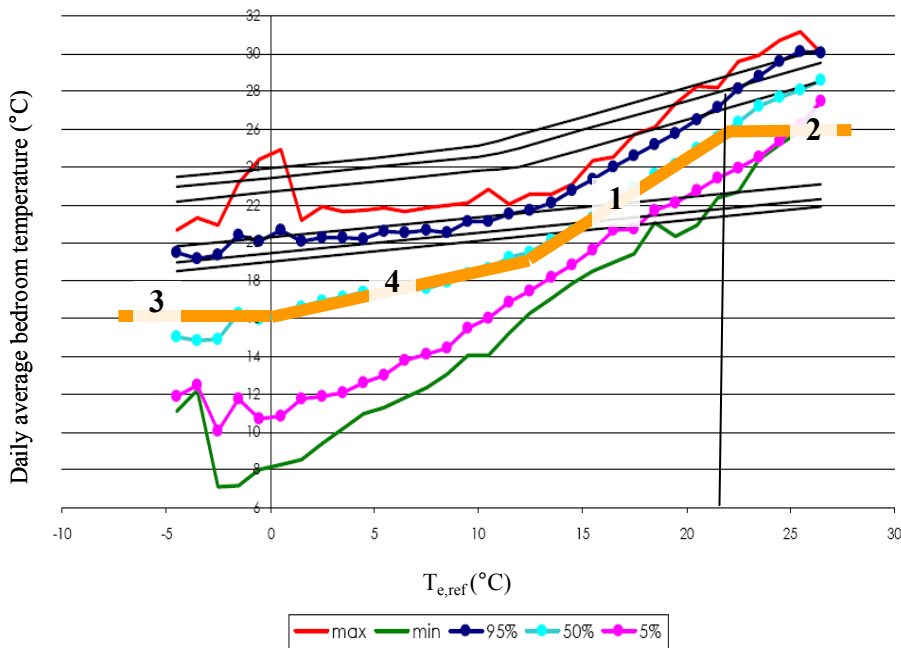


Figure 1.3: Daily average bedroom temperature in Belgium as function of $T_{e,ref}$. The graph shows minimum, maximum, 95-, 50-, and 5-percentiles (adapted from [45]). The thick orange line indicates the curve defined in current work. The black curves indicate the ATL 90-, 80- and 65-acceptability limits.

Based on a questionnaire survey for indoor thermal sensations during summer conditions in general, Maeyens et al. [41] found up to 50% of respondents complained about uncomfortably warm bedrooms (comparable with a PMV of 1 or more). 2/3rd of these complaints were on evening, night or morning temperatures.

The above given figure shows the daily mean bedroom temperature, which will generally be higher than the temperature during sleeping. This in fact highlights the contrast between the summer comfort temperature Maeyens calculated (i.e. 26.4°C) and the observations shown in that Figure 1.3, where only a minority had a ventilation system. This could be explained partly by Maeyen's underestimation of the clothing value of the bedding [46] as well as the required corrections to Fanger's conventional PMV-formula when evaluating thermal comfort in warm environmental conditions [20]. As no detailed information is available on bedroom temperatures during occupancy only, the 50-percentile curve is here accepted as representing the neutral temperature for summer conditions, indicated by the orange line segment 1 in Figure 1.3. However, the value of 26°C, indicated by CIBSE as the limit in the absence of an elevated air speed, is set here as the upper limit. It is indicated by the orange line segment 2 in Figure 1.3.

The *winter* comfort temperature for bedrooms, indicated by CIBSE, is 17°C [42]. Chalkey and Cater [47] indicate comfort temperatures of 15 to 17°C, but they do not give any reference for that. Humphreys [43] shows with his measurements in dwellings good sleep quality, even for bedroom temperatures as low as 12°C. However, Collins [48] and Hartley [49] indicate the World Health Organisation's bedroom temperature limit of 16°C, because of a decreasing resistance to respiratory infections once below this temperature.

For the heating season, a strong correlation exists between the temperatures in bedrooms also used for other activities (e.g. watching TV, homework, etc.) and the living room temperature. These bedrooms, requiring temperatures in accordance to the activity level and clothing value during these activities, are represented by the 95-percentile curve in Figure 1.4, almost equal to the median of the living room temperatures, measured during the same monitoring campaign, at least for the heating season days with mean outdoor temperatures below 15 °C (as shown in Figure 1.4 below). The other bedrooms, used for sleeping only, are often not heated, in some cases resulting in cold to very cold conditions [50], [51].

The course of the bedroom's neutral temperature, as a function of the outdoor temperature, will therefore differ from the shape shown in Figure 1.2: the neutral bedroom temperature is limited in both summer and winter conditions. The above given upper limit as defined by CIBSE [42] will be taken for the summer estimate, while in this dissertation the WHO value of 16°C will be accepted as minimum of the neutral temperature for winter conditions (indicated by the orange line segment 3

in Figure 1.3). According to the 50-percentile curve, this corresponds to reference outdoor temperatures of 0°C and lower. For somewhat warmer ambient conditions, the 50-percentile curve (orange line segment 4 in Figure 1.3) defines the trend, as was the case for summer conditions. For moderate winter-conditions, i.e. a reference outdoor temperature around 7°C, the resulting neutral bedroom temperature around 18°C is confirmed as comfortable by the data of a UK study on residential thermal comfort [52].

The slope of the 50-percentile is different for cold versus warm conditions. The intersection of the two curves is calculated at a reference outdoor temperature of 12.6°C. For the case of no elevated air velocity in summer, the equations derived in this dissertation are given by:

$$T_n = 16^\circ C \quad \text{for} \quad T_{e,ref} < 0^\circ C \quad (1.6)$$

$$T_n = 0.21T_{e,ref} + 16 \quad \text{for} \quad 0^\circ C \leq T_{e,ref} < 12.6^\circ C \quad (1.7)$$

$$T_n = 0.69T_{e,ref} + 9.95^\circ C \quad \text{for} \quad 12.6^\circ C \leq T_{e,ref} < 23.3^\circ C \quad (1.8)$$

$$T_n = 26^\circ C \quad \text{for} \quad T_{e,ref} \geq 23.3^\circ C \quad (1.9)$$

It should be emphasized that the so-derived formulas might result in low values for the bedrooms. The reason is that in bedrooms used for sleeping only, the thermal comfort should in fact be evaluated for a person in bed, thus on a mattress and covered by beddings. Furthermore, it is common practice in Belgium to not heat the bedroom. The lower bedroom temperatures are generally compensated by better insulating nightwear and bedding.

1.4.3 Other rooms

Kitchen, living room and study room have physical activity levels comparable to those in offices, or just slightly more intensive: reclining, reading the newspaper, cooking etc. have metabolic rates in the range of 0.8 met to 1.4 met, comparable to office or general laboratory work. More adaptive options, however, are available (changing activity, going to another room, drinking cold or warm drinks, changing

garments -absence of dress codes -, opening windows and doors for ventilation and cooling, etc.). The neutral temperature can therefore be more dependent on the outside climate than what is generally accepted in offices.

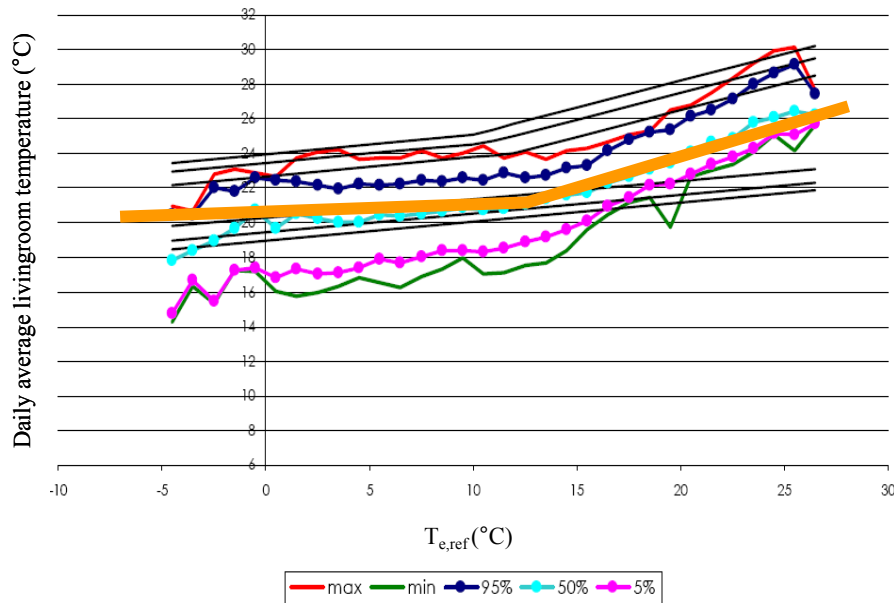


Figure 1.4: Daily average living room temperature in Belgium as function of $T_{e,ref}$: minimum, maximum, 95-, 50-, and 5-percentiles (adapted from [45]). The thick orange lines indicate the curve defined in current work. The black curves indicate the ATL 90-, 80- and 65-acceptability limits.

In the SCATS project [31], Nicol and McCartney developed an adaptive algorithm for comfort temperatures in terms of outdoor temperature. The relationships are based on empirical field study data of offices and public buildings in different European countries. The study included both naturally ventilated and air conditioned buildings, as well as buildings equipped with mixed systems. Their equations indicate, by a constant comfort temperature for lower external temperatures and an increasing comfort temperature for increasing ambient temperatures, that occupants are less adaptive to cold than to heat. This is in agreement with Jokl and Kabele [12] and with the observations in Belgian dwellings as shown in Figure 1.4. This is also confirmed by the ATL-method as the slope of the comfort ranges for the alpha buildings is less steep in colder outdoor conditions than that for warm weather; as can be seen in Figure 1.2 and as indicated in Figure 1.4. As the ATL-curve for the

alpha-buildings is set up with data for non-air-conditioned buildings, it is in fact better dealing with the presence of more adaptive possibilities.

Humphreys and Hancock [15] mention that temperature adaptation also occurs in response to indoor conditions, whereby people feel colder at the end of the day when the indoor temperature is kept constant. A statement that is confirmed by Oseland [53] for offices, but not for homes. The reason might be declining metabolic rates after a day sitting quietly for the office case, while at home the variation in activity intensity will probably be higher. Oseland also demonstrated experimentally that people feel warmer in their home than they do in their office at the same temperatures. Oseland mentions as possible reason the presence of furnishings (i.e. carpet, wall paper and furniture), as people tend to judge rooms with such features as being warmer. The people participating in his field study reported comfortable winter operative temperatures of 21.8°C and 20.4°C for office and home respectively. The latter value is indirectly confirmed by the data of Figure 1.4. The data of this figure give a daily mean indoor temperature and thus include night set-back effects. Translating that effect to a temperature during occupancy would result in winter comfort values close to the ones determined by Oseland in his experiment in the UK.

For their Belgian field study on summer comfort, Maeyens et al. [41] mention that 10% of the people judged the temperature in the living room on warm summer days to be uncomfortably high, comparable to 3 on the PMV scale [43]. The data shown in Figure 1.4, from another Belgian study [45], were measured around the same period. Combining these data with the conclusion of Maeyens et al., results in defining a neutral temperature that partly corresponds with the 50-percentile curve in Figure 1.4. The 50-percentile curve of Figure 1.4 agrees well with the 90% acceptable zone of the ATL-method for summer outdoor conditions. However, for winter conditions, the ATL 90-percentage acceptability indicates higher indoor temperatures. The reason is that the measured Belgian data are daily mean indoor temperatures; the effect of night set backs is thus incorporated. Therefore, the neutral temperatures during the heating season should not be the 50-percentile values. They should nevertheless start from the comfort values as observed by amongst other Oseland [54], and converge to the 50-percentile curve of Vandepitte et al. [45] at $T_{e,ref}$ equal to 12.5°C.

Therefore, in this dissertation, the concluding neutral temperatures for the zones with office-like activity level are defined by Eqs. (1.10) and (1.11). The so-defined

relations agree well with the comfort measurements in a wide range of buildings, analyzed by Nicol and Humphreys [55]. The buildings in that study were located in different climates worldwide and the data gathered spread a range of mean outdoor temperatures varying from below -20°C to above 30°C .

$$T_n = 20.4 + 0.06 \cdot T_{e,ref} \quad \text{for} \quad T_{e,ref} < 12.5^{\circ}\text{C} \quad (1.10)$$

$$T_n = 16.63 + 0.36 \cdot T_{e,ref} \quad \text{for} \quad T_{e,ref} \geq 12.5^{\circ}\text{C} \quad (1.11)$$

1.5 Local thermal discomfort

Local thermal discomfort could be caused by a non-uniform temperature distribution in the zone. Although Fanger [2] summarized the effect in an additional index, the lowest possible percentage of dissatisfied (LPPD (%)), it is generally treated differently in international standards on thermal comfort. Both ISSO 7730 [21] and ASHRAE 55 [8] discuss local thermal discomfort for several possible causes separately:

- draft
- radiant temperature asymmetry
- vertical air temperature difference
- floor surface temperature.

The discomfort for each of these causes is expressed as percentage of dissatisfied, PD (%). As for the LPPD, the PD should not be added to the PPD, as it will often be the same persons being sensitive to different types of discomfort.

Adaptive standards as the ATL [24] do not specifically mention calculation methods for the effect or decrease in comfort due to local thermal discomfort. However, there is no reason to not accept the methodology as outlined in the standards ISSO 7730 and ASHRAE 55, it might be somewhat conservative for environments with a wide range of adaptive options [14], [56].

1.6 Temperature variations

The above defined neutral temperatures will not be met continuously. A residential building is a dynamic system; the outdoor environment, the internal heat gains and the ventilation rates are just some of the constantly changing parameters influencing the indoor temperature. This dynamic character, obviously, is the most important reason to use BES programmes.

The real indoor temperature will be a value close to, or fluctuating around the neutral temperature. If these fluctuations are limited, they will not induce excessive complaints. These limitations are often formulated as restrictions on both the amplitude and the period of the variation ([2], [8], [21], [27]). Notwithstanding their mostly strictly mathematical formulation, often in the format as given by Eq. (1.12), implementing these restrictions in a general format in BES-programmes is not obvious.

$$\Delta T_{pp}^x < a \quad (1.12)$$

where ΔT_{pp} = the peak to peak temperature variation per time-interval ($^{\circ}\text{C}/\text{h}$)
 x = a constant exponent
 a = a constant $\left(\frac{^{\circ}\text{C}}{\text{h}}\right)^x$

The numerical result for the simulated thermal comfort could be influenced by the simulation time step, which can be a fixed user-defined value or can be selected to vary during a simulation as for example in *ESP-r*. When the simulation time step increases, temperature variations within smaller periods will not be taken into account. However, it is well known that increasing the simulation time step will negatively influence the quality of the numerical result.

Nevertheless, in the current dissertation, the indoor temperature fluctuations are evaluated. This can be done as the simulation time step for the evaluation of potential heat emitter/absorber elements is small and different potential elements are evaluated using exactly the same timestep. The limitations for amplitude and cycle frequency, implemented in the tool for evaluation of emitters/absorbers, are as defined by ASHRAE [8]. This standard suggests that for cyclic temperature variations, there are no restrictions if the peak to peak temperature difference does

not exceed 1.1K. If above this value, the temperature change shall not exceed 2.2K/h. For temperature drifts or ramps (monotonic steady change) the standard gives even more restricted limits. However, in his overview on transient thermal comfort conditions, Hensen [27] concludes that there is no evidence to not accept the 1.1K-2.2K/h limit for temperature drifts or ramps as well. Hensen further gives the remark that for homes and even offices, this limit might be conservative.

1.7 Acceptable thermal comfort ‘regions’ for residential buildings

The temperature ranges encountered in most standards ([2], [8], [21]), are symmetrically distributed around the neutral temperature:

$$T_n \pm a \quad (1.13)$$

with a = constant (°C)

As described by Henze et al. [57], the constant a is independent of the season with, for a 90% acceptability, values of 1.5 °C for ISO 7730 [21] and 2.5 °C for prEN 15251 [58]. That is in agreement with the symmetrical shape of the relation PMV-PPD, as shown in Figure 1.1. In their enquiries, Humphreys and Hancock [15], however, found an asymmetric relation between the desired thermal sensation and the actual sensation, as can be seen in Figure 1.5. The data were collected at university lectures and in selected dwellings throughout the UK. Such an asymmetry showing a preference for warmer environments is also described by Mayer [59]. His conclusions are based on results of earlier thermal comfort studies of the Fraunhofer Institut für Bauphysik, in which some 100 persons were involved. He gives no details on those comfort studies but emphasizes that his conclusions are confirmed by field study data of other researchers.

The asymmetry is further confirmed by the analysis of field study data by Fountain et al. [60]. They concluded that people’s preferences for non-neutral thermal sensations are common, that they vary asymmetrically around neutrality and that, in several cases, they are influenced by season. De Dear et al. [28] consider this idea of outdoor dependent temperature ranges. However, they observed no statistical significance in the 95% confidence level, regardless of building type or acceptability

level. Seasonal dependency can thus not be proven and, in this dissertation, the comfort band around the neutral temperature is thus considered having a constant width, independent of the season.

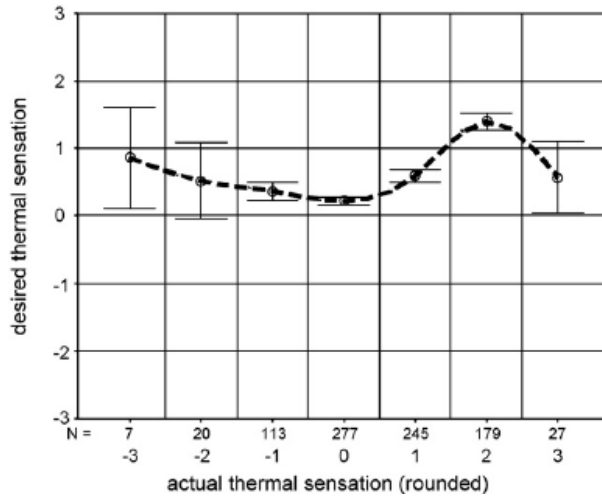


Figure 1.5: Dependence of the mean desired thermal sensation (-3 to +3 on adapted ASHRAE scale) on the actual sensation (similar scaling, with also the indication of the distribution of the test persons (N)) [15]

To account for both the enhanced sensitivity for cold versus heat and the non seasonal dependency, the following format for the temperature ranges is suggested in this dissertation:

$$T_{upper} = T_n + w\zeta \quad (1.14)$$

$$T_{lower} = T_n - w(1 - \zeta) \quad (1.15)$$

with T_{upper} = upper limit of comfort band (°C)

T_{lower} = lower limit of comfort band (°C)

w = width of comfort band (°C)

ζ = constant (≤ 1)

In the ASHRAE RP 884 study, De Dear and Brager [29] observed that occupants of residential buildings showed a low sensitivity to indoor temperature changes; the

gradient of their thermal sensation votes with respect to indoor operative temperature turned out to be 1 vote for every 3°C to 5°C change in temperature. Values in the same range are encountered in work of Oseland [54] and of Van der Linden et al.[23]. This, it is concluded in present analysis, defines the width of the comfort zone, the value of w in Eqs. (1.14) and (1.15); 5°C in case of 90% acceptability. Oseland reported a 7°C comfort band width in case of 80% acceptability.

This so defined width of the comfort band must thus be asymmetrically split around the neutral temperature. The thermal sensation at the neutral temperature leads to a value of 0 on the adapted 7 points ASHRAE scale (-3 to +3). From Figure 1.5 it is clear that the desired sensation in that case is an average 0.2 above neutral. Aiming a 10% PPD quality, this 0.2 represents on average 20% of the occupants. These 20% desire a warmer environment, on top of the 50% who already preferred a sensation in the 0 to 0.5-range on the ASHRAE-scale. This causes a 70%-30% split for the temperature band around neutral, resulting in ζ equal to 0.7.

Additionally, some extreme temperatures will cause restrictions. The above stated limit of 16°C for the bedroom is to be respected. For all other rooms the absolute lower limit is set to 18°C. This value is often encountered in the literature ([34], [61], [62]). The upper limits differ depending on the room. While the stringent limit of 26 °C for warm outdoor conditions is accepted for bedrooms in case of no elevated air speed, bathrooms and rooms with office like activities can have acceptable indoor temperatures of up to 30 °C in a 90% acceptability level and even around 31°C for a 80% level [24] during extreme warm summer outdoor conditions⁸.

The following restrictions must therefore be added to the statements of Eqs. (1.14) and (1.15):

for bedrooms:

⁸ These temperatures might seem high. It should be noted that the exact value of the highest acceptable temperature in a certain (residential) building will depend on a wide range of (adaptive) options such as the possibility for window opening and the possible discomfort (acoustics, air quality) associated with it as well as access to a garden or terrace.

$$T_{upper} = \min(26^{\circ}C, T_n + w\zeta) \quad (1.16)$$

$$T_{lower} = \max(16^{\circ}C, T_n - (1-w)\zeta) \quad (1.17)$$

for bathrooms and other rooms:

$$T_{upper} = \min(T_n + w\zeta, 30^{\circ}C) \quad (1.18)$$

$$T_{lower} = \max(18^{\circ}C, T_n - w(1-\zeta)) \quad (1.19)$$

1.8 Summary and conclusion on thermal comfort

Most BES programmes currently have the option to evaluate thermal comfort with the conventional criteria. These evaluation mechanisms have been set up for constant, office-like environments. Based on the literature, present analysis shows that because of the wide range of possibilities to adapt to the thermal environment, conventional algorithms are not adequate in case of residential buildings.

Thermal comfort in residential buildings shows a strong dependency on weather data, more specific on recent outdoor temperatures. Therefore the relations set up in this dissertation link the comfort temperatures to a form of outdoor temperature.

It is stated here that a residential building can be split up in three zones with markedly different thermal comfort requirements; bathroom, bedroom and other rooms. For each of these zones, the neutral temperatures, defined in the present analysis, are based on measurements described in the literature and in that sense do consider the special case of each of the zones. For the bathroom, the analysis is based on the comfort of both wet naked and dry clothed people with limited activity level. The relations for the bedrooms have been set up based on a theoretical study that applies the Fanger equation to the special case of sleeping covered bodies. It is combined with measurement data on Belgian bedrooms. For the other zones with activity levels close to those in offices and laboratories, the defined relation is set up comparing measurement data with the ATL method.

The resulting curves for the comfort temperatures, with a corresponding neutral thermal sensation, show a steeper slope for warmer outdoor conditions. This reflects that people adapt more easily to heat than they do to cold.

The asymmetric comfort band around this neutral temperature is set for the same reason. However, both the neutral temperatures and the comfort bands are restricted by upper and lower limits. In this dissertation, these limits have been defined based on information of the World Health Organisation and available experimental data. It must be emphasised, however, that currently there are only limited data available on residential thermal comfort. By including, or sometimes being restricted to office-related data, it is probable that the relations defined in this dissertation might be somewhat conservative.

The resulting correlations between indoor and outdoor temperature are presented in an algorithmic way to facilitate implementation in any BES code.

As stated in the introduction, the definition of residential thermal comfort is the first step in determining optimal heat/emission absorption elements. As this is now defined, the next step is to implement a structure that allows modelling any heat emission/absorption within a building. This is discussed in the next chapter.

References

- [1] L. Peeters, R. De Dear, J. Hensen, W. D'haeseleer, 2008, Thermal comfort in residential buildings: Comfort values and scales for building energy simulation, *Applied Energy*, vol. 86, pp. 772-780
- [2] P. Fanger, 1970, *Thermal Comfort: Analysis and applications in environmental engineering*, McGraw-Hill Book Company, United States. ISBN 0-07-019915-9
- [3] T. Doherty, E. Arens, 1988, Evaluation of the physiological bases of thermal comfort models, *ASHRAE Transactions* vol. 94, pp. 1371-1385
- [4] M. Humphreys, J. Nicol, 1998, Understanding the adaptive approach to thermal comfort, *ASHRAE technical bulletin*, vol. 14, pp. 1-14
- [5] ESRU, 2007, Released version 11.4, http://www.esru.strath.ac.uk/Programs/ESP-r_CodeDoc/esrures/comfort.F.html
- [6] T. Welfonder, M. Hiller, S. Holst, A. Knirsch, 2003, Improvements on the capabilities of TRNSYS, Eight International IBPSA Conference, Eindhoven, The Netherlands, August 11-14, 2003, pp. 1377-1384
- [7] O. Kalyanova, P. Heiselberg, 2007, Comparative Validation of Building Simulation Software: Modeling of Double facades; Final Report, IEA ECBCS Annex 43/SHC Task 34, Validation of Building Energy Simulation tools, Subtask E
- [8] ASHRAE 2004, ANSI/ASHRAE 55: Thermal Environmental Conditions for Human Occupancy, American Society of Heating, Refrigerating and Air-conditioning Engineers, Inc. Atlanta, USA
- [9] B. Jones, 2000, Capabilities and limitations of thermal models, Smart Controls and Thermal Comfort Project, Final Report (Confidential), Oxford Brookes University
- [10] M. Humphreys, J. Nicol, 2002, The validity of ISO-PMV for predicting comfort votes for everyday thermal environments, *Energy & Buildings*, vol. 34, pp. 667-684
- [11] J. Stoops, 2004, A possible connection between thermal comfort and health, paper LBNL 55134, Lawrence Berkeley National Laboratory, University of California
- [12] M. Jokl, K. Kabele, 2007, The substitution of comfort PMV values by a new experimental operative temperature, *Electronic proceedings of Clima 2007 WellBeing Indoors*, Helsinki, Finland
- [13] G. Brager, R. De Dear, 1998, Thermal adaptation in the built environment: a literature overview. *Energy & Buildings*, vol. 27, pp. 83-96
- [14] S. Kurvers, 2007, Technical university of Delft, The Netherlands, personal communication.
- [15] M. Humphreys, M. Hancock, 2007, Do people like to feel 'neutral'? Exploring the variation of the desired thermal sensation on the ASHRAE scale, *Energy & Buildings*, vol. 39, pp. 867-874

- [16] E. Shove, 2004, Social, architectural and environmental convergence, Environmental Diversity in Architecture, Koen Steemers, Mary Ann Steane (Eds).
- [17] M. Holmes, J. Hacker, 2007, Climate change, thermal comfort and energy: Meeting the design challenges of the 21st century, Energy & Buildings, vol. 39, pp. 802-814
- [18] D. Fiala, K. Lomas, 2001, The dynamic effect of adaptive human responses in the sensation of thermal comfort, Moving Thermal Comfort Standards into the 21st Century, Windsor, UK, Conference Proceedings, pp. 147-157
- [19] N. Baker, M. Standeven, 1996, Thermal comfort for free-running buildings, Energy and Buildings, vol. 23, pp. 175-182
- [20] P. Fanger, J. Toftum, 2002, Prediction of thermal sensation in non-air-conditioned buildings in warm climates, Proceedings of the 9th International Conference on Indoor Air Quality and Climate, Monterey, California, June 30- July 5
- [21] ISO, 2005, ISO 7730; Ergonomics of the thermal environment – Analytical determination and interpretation of thermal comfort using the PMV and PPD indices and local thermal comfort criteria, International Organisation for standardization, Switzerland
- [22] B. Olesen, K. Parsons, 2002, Introduction to thermal comfort standards and to the proposed new version of EN ISO 7730, Energy and Buildings vol. 34, pp. 537-548
- [23] A. van der Linden, A. Boerstra, A. Raue, S. Kurvers, R. De Dear, 2006, Adaptive temperature limits: A new guideline in the Netherlands. A new approach for the assessment of building performance with respect to thermal indoor climate, Energy and Buildings, vol. 38, pp. 8-17
- [24] S. Kurvers, A. van der Linden, A. Boerstra, A. Raue, 2005, Adaptieve Temperatuurgrenswaarden (ATG), ISSO 74: een nieuwe richtlijn voor de beoordeling van het thermisch binnenklimaat, Deel 1: Theoretische achtergronden, TvvL Magazine, juni 2005 (In Dutch)
- [25] K. Rehdanz, 2007, Determinants of residential space heating expenditures in Germany, Energy Economics, vol. 29, pp. 167-182
- [26] E. Sardanou, 2008, Estimating space heating determinants: An analysis of Greek households, Energy and Buildings, vol. 40, pp. 1084-1093
- [27] J. Hensen, 1990, Literature review on thermal comfort in transient conditions, Building and Environment, vol. 25, pp. 309-316
- [28] R. de Dear, G. Brager, 1997, Developing an adaptive model of thermal comfort and preference; Final Report Ashrae RP-884, Macquarie Research Ltd., Macquarie University, Sydney, Australia
- [29] R. De Dear, G. Brager, 1998, Developing an adaptive model of thermal comfort and preference, ASHRAE transactions, vol. 104 (1. a), pp. 145-167
- [30] C. Morgan, R. de Dear, 2003, Weather, clothing and thermal adaptation to indoor climate, Climate Research, vol. 24, pp. 267-284
- [31] F. Nicol, K. McCartney, 2000, Smart Controls and Thermal comfort Project: Final Report (Confidential), Oxford Brookes University

- [32] K. McCartney, J. Nicol, 2002, Developing an adaptive control algorithm for Europe: Results of the Scats project, *Energy and Buildings*, vol. 34, pp. 529-532
- [33] R. De Dear, G Brager, 2002, Thermal comfort in naturally ventilated buildings: revisions to ASHRAE Standard 55, *Energy & Buildings*, vol. 34, pp. 549-561
- [34] K. Parsons, 2002, The effect of gender, acclimation state, the opportunity to adjust clothing and physical disability on requirements for thermal comfort, *Energy and Buildings*, vol. 34, pp. 593-599
- [35] H. Hens, 2003, *Toegepaste Bouwfysica 1: Randvoorwaarden, prestaties, materiaaleigenschappen*, ACCO, Leuven, Belgium, ISBN 90-334-5511-0
- [36] D. Marret, 1981, *Qualite de la ventilation mecanique controlee; Influence du mode de chauffage sur le confort et les pertes thermique dans 'l habitat*, PhD thesis, Institut National Des Sciences Appliques De Lyon, France
- [37] Y. Kurazumi, et al., 2008, Radiative and convective heat transfer coefficients of the human body in natural convection, *Building and Environment*, vol. 43, pp. 2142-2153
- [38] J. Lammers, 1978, *Human factors, energy conservation and design practice*, Technical University of Eindhoven, the Netherlands, PhD thesis
- [39] Y. Tochihara, Y. Kimura, I. Yadoguchi, M. Nomura, 1998, Thermal responses to air temperature before, during and after bathing, *Proceedings of International Conference of Environmental Ergonomics*, San Diego, USA, pp. 309-313
- [40] B. Zingano, 2001, A discussion on thermal comfort with reference to bath water temperature to deduce a midpoint of the thermal comfort zone, *Renewable Energy*, vol. 23, pp. 41-47
- [41] J. Maeyens, 2001, *Ontwerpregels voor zomercomfort in woningen*, Master's thesis (Coach: H. Breesch, Promotor: A. Janssens), Department of Architecture and Urban Planning, University of Ghent, Belgium (In Dutch)
- [42] CIBSE, 2006, *Guide A: Environmental Design*, Chartered Institution of Building Services Engineers, London, ISBN 978-1-903287-66-8
- [43] M. Humphreys, 1979, The influence of season and ambient temperature on human clothing behaviour, *Indoor Climate*, Eds.: P. Fanger & O Valbjorn, Danish Building Research, Copenhagen
- [44] A. Janssens, A. Vandepitte, 2006, *Analysis of indoor climate measurements in recently built Belgian dwellings*, IEA annex 41, report n° A41-T3-B-06-10, University of Ghent, Belgium, department of Architecture
- [45] A. Vandepitte, 2006, *Analyse van binnenklimaatmetingen in woningen*, Masters thesis (Coaches: N. Vandenbossche, L. Willems, Promotor: A. Janssens), Department of Architecture and Urban Planning, UGent, Belgium (In Dutch)
- [46] Z. Lin, S. Deng, 2008, A study on the thermal comfort in sleeping environments in the subtropics – Measuring the total insulation values for the bedding system commonly used in the subtropics, *Building and Environment*, vol. 43, pp. 905-916

- [47] J. Chalkey, H. Cater, 1968, Thermal environment for the student of architecture, The Architectural Press LTD, London, ISBN 0-85139-635-6.
- [48] K. Collins, 1986, Low indoor temperatures and morbidity in the elderly, *Age and Ageing*, vol.15, pp. 212-220
- [49] A. Hartley, West Midlands Public Health Observatory: Health Issues; Fuel poverty, consulted online via www.wmpho.org.uk, December 2007
- [50] L. Peeters, J. van der Veken, H. Hens, L. Helsen, W. D'haeseleer, 2008, Control of heating systems in residential buildings; current practice, *Energy and Buildings*, vol. 40, pp. 1446-1455
- [51] K. Kiekens, 2007, Analyse en simulatie van installaties voor de gecombineerde productie van sanitair warm water en ruimteverwarming in lage energiewoningen, Master's thesis (Coach: L. Peeters, Promotor: L. Helsen), Applied mechanics and energy conversion, KULeuven, Belgium (in Dutch)
- [52] S. Hong, J. Gilbertson, T. Oreszczyn, G. Green, I. Ridley, 2008, A field study of thermal comfort in low-income dwellings in England before and after energy efficient refurbishment, *Building and Environment*, doi:10.1016/j.buildenv.2008.09.003
- [53] N. Oseland, 1995, Predicted and reported thermal sensation in climate chambers, offices and homes, *Energy and Buildings*, vol. 23, pp. 105-115
- [54] N. Oseland, 1994, A comparison of the predicted and reported thermal sensation vote in homes during winter and summer, *Energy and Buildings*, vol.21, pp. 45-54
- [55] J. Nicol, M. Humphreys, 2002, Adaptive thermal comfort and sustainable thermal standards for buildings, *Energy and Buildings*, vol. 34, pp. 563-572
- [56] R. de Dear, 2008, personal communication, Environmental and life sciences, Macquarie University, Sydney, Australia
- [57] G. Henze, J. Pfafferot, S. Herkel, C. Felsmann, 2007, Impact of adaptive comfort criteria and heat waves on optimal building thermal mass control, *Energy & Buildings*, vol. 39, pp. 221-235
- [58] prEN 15251, 2005, Criteria for the indoor environment including thermal, indoor air quality, light and noise, Beuth Verlag, Berlin, Germany
- [59] E. Mayer, 1998, Ist die bisherige Zuordnung von PMV und PPD noch richtig?, *KI Luft- und Kältetechnik*, vol. 12, pp. 575-577
- [60] M. Fountain, G. Brager, R. De Dear, 1996, Expectations of indoor climate control, *Energy & Buildings*, vol. 24, pp. 179-182
- [61] J. Healy, P. Clinch, 2002, Fuel poverty, thermal comfort and occupancy: results of a national household survey in Ireland, *Applied Energy*, vol. 73, pp. 329-343
- [62] M. Ubbelohde, G. Loisos, R. McBride, 2004, Comfort Reports: Advanced comfort criteria and adapted comfort & human comfort studies; section 1: advanced comfort criteria for ACC house, Davis Energy Group for the California Energy Commission

2 MODELLING BUILDING ENERGY SYSTEMS

The objective of any heating/cooling installation is to realise a satisfying thermal comfort in the volume of interest. The energy flux emitted by the heating/cooling equipment is far from the only source influencing the indoor climate. Various processes within and outside the volume of interest, interacting in a dynamic and complex manner, dictate the volume's thermal state. The heating/cooling system installed needs to react to this dynamically changing state and must guarantee the desired thermal comfort.

It is clear that modelling the heating/cooling installation to predict its in situ performance, makes sense only if the interaction with the volume of interest and its surroundings is accounted for. Different building energy simulation (BES) programs have been developed to take into account these dynamics.

To evaluate whether residential buildings require new developments in emission and production systems, the BES code ESP-r (Environmental Systems Performance,

Research version) has been extended with a rather abstract model for heating/cooling installations. The current account presents these new software developments. The thermal comfort algorithm, as defined in chapter 1, is incorporated in the new structure to determine the boundary conditions for the simulation.

2.1 Introduction

The thermal interactions between a building, the inhabitants and the environment are complex [1], [2]. Multilayered opaque and transparent structures are subject to constantly changing outdoor conditions: solar radiation, infiltration of fresh air and wind are just some of the outdoor sources affecting the indoor thermal environment. Within the building, air flows between zones as well as casual gains will cause additional fluctuations of the zonal heat load. These processes are shown in Figure 2.1. To ensure a thermally comfortable indoor environment, the heating/cooling system should compensate for possible temperature over- or undershoots caused by these casual gains and outdoor influences.

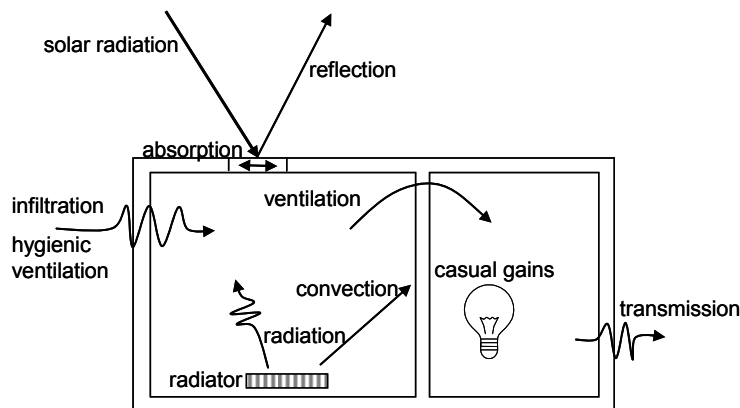


Figure 2.1: Some of the building energy flowpaths influencing the indoor thermal climate

To account for the complexities of these energy transfer processes occurring between the external environment, the indoor gains and the building itself, as well as among the various components and systems, building energy simulation (BES) is adopted as a standard technique [1], [3]. BES is a standard means used to analyse

the energy performance of a building as an integrated system. BES allows predicting the performance of a heating/cooling installation while still at the design stage and can thus lead to more energy efficient and comfortable buildings. New techniques can be evaluated by the use of BES, allowing to optimise their characteristics and to estimate the savings they might lead to. In that sense, *ESP-r* is used in the current research as an evaluation tool for the performance of a wide range of, rather abstract, heating/cooling systems. *ESP-r* analyses the building and its constituents simultaneously and in the transient domain [4]. All aspects of the model, building as well as plant, are considered as a collection of small finite volumes, between which energy and mass can flow. For each of these finite volumes, at each simulation time step, conservation laws can be applied.

These equations are passed on to the central numerical solver where they are regrouped in sub-sets, according to the physical process they represent. Several solvers specifically developed for each sub-set, work in tandem to solve the overall problem. The boundary conditions for this solution are provided by the climate data selected by the user and by user selected or defined control criteria [1], [5]. The software structure as explained above has been extended to represent the abstract heating/cooling installation in a (simple) straightforward way.

2.2 Status of *ESP-r* at project commencement

2.2.1 The structure of *ESP-r*

ESP-r uses a numerical discretisation technique by dividing a model into small volumes. Such a volume is named a control volume and is represented by a node. The conservation principles can then be applied to these control volumes and to the energy transfers between volumes in thermodynamic contact. In that way the resulting solution satisfies the conservation principles, independent of the number of control volumes [1], [2].

Simulating the thermal state of a building requires setting up the heat balances for all control volumes possibly affected by the relevant energy flows. This is called a *finite difference control volume heat balance approach* [6].

In case a more detailed analysis of fluid flows, distribution of physical properties within enclosed fluid volumes, or estimation of pressure losses is required the heat

balance approach is extended to incorporate the conservation of mass and momentum principles. This method is then termed a *control volume flux balance approach* [6].

Within *ESP-r* the control volume heat balance approach is applied at the building and plant level. The building level comprises the physical building structure and the thermal zones enclosed by that. The plant levels consist of all plant components. The level that considers the pressure driven flows, the fluid flow level, implies applying the control volume flux balance approach. A brief description of the basic physics with the characteristic equations for the different levels, focusing on energy and mass variations, will be given here. Next the operation of controls is described, followed by a discussion of the solution techniques. A more rigorous treatment can be found in Clarke [1], Underwood and Yik [2], Kelly [5], Beausoleil-Morrison [6], Aassem [7] and Hensen [8].

2.2.2 Basic physics in *ESP-r*

2.2.2.1 Building level

A building consists of a number of physically separated thermal zones, surrounded by the building fabric. A thermal zone is a volume of air enclosed by the physical limits of the zone, i.e. the internal and external walls. In case no detailed analysis of the state variables in the thermal zone is required, it is considered as one single volume symbolised by one single node. It is further referred to as a_i , i.e. air volume of zone i . The air is subject to a range of processes, influencing its thermodynamic properties, as can be seen in Figure 2.2.

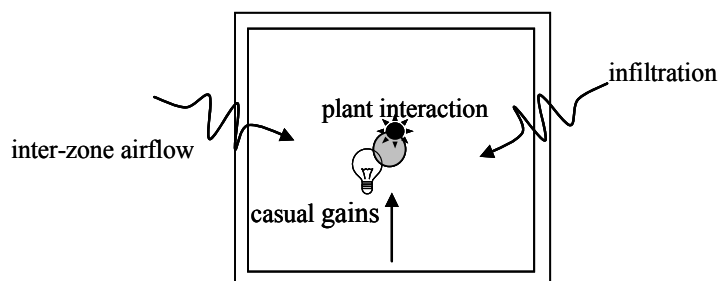


Figure 2.2: The heat balance of an air node symbolising a thermal zone.

These processes can be of three types:

1. Surface (s) to fluid (a) heat transfer (convection), $Q_{si,ai}$ (W),
2. Inter-zone airflow from zone j to zone i, $Q_{aj,ai}$ (W), or infiltration of fresh air from the exterior, $Q_{ext,ai}$ (W),
3. Casual gains $Q_{cas,i}$ (W) or possible plant component interactions, $Q_{pli,i}$ (W).

Radiant energy will be emitted straight to the surrounding surfaces and will thus not directly influence the energy processes in the air volume. The latter concerns only the energy gains that can be emitted by convection. Therefore, the overall energy balance of the node representing the air volume will only include the convective part of $Q_{cas,i}$ and $Q_{pli,i}$, given by $\alpha_i' Q_{cas,i}$ and $\alpha_i Q_{pli,i}$ (W). The fractions of convection, α_i' (-) and α_i (-), indicate the ratio of convective to overall heat transfer for the casual and plant gains respectively. The subscript i refers to the casual gain source i and plant component i¹. The radiant parts equal $(1 - \alpha_i') Q_{cas,i}$, and $(1 - \alpha_i) Q_{pli,i}$.

The overall heat balance for the air node thus results in:

$$\begin{aligned} \left(\begin{array}{l} \text{heat stored} \\ \text{in air volume} \\ \text{of zone i} \end{array} \right) &= \left(\begin{array}{l} \text{net convection} \\ \text{into air volume} \\ \text{of zone i} \end{array} \right) + \left(\begin{array}{l} \text{net advection by} \\ \text{inter-zone flow} \\ \text{into air volume} \\ \text{of zone i} \end{array} \right) + \left(\begin{array}{l} \text{net advection by} \\ \text{infiltration} \\ \text{into air volume} \\ \text{of zone i} \end{array} \right) \\ &+ \left(\begin{array}{l} \text{convective energy} \\ \text{from casual gains} \\ \text{in air volume} \\ \text{of zone i} \end{array} \right) + \left(\begin{array}{l} \text{convective energy} \\ \text{from plant interaction} \\ \text{with air volume of} \\ \text{zone i} \end{array} \right) \end{aligned} \quad (2.1)$$

$$V_{ai} \rho_{ai} c_{p,ai} \frac{\partial T_{ai}}{\partial t} = Q_{si,ai} + Q_{aj,ai} + Q_{ext,ai} + \alpha_i' Q_{cas,i} + \alpha_i Q_{pli,i} \quad (2.2)$$

¹ In this outline, only one casual gains source in zone i and one plant component interaction with zone i is considered. The subscript i thus links these sources to the zone they are located in.

where V_{ai} is the volume of thermal zone i (m^3), ρ_{ai} is the density of the air (kg/m^3), $c_{p,ai}$ is its specific heat at constant pressure (J/kgK), T_{ai} is its temperature (K) and t is the time (s).

The same principles can be applied to the solid material enclosing the thermal zone. Figure 2.3 schematically shows the thermal processes involved. The zonal enclosure of zone i has surface nodes, s_i , and inner nodes, s_{li} .

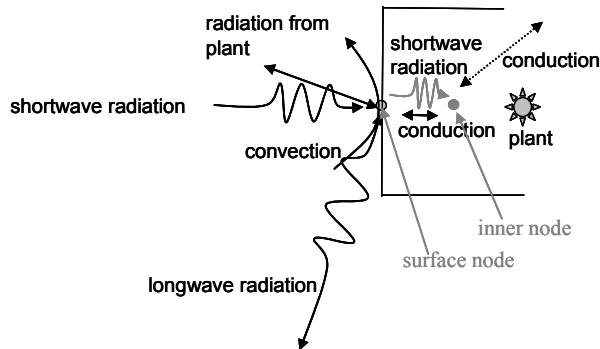


Figure 2.3: The heat balance of a finite part of the solid enclosing a thermal zone of a building.

Convective heat transfer, $Q_{ai,si}$ (W) occurs between the air at both sides of the solid and the surface of the solid. Longwave radiant heat transfer from sources inside the thermal zone includes both those originating from plant components in the thermal zone, $(1-\alpha_i)Q_{pli,i}$, and those from casual sources in that zone $(1-\alpha_i)Q_{cas,i}$. Longwave radiation also occurs between a surface, s' , in visible contact with the surface of the solid enclosure of zone i , i.e. $Q_{s',si}$ (W). Shortwave solar radiation, $Q_{solar,i}$ (W), can be partly absorbed, reflected and/or transmitted by the surface node. The transmitted part can affect the inner node of the solid volume, $Q_{solar_trans,soli}$ (W). Heat gains within the solid are represented by $Q_{soli,e}$ (W), which include gains from plant components located inside the solid volume. A solid volume, being surface or inner node, is also subject to conduction from the surrounding volumes s_{i+1} and s_{i-1} ²,

² The conductive heat transfer is given for a 1-dimensional representation only. *ESP-r* can handle 2- and 3-dimensional processes as well. For an extended outline of those equations the reader is referred to [1].

$Q_{si+/-1,si}$ (W) or sol_i+1 and sol_i-1 , $Q_{sol_i+/-1,sol_i}$ (W). Furthermore, conduction could also appear between surface and solid nodes: Q_{si,sol_i} (W). The overall energy balance will here be given for the inner node of a solid:

$$\begin{aligned} \begin{pmatrix} \text{heat stored in} \\ \text{inner solid} \\ \text{volume } i \end{pmatrix} &= \begin{pmatrix} \text{net conduction from} \\ \text{surrounding inner nodes} \\ \text{into inner solid volume } i \end{pmatrix} + \begin{pmatrix} \text{net conduction from} \\ \text{surrounding surface node} \\ \text{into inner solid volume } i \end{pmatrix} \\ &+ \begin{pmatrix} \text{transmitted solar} \\ \text{radiation passed on to} \\ \text{inner solid volume } i \end{pmatrix} + \begin{pmatrix} \text{energy source} \\ \text{in inner solid} \\ \text{volume } i \end{pmatrix} \end{aligned} \quad (2.3)$$

$$V_{sol_i} \rho_{sol_i} c_{sol_i} \frac{\partial T_{sol_i}}{\partial t} = Q_{sol_i+/-1,sol_i} + Q_{si,sol_i} + Q_{solar_trans,sol_i} + Q_{sol_i,e} \quad (2.4)$$

where V_{sol_i} is the volume of the specific inner solid node (m^3), ρ_{sol_i} is the density of the node (kg/m^3), c_{sol_i} is its specific heat (J/kgK) and T_{sol_i} is its temperature (K).

The energy balance for the surface node of the solid zonal enclosure follows the same logic.

2.2.2.2 Plant level

As with the building and the enclosed thermal zones, the control volume approach can also be applied to the plant network. The plant level consists of a group of component models, linked to form a circuit. Each of these plant-component models can be represented by one or more control volumes. For a water-based heating system, the components can be represented by 2 control volumes: one for the water and one for the solid material enclosing the water flow.

As for the solid enclosing the thermal volume of a building zone, also for the solid of a plant component, heat transfer through convection, conduction and radiation can take place (see Figure 2.4).

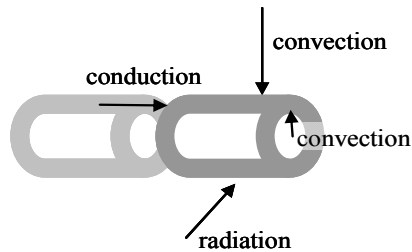


Figure 2.4: The heat balance of a finite part of the solid enclosing the water flow of a plant component.

Convective heat transfer occurs between the plant component's water node w_i , and the solid enclosure, represented by node p_{li} , i.e. $Q_{w_i,p_{li}}$ (W). Convective and radiant heat transfer might occur between the air in zone i and the solid plant enclosure, $Q_{i,p_{li}}$ (W). The convective part is represented by $\alpha_i Q_{i,p_{li}}$ (W), the radiant part by $(1-\alpha_i)Q_{i,p_{li}}$ (W). Radiant heat transfer can additionally occur between any other surface or object in visible contact with the specific plant component, i.e. $Q_{s',p_{li}}$ (W). Conduction might occur from the solid material of one plant component to the solid material of a surrounding plant component $p_{li\pm 1}$, i.e. $Q_{p_{li\pm 1},p_{li}}$ (W). Conductive heat transfer could also take place between a solid of a zone and a plant volume when that zonal solid volume encloses the solid plant volume. It results in a heat transfer $Q_{soli,p_{li}}$ (W). Heat gains in the solid plant volume are not considered here; the solid of the plant is the surrounding material undergoing the energy flows between the water transporting the heat or cold³, and the building zone.

The overall energy balance for the solid enclosure of a plant component is given by:

³ The concepts 'heat' and 'cold' are short terms used for convenience. To be thermodynamically correct, they should be replaced by internal energy at high and low temperature respectively.

$$\begin{aligned}
 \left(\begin{array}{l} \text{heat stored in solid} \\ \text{volume of plant} \\ \text{component i} \end{array} \right) &= \left(\begin{array}{l} \text{convection from} \\ \text{water into solid} \\ \text{volume of plant} \\ \text{component i} \end{array} \right) + \left(\begin{array}{l} \text{heat transfer between} \\ \text{zone i and volume of} \\ \text{plant component i} \end{array} \right) \\
 + \left(\begin{array}{l} \text{net radiation} \\ \text{into solid} \\ \text{volume of plant} \\ \text{component i} \end{array} \right) &+ \left(\begin{array}{l} \text{net conduction from} \\ \text{solid of surrounding} \\ \text{plant component into} \\ \text{solid volume of plant} \\ \text{component i} \end{array} \right) + \left(\begin{array}{l} \text{net conduction from} \\ \text{enclosing zonal building} \\ \text{structure into solid volume} \\ \text{of plant component i} \end{array} \right) \quad (2.5)
 \end{aligned}$$

$$V_{pli} \rho_{pli} c_{pli} \frac{\partial T_{pli}}{\partial t} = Q_{wi,pli} + Q_{i,pli} + Q_{s',pli} + Q_{pli+/-1,pli} + Q_{soli,pli} \quad (2.6)$$

where V_{pli} is the volume (m^3), ρ_{pli} is the density (kg/m^3), c_{pli} is the specific heat (J/kgK), T_{pli} is the temperature (K) of the solid plant enclosure.

Similarly, the heat balance for the water in the plant component can be set up. The processes involved are schematically shown in Figure 2.5 below.

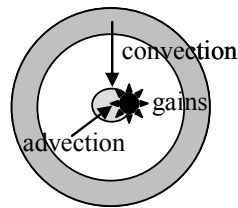


Figure 2.5: The heat balance of a water node symbolising the water enclosed by a plant component.

As can be seen in Figure 2.5, the water node of the plant component is subject to convection between the water and the surrounding solid enclosure $Q_{pli,wi}$ (W), to advective heat transfer by flow of water from other water volumes, $Q_{wi+/-1,wi}$ (W), and sensible heat gains from sources inside the control volume, $Q_{wi,e}$ (W). This last term could for example represent the energy flow the water volume receives from an ideal boiler.

This results in:

$$\begin{aligned} \left(\begin{array}{l} \text{heat stored in} \\ \text{water volume of} \\ \text{plant component i} \end{array} \right) &= \left(\begin{array}{l} \text{net convection into} \\ \text{water volume of} \\ \text{plant component i} \end{array} \right) + \left(\begin{array}{l} \text{net advection by water} \\ \text{flow into water volume} \\ \text{of plant component i} \end{array} \right) \\ &+ \left(\begin{array}{l} \text{energy gains} \\ \text{in water volume} \\ \text{of plant component i} \end{array} \right) \end{aligned} \quad (2.7)$$

$$V_{wi} \rho_{wi} c_{wi} \frac{\partial T_{wi}}{\partial t} = Q_{pli,wi} + Q_{wi+/-1,wi} + Q_{wi,e} \quad (2.8)$$

where V_{wi} is the volume (m^3), ρ_{wi} is the density (kg/m^3), c_{wi} is the specific heat (J/kgK), T_{wi} is the temperature (K) of the water node i .

2.2.2.3 Fluid flow level⁴

In case of pressure driven flows or the need for more detailed results concerning air or water flows, a fluid flow network needs to be modelled.

In that case, the principle of conservation of mass can be applied to a control volume of a certain fluid, for example air:

$$\left(\begin{array}{l} \text{net mass} \\ \text{transferred} \\ \text{into volume i} \end{array} \right) = 0 \quad (2.9)$$

$$\sum_j \dot{m}_{ij} = 0 \quad (2.10)$$

⁴ In the absence of a fluid flow level, simplified expressions can be used to estimate fluid flows such as infiltration of fresh air. More details on that can be found in [1].

where \dot{m}_{ij} is the mass flow rate (kg/s) between volumes i and j , and the summation is over all connected volumes.

Each of the flows associated with control volume i , can be expressed as a function of the pressures p_i (Pa) and p_j (Pa) and thus of the pressure difference Δp_{ij} (Pa):

$$\dot{m}_{ij} = f(p_i, p_j) = f(\Delta p_{ij}) \quad (2.11)$$

The same principles can be applied to other fluid flows in the model. These relations are non-linear. Therefore, an iterative solution technique must be used to achieve a solution for the fluid flow network. To successfully solve the above defined equation, the pressure of at least one control volume must be known.

2.2.3 Control logic in ESP-r

The above described set of equations for calculation of the physical quantities related to the simulation model is subject to the boundary conditions enforced by the climate and by user defined controls. Controls can be imposed on each level of the model: the thermal zones of the building level, the plant networks and the fluid flows.

A control consists of a *sensor*, an *actuator* and a *control law*. The sensor senses a certain variable such as a temperature or a valve position. The control law reacts based on the sensed condition and according to the predefined control logic. This logic defines the action taken by the actuator based on the condition sensed by the sensor.

In *ESP-r*, the control on the building level is often called *zone control*. It implies sensing a condition in a thermal zone of the building or outdoors and consequently reacting through the actuator located in that thermal zone. It is thus a single input, single output (SISO) system. This type of control can assign energy fluxes to the specific actuating point. This actuating point can e.g. be the node representing the zone air or a user-defined fixed split between convective energy emission into the zone air node and radiant energy emitted/absorbed in that zone. It thus determines the value of $Q_{pli,i}$ in equations (2.2) and (2.4).

At project commencement, the zone controllers had no inertia. The reason is that zone controls are normally used for a simplified representation of a plant interaction. Consequently start up and shut down effects do not need to be incorporated. However, time dependent characteristics as minimum time on and off are implemented in several zone controllers [9], [11].

Plant and mass controls follow a similar form of sensor, control law and actuator in the specific level, again a SISO-system. But they do not interfere in the energy balances in the same way as the zone controllers. Plant and fluid flow controls act on the coefficients of the energy balances of the explicitly modelled plant components. If a plant is modelled, the thermal interaction between plant and zone is through a coupling zone control. The latter zone control then acts as a conduit for energy exchanges between plant and zone.

Plant and fluid control laws support a detailed assessment of equipment use and control system design [3]. Hence, they do allow incorporating transient effects, defining temperatures of components and circulating fluids as well as mass flow rates in the explicitly defined components.

Various plant controls acting on one plant network can be active simultaneously. The same is possible for flow controls on flow networks. *ESP-r*, however, allows only a single zone controller for a given thermal zone at each moment. Nevertheless, a structure is available to define a dominating controller, which is named global controller [10]. It can be combined with multiple zone/plant/fluid controllers and thus handle multiple inputs and react through multiple actuators. It is thus a multiple input, multiple output (MIMO) control.

Generally, global controllers are used as hierarchical control systems. A hierarchical control can be organised by a non-iterative or an iterative approach. For a non-iterative approach, the different sensed variables are inputs to a global management system. This system determines, according to the predefined global logic, the values of a range of outputs. It thus holds the overall logic and requires no additional control algorithms in the hierarchically lower levels. The iterative global control as implemented in *ESP-r*, communicates with hierarchically lower controls and can overrule their decisions. It operates by collecting the desired actuator outputs, as defined by the hierarchically lower controllers. Consequently, it processes the desired actions and checks whether they are according to the logic of the global control algorithm. Then, a separate routine is called, which enables a second pass

within the same timestep with identical state variables as for the first pass. During this second pass, the global control can overrule/overwrite conflicting actuating signals. These values are then further processed to solve the overall energy balance equation sets for that timestep.

The global controller scheme of interest for the structures modelled in the framework of this dissertation is visualized in Figure 2.6. In this case, the hierarchically lower controls are zone controls. They sense a condition in the zone and determine the desired actuating signal, i.e. an energy flux. In the absence of a global control, the energy balances of the zonal air and solid enclosure could now be processed. In case a global control is active, this hierarchically higher control first collects the desired actuating signals of the different thermal zones. It checks whether the different desired fluxes are in accordance with the global controller logic and within the second pass possibly overwrites zonal fluxes. The zonal energy balances now have the final plant interaction flux $Q_{pl,i}$ for further processing.

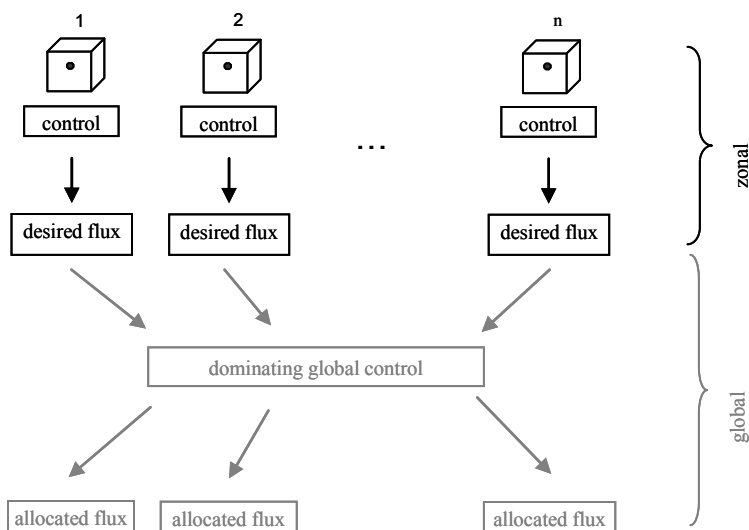


Figure 2.6: Structure and decision logic of global controller.

2.2.4 Solution technique within *ESP-r*

As the equations for the different parts of the model have now been introduced, they have to be arranged in a format suitable for simultaneous solution. They are organised by level: building, plant or flow.

Interactions between levels are handled as bi-directional excitations on the different levels involved through common variables: physical state variables that occur in the heat balance equations of these multiple levels. Firstly, the heat balances in each level are solved, based on assumed values of the coupled variables and the physical states in surrounding volumes. Then, an iterative process is started to achieve a solution within predefined convergence criteria.

The thermal solution procedure involves solving the above given heat balances Eqs, (2.2), (2.4), (2.6) and (2.8). The procedure is described here focussing first on the air within a zone i . The heat-transfer processes possibly involved are thus convection, advection and heat gains from sources in the volume of interest⁵. This allows generalising Eq. (2.2) in the format given by Eq. (2.12). $Q_{sj,ai}$ is a generalised format for the convective heat transfer (W) possibly occurring between all surrounding or enclosed solid volumes j and the volume of interest. Similarly, $Q_{ak,ai}$ is a generalised format for the advective heat transfer (W) possibly occurring between all surrounding air volumes k and the air volume of interest. $\alpha_i Q_{pli,i}$ is the convective part of the internal heat gains (W) possibly occurring in the air volume of interest, where for the sake of clarity the gains are limited to plant interactions.

$$V_{ai} \rho_{ai} c_{p,ai} \frac{\partial T_{ai}}{\partial t} = \sum_j Q_{sj,ai} + \sum_k Q_{ak,ai} + \alpha_i Q_{pli,i} \quad (2.12)$$

This equation is valid for all physical states and thermal processes occurring at a certain moment t (s). The derivative term related to the thermal capacity can be rewritten as a function of the finite time difference Δt (s), i.e. the simulation timestep. Using a backward difference scheme, this results in Eq. (2.13), where for ease of notation the air volume V_{ai} (m^3) the air density ρ_{ai} (kg/m^3) and the specific

⁵ For an extensive elaboration on the solution procedures the reader is referred to [1]

heat at constant pressure of the air in the zone, $c_{p,ai}$ (J/kgK), are here considered to be time invariant⁶.

$$V_{ai} \rho_{ai} c_{p,ai} \frac{T_{ai}(t + \Delta t) - T_{ai}(t)}{\Delta t} = \sum_j Q_{sj,ai}(t) + \sum_k Q_{ak,ai}(t) + \alpha_i Q_{pli,i}(t) \quad (2.13)$$

Dividing by the volume V_{ai} and applying a generalized trapezoidal scheme, i.e. a mix of a forward difference and a backward difference scheme, the resulting equation becomes:

$$\begin{aligned} 2\rho_{ai} c_{p,ai} \frac{T_{ai}(t + \Delta t)}{\Delta t} - \frac{\sum_j Q_{sj,ai}(t + \Delta t) + \sum_k Q_{ak,ai}(t + \Delta t) + \alpha_i Q_{pli,i}(t + \Delta t)}{V_i} \\ = 2\rho_{ai} c_{p,ai} \frac{T_{ai}(t)}{\Delta t} + \frac{\sum_j Q_{sj,ai}(t) + \sum_k Q_{ak,ai}(t) + \alpha_i Q_{pli,i}(t)}{V_i} \end{aligned} \quad (2.14)$$

The processes of convection and advection depend, amongst others, on the temperature differences between the solid or fluid volumes involved. Replacing the general forms by the basic equations representing these physical processes (Eqs. (2.15) and (2.16) respectively), results in Eq. (2.17) where $\bar{h}_{sj,ai}(t)$ is the surface averaged convective heat transfer coefficient at time t (W/m²K). For the ease of notation, the convective heat transfer process is considered to be linear here. It will be discussed in more detail in chapter 3⁷. $A_{sj,ai}$ is the contact area for the convective heat transfer between solid volume j and air volume i (m²), $T_{sj}(t)$ is the temperature of that solid at time t (K). $\dot{m}_{ak,ai}$ is the mass flow rate between air volume k and the air volume of interest i at time t (kg/s) and $T_{ak}(t)$ is the temperature of the air of volume k at time t (K). $c_{p,a}$ is the specific heat capacity of the air exchanged at constant pressure (J/kgK).

⁶ This time-invariance is set here for ease of notation. Within ESP-r, these values are adapted during the simulation.

$$Q_{sj,ai}(t) = \bar{h}_{sj,ai}(t) A_{sj,ai} (T_{sj}(t) - T_{ai}(t)) \quad (2.15)$$

$$Q_{ak,ai} = \dot{m}_{ak,ai}(t) c_{p,a} (T_{ak}(t) - T_{ai}(t)) \quad (2.16)$$

All grouped together, this leads to:

$$\begin{aligned} & \left[\frac{2\rho_{ai}c_{p,ai}}{\Delta t} + \frac{\sum_j \bar{h}_{sj,ai}(t+\Delta t)A_{sj,ai}}{V_{ai}} + \frac{\sum_k \dot{m}_{ak,ai}(t+\Delta t)c_{p,a}}{V_{ai}} \right] T_{ai}(t+\Delta t) \\ & - \frac{\sum_j \bar{h}_{sj,ai}(t+\Delta t)A_{sj,ai}}{V_{ai}} T_{sj}(t+\Delta t) - \frac{\sum_k \dot{m}_{ak,ai}(t+\Delta t)c_{p,a}}{V_{ai}} T_{ak}(t+\Delta t) - \frac{\alpha_i Q_{pli,i}(t+\Delta t)}{V_{ai}} = \\ & \left[\frac{2 \cdot \rho_{ai} c_{p,ai}}{\Delta t} + \frac{\sum_j \bar{h}_{sj,ai}(t)A_{sj,ai}}{V_{ai}} + \frac{\sum_k \dot{m}_{ak,ai}(t)c_{p,a}}{V_{ai}} \right] T_{ai}(t) \\ & + \frac{\sum_j \bar{h}_{sj,ai}(t)A_{sj,ai}}{V_{ai}} T_{sj}(t) - \frac{\sum_k \dot{m}_{ak,ai}(t)c_{p,a}}{V_{ai}} T_{ak}(t) - \frac{\alpha_i Q_{pli,i}(t)}{V_{ai}} \end{aligned} \quad (2.17)$$

This is the basic equation used in *ESP-r* for calculating a fluid volume's temperature at time $t+\Delta t$. The term in the first rectangle, indicated in black, is known as the self-coupling coefficient as it relies on information directly related to the fluid volume of interest. The terms in the second and third rectangle, indicated in grey, are the cross-coupling coefficients as they provide the link to other volumes exchanging thermal energy with the volume of interest. The right hand side of this equation consist of terms related to physical properties at time t . It thus considers known values only

⁷ Within *ESP-r*, the convective heat transfer coefficient is linearised, however, updated to account for changed conditions. This is done to enable fast efficient solution methods. For an extended discussion of the linearisation of non-linear processes within *ESP-r* the reader is referred to [5]

and can therefore be replaced by a single constant⁸. Note that the derived equation gives an equal weight to the backward and forward differentiation, i.e. a Crank-Nicholson formulation, a technique applied to achieve high accuracy and a stable solution [2]. Within *ESP-r* the user can change this weighing.

Similar equations, containing self-coupling and cross-coupling coefficients can be set-up for the zone's surface nodes. The zonal heat balance for a single air volume i , surrounded by n surfaces, results in a matrix schematically described by Eq. (2.18). $T_{si}(t+\Delta t)$ indicates the surface temperature of solid i (K), for i from 1 to n . The right hand side of this equation holds the known terms, or the assumed conditions in the surrounding zones.

$$\begin{bmatrix} \text{matrix holding self-coupling,} \\ \text{cross-coupling and plant interaction} \\ \text{coefficients} \end{bmatrix} \times \begin{bmatrix} T_{ai}(t + \Delta t) \\ T_{s1}(t + \Delta t) \\ T_{s2}(t + \Delta t) \\ \dots \\ T_{sn}(t + \Delta t) \\ Q_{pl,i}(t + \Delta t) \end{bmatrix} = [\text{known terms}] \quad (2.18)$$

This matrix is then reduced as far as possible to allow extracting characteristic equations that embody the dynamics of the processes of interest. Focussing on plant interaction within a zone, the so-derived characteristic equation⁹ results in:

$$A \cdot T_{ai}(t + \Delta t) + B \cdot Q_{pl,ai}(t + \Delta t) = C \quad (2.19)$$

⁸ This equation deals with 1-D heat flow only. In *ESP-r* 3-D heat flow can be simulated using computational fluid dynamics [6].

⁹ This characteristic equation is often used in *ESP-r*'s zone controls. It enables estimating the thermal flux as a function of the desired temperature or vice versa. As the equation is based on amongst others temperature dependent material properties, the estimated value will not be exactly the same as the finally calculated value. To improve the estimation, the forward and backward reduction processes could be repeated till a desired accuracy is achieved. Such iterative estimation techniques could be based on available subroutines as the `mzrcpl` located in `bcfunc.F`.

The coefficients A, B and C are the modified coefficients resulting from the matrix processing. They indirectly hold current timestep zonal characteristics as well as future timestep estimated values related to processes and physical states within the zone and the surrounding zones.

The equation is given for the air temperature. However, the reduction and solution process can focus on surface and intra-constructural nodes as well. When using a mixed air - mean radiant control point, the use of the above derived Eq. (2.19) requests 'translating' the desired mixed value into an air or surface temperature before applying the derived relation¹⁰. An overview of the different solution schemes, depending on the zonal control point location, is given below:

The back substitution processes enable calculating the new nodal temperatures for all surfaces of the zone. The solution of this matrix, however, is only a part of the solution process of the whole building.

¹⁰ When further recalling this equation, it is supposed to be combinable with any kind of sensor. The 'translation' to air or surface temperatures is then not repeated, however it is assumed to be accounted for.

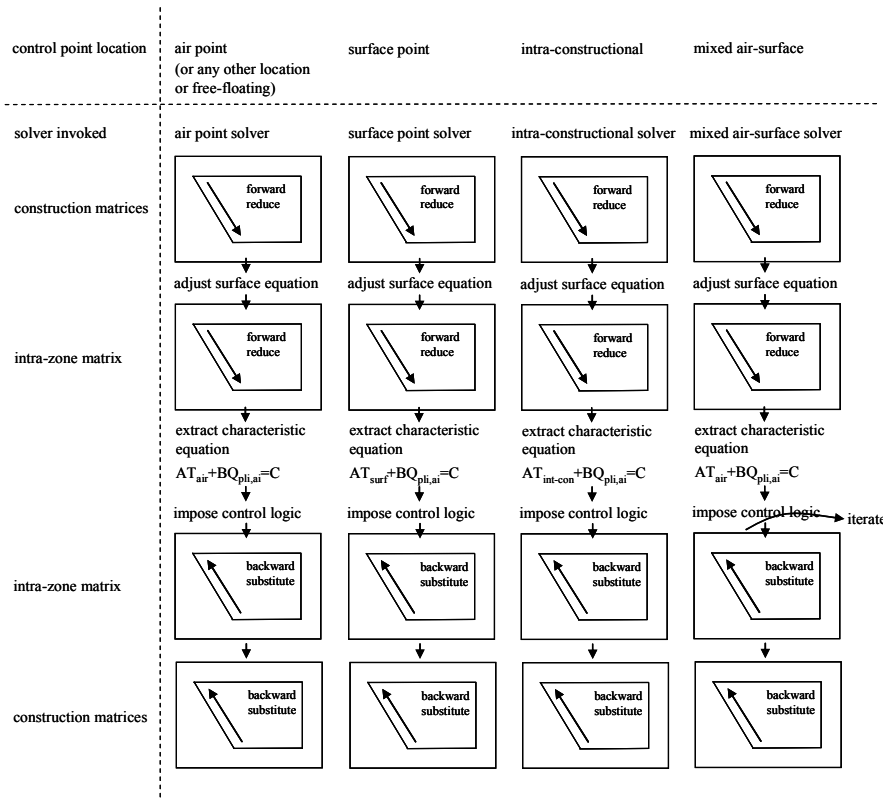


Figure 2.7: Numerical solution as a function of the control point location [10].

Within *ESP-r* each level, i.e. building, plant and flow, employs a solution method optimised for the specific domain equation types. These general solution methods are embedded in a higher level global solver that dictates the actions of the sub-solvers according to the outline¹¹ of Figure 2.8 ([1], [12], [13]). This scheme shows the zone by zone solution. That implies that the first zone solved at a certain timestep takes into account last-timestep nodal temperatures of the surrounding zones in its calculation process. Further zones will then be calculated with updated nodal temperatures of all already processed zones.

¹¹ In this outline the use of an intermediate calculation for the plant level is ignored. However, *ESP-r* allows the user to define a different and smaller plant simulation time step compared to the building simulation time step for combined building-plant simulation.

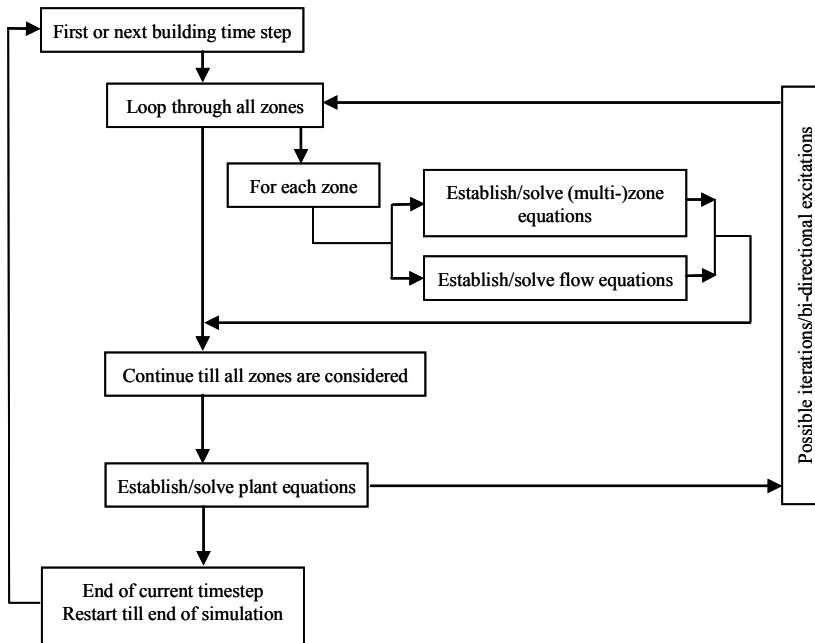


Figure 2.8: Outline of solution procedure in *ESP-r*

The matrix organization of the equations implies that the same physical processes will be handled in the same way, independent of how the model has been set up. So is the injection of heat due to plant interactions done by the coupling term Q_{pli} of Eq. (2.18). Iterations within a zonal loop ensure stable solutions for all zones processed.

More details on the solution methodology and the matrix organization can be found in [1].

2.2.5 Validation of *ESP-r*

Standard tests have been conducted to evaluate *ESP-r*'s accuracy in predicting/calculating different aspects related to energy in buildings [14], [15]. It

involves several BESTEST¹²-cases for building envelope and HVAC aspects. For these BESTEST inter-model comparisons are set up. ESP-r generally showed to be in agreement with the outcome of other BES-codes. However, for cooling loads the ESP-r IEA annex 21 [16] results showed to deviate from the results of the other building simulation codes. This was mainly due to different assumptions for the convection coefficients for internal convection: ESP-r applied correlations described in the literature, while most other codes used constants. These coefficients are shown to influence the results significantly.

ESP-r has further been validated for specific models or aspects throughout research projects as the IEA ECBCS Implementing Agreement annex 1, 4, 21 and 42 [16], [17],[18] the BRE/EDF validation project and the PASSYS project [14], [16].

An extended overview of ESP-r's testing and validation history can be found in [19].

2.3 Implicit plant simulation¹³

The general question that prompted consideration of a new way of plant simulation in ESP-r was related to optimal heating/cooling systems. That means questioning current technologies and possibly defining tendencies for future developments in the areas of heat emitters/absorbers, distribution networks and heat/cold production systems.

The problem clearly focuses on plant configurations and how they interact with the building. In the framework of current research, however, it is more convenient to tackle the problem without introducing an explicit plant level in the simulation model. So, instead of explicitly defining a plant, an *implicit approach*¹⁴ is taken. The

¹² The International Energy Agency, working with the U.S. National Renewable Energy Lab, has created a benchmark for building energy simulation programs. This benchmark is entitled "BESTEST –Building Energy Simulation Test and Diagnostic Method"

¹³ The ESP-r version containing the implicit approach is downloadable through the author's development branch. It is built in the ESP-r 11.5 release. The list of files that have been changed, as well as a brief description of the changes, can be found in Appendix B.

¹⁴ The term 'implicit' emphasises the indirect modelling of the plant level.

main reason is that this approach allows using energy flows and averaged temperatures, instead of exact temperatures and mass flow rates, although reducing modelling complexity is a fair advantage as well.

A reduced model has also been set up by Garcia-Sanz and is described in [20]. However, he did use mass flow rate data. His aim was to allow quickly testing the effect of certain control logic, more than focussing on the design of the different components. Similarly, Nielsen [21] defined a rough model for decisions in early design stages. She reduces the heating output to a single value, not considering the characteristics of the emission/absorption elements. For the current research, that approach is too rudimentary for defining the tendencies of heating/cooling equipment design. Another, at first sight promising, tool is described by Mathews and Richards [22]. They developed a software model that takes into account radiant and convective energy emission of a plant component based on a limited range of input data. As far as described, they, however, assume a zero-thermal capacity plant component model with a constant split between radiant and convective output for the energy emission. In later publications, Mathews et al. [23], [24] describe the tool *QUICKcontrol*. Although the name might suggest differently, it can be used for system sizing. Besides the fact that the tool has been developed for air conditioning, it includes existing components only. Furthermore, none of the here referred publications mentions the use of the heating equipment for both heating and cooling purposes.

The structure and physical logic of the implicit modelling approach and how it is implemented in the above described BES code *ESP-r* will be described hereafter. This explanation will allow reasoning about the implicit plant modelling approach.

2.3.1 The implicit plant structure

2.3.1.1 *The emission/absorption of heat in a thermal zone*

The emission/absorption of heat by any water-based heat exchanger involves radiant as well as convective heat transfer. The convective energy transfer affects the zonal air temperature. The radiation will influence the temperature of the surrounding surfaces. Recalling the heat-balance equations for zone air point, Eq. (2.2), and solid zonal enclosure, Eq. (2.4),

$$V_{ai} \rho_{ai} c_{p,ai} \frac{\partial T_{ai}}{\partial t} = Q_{si,ai} + Q_{aj,ai} + Q_{ext,ai} + \alpha_i' Q_{cas,i} + \alpha_i Q_{pli,i} \quad (2.2)$$

$$V_{si} \rho_{si} c_{si} \frac{\partial T_{si}}{\partial t} = Q_{ai,si} + Q_{si+/-1,si} + (1-\alpha) Q_{pli,i} + (1-\alpha') Q_{cas,i} + Q_{s',si} + Q_{si,e} \quad (2.4)$$

the term representing the interaction with a possible plant component i located in the thermal zone is given by $Q_{pli,i}$. This term, combined with α_i , can thus be used to represent a fictitious heat emitter/absorber.

Using the structure of the zone controllers and combining it with a mixed convective/radiant actuator allows determining a convective energy injection into the air node of the thermal zone, on the one hand, and a radiant injection into the solid zone enclosure, on the other hand. This structure can thus be used to represent the emission/absorption element¹⁵.

This approach implies that the heat emission/absorption element is treated as a single, isothermal node at temperature $T_{emit,i}$ (K) with infinitesimally small volume. The resulting heat balance of the implicit emitter/absorber is then given by Eq. (2.20):

$$C_{emit,i} \frac{\partial T_{emit,i}(t)}{\partial t} = Q_{pli}(t) - Q_{pli,i}(t) \quad (2.20)$$

$C_{emit,i}$ is the total capacity of the emitter/absorber (J/K), $Q_{pli}(t)$ (W) is the thermal power flux injected in the emitter/absorber at time t (s). Its value is defined by both the emitter/absorber element's control and the production device's characteristics and control. These controls can determine the desired thermal power flux based on

¹⁵ In fact, the heat emitter/absorber itself is not really implemented in the routine that holds the zone controllers. It is held in a separate file and can be called from the zone control routine in the absence of an implicit production system. If an implicit production unit is defined, the implicit emitter/absorber is called from a subroutine embedded in a hierarchically higher decision algorithm managing the calls to the zone controllers. And therefore, the implicit emission/absorption element uses the facility this algorithm offers for the zone controllers, without really being one.

the relation given by Eq. (2.20). This will be briefly described hereafter and further elaborated in chapter 6. $Q_{pii,i}(t)$ is the heat exchange between plant component i and zone i (W).

The thermal power flux $Q_{pii,i}$ is the term interacting with the zone. Its output is therefore an amount of convection and an amount of radiation. Both processes are temperature dependent in a different non-linear way. The ratio between the amount of convection and the total amount of heat emitted/absorbed for a given element i , i.e. α_i (-), will thus not be constant. To calculate the instantaneous ratio, a generic model has been set up representing any type of water-based heat emitter/absorber.

The model is discussed in detail in chapter 3. A generalised format is given by:

$$Q_{pii,i}(t) = f(T_{emit,i}(t), MRT_i(t), T_{ai,i}(t)) \quad (2.21)$$

where $MRT_i(t)$ (K) indicates the mean radiant temperature as observed by the element¹⁶ of zone i , which will be discussed in more detail in the next chapters.

Equations (2.20) and (2.21) can then be combined to determine the heat emission/absorption $Q_{pii,i}(t)$ as well as the average emitter's/absorber's temperature $T_{emit,i}$ (K) and based on the instantaneous value for the amount of convection over total energy delivered, i.e. α_i . This constantly adapted value is then passed to the correct subsolver to account for an accurate actuation.

The emitter/absorber logic is schematically presented by the grey box in Figure 2.9. The flow of information to and from the emitter/absorber is indicated in italic.

¹⁶ The mean radiant temperature might be hard or even impossible to measure physically. However, in the current abstract analysis, that is not a restriction as it can be calculated within the code.

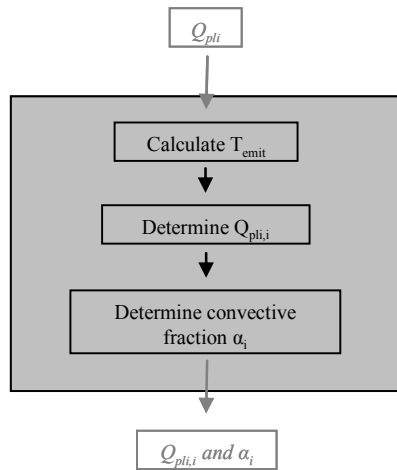


Figure 2.9: Schematic representation of the implicit heat emitter/absorber logic. The grey box indicates the processing of information within the heat emitter/absorber model. The information flow to and from the emitter/absorber is indicated in italic.

2.3.1.2 The distribution of thermal energy to the thermal zone

The distribution system transports the heat/cold at any moment from the production unit to the heat emitter/absorber and back. During this process energy is lost, due to temperature differences between the transported water and the surroundings of the pipe. Some of these losses might be recovered as they occur in heated/cooled zones reducing their demand for thermal energy.

In the implicit modelling approach, no detailed information is available on exact location of the elements within the zones. Consequently, the piping network is not defined either. The European standard CEN 15316-2-3 [25] suggests a method for estimation of the distribution losses using early design stage information. The method is set up for heating systems only. When comparing the results with

simulations performed in the framework of the el²ep-project¹⁷ [26], it is clear that the European standard simplified method overestimates the losses¹⁸.

The *TRNSYS*-simulations, described by Van der Veken, et al. [26], were performed for different combinations of heat emission and production systems for a terraced house built according to the Belgian standards. The average distribution efficiency calculated based on these simulation results is 97.9 % with a standard deviation of only 0.6. The pipes in the simulation model were not insulated and thermal losses within heated zones were not considered as losses for calculation of the distribution efficiency. The latter approach of not incorporating possible losses to heated zones, is also taken by Ast [27]. He achieves efficiencies that are even higher, due to the insulation of the pipes in his models: values of 98.6% to even 99%, depending on the control strategy for heat production and emission. Eisenman [28] comes up with distribution efficiencies for low energy buildings in the range of 92.2% to 93.3%. These values are clearly lower as she does not consider insulated pipes and does not incorporate the losses to the heated zones. Her efficiency numbers are based on what arrives at the heat emission element(s) versus what was injected in the distribution system by the production device. It is clear that exact values for the distribution efficiency are hard to define, as they are shown to depend on what is considered as useful energy, controls for temperatures and flow rates and how the distribution system is set-up as well as on non-distribution system dependent characteristics¹⁹. As the distribution system is not the main focus of the current research, it is here accepted to treat the distribution losses by incorporating an efficiency $\eta_{\text{distribution}}$ equal to an average constant value independent of the case considered. This average is set to the 97.9% as defined in [26].

¹⁷ El²ep stands for extreme low energy and pollution. The aim of the project was to define concepts for (extreme) low energy buildings, optimised for energy consumption, ecological impact and cost.

¹⁸ The standard mentions this overestimation of the simplified method and suggests its use only for estimation of the losses in an early design stage.

¹⁹ It is clear that the building design and the geometrical ‘stacking’ of the heated and unheated zones will influence the losses. A more detailed model for the calculation of the distribution losses might therefore be a further improvement of the implicit approach.

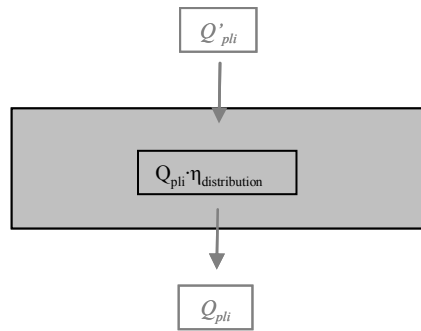


Figure 2.10: Schematic representation of the implicit distribution system logic. The grey box indicates the processing of information within the distribution system model. The information flow to and from the distribution system is indicated in italic.

The distribution logic is schematically presented by the grey box in Figure 2.10. The flow of information to and from the distribution model is indicated in italic. Q'_{pli} (W) indicates the thermal flux the distribution system receives from the production device and transports to emitter/absorber element i .

2.3.1.3 Producing the heat

The aspects of heat emission/absorption in the zones and distribution to the zones have been discussed. The remaining implicit plant component is the production unit. Unlike the other components, this part of the installation has to be able to deal with multiple inputs and multiple outputs (MIMO). It can thus not be embedded in the structure of the zone controllers. As described above, the structure of the global controllers can be used to handle such MIMO-issues. It has been implemented previously in *ESP-r* to handle building management systems and is perfectly suited to hold the logic of the implicit production unit.

The structure of the global controller is extended to contain both the control of the production unit and the production unit itself. The control collects the requested thermal fluxes of the controllers of the heat emitters/absorbers in the different zones. The production control then reacts to these demands according to its logic as will be discussed below. Once the decision on the total energy to be produced is taken by the controller, the implicit production unit model is entered. It receives the demand,

Q_{prod} (W), requested by its control. It performs the primary energy calculation²⁰ based on user-selected efficiency characteristics, adds start up and shut down dynamics and finally divides the available energy amongst the different zones proportional to their demand. However, it does not directly allocate the thermal fluxes to the zones. For each zone, it first calls the distribution logic. The thermal power flux it passes on to the distribution model is indicated by Q'_{pli} (W).

The logic of the production unit is schematically presented by the grey box in Figure 2.11. The flow of information to and from the implicit production model is given in *italic*.

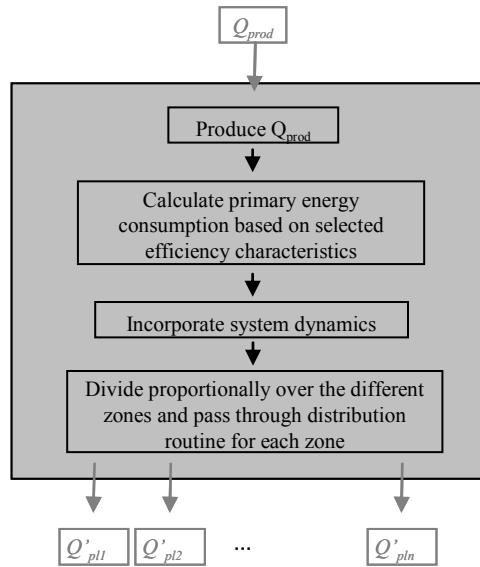


Figure 2.11: Schematic representation of the implicit production unit logic. The grey box indicates the processing of information within the implicit production system model. The information flow to and from the production system is indicated in *italic*.

2.3.1.4 Controlling the implicit plant components

All implicit hardware installation components are now described. As for any plant, also the implicitly modelled plant components need to be controlled. Whether the

²⁰ It might seem unlogic to first perform the primary energy calculations. However, it is computationally more efficient. For more information is referred to chapter 5.

control is ideal or whether it models a realistic control type, each plant component needs a signal to continue, modify or interrupt an action.

The controls for emission/absorption of heat in a zone are implemented in the structure of the zone controllers²¹. The user can only specify one control for each emitter/absorber. However, this control can, as in reality, be overruled by a hierarchically higher control such as a production unit control. The emission/absorption controllers sense a condition in the zone of interest. In the implicit structure developed in the framework of this dissertation, this is the operative temperature $T_{op,i}$ (K). As elaborated in chapter 1 this will here be considered a mix of 50% zone air temperature and 50% mean radiant temperature. The controller then decides on the required reaction to that sensed condition. It can therefore use the above given Eq. (2.20). This requested thermal power flux is then passed on to the global level²². This flux is here indicated by Q''_{pli} (W).

Different controls are implemented, varying from an ideal controller dealing with start up calculations to a thermostatic radiator valve as will be elaborated in chapter 6 and appendix D. Their main structure is similar and schematically represented by the grey box in Figure 2.12. The flow of information to and from the controllers of the implicit heat emitter/absorber is indicated in italic.

²¹ The emitter/absorber controls are embedded in a separate file but called from a routine in the structure holding the zone controllers

²² In case no global level has been defined, the zone controller routine calls the implicit emitter/absorber logic.

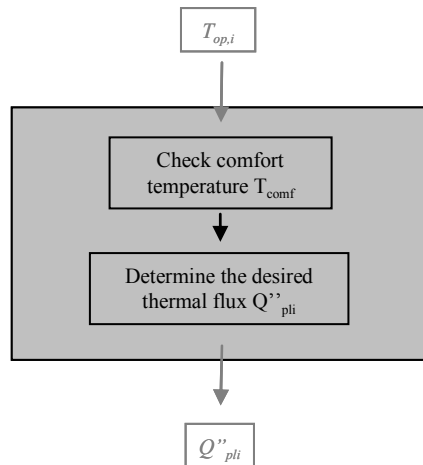


Figure 2.12: Schematic representation of the controller of the implicit heat emitter/absorber. The grey box indicates the processing of information within the implicit emitter/absorber control model. The information flow to and from this control is indicated in *italic*.

While the emitter/absorber element's controllers are located within *ESP-r*'s zonal level, the controllers for the implicit production device are implemented in the structure of the production device itself, i.e. the structure of the global controllers. They are called while processing zone by zone. However, they only start taking action if all zones have been processed during that particular simulation timestep (see Figure 2.8). All requested demands are then gathered and evaluated. The action that the selected production controller decides on depends on its logic. When representing a central room thermostat, the demand of a specific single zone is decisive. For other controls, all zones in the building are considered for calculation of an average cooling and an average heating demand. This possible average cooling demand is compared to the possible average heating demand and the reaction is determined by the highest average demand.

The production control logic then determines the desired thermal energy, according to its logic. It checks whether this thermal flux can be delivered given limitations as lock out time and thermal power constraints. The final requested energy demand is passed on to the production system algorithm.

This process is schematically represented by the grey box in Figure 2.13. The flow of information to and from the controllers of the implicit production unit is indicated in *italic*.

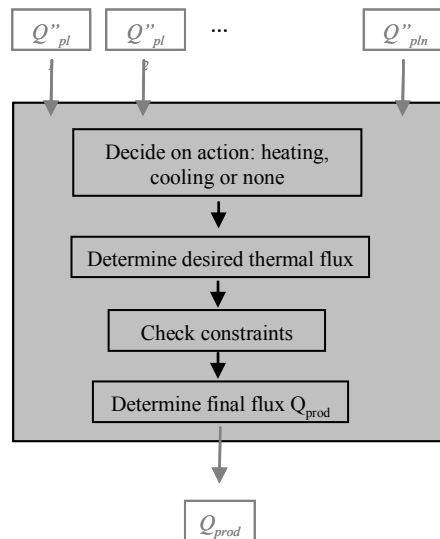


Figure 2.13: Schematic representation of the controller of the implicit production device. The grey box indicates the processing of information within the implicit production system control model. The information flow to and from the production control is indicated in *italic*.

2.3.1.5 The combined action of all implicit plant parts

The combined action of all of the above presented parts of the implicit plant modelling approach is presented in the scheme of Figure 2.14.

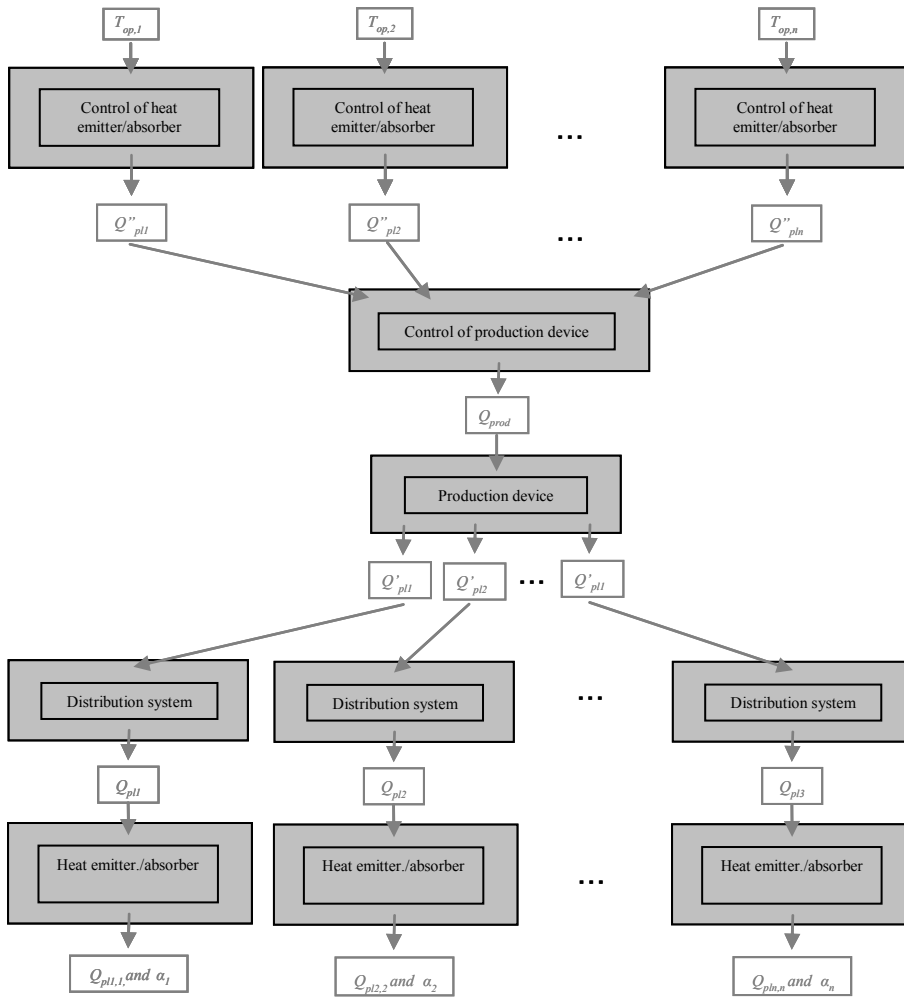


Figure 2.14: Schematic representation of the combined action of all implicit plant modelling parts. The grey boxes indicate the implicit plant component models. The information flow to and from these components is indicated in *italic*.

2.3.2 The advantages of the implicit approach

ESP-r offers a wide range of plant components with varying complexity. These components can be combined with a broad range of controls implemented at the plant level. It seems presumptuous to question the use of that structure.

However, there are several reasons to work at the building level and to define the whole abstract heating/cooling system in that level.

This implicit structure allows step by step building and testing of a possible plant. Each of the components can first be optimised and then translated into a realistic overall heating/cooling installation. Furthermore, the implicit heat *emitter/absorber model* can be used separately, to evaluate the performance of an emission/absorption element in a given zone, without even connecting it to a production unit. This is a useful approach when the focus is on the optimisation of single zones and not or not yet on the combined action of the whole installation.

Using the node in the thermal zone as an actuating point also excludes effects concerning the exact configuration and location of the emission/absorption element. Therefore, it allows focusing on the set of characteristics for the emission/absorption elements and requirements for the production system. The detailed effects of the emitter's/absorber's configuration and location can only be examined after translating that set of characteristics to a real heat exchanger and perform a detailed analysis on it. That is beyond the scope of current research.

The *emitter/absorber controllers* can be added to these emitters/absorbers. The control of heating and cooling in this implicit approach can be ideal. However, more realistic implicit controllers are added by the current author to increase the usefulness of the implicit approach. The use of the ideal control is to avoid the simulation results to be dominated by the impact of the controller, as for the current research the focus is on the hardware. The dominating impact of the controller has been reported by Peeters et al. [29], Kiekens [30] and Crommelin and Ham [31] based on simulation results, and confirmed by Weitzmann et al. [32] based on measurements.

A *production unit* can be selected in the next step and finally this unit can be combined with its appropriate *production system control*.

This whole approach allows starting from the desired thermal comfort and defining the characteristics of the heating/cooling installation step by step to achieve that comfort.

This approach thus enables determining tendencies for the development of specific installation components. That has been the reason to develop the implicit modelling approach.

2.4 Summary and conclusions on modelling building energy systems

ESP-r is a research oriented simulation program. It uses the finite difference control volume heat balance approach to define the physical state of thermal zones, building structure and plant components. That way, it creates an almost perfect environment for simulation of abstract, theoretical and even non-existing systems.

Therefore, the building simulation code *ESP-r* was used to define, besides the already existing explicit plant modelling structure, an *implicit plant modelling approach*. The main advantage of that approach is that it allows simulating fictitious heating/cooling systems based on energy flows and average element temperatures. That permits focusing on the performance of the different components, without defining detailed controls that might dominate the overall result. In addition, the time-saving side effect for defining and comparing plant configurations through simulations is positive as well. The approach, however, has some drawbacks as well. For the emitter/absorber element, the detailed temperature distribution within such element is not accounted for. This could cause differences between simulated and real energy output, especially in transient regimes. This location independency also prevents a detailed model of the distribution network. Concerning the production devices, a rough temperature model prevents detailed performance analysis such as on when and how much condensation would appear in case of a condensing boiler.

As now the main structure is sketched, the different implicit installation components and controls have to be described in more detail. The most crucial component model, in the context of the current research, is the one representing the heat emission/absorption element itself. Its model logic is the subject of the next chapter.

References

- [1] J. Clarke, 2001, *Energy Simulation in Building Design*, Butterworth Heinemann, Oxford, ISBN 0-7506-5082-6
- [2] C. Underwood, F. Yik, 2004, *Modelling Methods For Energy In Buildings*, Blackwell Publishing, ISBN 0-632-05936-2
- [3] J. Hand, 1998, *Removing barriers to the use of simulation in the building design professions*, PhD dissertation, University of Strathclyde, Glasgow, UK
- [4] Jensen, S., 1993, *Validation of Building Energy Simulation programs, Part 1 & 2*, Research Report PASSYS Subgroup Model Validation and development, EUR 15115, TIL, CEC, Brussels
- [5] N. Kelly, 1998, *Towards a design environment for building-integrated energy systems: the integration of electrical power flow modelling with building simulation*, PhD dissertation, University of Strathclyde, Glasgow, UK
- [6] I. Beausoliel-Morisson, 2000, *The adaptive coupling of heat and air flow modelling within dynamic whole-building simulation*, PhD dissertation, University of Strathclyde, Glasgow, UK
- [7] E. Aassem, 1993, *Practical simulation of buildings and air-conditioning systems in the transient domain*, PhD dissertation, University of Strathclyde, Glasgow, UK
- [8] J. Hensen, 1991, *On the thermal interaction of building structure and heating and ventilating system*, PhD dissertation, Technical University of Eindhoven, The Netherlands
- [9] H. Rijal, P. Tuohy, M. Humphreys, F. Nicol, A. Samuel, J. Clarke, 2007, *Using results from field surveys to predict the effect of open windows on thermal comfort and energy use in buildings*, *Energy and Buildings*, vol. 39, pp. 823-836
- [10] J. MacQueen, 1997, *The modelling and simulation of energy management control systems*, PhD dissertation, University of Strathclyde, Glasgow, UK
- [11] Energy Systems Research Unit, 2001, *Data Model Summary Esp-r Version 9 Series*, Energy Systems Research Unit, University of Strathclyde, Glasgow, UK
- [12] I. MacDonald, 2002, *Quantifying the effects of uncertainty in building simulation*, PhD dissertation, University of Strathclyde, Glasgow, UK
- [13] ESRU, 2001, *Flowchart of the Structure of the Main Controller of the Simulator bps, Routine mznnuma.*, ESRU Publication, University of Strathclyde, Glasgow, UK
- [14] D. Crawley, J. Hand, M. Kummert, B. Griffith, 2005, *Contrasting the capabilities of building energy performance simulation programs*, joint report of United States department of Energy, University of Strathclyde and

- University of Wisconsin; http://apps1.eere.energy.gov/buildings/tools_directory/pdfs/contrasting_the_capabilities_of_building_energy_performance_simulation_programs_v1.0.pdf
- [15] K. Haddad, I. Beausoleil-Morisson, 2001, Results of the HERS BESTEST on an energy simulation computer program, ASHRAE Transactions, pp. 713-721
- [16] P. Strachan, 2000, ESP-r: summary of validation studies; Technical report, available online: <http://www.esru.strath.ac.uk/Documents/validation.pdf>
- [17] I. Beausoleil-Morisson, P. Strachan, 1999, On the significance of modeling internal surface convection in dynamic whole-building simulation programs, Ashrae-transactions, Symposia
- [18] I. Beausoleil-Morisson, A. Ferguson, N. Kelly, 2007, Inter-model comparative testing and empirical validation of annex 42 models for residential cogeneration devices, International Energy Agency, ECBCS annex 42, operating agent I. Beausoleil-Morisson
- [19] P. Strachan, G. Kokogiannakis, I. Macdonalds, 2008, History and development of validation with the ESP-r simulation program, Building and Environment, vol. 43, pp. 601-609
- [20] M. Garcia-Sanz, 1997, A reduced model of central heating systems as a realistic scenario for analyzing control strategies, Applied mathematical modeling, vol. 21, pp. 535-545
- [21] T. Nielsen, 2005, Simple tool to evaluate energy demand and indoor environment in the early design stages of a building, Solar Energy, vol. 78, pp. 73-83
- [22] E. Mathews, P. Richards, 1989, A tool for predicting hourly air temperatures and sensible energy loads in buildings at sketch design stage, Energy and buildings, vol. 14, pp. 61-80
- [23] E. Mathews, E. van Heerden, D. Arndt, 1999, A tool for integrated HVAC, building, energy and control analysis. Part I: overview of quick control, Building and Environment, vol. 34, pp. 429-229
- [24] E. Mathews, E. van Heerden, 1999, A tool for integrated HVAC, building and control analysis. Part II: control simulations with QUICKcontrol, Building and Environment, vol. 34, pp. 451-467
- [25] CEN, 2007, Heating systems in buildings - Method for calculation of systems energy requirements and system efficiencies, Part 2-3: Space heating distribution systems, European committee for standardization.
- [26] J. Van der Veken, L. Peeters, H. Hens, L. Helsen, W. D'haeseleer, 2006, Economy, energy and ecology based comparison of heating systems in dwellings, 3rd International Buildings Physics Conference, Montreal, Canada, electronic proceedings

-
- [27] H. Ast, 1989, Energetische Beurteilung von Warmwasserheizanlagen durch rechnerische Betriebssimulation, PhD dissertation, University of Stuttgart, Germany
 - [28] G. Eisenmann, 1997, Entwicklung einer allgemeinen Bewertungsmethode für Heiz- und Trinkwasserwärmungssysteme am Beispiel einer Wohnung in einem Mehrfamilienhaus, PhD thesis, University of Stuttgart, Germany
 - [29] L. Peeters, J. Van der Veken, H. Hens, L. Helsen, W. D'haeseleer, 2008, Control of heating systems in residential buildings: Current practice, *Energy and Buildings*, vol. 40, pp. 1446-1455
 - [30] K. Kiekens, 2007, Analyse en simulatie van installaties voor de gecombineerde productie van sanitair warm water en ruimteverwarming in lage-energiewoningen, Masters thesis (Coach L. Peeters, Promotor L. Helsen.), Division of Applied Mechanics and Energy, University of Leuven (KUL), Belgium
 - [31] R. Crommelin, P. Ham, 1987, The influence of modifications in a central heating system of a dwelling on the energy consumption, calculated with a dynamic model, *Energy and Buildings*, vol. 10, pp. 1-17
 - [32] P. Weitzmann, J. Kragh, P. Roots, S. Svendsen, 2005, Modelling floor heating systems using a validated two-dimensional ground-coupled numerical model, *Building and Environment*, vol. 40, pp. 153-163

3 HEAT EMISSION/ABSORPTION ELEMENTS

Using the implicit modelling approach as described in chapter 2, a generic model needs to be set up for the simulation of any existing or fictitious heat emission/absorption element. The derivation of such a model is described in the present chapter.

Reducing any emitter to a point in the zone, the output of that emitter/absorber is an amount of convective and radiant energy. The implicit approach uses energy fluxes instead of exact temperatures and mass-flow rates in the plant model. Consequently, there is insufficient data to make a detailed analysis of the energy emission/absorption based on temperature distributions within the emission/absorption element itself and of effects due to the exact shape and location of the element within the zone. Therefore, a theoretical analysis is given showing that it is possible to accurately approximate the energy fluxes based on a limited number of empirically determined parameters.

3.1 Introduction

In the implicit modelling approach, the emitter/absorber element is considered as a point in the zone. What is of importance, are the energy fluxes emitted by the element into the zone. The temperature of the emitter's/absorber's surface is thus assumed to be equal to the average temperature of the water in it [1], [2]. The distribution of the temperatures over the surface of the emitter/absorber is neglected and the element is considered as an isothermal 'box'. The heat-transfer processes between this emission/absorption element and the zone it is located in are of two kinds: *radiation* and *convection*.

Longwave radiant heat transfer occurs between the surface of an emission/absorption element and surfaces in visible¹ contact with it. Reflection may cause radiant exchange between surfaces not in direct visible contact. Radiant heat exchange is determined by the temperature difference, properties such as the emissivity, and geometrical properties such as the surface area.

Convective heat-transfer can be natural convection or forced convection. Natural convection, or thermobuoyancy induced convection, is caused by changes in the thermo-physical properties of the air due to the temperature difference between the emitting/absorbing surface and the zonal air. The calculation of the heat flux for natural convection can be rather complex, as it depends upon, amongst others, the orientation and temperature of the emitting/absorbing surface, the location compared to other objects in the zone and the shape of the emitter/absorber. For forced convection, the movement of the air around the emitting/absorbing element is the main driving force. The heat flux for forced convection thus depends on the air velocity, and is related to geometrical properties as well as to the temperature difference between emitter/absorber and zonal air. When forced convection appears in a case with a temperature gradient, it is likely that buoyancy forces will introduce natural convection. In that case, the effects are described by the theory of mixed convection.

¹ To be exact, the range for thermal radiation is wider than the wavelengths that are in the visible range. The latter is limited to wavelengths of 0.4 μm to 0.7 μm , while the range of wavelengths for thermal radiation is from 0.1 μm to 100 μm .

The processes of radiation and convection occur simultaneously in a heat emitter/absorber. The effect of radiation is to alter the surface temperature of the emitter/absorber, which in turn influences the heat transferred by convection and vice versa. However, for transparent fluids such as air, the standard equations of convection and radiation can still be applied. The coupling is through the common influence on the emitter's/absorber's surface temperature.

Several modelling techniques for heat emission/absorption systems have been described in the literature. Lianzhong and Zaheeruddin [2] use a control-volume modelling technique for a baseboard heater. The model could be extrapolated to represent more radiant systems and the effects of forced and mixed convection. However, the required data are far too detailed for the implicit approach taken in the research reported on in this dissertation. Xu, Fu and Di [3] based their radiator model on a similar experimentally derived formula as will be used in this dissertation. They applied the formula to a heating case. However, they accepted the formula as it is, without evaluating the temperature range it could be used for. As will be shown in this chapter, the use of that formula, without improvements, is not suitable for cooling with radiators or for radiant systems in general.

Strand and Baumgartner [4], as well as Laouadi [5], derive models for radiant heating and cooling systems to be embedded in a building energy simulation code. They assume an isothermal radiating surface which they indirectly provide with heat. The processes of radiation and convection are then supposed to be described by the already embedded heat balance equations within the simulation software. This procedure is obviously not suitable for representing heat emitter/absorber elements applying forced convection. Ho et al. [6] describe a floor heating model. They assume a constant convective heat transfer coefficient. An assumption that is inadequate in case of simulation of the performance in the wider temperature range as used for both heating and cooling.

Therefore, in this dissertation, an empirically derived formula, commonly encountered in various BES programs, is analysed and is shown to accurately determine the energy output of the emitter. It is shown that the amount of convective to overall heat transfer is variable but that it can be calculated for any case using two additional parameters. Based on that discussion, the generic model of the implicit emission/absorption element is proposed.

3.2 The physics of an emission/absorption element

3.2.1 The basic processes of heat transfer: Radiation

Thermal radiation is electromagnetic radiation emitted by a body at a temperature above 0K. Net thermal radiant exchange between bodies is a function of a temperature difference between the body itself and the surroundings in visible contact². Besides the temperature difference, also the emissivity ε (-), the surface area A_r (m²) and the view factor F (-) influence the emitted/absorbed flux. The emissivity is defined as the ratio of the emissive power of the surface of interest compared to the emissive power of a black body at the same temperature. The emissivity of the heat emitter/absorber is given by the symbol ε_{emit} (-). The surface A_r is the emitter's/absorber's total surface area exposed to the surroundings. Generally, the heat transfer by radiation is given by Eq. (3.1).

$$Q_r = \varepsilon_{emit} \sigma A_r (T_{emit}^4 - T_s^4) \quad (3.1)$$

where σ is the Stefan Boltzmann constant (5.67×10^{-8} W/m²K⁴), T_{emit} (K) is the emitter's/absorber's temperature, T_s (K) is the viewfactor weighted surface temperature of the surrounding surfaces i to n as given by Eq. (3.2):

$$T_s^4 = \sum_i^n F_i T_{si}^4 \quad (3.2)$$

where the view factor F_i determines the percentage of the receiving surface i that accounts for radiant energy from the emitting/absorbing surface. F_i is a geometrical property. T_{si} (K) is the surface temperature of surrounding surface i . As mentioned by Fanger [7], for small temperature differences between the surfaces of the enclosure, the above given Eq. (3.2) can be approximated by:

² As long as it concerns non-reflecting surfaces.

$$T_s = \sum_i^n F_i T_{si} \quad (3.3)$$

As the view factor depends on the location of the emitter/absorber, the above given viewfactor weighted surface temperature of the zonal enclosure is approximated by the area weighted surface temperature. Such simplification introduces an error, which will be discussed in Chapter 4. The area weighted mean radiant temperature will further be referred to as MRT (K). Equation (3.1) can thus be rewritten as:

$$Q_r = \varepsilon_{emit} \sigma A_r (T_{emit}^4 - MRT^4) \quad (3.4)$$

This relation can be linearized to the format given by e.g. [8], [9]:

$$Q_r = A_r \bar{h}_r (T_{emit} - MRT) \quad (3.5)$$

where \bar{h}_r (W/m²K) is the surface averaged radiant heat transfer coefficient. This linearization is accurate in case:

$$\frac{1}{4} \left(\frac{T_{emit} - MRT}{\left(\frac{T_{emit} + MRT}{2} \right)} \right)^2 \ll 1 \quad (3.6)$$

For normal water-based heating/cooling installations in buildings, this condition is satisfied [9]. The linearised radiant heat transfer coefficient then equals:

$$\bar{h}_r = 4\varepsilon\sigma \left(\frac{T_{emit} + MRT}{2} \right)^3 \quad (3.7)$$

3.2.2 The basic processes of heat transfer: Convection

Convection is heat transfer that is due to the movement of fluid particles along an element at a different temperature. In case of natural convection, the fluid flow is

induced by buoyancy forces. Forced convection occurs when the fluid flow is caused by external forces as a fan or pump.

The convective heat transfer coefficients are generally presented as a function of dimensionless numbers: Reynolds number, Re (-), Prandtl number, Pr (-), and Grashof number (-). They are given by Eqs. (3.8), (3.9) and (3.10) respectively.

$$Re = \frac{VL}{\nu} \quad (3.8)$$

V (m/s) is the air velocity, L (m) is a characteristic length and ν (m^2/s) is the kinematic viscosity.

$$Pr = \frac{\nu}{\alpha} \quad (3.9)$$

α (m^2/s) indicates the thermal diffusivity.

$$Gr = \frac{gL^3\beta_v\Delta T}{\nu^2} \quad (3.10)$$

where g is the gravitational acceleration (m/s^2), β_v is the volumetric thermal expansion coefficient ($1/K$), ΔT (K) the difference between the free stream and the surface temperature of the emitting/absorbing element.

3.2.2.1 *Natural convection*

The heat transfer in the very first layer of fluid next to the surface takes place by conduction. Heat is then transferred by convection to or from the surrounding air through a boundary layer. Gravitation then causes the lighter warmer air to move upwards, the heavier colder air to go downwards. This process is known as natural, or thermobuoyancy-driven, convection. In case of vertical emitting surfaces with no non-vertical constraints close to it, the thermally induced flows are parallel to gravitation. In case of non-vertical obstacles or inclined emitting/absorbing planes, the flow is somewhat slowed down.

It is thus clear that the natural convective heat transfer, $Q_{c,n}$ (W), is correlated to the temperature difference, as shown by the convective heat transfer equation:

$$Q_{c,n} = \bar{h}_{c,n} A_{c,n} (T_{emit} - T_a) \quad (3.11)$$

where $\bar{h}_{c,n}$ (W/m²K) is the surface averaged natural convective heat transfer coefficient, $A_{c,n}$ (m²) is the surface of the emitter/absorber in contact with the fluid – here air, T_{emit} (K) the above mentioned temperature of the emitter/absorber and T_a (K) the temperature of the surrounding fluid, in this case air³.

The convective heat transfer coefficient itself, $\bar{h}_{c,n}$, is a function of the geometry and location of the heat emitting/absorbing element, and properties of the fluid surrounding the element. Those properties are evaluated at film temperature, i.e. the mean of the free stream temperature and the surface temperature. In the literature several correlations have been described for convection coefficients in different set ups ([10], [11], [12], [13], [14]). $\bar{h}_{c,n}$ is generally given as a function of the dimensionless Rayleigh number (Ra):

$$\bar{h}_{c,n} = cRa^n \quad (3.12)$$

where c (W/m²K) and n (-) depend on the geometry. The Rayleigh number is a product of the dimensionless Grashof (Gr) and Prandtl (Pr) numbers. The former is related to the temperature difference as well as on geometrical properties and both depend on temperature related physical properties.

However, in this dissertation, it is assumed that for a given emission/absorption element with a given geometry, $\bar{h}_{c,n}$ is a function of the temperature difference $T_{emit} - T_a$ only (Eq. (3.13)). The error by accepting this simplification is discussed in Chapter 4.

³ The reference air temperature is considered as the temperature of the air in the middle of the zone at around 1.2 m height. In this dissertation, this is considered to be the temperature of the node representing the zonal air.

$$\bar{h}_{c,n} = a(T_{emit} - T_a)^b \quad (3.13)$$

with a ($\text{W}/\text{m}^2\text{K}^{1+b}$) and b (-) constants for a given emitter/absorber geometry. The simplification of accepting these coefficients a and b as being constant is in accordance with [15], [16] and is as used by Gong and Claridge [17] for their research on heat radiator positions.

Table 3-1 shows geometry-dependent correlations for a and values for the power coefficient b for some heat emitter/absorber configurations. It should be noted that free convection correlations for more complicated configurations are hardly described in the literature (indicated in the table below by NA: not available). However, the power coefficient b can generally be found. It is this coefficient that is of importance in the further analysis described in the current chapter.

Emitter type	a	b
Heated floors/Cooled ceilings	2.13	0.31
Heated ceilings	$0.704/D^{0.601}$	0.133
Partly heated ceiling	$1.736/D^{0.52}$	0.16
Heated wall	$1.823/D^{0.121}$	0.293
Vertical or inclined surface	NA	1/3
Cooled floor	0.134	1/4
Multiple plates connected by fins	NA	0.4
Tubes with fins in casing	NA	0.5

Table 3-1: Values of coefficient a and power-factor b for natural convection according to the expression $\bar{h}_n = a(T_{emit} - T_a)^b$ ([12], [14], [15], [17], [18], [19]). D indicates the hydraulic diameter (m) which is the ratio of $4 \times$ Area over the wetted perimeter.

3.2.2.2 Forced convection

When the fluid flow is induced by external means, the process is termed forced convection. As the particles are moving faster compared to the case of natural

convection, it is clear that forced convective heat transfer will generally be more effective.

The general format of the equation for forced convection equals that of natural convection:

$$Q_{c,f} = \bar{h}_{c,f} A_{c,f} (T_{emit} - T_a) \quad (3.14)$$

where $Q_{c,f}$ (W) is the forced convective heat flux, $\bar{h}_{c,f}$ (W/m²K) is the surface averaged forced convective heat transfer coefficient, $A_{c,f}$ (m²) is the surface of the emitter/absorber in contact with the moving fluid – here air, T_{emit} (K) the above mentioned temperature of the emitter/absorber and T_a (K) the temperature of the surrounding fluid, i.e. air.

Contrary to natural convection, no general format can be given for the forced convection coefficient. This coefficient strongly depends on the geometry of the heat emission/absorption element, which can be seen by comparing Eqs. (3.15), (3.16) and (3.17) valid for flow over a flat plate or across a cylinder, cross-flow over a cylinder and flow over a sphere respectively.

$$\bar{h}_{c,f} = c \text{Re}^n \text{Pr}^m \quad (3.15)$$

$$\bar{h}_{c,f} = \frac{\lambda}{D} \left[0.3 + \frac{0.62 \text{Re}^{1/2} \text{Pr}^{1/3}}{\left(1 + \left(\frac{0.4}{\text{Pr}}\right)^{2/3}\right)^{1/4}} \left(1 + \left(\frac{\text{Re}}{28200}\right)^{5/8}\right) \right]^{4/5} \quad (3.16)$$

$$\bar{h}_{c,f} = \frac{\lambda}{D} \left[2 + (0.4 \text{Re}^{1/2} + 0.06 \text{Re}^{2/3}) \text{Pr}^{0.4} \left(\frac{\mu_\infty}{\mu_s}\right)^{1/4} \right] \quad (3.17)$$

where c (W/m²K) is a constant, n (-) and m (-) are dimensionless constants, λ is the thermal conductivity (W/mK), D is the cylinder or sphere's diameter (m) and μ_∞

(kg/ms) and μ_s (kg/ms) refer to the dynamic viscosity of the zone air and emitter's/absorber's surface respectively.

Because the forced convection coefficient can not be written in a geometry-independent format, forced convection can not be considered in detail in the implicit approach⁴ and is therefore not considered in the current analysis.

3.2.2.3 *Mixed convection*

Forced convection will seldom appear solely in case of water-based heating/cooling systems in residential buildings. Whether both forced and natural convection need to be taken into account or whether one could be neglected depends on the Archimedes number, i.e. the ratio Gr/Re^2 . If the Archimedes number is much smaller than 1, forced convection is dominant and natural convection could be neglected. An Archimedes number much higher than 1 implies the opposite, i.e. natural convection dominates. For an Archimedes number close to 1 both forced and natural convection need to be taken into account. Commonly encountered correlations for convection coefficients for mixed convection $\bar{h}_{c,m}$ (W/m²K) are based on those for natural and forced convection:

$$\bar{h}_{c,m}^k = \bar{h}_{c,f}^k \pm \bar{h}_{c,n}^k \quad (3.18)$$

where k is an exponent depending on the configuration and flow direction. Whether to add or subtract the convection coefficient for natural convection from the one for forced convection depends on the flow direction: adding is for assisting or transverse flows, subtracting is for opposing flows.

It should be noted that the above given correlation for mixed convection is a first approximation only. More accurate correlations can be found in amongst others [11]. As mentioned above, forced convection will not be discussed further in the current analysis, the discussion of mixed convection in the context of the implicit

⁴ This can be changed easily afterwards, but requires more detailed model input data. For the aim of the optimisation here, however, the shape-independency is crucial.

approach is limited to Appendix A. In that appendix the formulation is given for a case of assisting flows.

3.3 An empirically derived formula for the heat output

All processes possibly involved in water-based heat emission/absorption have been theoretically described above. However, relationships often encountered in the literature are based on experimental data. A commonly used empirically-based formula will be analysed hereafter. Based on this analysis for a non-specified element, a general format for an emission/absorption element can be set up. Such format can be used in the implicit plant modelling approach.

3.3.1 Steady-state thermal output

The steady-state heat emission, Q_{emit} (W), of a radiator is correlated to the difference ΔT (K) between the mean radiator temperature and the zonal temperature. A well-known relationship to quantify this steady-state emission is given by:

$$Q_{\text{emit}} = Q_{\text{emit},N} \left(\frac{\Delta T}{\Delta T_N} \right)^n \quad (3.19)$$

$Q_{\text{emit},N}$ (W) is the radiator output in reference conditions, or so-called nominal conditions⁵. ΔT_N is the temperature difference between emitter and room air for the nominal case. In this formula ΔT and ΔT_N use the arithmetic mean of the water inlet and exit temperature of the radiator. n is the dimensionless radiator exponent, with typical values in the range of 1.1 to 1.4. The same approach is used in standards, as

⁵ The nominal conditions were defined during IEA ECBCS annex 10 [20] as a water supply temperature of 90°C, a water exit temperature of 70 °C (thus average radiator temperature approximately 80°C) and indoor air equal to mean radiant zonal temperature and set to 20°C. And thus $\Delta T = 60$ K. In the EN 442 [21], the nominal temperature difference has been decreased to 50 K.

the European EN 442⁶ [21] for testing and rating of radiators and convectors and prEN 15377 for embedded water-based surface heating and cooling systems [22].

As Stephan mentions in the IEA ECBCS annex 10 report [20], the relation (3.19) is not valid for low mass-flow rates when a temperature difference calculated based on the arithmetic mean of the radiator is used. He therefore proposed using a logarithmic temperature difference:

$$\Delta T_{\text{lg}} = \frac{T_{\text{su}} - T_{\text{ex}}}{\ln \left(\frac{T_{\text{su}} - T_{\text{ex}}}{T_{\text{ex}} - \frac{(T_{\text{a}} + MRT)}{2}} \right)} \quad (3.20)$$

with T_{su} (K) the radiator water supply temperature, T_{ex} (K) the radiator water exit temperature, T_{a} (K) the zone air temperature and MRT (K) the mean radiant temperature.

Using a so-defined temperature difference, results in a somewhat different value for the radiator exponent n . Stephan mentions [20] the so-derived radiator exponent to be nearly the same⁷ as the one based on the arithmetic mean temperature difference. Stephan therefore proposes to use this last n -value. For small temperature differences, Stephan [20] and Hensen [23] mention that the above given equation (3.20) might cause numerical instability and therefore the difference calculated based on the arithmetic mean should be used in those cases.

⁶ This standard also lists the nominal fraction of radiant heat output to overall heat output for different configurations. According to the nomenclature used in current dissertation this fraction of radiation is referred to as $(1-\alpha_N)$.

⁷ For a range of data as provided by Stephan [20], the difference was calculated by the current author and it did not exceed the value of 0.5%.

The use of equation (3.19) in combination with (3.20) is commonly encountered in building simulation: *TRNSYS* [24], *IDA Ice* [25] and *ESP-r*⁸ [26] all use this approach.

3.3.2 Cooling

No references have been found that validate or disprove the use of the empirical relationship for cooling (i.e. ‘absorption’ in the context of the emission/absorption element). Mathematically, the formula is not automatically suitable for cooling. However, introducing absolute values for temperature differences solves that problem:

$$Q_{emit} = \frac{\Delta T}{|\Delta T|} Q_{emit,N} \left(\frac{|\Delta T|}{\Delta T_N} \right)^n \quad (3.21)$$

3.3.3 Thermally activated building elements

The empirical formula is set up for radiators and convectors. However, a similar formula is often used for floor heating and ceiling cooling systems, generally termed Thermally Activated Building (TAB) elements as well [22]. The question then rises whether floor cooling and ceiling heating can be modelled with the same formula. The European standard prEN 15377 [22] applies a fixed overall heat transfer coefficient, i.e. combined radiant and convective, for such cases as well as for wall heating and cooling. The validity of the above given empirical radiator formula for TAB elements will be discussed later in this chapter as well as in chapter 4.

3.3.4 Introducing dynamics

The dynamical performance of the radiator is given by applying the conservation of energy principle. Using the arithmetic mean radiator temperature, this results in:

⁸ The plant level in *ESP-r* allows the user to select a 2- or an 8-node radiator model. The latter is more complex, but results in more realistic performance data.

$$C_{emit} \frac{\partial T_{emit}}{\partial t} = Q_{pl} - Q_{emit} = Q_{pl} - Q_{emit,N} \left(\frac{\Delta T}{\Delta T_N} \right)^n \quad (3.22)$$

where C_{emit} (J/K) represents the total capacity of the emitter, t (s) is the time and Q_{pl} (W) is the thermal power flux a radiator receives, through the distribution system, from the production system. Here the emitted thermal power flux Q_{emit} (W) has been substituted by the relation given in Eq. (3.19).

It is clear that using this formula, it is assumed that the radiator heats up uniformly. The accuracy of this assumption strongly depends on the radiator configuration and this will be discussed in chapter 4.

3.4 Linking the empirically derived formula with theory

In this section, the described empirically derived formula is linked with the above given theory of the different processes possibly involved in water-based heating/cooling.

3.4.1 An amount of radiation and an amount of convection

Theoretically, any heat emitter/absorber exchanges an amount of heat with the environment by both radiation and convection:

$$Q_{emit} = Q_r + Q_{c,n} \quad (3.23)$$

Assuming a constant linear relation for the radiant heat transfer (Eqs. (3.5) and (3.11)), this can be rewritten as:

$$Q_{emit} = \bar{h}_r A_r (T_{emit} - MRT) + \bar{h}_{c,n} A_{c,n} (T_{emit} - T_a) \quad (3.24)$$

And further simplified to:

$$Q_{emit} = C_1 (T_{emit} - MRT) + C_2 (T_{emit} - T_a)^{b+1} \frac{(T_{emit} - T_a)}{|T_{emit} - T_a|} \quad (3.25)$$

with C_1 (W/K) considered as being constant over a limited temperature range. C_2 (W/K^{b+1}) is a temperature independent constant.

Replacing the emitter's/absorber's output, Q_{emit} , by the empirically proposed Eq. (3.21), thereby using the arithmetic mean of the emitter's temperature, results in:

$$\left(\frac{\Delta T}{|\Delta T|} \right) (\Delta T) Q_{emit,N} \left(\frac{|\Delta T|}{\Delta T_N} \right)^n = C_1 (T_{emit} - MRT) + C_2 (T_{emit} - T_a)^{b+1} \frac{(T_{emit} - T_a)}{|T_{emit} - T_a|} \quad (3.26)$$

This relationship should be correct in the nominal conditions:

$$Q_{emit,N} = C_1 \Delta T_N + C_2 \cdot \Delta T_N^{b+1} \quad (3.27)$$

where ΔT_N (K) is the positive difference between nominal average emitter/absorber temperature and nominal room temperature. Note that for the EN442-nominal case the zonal air temperature T_a equals the zonal mean radiant temperature MRT.

In the proximity of the nominal conditions also the slope, or the first derivative to the temperature difference, should be the same for both the empirically established and the theoretical formula:

$$\frac{Q_{emit,N}}{\Delta T_N^n} n \Delta T_N^{n-1} = C_1 + C_2 (1+b) \Delta T_N^b \quad (3.28)$$

For the nominal conditions, also the fraction of convection α_N (-) should be similar for both the empirically established and the theoretical formula:

$$\alpha_N Q_{emit,N} = C_2 (T_{emit} - T_a)^{b+1} \quad (3.29)$$

Combining Eqs. (3.27), (3.28) and (3.29) allows calculating the constants C_1 , C_2 and determining the relation between n , α_N and the power coefficient b :

$$C_1 = \frac{Q_{emit,N}}{\Delta T_N} (1 - \alpha_N) \quad (3.30)$$

$$C_2 = \frac{Q_{emit,N} (n-1)}{\Delta T_N^{1+b} b} \quad (3.31)$$

$$\alpha_N = \frac{(n-1)}{b} \quad (3.32)$$

3.4.2 Extrapolating the correlations

So far, the empirically established formula has only been used for the nominal case.

Considering the radiant heat transfer, the value of C_1 , depends on material and geometrical properties of the surface of the emission element, on the average of the emitter's/absorber's and zonal surface temperatures and on its location in the zone. Hence, it is valid for any combination of emitter/absorber and room air and surface temperatures and for any type of emitter/absorber. Consequently, there is no theoretical argument to not accept this value for cooling with a heat emission/absorption element as long as the condition for the linearization of the radiant heat transfer coefficient is fulfilled (Eq. (3.6)).

For natural convection, the convection coefficient depends on a and b . For a given configuration, a and b are constant for the case the emitter is heating the zone. This is valid for any type of emitter, whether it is a convector, a radiator or a zone's surface. Mohammadi et al. [15] studied convection in a radiator-heated dwelling cell. The radiator is composed of a single pane, with some lamella at the back side. The authors of that publication analysed the heat transfer processes and concluded

convection correlations for the front side to be valid at the back side of the radiator as well.

If the flow is not hindered in the proximity of the emitting/absorbing element, the value of b is the same for both heating and cooling. This is correct in case of vertical emission/absorption elements [27]. However, the proximity of especially horizontal disturbances will influence the flow pattern as will the temperature of the element itself. The resulting stratification is described for well-controlled test conditions by amongst others Marret [28]. He performed multiple tests in a test chamber with variation of radiator types and positions, thermal quality of the window and building envelope and changes in infiltration rate. Marret indicated an infiltration rate of 0.7 AC/h to positively affect the temperature stratification in the room. As expected, the temperature distribution showed to be affected by the location of the radiator in the zone. However Marret showed the effect to be less important when using a better insulated zonal enclosure and applying an improved window quality. Myhren and Holmberg [29] tested the influence of different heating elements on the temperature stratification and the air velocity in a testroom. They observed considerable differences in temperature distribution over the whole room depending on emitter's geometry and temperature as well as a considerable impact of the applied ventilation strategy. Effects of stratification and more general additional losses due to non-optimal emitter locations are also described in [30] and [31]. Based on this overview, it is clear that the implicit model - using a 1-node approach - cannot account for such location and configuration dependent effects. Therefore, the vertical emitting/absorbing elements will be characterized by a single convective heat transfer coefficient.

Horizontal surfaces emitting/absorbing heat will result in an even more stratified temperature distribution in the room. For floor heating systems, Table 3-1 shows a value of 0.308 for b . In such configuration, the heated air is not limited in its upwards movement. However, in case of using the same system for cooling, a layer of cold air is formed above the absorbing floor. Theoretically, the flow in this layer is limited. Values of 0.2 for b in case of a cooling horizontal surface facing upwards, have been reported in the literature [12]. The same, but opposite effects will occur for a ceiling heating. Most of the correlations found in the literature are based on experiments in well-controlled non-ventilated and empty rooms. The reported correlations for floor heating and for ceiling cooling show some agreement (Figure 3.1). The correlation found for floor cooling and ceiling heating, however, show considerable deviations one from another (Figure 3.2).

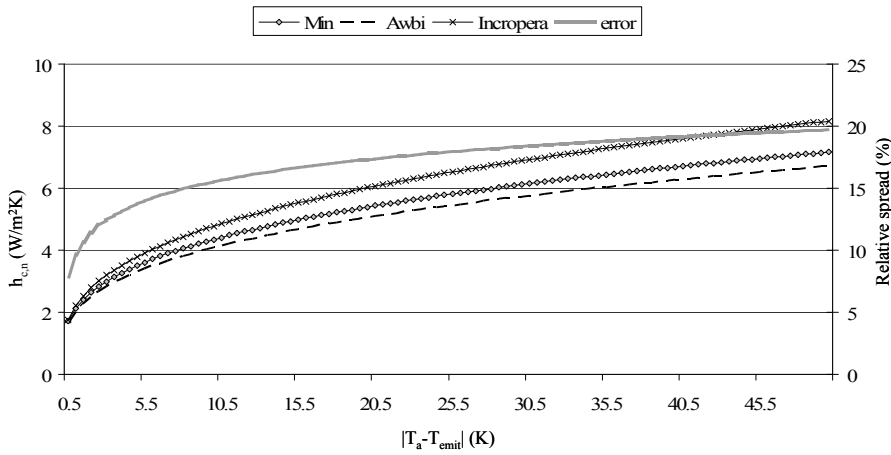


Figure 3.1: Comparison of different correlations for convection coefficients for ceiling cooling or floor heating cases as a function of absolute value of the temperature difference between air, $T_a(K)$ and emitter/absorber $T_{emit}(K)$. Left hand vertical axis gives the convection coefficient for natural convection for the different correlations, the right vertical axis shows the relative spread defined as the difference between the highest and the lowest coefficient divided by the average of the three coefficients.

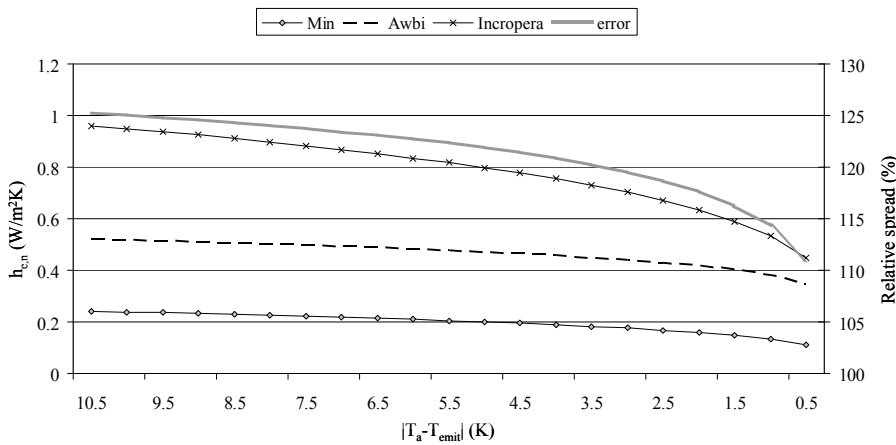


Figure 3.2: Comparison of different correlations for convection coefficients for ceiling heating or floor cooling as a function of the absolute value of the temperature difference between the air, $T_a(K)$ and emitter/absorber $T_{emit}(K)$. Left hand vertical axis gives the convection coefficient for natural convection for the different correlations, the right vertical axis shows the relative spread defined as the difference between the highest and the lowest coefficient divided by the average of the three coefficients.

Min [32] reports a correlation set up based on measurement data of a non-ventilated 3-dimensional room. Also Awbi and Hatton [33] derived their correlation based on experiments in a full-scale test room without ventilation. The correlation given by Incropera and Dewitt [34] is for horizontal plates where no edge-conditions are considered. As can be seen in the above figures this leads to an overall higher value for the convective heat transfer coefficient.

In the real context of a residential building, the stratified lower layer of cold air in case of floor cooling will be activated by people moving around and by infiltration of fresh air. This will increase the value of the convection coefficient for natural convection. For the case of a ceiling heating, the effects will be less pronounced and the convection coefficients will be closer to those given in the figures above. The reason is that disturbances in the top layer are less likely as people moving around and cold fresh air will mainly affect the colder lower layers [29]. This tendency of higher convection coefficients for floor cooling compared to ceiling heating is confirmed by the values given by the European standard for embedded emitting/absorbing systems [22]. Also the Rehva guidebook on low temperature heating and high temperature cooling [35] indicates the same tendency: $1.5 \text{ W/m}^2\text{K}$ for floor cooling and $0.5 \text{ W/m}^2\text{K}$ for ceiling heating. The latter value agrees well with the correlation of Awbi shown in the above Figure 3.2. For floor cooling values in the range of the REHVA-coefficient of $1.5 \text{ W/m}^2\text{K}$ were calculated by Michel et al. [36] based on the results of their extended lab study. They varied a range of parameters ending up with an average convection coefficient for floor cooling in the range of $1.6 \text{ W/m}^2\text{K}$. The infiltration rate in the test chamber used by Michel et al. varied from 0.5 to 1 AC/h and furniture was added in order to achieve conditions comparable to those in offices and residential buildings. The average value of $1.6 \text{ W/m}^2\text{K}$ showed to increase with increasing temperature difference between cooling floor and room air temperature. However, not enough data were shown to allow setting up a well-fitted correlation. These values of $1.6 \text{ W/m}^2\text{K}$ and $1.5 \text{ W/m}^2\text{K}$ are higher than the suggestions of Awbi et al. [33]. It can be explained by the before mentioned less pronounced effect of disturbances on stratified layers close to the ceiling compared to layers above the floor. Awbi et al. did not consider such disturbances in their experiments.

It is clear that stratification is an important effect when evaluating thermal comfort. It has also been shown by the above mentioned authors that not only the characteristics of the element, but especially its location in the zone, the thermal

quality of the zonal enclosure, including the transparent parts, as well as the infiltration/ventilation strategy will be of importance.

Stratification will partly be reduced by the above described effect of flow due to people moving around, opening doors, etc. Moreover, the discomfort associated with stratification will stimulate the use of facilities increasing intra-zonal air circulation. The effect of increased air movements due to ventilation can result in local convection coefficients being up to 10% higher than expected, as mentioned by Wallenten [16]. He further emphasizes setting up accurate correlations to be difficult, also due to the lack of experimental data for realistic cases.

It can thus be concluded that the real value of b will be somewhat 'variable'. As described above, the largest variation will occur in the horizontal emitting/absorbing surfaces. Therefore, in this dissertation a difference is made between mainly vertical emitting/absorbing elements and horizontal elements. These last ones are assumed to be embedded in a horizontal part of the zonal enclosure; either the floor or the ceiling. For these elements, the correlations for floor heating and ceiling cooling will be temperature dependent and thus of the format given by Eq. (3.13), while due to lack of more accurate correlations a constant convection coefficient ([35]) for cooling floors and heating ceilings will be used. The resulting calculation thus depends on the element modelled, as schematically presented in Figure 3.3:

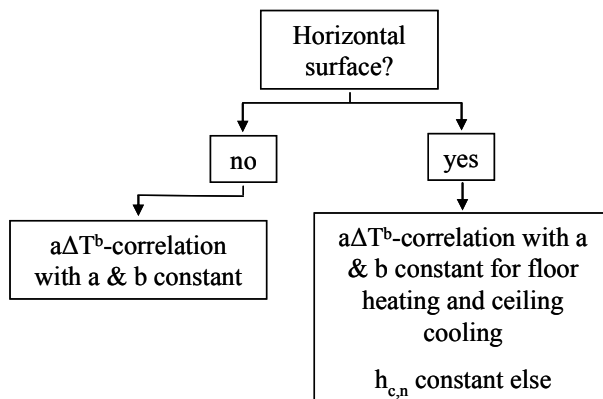


Figure 3.3: Schema showing the calculation methodology for the convective heat transfer coefficient as a function of the element modelled.

The above given discussion emphasizes the importance of a thorough CFD-analysis once the optimal characteristics of the emitter are defined. A far-from optimal

location in the zone can drastically reduce the effects of a well-designed emitter/absorber. Furthermore, it is clear that there is still a lot to be done on the determination of convection coefficients in residential settings and their sensitivity to commonly encountered disturbances such as people moving around, infiltration/ventilation patterns and furniture.

3.5 Comparing the empirically derived formula with theory

The empirically derived formula has now been linked to the theory. The coefficients for radiation and natural convection can be calculated based on the data of the nominal case⁹. The results for a purely theoretically calculated output will now be compared to the results based on the empirical relationship. This will be done for a general case and not for the specific cases of heating ceilings and cooling floors.

3.5.1 An amount of convection and an amount of radiation

The empirically derived formula assumes a linear relation with the temperature difference for the radiant emission. The convective heat flux is proportional to the $(b+1)^{\text{th}}$ power of the temperature difference.

Reducing the empirically based relation to the terms related to these temperature dependencies, results in:

$$\left(\frac{\Delta T}{|\Delta T|} \right) \Delta T^n \quad (3.33)$$

Applying the same reduction to the theoretical formulation, results in:

⁹ Except for a emitter/absorber that is a horizontal TAB where the nominal condition is a cooling case for a floor TAB and a heating case for a ceiling TAB.

$$x\Delta T + \left(\frac{\Delta T}{|\Delta T|} \right) (1-x) |\Delta T|^{b+1} \tag{3.34}$$

where x (-) indicates a fraction of radiation.

These functions (Eqs. (3.33) and (3.34)) are plotted in Figure 3.4. The value of ΔT^n , which in fact shows the course of the empirically established formula, is plotted for radiator exponents of $n=1.1$ and $n=1.3$. The course of the function given by Eq. (3.33), further referred to as $f(x)$, is shown for b equal to $1/3$ and for a variation in x -values. This x indirectly indicates the percentage of radiant compared to the overall output.

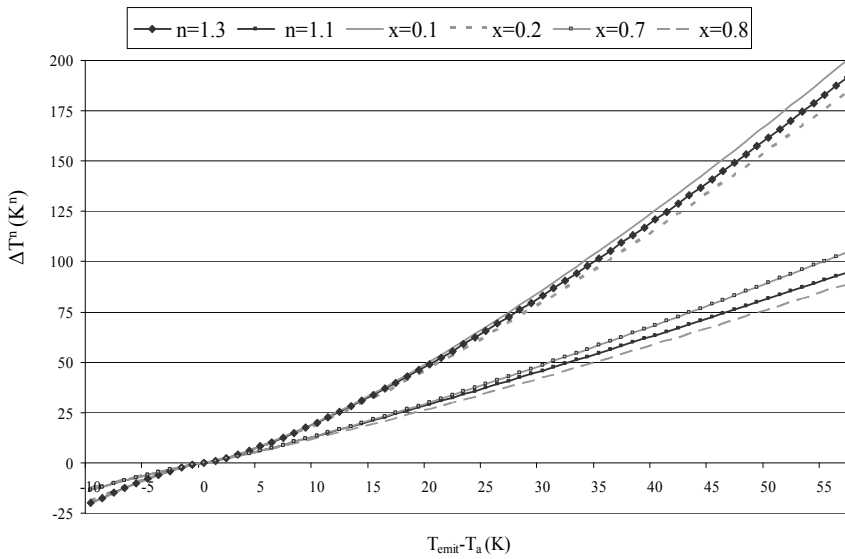


Figure 3.4: Course of ΔT^n as a function of the temperature difference between emitter/absorber and air for $n=1.1$ and $n=1.3$, indicated in black, and $x\Delta T + \left(\frac{\Delta T}{|\Delta T|} \right) (1-x) |\Delta T|^{b+1}$ for variable x -values for a case with $T_a=MRT$ and $b=1/3$, indicated in grey.

The chart shows the curve for ΔT^n for n equal to 1.3 to be in between those of $f(x)$ for x equal to 0.1 and 0.2. For ΔT^n with n much smaller, i.e. equal to 1.1, the curve is situated in between those of the functions $f(x)$ for x -values of 0.7 and 0.8. It thus

indicates that for high values of the radiator exponent, the amount of natural convection is high. Highly radiant emitters/absorbers (x rather high) are indicated to result in low n-values. This emphasises the empirically established formula relying on a linear relationship for these phenomena.

To calculate the radiant heat transfer characteristics, Eqs (3.5) and (3.7) can be combined:

$$\varepsilon\sigma A_r = \frac{8C_1}{4(T_{emit,N} + MRT_N)^3} \quad (3.35)$$

The emissivity, ε (-), the Stefan Boltzmann constant, σ (W/m²K⁴), the viewfactor, F (-) and the surface area for radiation, A_r (m²), are all temperature independent. The radiant output for any non-nominal temperature difference can consequently be calculated correctly, based on Eqs. (3.1) and (3.35):

$$Q_r = \frac{8C_1}{(T_{emit,N} + MRT_N)^3} (T_{emit}^4 - MRT^4) \quad (3.36)$$

By applying this formula for calculation of the radiant output, the outcome will differ from what is calculated based on the linear temperature dependency as indirectly embedded in the empirically established formula. The latter assumes a constant radiant heat transfer coefficient, of which the value is determined by the nominal conditions. The difference will increase for cases further removed from the nominal conditions. Consequently, a more radiant emitter/absorber results in a larger relative approximation, i.e. the ratio of the empirically calculated versus the theoretically calculated output. This ratio, expressed in percentages, is shown in Figure 3.5.

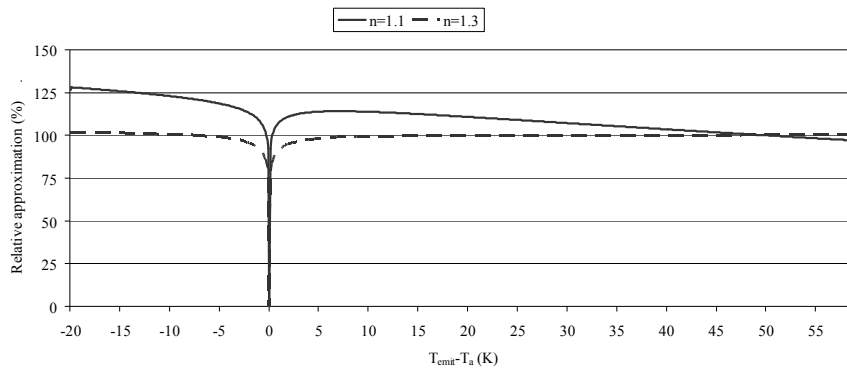


Figure 3.5: Relative approximation of empirically calculated versus theoretically calculated total energy output of a heat emission/absorption element for a case with $T_a = MRT$ and a nominal condition $T_{a,N} = MRT_N = 20^\circ\text{C}$, $\Delta T_N = 50\text{K}$, and $b = 1/3$, for $n = 1.1$ and $n = 1.3$.

The relative approximation, as shown in Figure 3.5, is indeed worse for lower n -values. The overestimation of the radiant energy emission is due to the high average emitter/absorber temperature in the nominal condition.

For small temperature differences, Figure 3.5 shows the relative approximation to be significant. The explanation is given by equation (3.37).

$$\lim_{T_{emit} \rightarrow MRT} (T_{emit}^4 - MRT^4) \gg (T_{emit} - MRT) \quad (3.37)$$

When the average emitter temperature is exactly equal to the zonal air temperature, no heat output occurs. Both calculation methods will then result in a zero output. However both calculation methods show a continuous and smooth behaviour, the calculation of their ratio causes a numerical discontinuity. This can be seen in the above given Figure 3.5.

3.5.2 The amount of convection compared to the total energy output of the heat emitter/absorber

Currently, the actuating point in the zone by use of an *ESP-r* zone controller can emit/absorb a fixed amount of convective heat and thus also a fixed amount of radiant heat. Also Xu et al. [3] use a constant ratio between convection and radiation. They refer to a publication where the convective and radiant output of

normal radiators has been measured, but give no description on the circumstances, the temperature range or the accuracy. The graphs of the measurement data [37] on which they based their assumption, show a temperature range of 50°C to 70°C for the average temperature of the emitter. And even for the small temperature range considered, the graphs indicate non-negligible changes to the ratio of convection to overall output. The average fraction of convection of an emitter further shows to strongly depend on its shape.

Figure 3.6 shows the percentage of convective over total heat emitted by an emission element with an average radiator exponent of $n=1.2$ and $\Delta T_N=50$ K. The average percentage of convection over total thermal output, excluding the discontinuity at zero temperature-difference, is 52.8% when calculated theoretically and 49% with the empirical formula, with standard deviations of 7.7 and 6.3 respectively.

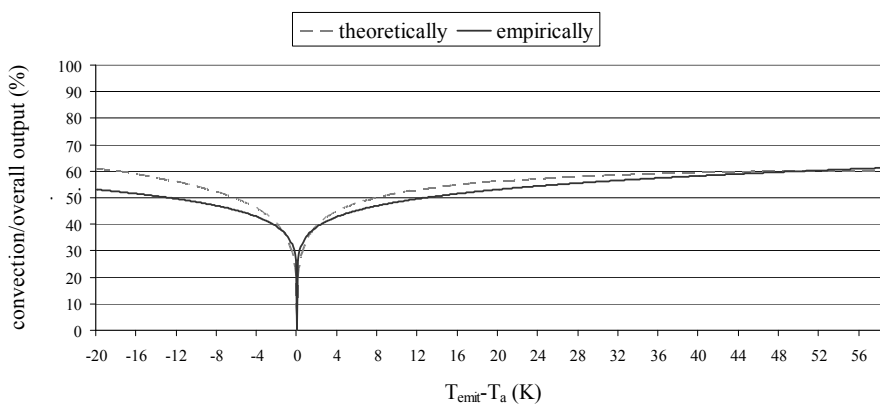


Figure 3.6: % convective energy output versus total energy output of a heat emission/absorption element calculated based on a nominal case with $n=1.2$, $\Delta T_N=50$ K, $T_{a,N}=MRT_N=20^\circ\text{C}$ and $b=1/3$.

Furthermore, Figure 3.6 shows that the percentage of convection can only be considered constant when the difference $T_{\text{emit}}-T_a$ varies over a limited range. The agreement between the results for the empirically established formula and the theoretical calculation is limited in case of cooling (deviation of up to 8 percent points) and in case of small to moderate positive ΔT (deviation of up to 4 percent points). This can be explained by the above described effect of the overestimation of the radiant part due to the use of a linear radiant heat transfer coefficient calculated based on a nominal condition characterised by a high average emitter/absorber temperature.

3.6 The effect of changes to the empirically derived formula

Based on the above given comparison between theoretical and empirical correlations, the weaknesses of the empirical formula have been demonstrated. In the section hereafter some changes are proposed so as to improve the agreement between empirically derived relation and theory.

3.6.1 Using the average fraction of convection to calculate the room temperature

A minor improvement compared to the formula is the use of a weighted average of the mean radiant temperature, MRT^{10} , and the air temperature, T_a . Using the average ratio of heat emitted/absorbed by convection over the total energy output, α , as a weighing factor, results in an 'adjusted' ΔT given by:

$$\Delta T = T_{emit} - (\alpha \cdot T_a + (1 - \alpha) \cdot MRT) \quad (3.38)$$

The effect of such a correction is shown by Figure 3.7, for a case with a radiator exponent of $n=1.3$, ΔT_N of 50 K, b of $1/3$, air temperature T_a of 22 °C and mean radiant temperature MRT of 20 °C. The empirical calculation is performed using 50% air, 50% mean radiant temperature split as suggested by Stephan [20]. It is clear that the adjusted temperature difference increases the accuracy of the results, even for the plotted case having a small amount of radiation.

¹⁰ The calculation of the MRT as used for TAB's will be discussed in the section on the implicit emitter/absorber model in the current chapter.

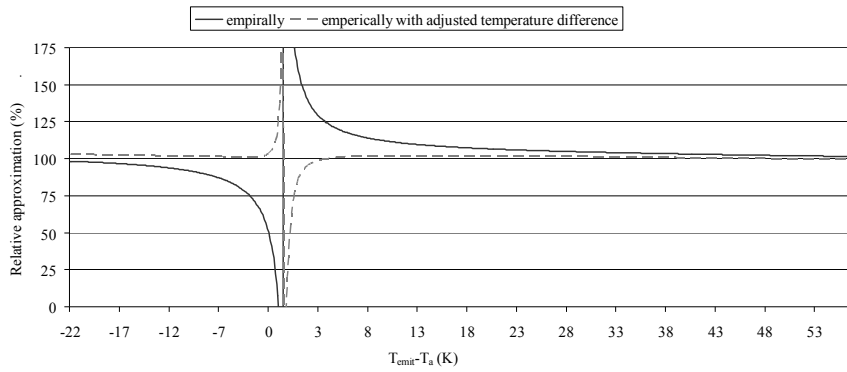


Figure 3.7: Relative approximation of heat output empirically calculated (based on Eq. (3.19)), without and with adjusted temperature difference, compared to theoretical calculation in case $T_a=22^\circ\text{C}$ $MRT=20^\circ\text{C}$ and with $T_{emit,N}=70^\circ\text{C}$, $T_{a,N}=MRT_N=20^\circ\text{C}$, $b=1/3$ and for $n=1.3$.

The effects that occur for temperature differences $T_{emit}-T_a$ approaching 0 are again due to discontinuities resulting from the calculation of a ratio of two values approaching 0. The difference between T_a and MRT results in a relatively larger portion of positive radiant energy emission for emitter/absorber temperatures close to, but smaller than the MRT. The overall energy emission for the theoretical calculation is positive. In contrast, for the conditions whereby T_a -MRT is slightly positive, the empirical calculation results in a negative energy emission.

3.6.2 Choosing average conditions as nominal conditions

The use of an adapted nominal condition can further improve the accuracy of the results, as can be seen in Figure 3.8. The results are shown for an empirical versus theoretical calculation with $T_{emit,N}=70^\circ\text{C}$ and for $T_{emit,N}=38.5^\circ\text{C}$. For the theoretical calculation, the heat transfer coefficients for convection and radiation are based on Eqs. (3.31) and (3.35) respectively. The graph shows that the use of nominal conditions close to the temperature range of interest, improves the overall accuracy of the empirical formula: an average accuracy of 114.0% for the $T_{emit,N}=70^\circ\text{C}$ – conditions versus 102.6% for the average nominal conditions.

Again the discontinuity shown is due to calculating the ratio of two values approaching 0. The formulas themselves are continuous.

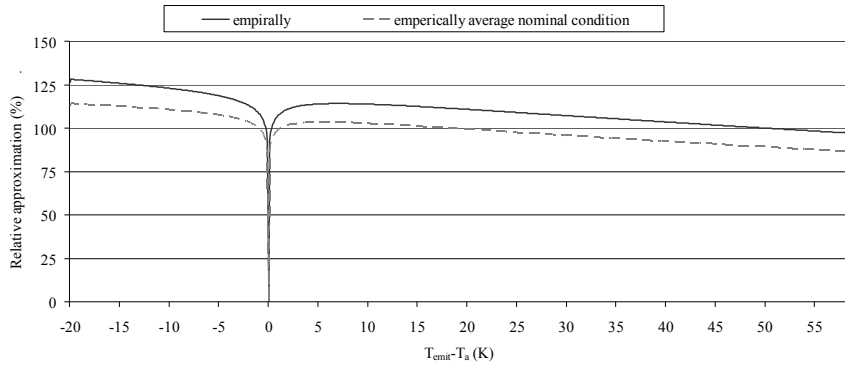


Figure 3.8: Relative approximation of empirically calculated versus theoretically calculated heat output with $T_{emit,N}=70^{\circ}\text{C}$ and a more average $T_{emit,N}=38.5^{\circ}\text{C}$ respectively for a heat emission/absorption element in case $T_a=20^{\circ}\text{C}$, $MRT=20^{\circ}\text{C}$ and $b=1/3$ and for $n=1.1$, $T_a=MRT$, $T_N=20^{\circ}\text{C}$.

3.6.3 The overestimated radiant heat emission

The assumption of a linear relationship with the temperature difference introduces an overestimation of the radiant output for the empirically established formula, as described above. Calculating the radiant heat transfer coefficient for temperature differences that significantly differ from the nominal conditions therefore introduces an error.

To correct for the resulting error, the linear radiant heat transfer coefficient calculated for the nominal conditions, C_1 , is rescaled:

$$C_1 \Delta T \rightarrow C_1 \left(\frac{\frac{T_{emit} + MRT}{2}}{\frac{T_{emit,N} + MRT_N}{2}} \right)^3 \Delta T \quad (3.39)$$

where, as mentioned above, the values of T_{emit} , as well as $T_{emit,N}$ and MRT must be given in absolute temperatures.

This expression could be considered as a 'natural' adaptation of Eq. (3.30) to take into account the indirect temperature scaling embedded in Eq. (3.7). Using this formula allows calculating the difference between the radiant output calculated

using the nominal versus the corrected radiant heat transfer coefficient. This difference can then be subtracted from the energy output calculated based on the empirical formula:

$$Q_{emit} = Q_{emit,N} \left(\frac{\Delta T}{|\Delta T|} \right) \left(\frac{|\Delta T|}{\Delta T_N} \right)^n - \left[C_1 \Delta T - C_1 \left(\frac{T_{emit} + MRT}{2} \right)^3 \right] \Delta T \quad (3.40)$$

After rearranging and replacing C_2 by the expression given by Eq. (3.31), this results in the ‘adapted empirical formula’ given by Eq. (3.41).

$$Q_{emit} = Q_{emit,N} \left(\frac{\Delta T}{\Delta T_N} \right) \left[\left(\frac{|\Delta T|}{\Delta T_N} \right)^{n-1} - (1 - \alpha_N) \left(1 - \left(\frac{T_{emit} + MRT}{T_{emit,N} + MRT_N} \right)^3 \right) \right] \quad (3.41)$$

Figure 3.9 shows the comparison between the non-adapted, i.e. the empirical formula, and the adapted empirical formula for radiator exponent values of $n=1.1$ and $n=1.3$. It is clear that the correction is especially of importance for low n -values, i.e. in cases with a high proportion of radiant emission.

Again the discontinuity shown is due to comparing with the theoretically calculated emission/absorption. For small temperature differences emitter/absorber versus zone air and MRT temperature, this results in a ratio of two values approaching 0. The formulas themselves are continuous.

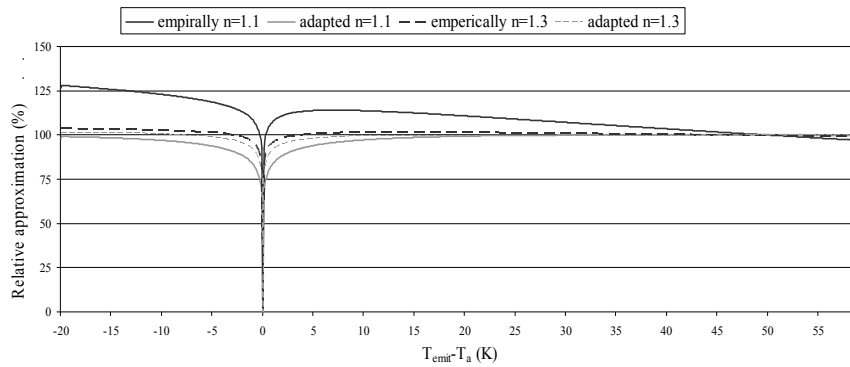


Figure 3.9: Relative approximation of heat output empirically calculated without (Eq. (3.19)) and with a correction factor (Eq. (3.41)) versus theoretically calculated for a heat emission/absorption element in case $T_{air}=MRT$ and with a nominal condition $T_a=MRT_N=20^{\circ}C$, $\Delta T_N=50K$, $b=1/3$, for $n=1.1$ and $n=1.3$.

3.6.4 The effect of the three corrections simultaneously

The simultaneous application of the weighing for the zone temperature, the use of an adapted nominal condition, i.e. in this case lower average emitter/absorber temperature, and the introduction of the ‘correction’ factor according to Eq. (3.41), clearly improves the accuracy (Figure 3.10).

The overall result has an accuracy close to 100% when compared to the theoretical calculation, even in this case with a high proportion of radiation as the radiator exponent equals 1.1.

To emphasize that the discontinuity in the above given Figures is not a consequence of an instability in the formulas, the thermal fluxes calculated based on the empirical and the corrected formula are shown in Figure 3.11. In this figure also the absolute and relative difference between the two formulas is given.

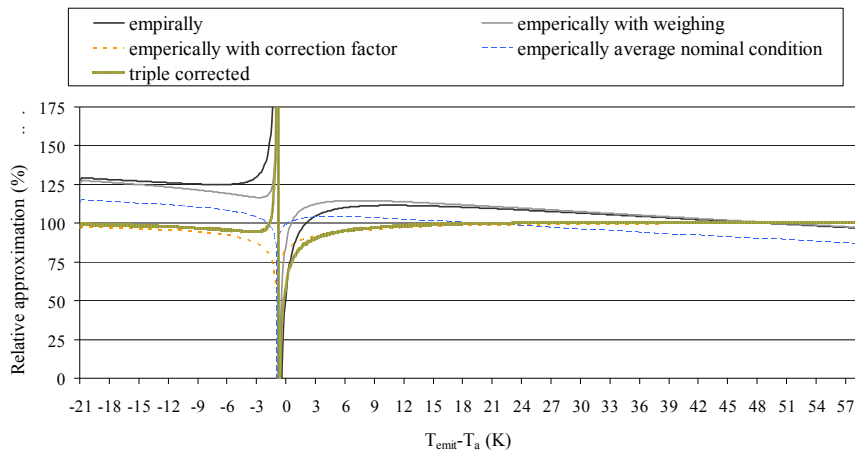


Figure 3.10: Relative approximation of the empirically established formula, and the same formula with 'adjusted' room temperature calculation (Eq.(3.38)), average nominal conditions and the adjusted formula accounting for the overestimated radiant output (Eq. (3.41)), versus theoretically calculated. The results are shown for separate and simultaneous application of the three 'corrections'. Results are given for a heat emission/absorption element in case of $T_{air}=22$ °C, $MRT=20$ °C and with a nominal condition $T_a=MRT_N=21$ °C, $\Delta T_N=30$ K, $b=1/3$, for $n=1.1$.

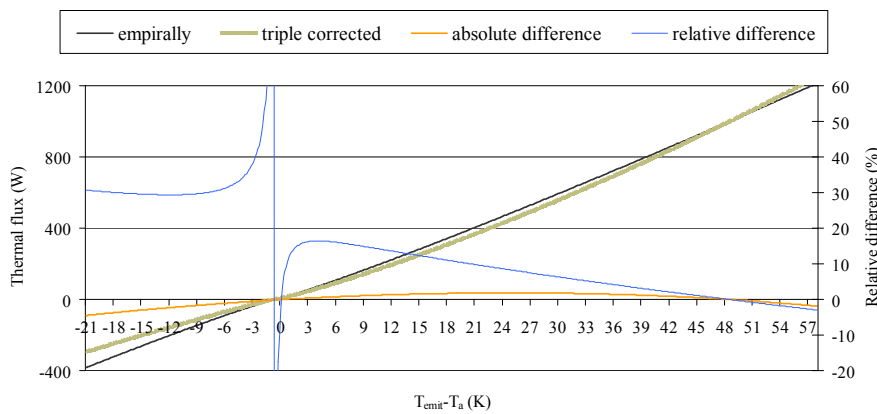


Figure 3.11: Thermal flux calculated with the empirically established formula, and the same formula with 'adjusted' room temperature calculation (Eq.(3.38)), average nominal conditions and the adjusted formula accounting for the overestimated radiant output (Eq. (3.41)). The absolute difference between empirically calculated flux and flux calculated applying Eq. (3.41) is also given. The relative difference, calculated as the absolute difference divided by the result of Eq. (3.41), is to be read compared to the right hand side vertical axis. Results are given for a heat emission/absorption element in case of $T_{air}=22$ °C, $MRT=20$ °C and with a nominal condition $T_a=MRT_N=21$ °C, $\Delta T_N=30$ K, $b=1/3$, for $n=1.1$.

3.7 The evaluation of the indoor climate resulting from the heat emission/absorption

As stated in chapter 1, the evaluation of the indoor climate is through the operative temperature, i.e. a combination of the zonal air temperature and the temperature of the surrounding surfaces. In the implicit approach, the zonal air temperature is a single value (chapter 2). It is thus the same value for both the occupants of the zone and the emitting/absorbing element in that zone. As described earlier in this chapter, the temperature of the surrounding surfaces as experienced by a surface, the MRT, depends on geometrical properties. It will thus depend on the position/location of the occupant or emitter/absorber. For the latter, the influence of the surface temperature of a possible occupant will be small. For the occupant, however, the influence of the surface temperature of the emitting/absorbing element might be substantial.

For the mean radiant temperature experienced by an occupant in case of an emitter/absorber located in the zone and not part of the zonal enclosure, an area weighted calculation strategy, without incorporation of the emitter's/absorber's temperature is applied. The assumption is that the unknown surface area of the emitting/absorbing element will generally be small compared to the total surface area of all parts of the zonal enclosure. The so-introduced error will be discussed in chapter 4.

In case it concerns TAB elements, it is assumed that the whole surface is activated, being the whole floor, ceiling or wall. The surface area of a TAB element is thus generally large. The impact of the surface temperature on the mean radiant temperature depends on the orientation of that surface as well as on the unknown location of the point in which the MRT is evaluated. Furthermore, with the implicit model no surface temperature of the TAB element is known. The only temperature available is the average temperature of the element. This will generally be an overestimation compared to the surface temperature of the element in case of

heating and an underestimation in case of cooling¹¹. Therefore, the proposed MRT-calculation for the evaluation of the indoor thermal comfort in case of a TAB element uses the average temperature of the emitter/absorber in an area-weighted calculation strategy. The error compared to a more correct modelling approach is discussed in chapter 4.

This MRT-calculation is applied for the evaluation of the indoor thermal environment. It is thus also this value that will be used as input to the zonal emitter/absorber controller.

3.8 The generic emitter model for the implicit approach

The empirically derived formula, with the three corrections as described above, shows to accurately estimate the heat transfer for water-based heating and cooling. These processes can be any combination of radiation and natural convection. This improved formula will be used to represent the implicit emitter/absorber, as will be described in the section below

3.8.1 Overall scheme related to model input data

The scheme of Figure 3.12 shows the overall calculation logic for the determination of the heat transfer coefficient for convection.

¹¹ One could argue to adapt the model in order to inject the thermal flux directly into the building structure in case of a TAB. However, that assumes that the position of the active layer within the building structure is known. In a general model, the building structure is composed of layers with specific thickness. A TAB element with a certain capacity might require activating only a part of a given layer. Such an approach would be applicable to models with special construction layers of which the thickness of the different layers can be varied according to the selected emitter's/absorber's capacity. Such an approach would affect the generality of the implicit model and will thus not be adopted.

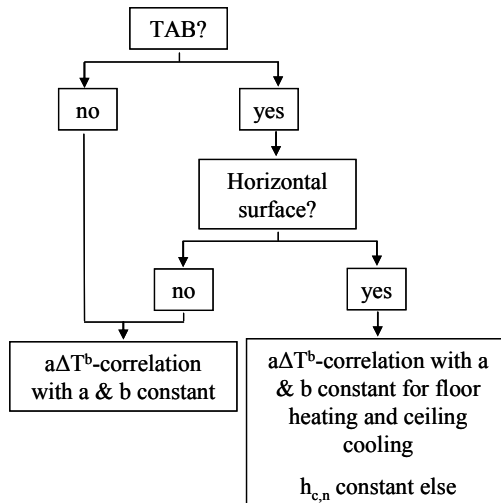


Figure 3.12: Overall scheme showing the calculation methodology as a function of the element modelled.

3.8.2 The model parameters

The implicit plant modelling structure is set up with as main purpose the determination of the optimal emission elements in a given context. It is thus important to have a generic model, which is able to represent any heat emitter/absorber. On the one hand, the selected set of parameters must thus be large enough in order to allow accurately defining a given emitter/absorber. On the other hand, however, using less parameters simplifies the optimisation problem.

The use of the empirical formula, without any ‘improvements’, has been shown to not correctly represent radiators and convectors in cases of cooling, and more radiant systems in general. The adjustments that have been suggested in this chapter indicate the possibility to improve the empirical formula to be valid for water-based emitters/absorbers both for heating and cooling. The parameters required for this formula, are Q_N , n , α_N and the nominal temperatures (see Table.3-2). The parameter β indicates whether or not the element is a TAB element; either located in the floor, ceiling or wall structure. This information is required for both the MRT-refinement and the selection of the correct convection coefficient.

Therefore, in the model structure as implemented for the current research, the parameters as given by Table.3-2 are selected. The values defining the nominal

conditions, $T_{a,N}$ and $T_{emit,N}$ are fixed¹². As there can be multiple emitters/absorbers in a building model, all of the characterizing parameters for a given emitter/absorber i are given a subscript for identification.

Parameter	Symbol
Nominal capacity (W)	$Q_{emit,i,N}$
Radiator exponent (-)	n_i
Nominal air temperature (°C) (assumed to be equal to nominal air temperature according to the European standard [15])	$T_{ai,N}$
Nominal mean radiant temperature (°C) (assumed to be equal to nominal mean radiant temperature according to the European standard [15])	$MRT_{i,N}$
Nominal average emitter/absorber temperature (°C)	$T_{emit,i,N}$
Maximum emitter's temperature (°C)	$T_{emit,i,max}$
Minimum emitter's temperature (°C)	$T_{emit,i,min}$
Fraction of convection at nominal conditions (-)	$\alpha_{i,N}$
No TAB or TAB element with specification of location (-)	β_i
Heat capacity of the emitter/absorber, i.e. water and casing (J/K)	$C_{emit,i}$

Table.3-2: Input parameters as used for the heat emitter/absorber simulation model.

3.8.3 The steady state model

In the implicit modelling approach, as described in chapter 2, the desired zonal heating/cooling flux is determined by the control of the emission/absorption element¹³. The production level, however, finally decides which amount of energy is allocated to the specific emission/absorption element. After passing through the distribution system, the amount of thermal power Q_{pli} (W) is the input for the specific emission element.

¹² These nominal conditions will not be varied throughout the optimisation process. They are then fixed at average nominal conditions.

¹³ It is the control of the emitter that accounts for avoiding condensation, as will be explained in chapter 6.

In a steady state modelling approach, this amount of power Q_{pli} equals the emitted thermal power $Q_{emit,i}$:

$$Q_{emit,i} = Q_{pli} \quad (3.42)$$

This thermal power has to be divided in an amount of radiation and an amount of convection. To determine this split, the average temperature of the emitter, $T_{emit,i}$ must be known. This temperature can be calculated using the corrected empirical formula, given by combining Eqs. (3.38) and (3.41). The resulting Eq. (3.43) is a differentiable continuous polynomial function of $T_{emit,i}$. This equation can thus be solved to define $T_{emit,i}$ applying iterative techniques such as Newton-Raphson.

The MRT used is based on current timestep values when calculating the emitted power for the next timestep.

$$Q_{pli} = Q_{emit,i,N} \left(\frac{T_{emit,i} - (\alpha_{i,N} T_{ai} + (1 - \alpha_{i,N}) MRT_i)}{T_{emit,i,N} - (\alpha_{i,N} T_{ai,N} + (1 - \alpha_{i,N}) MRT_{i,N})} \right) \left[\left(\frac{|T_{emit,i} - (\alpha_{i,N} T_{ai} + (1 - \alpha_{i,N}) MRT_i)|}{T_{emit,i,N} - (\alpha_{i,N} T_{ai,N} + (1 - \alpha_{i,N}) MRT_{i,N})} \right)^{n-1} - (1 - \alpha_{i,N}) \left(1 - \left(\frac{T_{emit,i} + MRT_i}{T_{emit,i,N} + MRT_{i,N}} \right)^3 \right) \right] \quad (3.43)$$

For floor cooling and ceiling heating, the following equation applies:

$$Q_{pli} = Q_{emit,i,N} \left(\frac{T_{emit,i} - (\alpha_{i,N} T_{ai} + (1 - \alpha_{i,N}) MRT_i)}{T_{emit,i,N} - (\alpha_{i,N} T_{ai,N} + (1 - \alpha_{i,N}) MRT_{i,N})} \right) (1 - \alpha_{i,N}) \cdot \left(\frac{T_{emit,i} + MRT_i}{T_{emit,i,N} + MRT_{i,N}} \right)^3 + \bar{h}_{c,n} A_{TAB} (T_{emit,i} - (\alpha_{i,N} T_{ai} + (1 - \alpha_{i,N}) MRT_i)) \quad (3.44)$$

where $\bar{h}_{c,n}$ is the above mentioned value of 1.5 W/m²K in case of floor cooling and 0.5 W/m²K in case of ceiling heating. A_{TAB} (m²) is the surface area of the zone.

Based on the so-calculated average emitter temperature $T_{emit,i}$, the correct radiant heat output can be calculated combining Eqs. (3.1), and (3.35). As the nominal air temperature $T_{ai,N}$ is equal to the nominal mean radiant temperature $MRT_{i,N}$, the radiant output is determined based on the following formula:

$$Q_{emit,i,rad} = \frac{Q_{emit,i,N}}{\Delta T_{i,N}} (1 - \alpha_{i,N}) \frac{1}{\left(\frac{T_{emit,i,N} + T_{ai,N}}{2} \right)^3} (T_{emit,i}^4 - MRT_i^4) \quad (3.45)$$

The convective heat output is then calculated as the difference between total and radiant power output.

As described in chapter 2, the implicit modelling of the emission/absorption element uses the mixed actuating structure which enables splitting a heat flux in a radiant and a convective part. The convective heat flux is allocated to the zone air node and the radiant part to the node representing the zone's solid enclosure. The input to that mixed actuating structure is the total energy delivered by the emission element to the zone, $Q_{emit,i}$, combined with the fraction of instantaneous convective over total power, i.e. α_i :

$$\alpha_i = \frac{Q_{emit,i} - Q_{emit,i,rad}}{Q_{emit,i}} \quad (3.46)$$

Figure 3.13 schematically presents the sequence of calculations, applied to a zone i ¹⁴, where the implicit emitter/absorber is indicated in the grey box.

¹⁴ In this dissertation it is assumed to have only one emission/absorption element representing controller per zone. However, the set of parameters, the model and the solution techniques could be translated to handle multiple emitters/absorbers per zone.

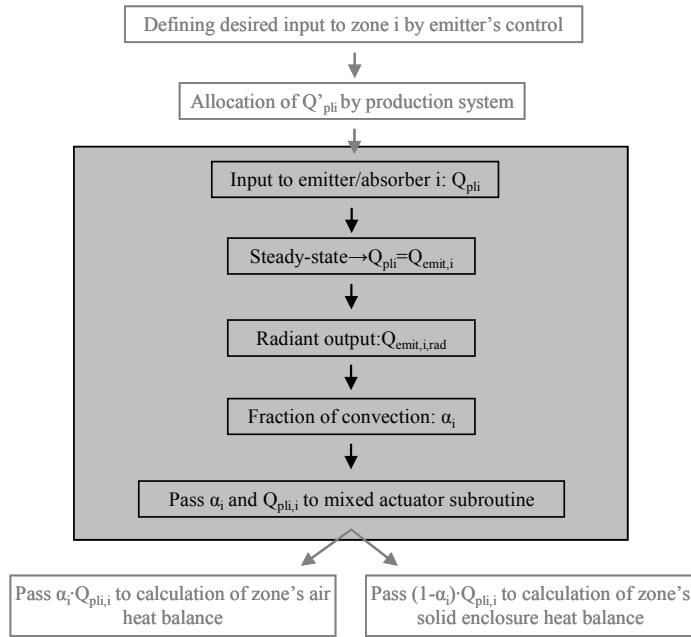


Figure 3.13: Schematic overview of the calculations for the implicit emission/absorption element (indicated by the grey box) using a steady state approach. The previous and following calculations steps, which occur 'outside' the emitter/absorber model, are briefly described and indicated. Q_{pli} is the thermal power received by emitter/absorber i through the distribution system, $Q_{emit,i}$ is the thermal power emitted in zone ai and equals $Q_{pli,i}$ in the assumption of a single emitter per zone and a steady state approach. α_i is the fraction of convection for that particular case.

3.8.4 Introducing dynamics

The dynamic behaviour of an emission/absorption element has an important influence on the achieved indoor temperatures. Using the implicit modelling approach, the emitter/absorber is assumed to be a single isothermal element. The total thermal heat capacity $C_{emit,i}$ of the emitter/absorber, i.e. the combined capacity of the water and the metal casing, is then allocated to the isothermal element.

In the dynamic performance calculation using the empirical formula (Eq. (3.22)), the emitter's/absorber's thermal output $Q_{emit,i}$ can be replaced by the 'corrected' formula (which results from combining Eqs. (3.38) and (3.41)). The resulting heat

balance equation of the emission/absorption element is given by Eq. (3.47) below (Eq.(3.48) for floor cooling or ceiling heating).

$$C_{emit,i} \frac{\partial T_{emit,i}}{\partial t} = Q_{pli} - Q_{emit,i,N} \left(\frac{T_{emit,i} - (\alpha_{i,N} T_{ai} + (1 - \alpha_{i,N}) MRT_i)}{T_{emit,i,N} - (\alpha_{i,N} T_{ai,N} + (1 - \alpha_{i,N}) MRT_{i,N})} \right) \cdot \left[\left(\frac{|T_{emit,i} - (\alpha_{i,N} T_{ai} + (1 - \alpha_{i,N}) MRT_i)|}{T_{emit,i,N} - (\alpha_{i,N} T_{ai,N} + (1 - \alpha_{i,N}) MRT_{i,N})} \right)^{n-1} - (1 - \alpha_{i,N}) \left(1 - \left(\frac{T_{emit,i} + MRT_i}{T_{emit,i,N} + MRT_{i,N}} \right)^3 \right) \right] \quad (3.47)$$

$$C_{emit,i} \frac{\partial T_{emit,i}}{\partial t} = Q_{pli} - Q_{emit,i,N} \left(\frac{T_{emit,i} - (\alpha_{i,N} T_{ai} + (1 - \alpha_{i,N}) MRT_i)}{T_{emit,i,N} - (\alpha_{i,N} T_{ai,N} + (1 - \alpha_{i,N}) MRT_{i,N})} \right) \cdot (1 - \alpha_{i,N}) \left(\frac{T_{emit,i} + MRT_i}{T_{emit,i,N} + MRT_{i,N}} \right)^3 - \bar{h}_{c,n} A_{TAB} (T_{emit,i} - (\alpha_{i,N} T_{ai} + (1 - \alpha_{i,N}) MRT_i)) \quad (3.48)$$

Within the ESP-r coding this derivative is changed into a differential. Iterative solution techniques such as Newton-Raphson can then be applied to solve this equation to determine the average temperature of the emission/absorption element ($T_{emit,i}$).

The sequence of calculations of the dynamic heat emitter/absorber is shown in Figure 3.14.

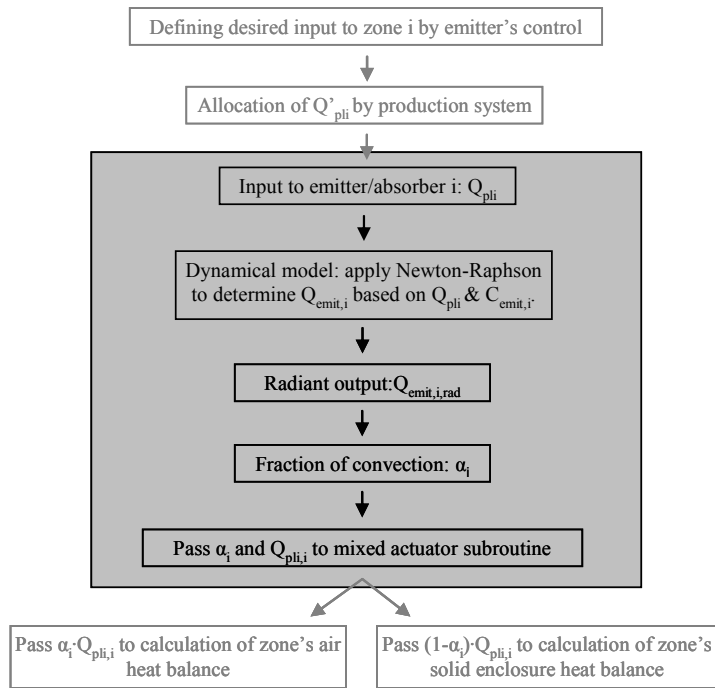


Figure 3.14: Schematic overview of the calculations for the dynamic implicit emission/absorption element (indicated by the grey box). The previous and following calculations steps, which occur 'outside' the emitter/absorber model, are briefly described and indicated. Q_{pli} is the thermal power received by emitter/absorber i through the distribution system, $Q_{emit,i}$ is the thermal power emitted in zone i and equals $Q_{pli,i}$ in the assumption of a single emitter per zone and a steady state approach. α_i is the fraction of convection for that particular case.

3.9 Heat emission/absorption of real elements

3.9.1 Radiators and convectors

The empirical formula is used in multiple simulation programs, as mentioned above. It is also commonly used in several national and international standards such as the German DIN 4704 [38] and the European CEN 2003[21].

It has been shown earlier in this chapter that, when comparing the model with theory, the major shortcoming is the overestimation of the radiant part. This overestimation is especially pronounced for low temperature heating cases and for

cooling in general. By applying the above suggested ‘corrections’, this deficit is accounted for.

3.9.2 Heated or cooled elements as part of the zonal enclosure

When techniques such as floor heating or ceilings cooling are applied, the emitting/absorbing element is not actually located within the zone, but is part of the zonal enclosure. In the presence of a TAB element, the conductive heat transfer within the building structure increases. This results in an increased heat transfer to the zones in direct contact with the heating/cooling building element. Using the generic implicit approach, no difference is made whether it concerns a thermally activated building element or an emitting/absorbing element within the zone. The resulting modelling error will be discussed in the validation part (Chapter 4).

Another effect that is not accounted for using the implicit approach is solar radiation heating up the TAB element. This will be discussed in chapter 4.

3.10 Summary and conclusion on implicit heat emitter/absorber model

The power emission of any heat emitter/absorber is by convection and by radiation. The empirically derived formula, often used in building-energy simulation, has been described and discussed. It has been shown that this relation can be used for emission elements with a mainly convective output such as conventional radiators and convectors. The amount of radiant output, however, is overestimated. This is due to the indirect calculation of the linear heat transfer coefficient for radiation at nominal, rather high, temperatures.

The formula has been ‘corrected’ in this chapter to account for the overestimation of the radiant output:

$$Q_{emit,i,N} \left(\frac{T_{emit,i} - (\alpha_{i,N} T_{ai} + (1 - \alpha_{i,N}) MRT_i)}{T_{emit,i,N} - (\alpha_{i,N} T_{ai,N} + (1 - \alpha_{i,N}) MRT_{i,N})} \right) \cdot \left[\left(\frac{|T_{emit,i} - (\alpha_{i,N} T_{ai} + (1 - \alpha_{i,N}) MRT_i)|}{T_{emit,i,N} - (\alpha_{i,N} T_{ai,N} + (1 - \alpha_{i,N}) MRT_{i,N})} \right)^{n-1} - (1 - \alpha_{i,N}) \left(1 - \left(\frac{T_{emit,i} + MRT_i}{T_{emit,i,N} + MRT_{i,N}} \right)^3 \right) \right] \quad (3.49)$$

This formula needs to be replaced by Eq. (3.50) in case of floor cooling or ceiling heating.

$$Q_{emit,i,N} \left(\frac{T_{emit,i} - (\alpha_{i,N} T_{ai} + (1 - \alpha_{i,N}) MRT_i)}{T_{emit,i,N} - (\alpha_{i,N} T_{ai,N} + (1 - \alpha_{i,N}) MRT_{i,N})} \right) \cdot (1 - \alpha_{i,N}) \left(\frac{T_{emit,i} + MRT_i}{T_{emit,i,N} + MRT_{i,N}} \right)^3 - \bar{h}_{c,n} A_{TAB} (T_{emit,i} - (\alpha_{i,N} T_{ai} + (1 - \alpha_{i,N}) MRT_i)) \quad (3.50)$$

It has been shown that due to these improvements the heat emission/ absorption of any element is calculated with more accurate agreement between the theoretical calculation and the well established empirical calculation. Based on these formulae (either Eq. (3.49) or Eq. (3.50)), the implemented algorithm for the generic model of a heat emission/absorption element has been presented. This model can consequently be used for the optimisation process so as to select the set of characteristics that leads to minimum energy consumption while achieving the desired thermal comfort. This is further discussed in chapter 6.

The next chapter, i.e. chapter 4, will focus on the verification of the model presented here. How the model is embedded in *ESP-r* is schematically described in appendix B.

References

- [1] M. Baelmans, 2006, Heat transfer course HENRAD Herentals, course documents, Applied Mechanics and Energy Conversion, University of Leuven (KULeuven), Belgium (not published)
- [2] L. Lianzhong, M. Zaheeruddin, 2006, Dynamic modeling and simulation of a room with hot water baseboard heater, *International journal of energy research*, vol. 30, pp. 427-445
- [3] B. Xu, L. Fu, H. Di, 2008, Dynamic simulation of space heating systems with radiators controlled by TRV's in buildings, *Energy and Buildings*, vol. 40, pp. 1755-1764
- [4] R. Strand, K. Baumgartner, 2005, Modeling radiant heating and cooling systems: integration with a whole-building simulation program, *Energy and Buildings*, vol. 37, pp. 389-397
- [5] A. Laouadi, 2004, Development of a radiant heating and cooling model for building energy simulation software, *Building and Environment*, vol. 39, pp. 421-431
- [6] S. Ho, R. Hayes, R. Wood, 1995, Simulation of the dynamic behaviour of a hydronic floor heating system, *Heat Recovery Systems and CHP*, vol. 15, pp. 505-519
- [7] P. Fanger, 1970, *Thermal Comfort: analysis and applications in environmental engineering*, McGraw-Hill, New York, ISBN 0-07-019915-9
- [8] J. Lienhardt, J. Lienhardt, 2006, *A heat transfer textbook*, 3rd edition, Phlogiston Press, Cambridge, Massachusetts, available online (<http://web.mit.edu/lienhard/www/ahttv131.pdf>)
- [9] H. Hens, 2003, *Bouwfysica 1, Warmte- en massatransport*, ACCO, Leuven, Belgium, ISBN 90-334-5412-1 (In Dutch)
- [10] Y. Çengel, 1997, *Introduction to thermodynamics and heat transfer*, Mc Graw Hill, ISBN 0-07-011498-6
- [11] S.Kakaç, Y. Yener, 1995, *Convective heat transfer; second edition*, CRC Press, Boca, Florida, ISBN 0-8493-9939-4
- [12] H. Awbi, A. Hatton, 1999, Natural convection from heated room surfaces, *Energy and buildings*, vol. 30, pp. 233-244
- [13] J. Clarke, 2001, *Energy Simulation in Building Design*, Butterworth Heinemann, Oxford, ISBN 0 7506 5082 6
- [14] I. Beausoleil-Morisson, 2000, *The adaptive coupling of heat and air flow modelling within dynamic whole-building simulation*, PhD dissertation, University of Strathclyde, Glasgow, UK
- [15] M. Mohammedi, F. Lainault, F. Milcent, J. Petit, 2002, *Modelisation en regime transitoire des mouvements convectifs dans une cellule d'habitation (Transient modelling of convective movements in a dwelling cell)*, *International Journal of Thermal Sciences*, vol. 41, pp. 709-720
- [16] P. Wallenten, 2001, Convective heat transfer coefficients in a full-scale room with and without furniture, *Buildings and Environment*, vol. 36, pp. 743-751

- [17] X. Gong, D. Claridge, 2007, Impact of the position of the radiators on energy consumption and thermal comfort in a mixed radiant and convective heating system, AHSRAE transactions, vol. 55, pp. 494-503
- [18] S. Churchill, H. Chu, 1975, Correlating equations for laminar and turbulent free convection from a vertical plate, International Journal of heat and mass transfer, vol. 18, pp. 1323-1329
- [19] E. Maes, 2007, JAGA, Diepenbeek Belgium, personal communication
- [20] W. Stephan, 1988, International Energy Agency annex 10, System simulation: radiator, University of Stuttgart, Germany
- [21] CEN, 2003, EN 442-2; Radiators and convectors-Part 2: Test methods and rating, European Committee for standardization
- [22] CEN, 2005, prEN15377: Heating systems in buildings; design of embedded water based surface heating and cooling systems, European Committee for standardization
- [23] J. Hensen, 1991, On the thermal interaction of building structure and heating and ventilating system, PhD dissertation, Technical University of Eindhoven, The Netherlands
- [24] TRNSYS 16, 2006, Technical Reference Manual, Solar Energy Laboratory, University of Wisconsin, Madison
- [25] O. Kalyanova, P. Heiselberg, 2007, Comparative Validation of Building Simulation Software: Modeling of Double facades; Final Report, IEA ECBCS Annex 43/SHC Task 34, Validation of Building Energy Simulation tools, Subtask E, pp. 231
- [26] ESRU, 2002, The ESP-r system for building energy simulation; User guide version 10 series, Environmental Systems Research Unit, University of Strathclyde, Glasgow, UK
- [27] A. Bejan, 2004, Convection heat transfer, Wiley, Hoboken, New Jersey, ISBN 0-471-27150-0
- [28] D. Marret, 1981, Qualite de la ventilation mecanique controlee; influence du mode de chauffage sur le confort et les pertes thermiques dans l' habitat, PhD thesis, Institut Nationales Des Sciences Appliques de Lyon et L'universite Claude Bernard Lyon
- [29] J. Myhren, S. Holmberg, 2008, Flow patterns and thermal comfort in a room with panel, floor and wall heating, Energy and Buildings, vol. 40, pp. 524-536
- [30] A. de Grave, 1973, Oliestook in de woning, Cedicol, Brussels, Belgium
- [31] ISSO, 2000, ISSO 66; Vermogen van radiatoren en convectoren in niet-genormeerde toepassingen, Instituut voor studie en stimulering van onderzoek op het gebied van gebouwinstallaties, Rotterdam, The Netherlands
- [32] T. Min, L. Schutrum, G. Parmelee, J. Vouris, 1956, Natural convection and radiation in a panel-heated room, Heat Piping and Air Conditioning, May, pp. 153-160
- [33] H. Awbi, A. Hatton, 1999, Natural convection from heated room surfaces, Energy and Buildings, vol. 30, pp. 233-244
- [34] F. Incropera, D. Dewitt, 1996, Fundamentals of heat and mass transfer, Wiley, New York, ISBN 0-471-30460-3

-
- [35] J. Babiak, B. Olesen, D. Petras, 2007, Low temperature heating and high temperature cooling: embedded water-based surface heating and cooling systems, REHVA, Forssa, Finland, ISBN 2-9600468-6-2
 - [36] E. Michel, F. Bonnefoi, A. Deves, 2001, Heating/Cooling floors: European Survey, Tests and Sizing method, Clima, 7th Rehva World Congress, Napoli, Italy
 - [37] X. Zang, W. Chen, W. Yu, 1994, Experimental study on the ratio between radiation and convection of normal radiators, Hetaing, Ventilation and Air Conditioning, vol. 6, pp. 13- 15 (in Chinese; relevant parts translated by Peng Wu, Department of Mechanical Engineering, KULeuven, Belgium)
 - [38] DIN, 1984, Prufung von Raumheizungskorpern, DIN 4704 Teil 4, Deutsches Institut fur Normung

4 MODEL VERIFICATION

In this chapter the model of the implicit heat emitter/absorber, as deduced in chapter 3, is verified. To do so, the general theoretical formulas are first evaluated comparing them to more accurate ones set up for specific cases. This comparison is made for both radiation and natural convection.

The area-weighted calculation strategy for the mean radiant temperature is compared to the viewfactor weighted strategy. This is done from the point of view of the emitting/absorbing element as well as from the point of view of an omnidirectional observant in the zone. Also the use of the average element's temperature versus its surface temperature is checked. For the case of a TAB element this is done based on a simple model validated using measurement data.

Measurement data are used for the steady state validation of the emitter/absorber located in the zone. For the implicit heat emitter/absorber being part of the zonal enclosure, the verification is based on a theoretical analysis. The dynamical performance of the implicit emission/absorption element located in the zone is compared to a model presented in the literature. An analytical comparison is made

for the verification of the dynamics of the emitter/absorber located within the solid zonal enclosure.

4.1 Theoretical analysis:

4.1.1 Uncertainty on the heat transfer coefficients

4.1.1.1 Radiation

Radiation satisfies the Stefan Boltzmann law. Radiant heat transfer is thus related to the difference of the fourth power of the absolute temperatures of both surfaces (Eq. (3.1)). The error introduced by linearization of this radiant heat transfer equation is limited when the temperature range of interest is small. That the empirical formula (Eq. (3.19)) is thus only correct for a limited temperature range around the nominal conditions has been shown above. By using the ‘improved’ formula (Eqs. (3.49) and (3.50)), as set up in chapter 3, the linearized radiant heat transfer coefficient is recalculated at each timestep. The deviation of the calculation of the radiant output when using a fixed linear radiant heat transfer coefficient, as incorporated in the empirical formula compared to the fourth power temperature difference calculation is graphically represented in Figure 4.1. This figure also shows the deviation of the constantly recalculated linear radiant heat transfer coefficient, as used in the improved formula, versus the fourth power method. This ‘improved’ calculation method shows deviations that are limited to less than 1%. The non-improved calculation results in deviations that are relatively limited in the proximity of the nominal point, but get large (i.e. up to 25%) when further removed from this point.

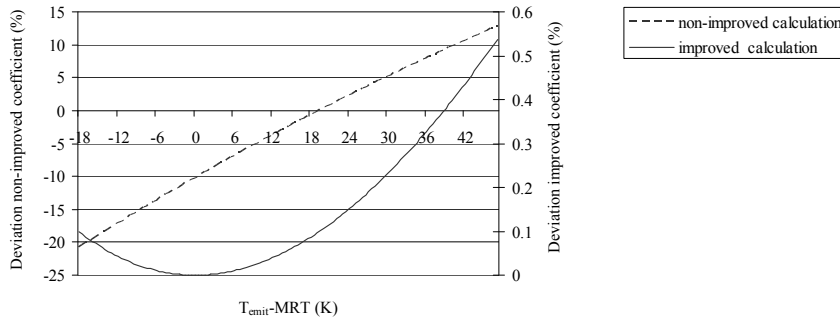


Figure 4.1: Deviation between the radiant heat output calculated with the non-improved and the improved formula ((3.19) and (3.49) respectively) and the fourth power Stefan Boltzmann calculation. The left vertical axis shows the results for the non-improved calculation method, the right axis shows the results for the improved calculation method. The former is here determined at nominal conditions of T_{emit} equal to 43°C and MRT equal to 23 °C.

4.1.1.2 Convection

Both the adapted and non-adapted formula of Stephan uses the correlation of Eq. (3.13) for the calculation of the convection coefficient. The coefficient is determined at nominal conditions only. To evaluate the accuracy of this simplified correlation it is compared, for the case of a vertical isothermal emitter/absorber, to the Churchill and Chu [1] correlation specifically derived for such a configuration (Eq. (4.1)).

$$\bar{h}_{c,n} = \frac{\lambda Nu}{L} = \left(0.825 + \frac{0.387 Ra^{1/6}}{\left(1 + \left(\frac{0.492}{Pr} \right)^{9/16} \right)^{8/27}} \right)^2 \quad (4.1)$$

where λ (W/mK) is the conductivity of the air, Ra (-) is the Rayleigh number, and Pr (-) is the Prandtl number of the air. Both dimensionless numbers, Ra and Pr are calculated based on temperature-dependent physical state quantities.

Figure 4.2 shows the convection coefficients for the calculation method of Eqs. (3.13) and (4.1). The deviation of the simplified correlation to the more detailed calculation is given as well. For the temperature range of interest for water-based heating and cooling, the graph shows an obvious agreement between both calculation methods: an average deviation of 0.3% with a maximum value of 3.9% for the very small temperature difference.

The agreement is especially good for the positive temperature differences. The higher deviation for the negative temperature differences is due to the selected a- and b-values in the temperature difference-correlations at a positive nominal emitter/absorber temperature of 40°C.

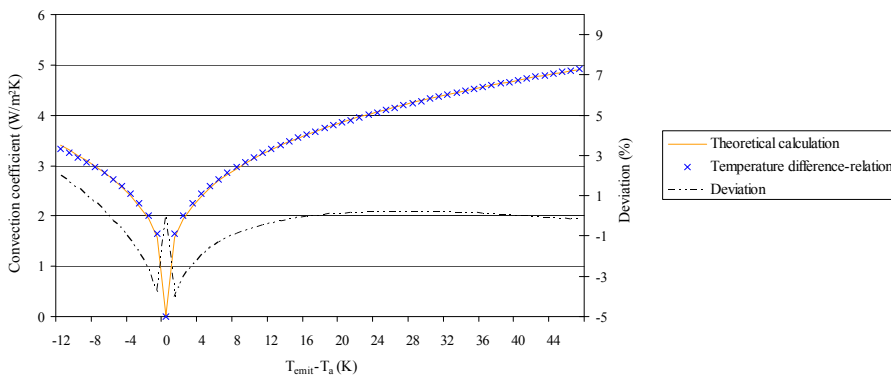


Figure 4.2: Convection coefficients for the simplified temperature difference related correlation of Eq. (3.13) versus the more detailed theoretical methodology of Eq. (4.1), shown on the left hand side axis. The deviation of the simplified versus the detailed calculation method is shown on the right hand side axis. The simplified correlation is here determined at nominal conditions of $T_{emit,N}$ equal 40°C and $T_{a,N}$ equal to 23 °C.

The same comparison was made based on a correlation for a cylinder [2]:

$$\bar{h}_{c,n} = \frac{\lambda Nu}{L} = \left(0.60 + \frac{0.387 Ra^{1/6}}{\left(1 + \left(\frac{0.559}{Pr} \right)^{9/16} \right)^{8/27}} \right)^2 \quad (4.2)$$

The resulting comparison is shown in Figure 4.3.

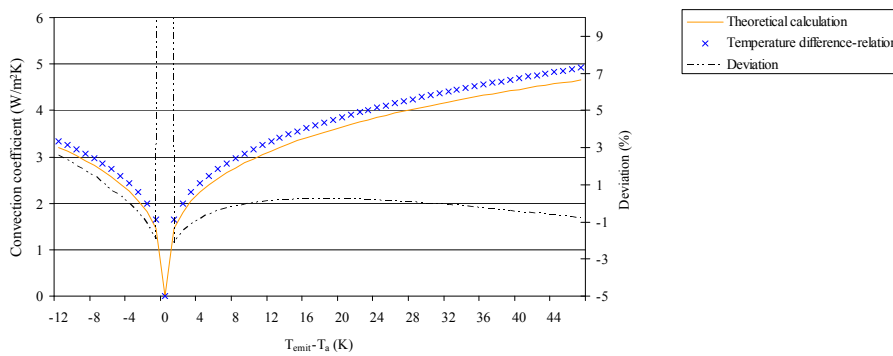


Figure 4.3: Convection coefficients for the simplified temperature difference related correlation of Eq. (3.13) versus the more detailed theoretical methodology of Eq. (4.2), shown on the left hand side axis. The deviation of the simplified versus the detailed calculation method is shown on the right hand side axis. The simplified correlation is here determined at nominal conditions of T_{emit} equal 40°C and $T_{a,N}$ equal to 23 °C.

The deviation is slightly higher, but still acceptable with a maximum of 2.8% for -12 °C. The average deviation equals 0.6%. The computed value of the deviation for a zero-temperature difference looks high, due to dividing by an almost-zero value.

4.1.2 Accuracy of the mean radiant temperature calculation

4.1.2.1 MRT for the emission/absorption of heat

The radiant heat emission of the implicit heat emitter/absorber is calculated based on the area-weighted MRT-calculation. To evaluate the so-introduced error, this calculation is compared to a viewfactor-weighted fourth-power MRT-calculation for a simple room.

The viewfactors are calculated based on commonly encountered formulae [3].

TAB element; floor heating/cooling

Both the simplified and the viewfactor-calculated MRT are applied to a simple zone (shown in Figure 4.4).

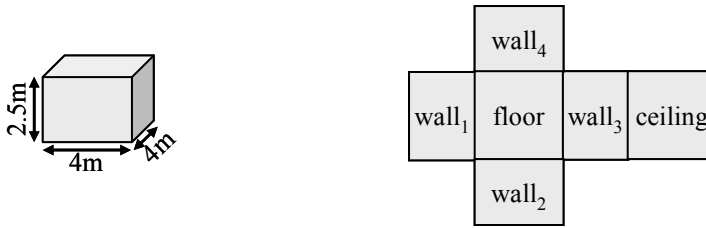


Figure 4.4: Simple box with indication of surface names for MRT 'observed' by floor.

The required viewfactors are summarized in Table 4-1.

wall ₁	wall ₂	wall ₃	wall ₄	ceiling
0.165	0.165	0.165	0.165	0.341

Table 4-1: Viewfactors for radiant heat exchange between floor and other surfaces.

For the implicit emitter/absorber model representing a TAB element, the heat exchange is through the plant injection term in the zonal energy balance. The heat is not injected into the active surface. The surface temperatures of all internal zonal surfaces are taken into account for the calculation of the mean radiant temperature the TAB element 'observes'. This simplified area-weighted formula is given by Eq. (4.3), the more refined viewfactor weighted strategy by Eq. (4.4).

$$MRT = \frac{1}{\sum_i A_i} \left(\sum_i A_i T_{si} \right) \quad (4.3)$$

$$MRT = \left(\sum_i F_i T_{si}^4 \right)^{1/4} \quad (4.4)$$

A_i (m^2) indicates the surface area of surface i with temperature T_{si} (K). F_i (-) is the viewfactor between 'the observer' and surface i .

The difference between both calculation methodologies is small, unless the surface temperatures deviate strongly from one another (Figure 4.5). The viewfactor-calculated approach gives more weight to the surface temperature of the ceiling, compared to the surface averaged approach. The deviation consequently shows the area weighted MRT to underestimate the influence of a change in surface temperature of the ceiling. It should be noted though that surface temperature variations in the zonal level in *ESP-r* are more limited than they would be in a real situation. One reason is that the zonal air is represented by a single node, so no stratification is considered. Another reason is that heat sources, such as fluxes originating from sources located in the zone or solar radiation¹, are divided over the different surfaces of the zonal enclosure and are not allocated to a specific surface only.

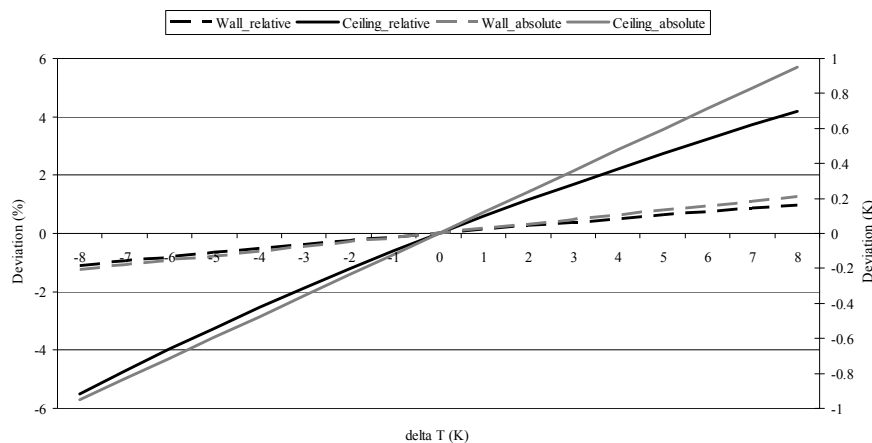


Figure 4.5: Deviation between viewfactor-weighted and surface weighted MRT-calculation 'observed' by the floor as a function of the temperature difference between the wall/ceiling and the floor. The results for all 4 walls are equal and are here given for 'wall' in general. The relative deviation (%) is the difference between the fourth-power viewfactor-calculated and the surface area-calculated MRT versus the former MRT calculation. The absolute deviation (K) is the difference between the fourth-power viewfactor-calculated and the surface area-calculated MRT.

¹ For the allocation of solar heat gains, a more refined technique can currently be selected in *ESP-r*. However, the standard method will, for the implicit approach, result in a smaller deviation for the MRT-calculation. The standard method is especially valuable due to the non-defined emitter/absorber element's location within the zone.

Radiator

The same comparison will here be made for the case no TAB element, but a radiator is installed in the zone. The radiator is assumed to have the same length as the wall and is given a height of 0.3 m.

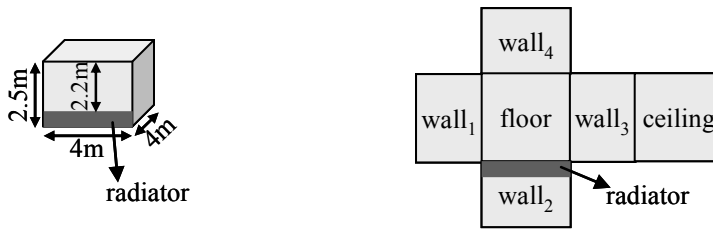


Figure 4.6: Simple box with indication of surface names for MRT 'observed' by radiator.

The resulting viewfactors are summarized in Table 4-2.

wall ₁	wall ₃	wall ₄	Floor	ceiling
0.140	0.140	0.132	0.446	0.141

Table 4-2: Viewfactors for radiant heat exchange between radiator and other surfaces.

The deviation for variations in surface temperature for the different parts of the zonal enclosure is given in Figure 4.7. The effect of changes to the temperature of wall₁ and wall₃ is for both calculation strategies almost equal. This is confirmed by an almost zero deviation, both absolute and relative, for wall_{1&3} in the graph. The other parts of the zonal enclosure get different weights in both calculation strategies, resulting in larger but opposite deviations for the floor and ceiling. Small variations in the surface temperatures of the zonal enclosure will, however, result in limited differences between both calculation strategies.

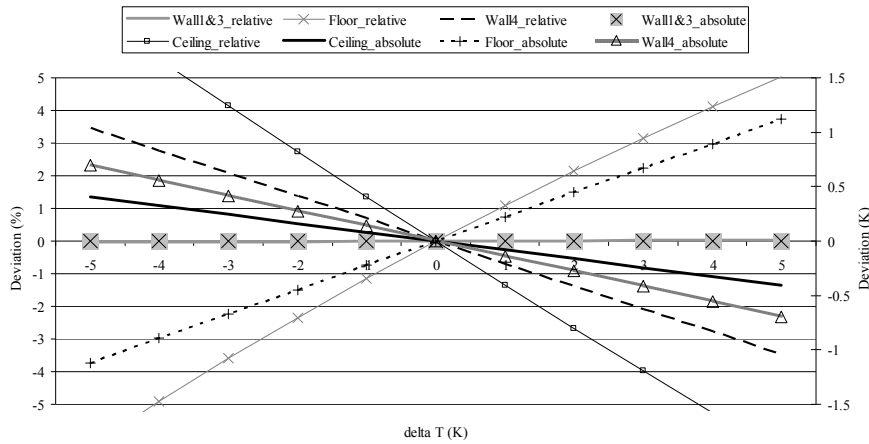


Figure 4.7: Deviation between viewfactor-weighted and surface weighted MRT-calculation ‘observed’ by the radiator as a function of the temperature difference between the wall/ceiling and the floor. The result for wall₁ equals that for wall₃ and is here given for ‘wall1&3’ in general. The relative deviation (%) is the difference between the fourth-power viewfactor-calculated and the surface area-calculated MRT versus the former MRT calculation. The absolute deviation (K) is the difference between the fourth-power viewfactor-calculated and the surface area-calculated MRT.

4.1.2.2 MRT for the evaluation of the thermal environment

TAB element; floor heating/cooling

The operative temperature as experienced by an occupant of the zone will here be calculated for the case of a floor heating/cooling system. The calculation is done once for an omnidirectional seated person and once for an omnidirectional standing person, both located in the middle of the zone. The viewfactors are calculated based on the formulas described in [4]. The authors of that publication did set up algorithms for the calculation of the viewfactors between a human body and rectangular surfaces surrounding it. The algorithms were compared to the more detailed calculations of Fanger and showed to agree well: for the vertical surfaces above or below seated persons the average deviation was 3.1% and for all other surfaces evaluated for either seated or standing persons the deviation was 1.4% only.

	wall ₁	wall ₂	wall ₃	wall ₄	floor	ceiling
seated person	0.123	0.123	0.123	0.123	0.362	0.146
standing person	0.148	0.148	0.148	0.148	0.245	0.163

Table 4-3: Viewfactors for occupant seating/standing in the middle of the zone.

Figure 4.8 shows the deviation between the detailed viewfactor-based calculation of the MRT and the simplified area weighted MRT calculation that does not consider the effect of changed floor temperatures due to the TAB element. The relative deviations (%) are given compared to the average surface and operative temperatures in degrees Celsius. All deviations are shown as a function of the temperature difference between floor and zonal surfaces.

It is assumed that the surface temperature of the TAB element is uniform. The resulting deviations are large: up to 22% for floor surface temperatures of 10K difference compared to the surface temperatures of the other parts of the zonal enclosure. Also the absolute difference on the operative temperature shows non-negligible deviations with an underestimation of up to 2K for the seated person when applying a simplified calculation and neglecting the surface temperature of the TAB element. Such a deviation could trigger the controller to inject (more) heat into the TAB element, while a comfortable indoor operative temperature is already achieved. In case the TAB element is cold compared to the rest of the zone, the simplified calculation overestimates the indoor operative temperature. This could result in triggering to restart or continue cooling, while there is no need for it.

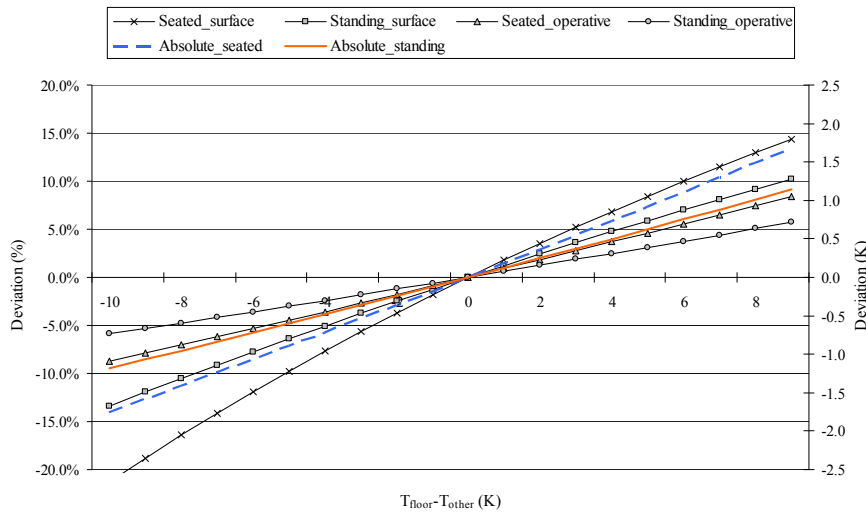


Figure 4.8: Relative deviation between viewfactor-weighted mean radiant temperature with correct floor temperature versus area-weighted mean radiant temperature of the zonal enclosure calculated without the changed temperature of the floor compared to a zonal temperature of 20°C, for seated and standing persons (Seated_surface and Standing_surface respectively), as well as the same relative deviation for the operative temperature for an air temperature of 293.15K (Seated_operative and Standing_operative respectively). The right vertical axis also indicates the absolute differences between the operative temperatures for the two calculation strategies, again for seated and standing persons (Absolute_seated and Absolute_standing respectively). All deviations and differences are shown as a function of the temperature difference between floor surface and average surface temperature of the zonal enclosure (all other surfaces are given a surface temperature of 293.15K).

In chapter 3, a strategy was proposed to use the average emitter's/absorber's temperature for the evaluation of the indoor thermal comfort in case the emitter/absorber is a TAB element. The calculation of the MRT should be area weighted, but taking into account the average temperature of the TAB element for the specific surface. The accuracy of the assumption of an average temperature will be discussed in the next paragraph. The accuracy of the use of the area weighted single power (Eq. (4.3)) versus view-factor weighted fourth-power MRT-calculation (Eq. (4.4)) is shown in Figure 4.9. An underestimation of up to 0.67K is shown for the seated person and less than 0.15K for the standing person for a heating case. Similar values, but then as overestimation, are shown for cooling cases.

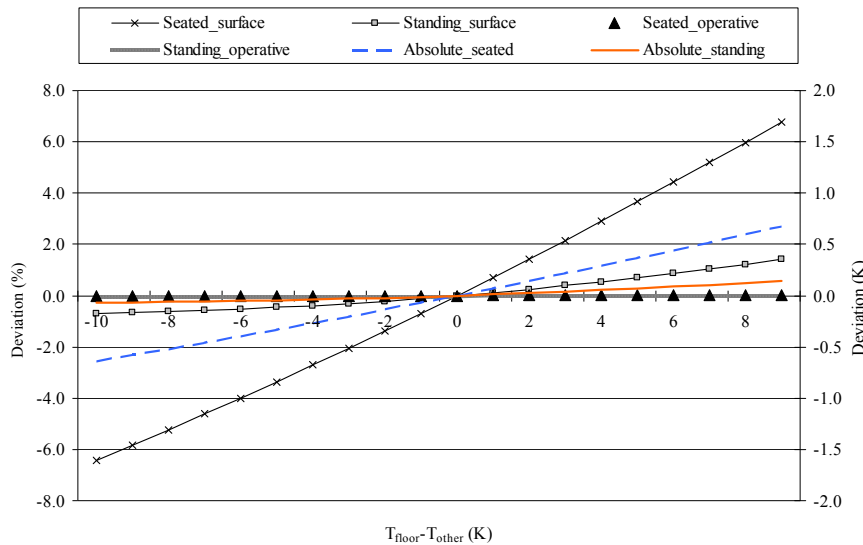


Figure 4.9: Relative deviation between viewfactor-weighted mean radiant temperature versus area-weighted mean radiant temperature of the zonal enclosure both with the changed temperature of the floor compared to a zonal temperature of 20°C, for seated and standing persons (Seated_surface and Standing_surface respectively), as well as the same relative deviation for the operative temperature for an air temperature of 293.15K (Seated_operative and Standing_operative respectively). The right vertical axis also indicates the absolute differences between the operative temperatures for the two calculation strategies, again for seated and standing persons (Absolute_seated and Absolute_standing respectively). All deviations and differences are shown as a function of the temperature difference between floor surface and average surface temperature of the zonal enclosure (all other surfaces are given a surface temperature of 293.15K).

The so-achieved values are for the specific geometry of the zone used for this verification. The difference will, of course, depend on the similarity of the weight of the viewfactor of a specific part of the zonal enclosure versus the ratio of its surface area versus the total surface area of the zonal enclosure. The deviation will thus be the highest for ceiling heating/cooling cases. While the case for floors showed the area-weighted methodology to underestimate the MRT when heating and overestimate when cooling, the opposite is the case for a thermally activated ceiling. The overestimation of the MRT when applying the area-weighted methodology is up to 0.57K when the difference between ceiling temperature and zonal temperature is up to 8K. For ceiling cooling with a temperature difference of 10K, the error equals 0.84K when applying the area-weighted calculation method. In this case it is an underestimation compared to the viewfactor weighted calculation strategy.

Radiator

For the surface temperature in a zone heated by a radiator the viewfactors are given in Table 4-4. The dimensions of zone and radiator are as shown in Figure 4.6 above. Again the temperature distribution within the radiator is neglected.

	wall ₁	Radiator	wall ₂	wall ₃	wall ₄	floor	ceiling
seated person	0.123	0.017	0.105	0.123	0.123	0.362	0.146
standing person	0.148	0.014	0.134	0.148	0.148	0.245	0.163

Table 4-4: Viewfactors for occupant seating/standing in the middle of the zone.

The resulting deviation, compared to the average surface and operative temperatures in degrees Celsius, as a function of the temperature difference between radiator and zonal surfaces, is shown in Figure 4.10. However the temperature difference radiator-zonal surfaces goes up to 40K, the absolute difference on the operative temperature is limited to less than 0.42K for the seated and only 0.31K for the standing person. The simplified calculation again underestimates the operative temperature in a heating case and overestimates for a cooling case.

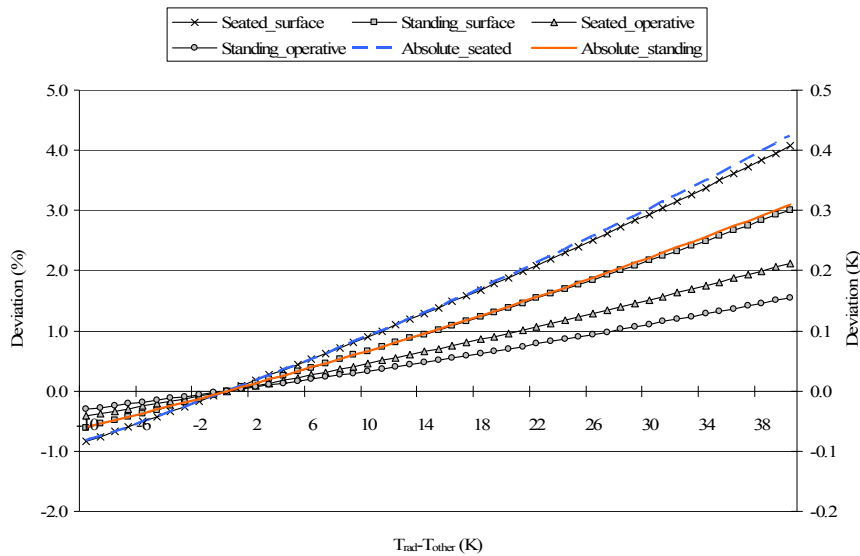


Figure 4.10: Relative deviation between viewfactor-weighted mean radiant temperature versus area-weighted mean radiant temperature of the zonal enclosure without the radiator compared to a zonal temperature of 20°C, for seated and standing persons (Seated_surface and Standing_surface respectively), as well as the same relative deviation for the operative temperature for an air temperature of 293.15K (Seated_operative and Standing_operative respectively). The right vertical axis also indicates the absolute differences between the operative temperatures for the two calculation strategies, again for seated and standing persons (Absolute_seated and Absolute_standing respectively). All deviations and differences are shown as a function of the temperature difference between radiator surface and average surface temperature of the zonal enclosure (all other surfaces are given a surface temperature of 293.15K).

4.1.2.3 The assumption of a homogeneous emitter/absorber element's temperature

TAB element

The heat emission/absorption of a TAB element is calculated based on the average temperature of the TAB element. The assumption of a homogeneous emitter/absorber element's temperature is checked for the case of a floor heating/cooling element. To do so, a resistance-model is set up that allows calculating the average temperature of the TAB element and of its surface temperature. This model is calibrated using data of the THERMAC-measurement

campaign (Figure 4.11, [5]). Due to the inaccuracy of the measurements, mainly due to the open and uncontrolled environment the measurements were conducted in, the analysis will here be limited to the steady behaviour.



Figure 4.11: TAB element as measured in the framework of the THERMAC-project [5] .

The model is set up based on 4 nodes: the water node representing the average water temperature (node 0), the water node representing the water at the surface of the plastic tubing (node 1), the plastic node (node 2) and the concrete node (node 3). The plastic node represents the tubes around the water, and the concrete node holds the characteristics of the reinforced concrete.

The resistance R_0 is related to the convective heat transfer from water to tubes. It is a function of the Nusselt number, which is determined by the Reynolds number as it concerns a turbulent flow. The resistances (R_1 and R_2) between the nodes are determined by the thickness of each of the layers and their thermal conductivity. The scheme of this model is shown in Figure 4.12.

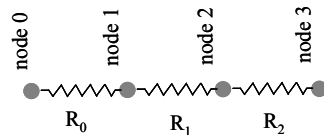


Figure 4.12: Scheme of simplified resistance model.

For the calibration of the model, the nodes 2 and 3 give the surface temperatures of plastic and concrete on the outermost side. The resistance R_0 ($\text{m}^2\text{K}/\text{W}$) is calculated as the inverse of the product of the convective heat transfer coefficient and the surface area. The resistances R_1 and R_2 ($\text{m}^2\text{K}/\text{W}$) are calculated based on:

$$R_i = \frac{d_i}{\lambda_i} \quad (4.5)$$

where d_i (m) is the thickness of the layer and λ_i (W/mK) is the thermal conductivity of the material composing that layer. The thickness of the plastic layer can be calculated based on the innermost and outermost water pipe diameter and the length of the pipes in the TAB element. For the concrete layer, the weight of the concrete element without piping combined with the density gives the thickness in the assumption of no inner open spaces. The assumption of neglecting the resistance of the inner air holes is based on the occurrence of internal air flows resulting from natural convection induced by the temperature difference of the concrete over the section [6]. This movement will reduce the actual thermal resistance of the sealed air holes.

The resulting surface temperature T_{surface} (K) can then be calculated based on Eq. (4.6) where q (W/m^2) indicates the emitted/absorbed thermal flux per square meter, which equals the injected flux in a steady state case, and \bar{T}_{water} (K) indicates the average of water inlet and outlet temperature.

$$T_{\text{surface}} = \bar{T}_{\text{water}} - q \frac{1}{\left(R_0 + \frac{d_1}{\lambda_1} + \frac{d_2}{\lambda_2} \right)^{-1}} \quad (4.6)$$

The model is validated by comparing the measured surface temperatures with the calculated ones. The results are shown for heating and cooling (Figure 4.13 and Figure 4.14 respectively). The measurements start with the element at room temperature. The element has a weight of 413 kg, this without water and pipes. The equivalent thickness of the concrete layer for the resistance model, i.e. the thickness d_2 , is 17.2 cm. For such a high thermal mass, steady state is only achieved after a few hours. The simple resistance model does not account for transient effects. This is clearly shown in the figures: accurate results are achieved only for calculations

based on data achieved in steady-state conditions, i.e. from 3.5 h on. This start up time agrees well with the values based on both simulations with Femlab (Finite element methodology-based software) software and simple calculations reported in the THERMAC handbook [5]. For those conditions, there is a good agreement between the simplified resistance model and the measurements.

The figures show the highest possible and lowest possible value for both the measurements and the calculated values. This is to account for the error on the measurements; i.e. 0.8K on the temperature measurements and 1.5% on the flow measurements. It should also be noted that the TAB element was measured in a non-conditioned, open zone².

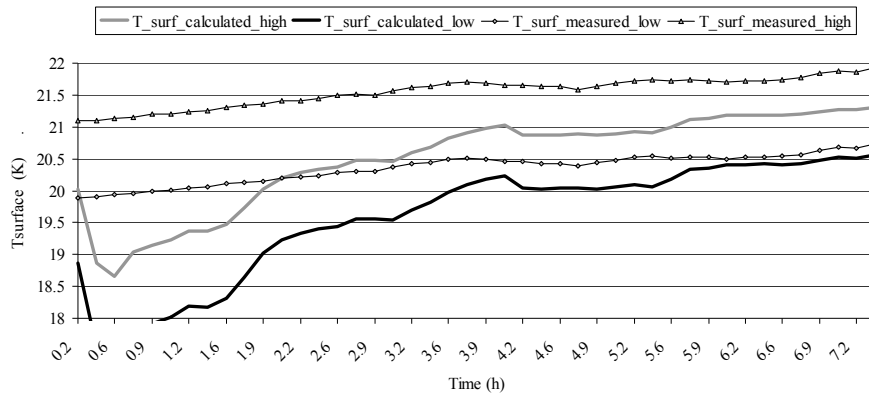


Figure 4.13: Measured surface temperatures and calculated surface temperatures for the TAB element in heating mode. The upper and lower values are determined by the accuracy of the measurement equipment.

² More accurate data were not available at the stage of this PhD. In the framework of [7] more detailed measurements will be performed in a well-controlled environment.

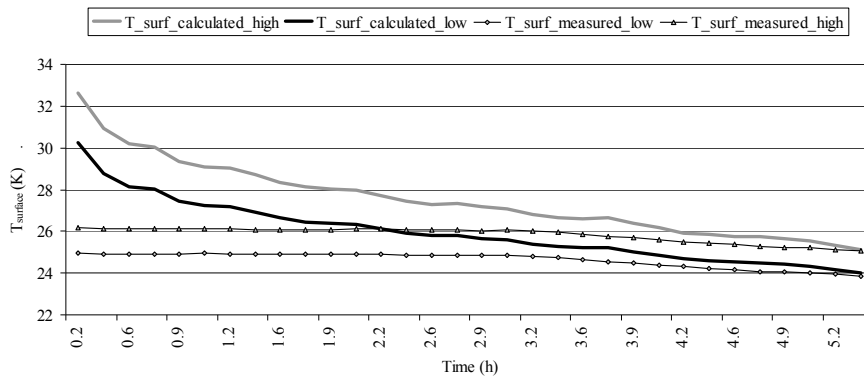


Figure 4.14: Measured surface temperatures and calculated surface temperatures for the TAB element in cooling mode. The upper- and lower values are determined by the accuracy of the measurement equipment.

The simple resistance model is consequently used to determine the difference between the average temperature of the emitter/absorber element as used in the implicit approach and the surface temperature. This is done for values for TAB element thicknesses commonly encountered in residential buildings, i.e. up to 8 cm and in the assumption that the TAB element is built up mainly in concrete.

It should be emphasized that the model is only validated for the specific TAB element configuration tested in the THERMAC-project as well as for the relatively high thermal fluxes tested, i.e. around 82 W/m^2 in heating mode and 103 W/m^2 in cooling mode.

The resulting deviations are shown in Figure 4.15 for the heating case and Figure 4.16 for a cooling case. The influence of the larger cooling flux compared to the heating flux results in larger deviations for the cooling case. The figures further confirm that the deviations increase with increasing thickness and remain acceptable only for small layer thickness.

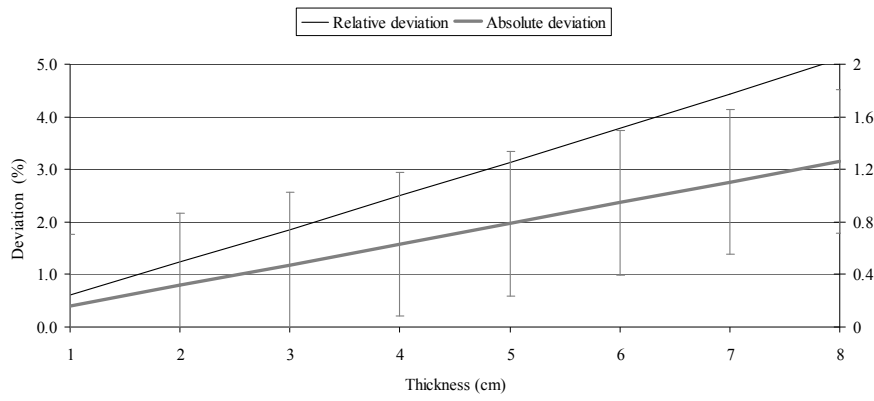


Figure 4.15: Relative and absolute deviation between average emitter/absorber temperature and surface temperature as a function of the thickness of the TAB element for a heating case. The spread due to the uncertainty on the measurement results is given for the absolute deviation (indicated by the vertical bars).

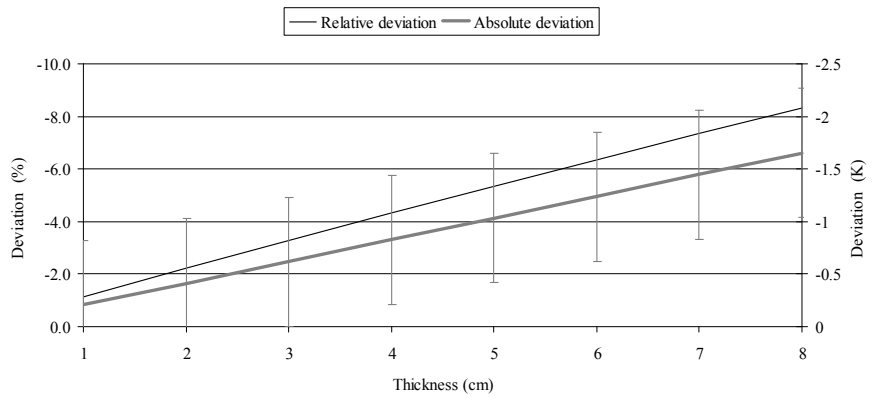


Figure 4.16: Relative and absolute deviation between average emitter/absorber temperature and surface temperature as a function of the thickness of the TAB element for a cooling case. The spread due to the uncertainty on the measurement results is given for the absolute deviation (indicated by the vertical bars).

As expected, the graphs show an overestimation of the temperature of the TAB element in a heating case and an underestimation in a cooling case. The deviation, even for moderate TAB element thickness, is large. It is possible to adapt the

formula of the implicit approach with an improved estimation of the surface temperature (Appendix A). However, it is not implemented in the code for the current analysis. The reason is that a relation must be determined between the average and the surface temperature. That relation can only be set up given material properties and more specific configuration details of the active element. There were no accurate data to validate such a relation. Furthermore, there is the absence of accurate convection coefficient correlations for the horizontal TAB elements. As discussed in chapter 3, the currently existing convection coefficient correlations show large deviations from one another and are measured in non-representative settings.

The combined effect of the use of the average emitter/absorber element's temperature and the area-weighted calculation strategy depends on the TAB element modelled. For floor heating cases, the average element's temperature is an overestimation, while the area-weighted MRT calculation is an underestimation. As an example a case where the average element's temperature that is overestimated by 1K in case of a floor heating system with 8K difference between floor and zonal temperature is compared to the correct calculation, i.e. viewfactor weighted with non-overestimated temperature. The resulting difference between the implicit method, i.e. the use of the overestimated average element's temperature combined with an area weighted MRT calculation, and the correct calculation will result in a difference of 0.07K and 0.4K on the operative temperature experienced by a seated, respectively standing person. These errors are small. However, when making the same comparison for a ceiling heating system, the resulting deviations on the operative temperature are 0.8K and 0.7K for seated and standing persons respectively. The deviations are overestimations in this case. Therefore, it is important to apply the model with special care in case of active ceilings with large capacity.

Care should also be taken for modelling wall heating systems. The viewfactor weighted and area-weighted MRT calculations might show small differences. In that case a deviation between average element's temperature and element's surface temperature is directly translated in an error on the operative temperature that is close to half of the deviation on the MRT.

Radiator

The use of an overall average emission/absorption element's temperature for radiators/convectors is based on the assumption that the water temperature equals the radiator's surface temperature. As the thickness of the metal casing is in the range of 1.25 mm [8] and the heat transfer resistance between water and radiator plate is negligible, it is clear that this is an acceptable assumption.

However, it should be emphasized that the agreement between the average emitter's/absorber's temperature and the average of water inlet and outlet temperature strongly depends on the elements configuration.

4.1.2.4 Solar radiation

In the standard *ESP-r* procedure, solar gains that enter the zone are divided over the different surfaces of the zonal enclosure. The local effect on, for example, the floor is thus not simulated.

The difference is generally limited in residential buildings, as the solar radiation heats up only a part of the floor. Assume the floor in the above described zone (dimensions 4m*4m*2.5m) is heated up by averagely 1K. As shown in Figure 4.9, the effect on the MRT observed by the occupant is limited to less than 0.02K in case of a standing person, 0.07K for a seated person. Assuming the floor is a TAB element, the use of the standard *ESP-r* approach will have little influence on the MRT observed by the floor. Temperature increases of walls and ceiling will be limited to less than 0.3K. Figure 4.5 shows that for such temperature increases, the effect on the MRT is less than 0.07K. However the increase in surface temperature will influence the heat emission/absorption as well. This effect might be substantial (in the order of up to 10%), but still less decisive than the inaccuracy of the convective heat transfer coefficients for horizontal elements.

Furthermore, it is difficult to estimate what percentage of incoming solar radiation will be stored in the active floor or in any other TAB element. Chatziangelidis and Bouris [9] did such analysis for a single and dual zone building located in Athens, Greece. They showed that the amount of solar radiation reaching a floor can be substantial (up to 30% of the direct solar radiation coming from the window). But the building considered was empty. The effect of furniture and decoration was not

investigated. These ‘disturbances’ make it hard to generalize the approach and estimate the potential effects.

4.2 Steady state behaviour of the emitter/absorber model

4.2.1 Emitter/absorber located in the zone.

To evaluate the implicit emitter/absorber model applied to the case of steady emission of a radiator, an existing model is adapted and calibrated using measurement data [10]. The model is based on [11]. It is valid for panel radiators and describes the different processes around each radiator panel. The front and back panel of the radiator emit heat by convection and radiation. Between the radiator panels only convective heat transfer occurs. Fluid flow velocities are calculated based on thermal and hydraulic balances.

The model was programmed in MATLAB [12], but reprogrammed for the current analysis using 2 temperature dependent heat transfer coefficients: one for the outer plates of the radiator, one for the convective heat transfer between the plates. The general format of these coefficients is given by:

$$\bar{h}_{c,n} = a\Delta T^b \quad (4.7)$$

where a is a coefficient given in $\text{W}/\text{m}^2\text{K}^{1+b}$ and b is a dimensionless coefficient. One could argue to use a more detailed correlation. However, the accuracy of the measured temperatures and the lack of enough detailed data made it impossible to correctly calibrate such correlations.

The friction coefficients are implemented in the model based on correlations as given in [13]. Losses at entrance and exit of the spaces between panels and between panel and back wall are arbitrarily set to 1.5%.

The program structure allows determining the power output for a given set of average water, zonal air and mean radiant temperature.



Figure 4.17: Radiator measured in framework of IWT-project [10].

The data used for calibration were measured in the framework of an IWT-project [10]. The studied radiator is shown in Figure 4.17. It is a radiator with two plates with both, at the inner side, lamella to improve the heat emission (Figure 4.18). The radiator exponent is 1.32, and the nominal fraction of convection is around 0.8. The radiator height is 0.5 m, the width is 1.1 m.

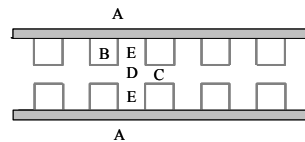


Figure 4.18: Schematic representation of radiator measured in framework of IWT-project [10].

Two power-measurements were available, as well as a range of temperature measurements involving zonal air and surface temperatures, water in- and outlet temperatures and the temperature of the air leaving the split between the two radiator panels. The measurements cover a range of average water temperatures varying from 60°C to 80°C.

The maximum error on the water temperature measurements was $\pm 0.33\text{K}$, the error on the mass flow rates was less than 1%. The overall error on the thermal power was less than 2%. The air and surface temperatures were measured with an accuracy of $\pm 0.5\text{K}$. To calibrate the MATLAB-model, the 2 thermal output data were compared to those calculated using the MATLAB-model. The temperatures of the

thermocouple located just above the radiator between the two radiatorpanels were compared to the values calculated for this parameter in the MATLAB-model. As the accuracy of the thermal power is obviously better, more weight was given to those data in the calibration. The effect of changes, determined by the error on the different inputvalues, was shown to be limited to 3.5 %. As no data out of the 60°C to 80°C-range were available, the comparison between the results using the MATLAB-model and the implicit formula is limited to that range³.

The calibrated model is consequently used to determine the power output as a function of the average water temperature, zonal air and mean radiant temperature. These values are compared to the ones calculated with the implicit emitter/absorber model. The results are shown in Figure 4.19 and Figure 4.20. The first figure gives the calculated thermal outputs as a function of the average water temperature. As shown, the implicit model agrees well with the results of the MATLAB-model: for the given temperature range the implicit formula results in values that lie within the uncertainty band. The difference is minimal around 343K. The reason is that 1 of the 2 thermal output measurements were at that average water temperature and therefore those conditions were selected as nominal conditions for the implicit formula. Figure 4.20 shows the relative and absolute deviations of the implicit formula compared to the MATLAB-calculation.

The results applying the conventional empirical radiator formula are not shown, as they are almost equal to the results for the implicit formula due to the limited temperature range, the high n-value (1.32) and the limited fraction of radiation (0.2).

³ The reason that it is difficult to extrapolate, is the simplification of using 2 convection coefficients of the format given by Eq. (4.7) and thus determine the temperature dependency of the heat emission by that. In fact, the heat transfer between the panels is governed by 4 convection coefficients: one for the enclosures formed by the panels and the lamella (B on Figure 4.18), one for the remaining small space between the lamella of the different plates (C on Figure 4.18), one for the heat transfer between two small spaces between the lamella of the different plates (D on Figure 4.18) and one for the remaining space between a radiator plate and two lamella of that plates (E on Figure 4.18). The currently measured data do not allow determining such correlations. Consequently the so-calibrated MATLAB model can not be used to draw conclusions for heat emission over a wider temperature range.

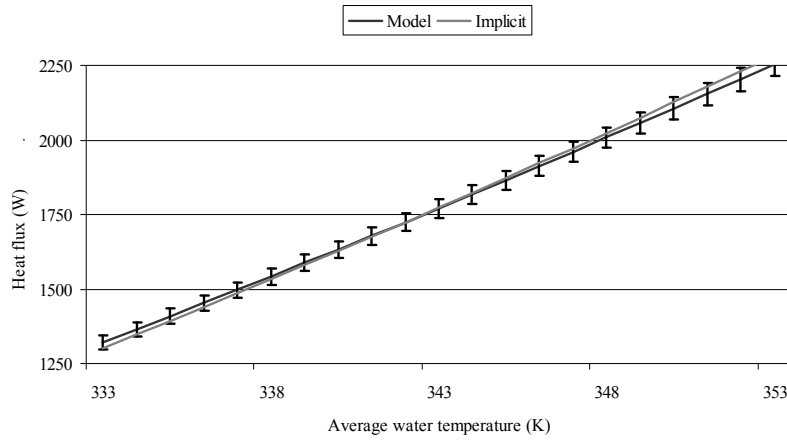


Figure 4.19: Calculated thermal output of radiator. The value as calculated by the MATLAB-model is indicated by 'Model', the value calculated based on the implicit model is indicated by 'Implicit'. The error bars indicate the possible error due to measurement inaccuracy.

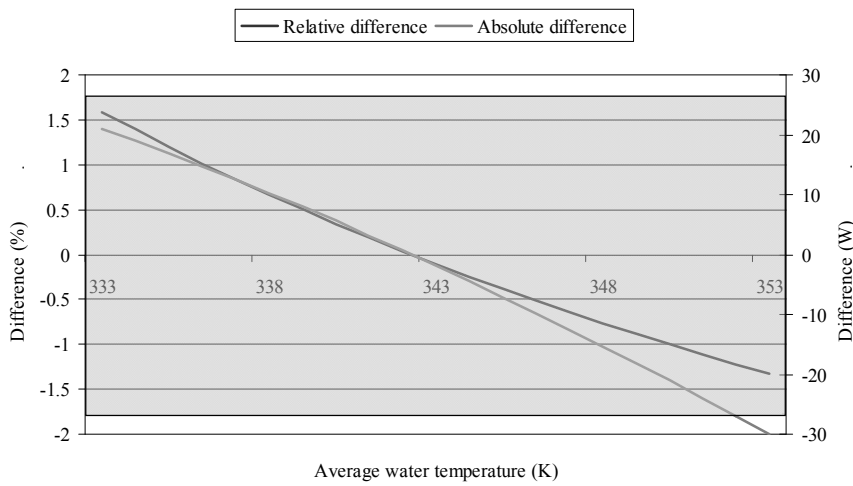


Figure 4.20: Relative and absolute difference between the thermal output of radiator calculated based on the MATLAB-model versus the implicit formula. The grey zone indicates the above mentioned error band of 3.48% for the relative difference.

4.2.2 Emitter/absorber located within the zonal enclosure.

To evaluate the implicit emitter/absorber model applied to the case of a TAB element, the starting point is the thermal condition achieved in the zone of interest. That implies that the convective and radiant output to the zone should be the same for the implicit emitter/absorber model representing the TAB element and a situation with a heat injection into the thermally active layer of the building element. For the same split convection-radiation, the achieved indoor air temperature will be the same. Also the zonal mean radiant temperatures will be the same, due to radiant exchanges between surfaces till a stage of equilibrium is achieved, i.e. when all surfaces are at equal temperatures. This is described, amongst others, by Underwood and Yik [14].

The losses to the surrounding zones, except the zone on the other side of the active building element, are thus treated correctly when using the implicit approach. For the losses to this specific neighbouring zone, the principle of the implicit approach is here compared to a simplified analytical solution.

4.2.2.1 *Implicit approach; determination of the losses to the zone separated by the thermally activated building element.*

In the implicit approach, the TAB element is considered as a single node. The losses $Q_{i,j}$ (W) from the heated/cooled zone i , to the receiving zone j , can be calculated based on the thermal transmittance $U_{i \rightarrow j}$ ($\text{W}/\text{m}^2\text{K}$), the surface area A (m^2) of the TAB element and the operative temperatures $T_{op,i}$ (K) and $T_{op,j}$ (K) of the two zones.

$$Q_{i,j} = U_{i \rightarrow j} A (T_{op,i} - T_{op,j}) \quad (4.8)$$

The temperature will drop in the direction from zone i to zone j in case of heating. In case of cooling, it will obviously be a temperature rise in that direction.

4.2.2.2 *Analytical calculation of the losses to the zone separated by the TAB element*

For the analytical calculation it is necessary to first determine the temperature of the active layer T_{AL} (K) of the heated/cooled building element. The emitted thermal power must equal the emitted power $Q_{pl,i}$ (W) as calculated using the implicit

approach. The thermal permeance $P_{AL \rightarrow i}$ must now be calculated from the active layer AL to zone i:

$$Q_{pli,i} = P_{AL \rightarrow i} A (T_{AL} - T_{op,i}) \quad (4.9)$$

Rearranging this relation enables determining T_{AL} :

$$T_{AL} = \frac{Q_{pli,i}}{P_{AL \rightarrow i} A} + T_{op,i} \quad (4.10)$$

In a heating case, the highest temperature will thus be T_{AL} . The temperature will drop in the direction to both zone i and zone j. In a cooling case, the temperature T_{AL} will be the lowest, with consequently increasing temperatures in the directions to zone i and j.

Based on this temperature T_{AL} , the losses $Q_{AL,j}$ to the surrounding zone can be calculated using the permeance from layer AL to zone j:

$$Q_{AL,j} = P_{AL \rightarrow j} A (T_{AL} - T_{op,j}) \quad (4.11)$$

Combining Eqs. (4.10) and (4.11) results in a relation for the losses to zone j, i.e. $Q_{AL,j}$ (W):

$$Q_{AL,j} = \frac{P_{AL \rightarrow j}}{P_{AL \rightarrow i}} Q_{pli,i} + P_{AL \rightarrow j} A (T_{op,i} - T_{op,j}) \quad (4.12)$$

4.2.2.3 *The difference between the implicit approach and the analytical calculation*

As now the losses to zone j have been defined for both approaches, the difference Δ (W) can be calculated:

$$\Delta = \frac{P_{AL \rightarrow j}}{P_{AL \rightarrow i}} Q_{pli,i} + P_{AL \rightarrow j} A \cdot (T_{op,i} - T_{op,j}) - U_{i \rightarrow j} A (T_{op,i} - T_{op,j}) \quad (4.13)$$

After rearranging, this leads to:

$$\Delta = \frac{P_{AL \rightarrow j}}{P_{AL \rightarrow i}} Q_{pli,i} + (P_{AL \rightarrow j} - U_{i \rightarrow j}) A (T_{op,i} - T_{op,j}) \quad (4.14)$$

Generally the second term is negligible due to small differences between the thermal permeance of the layer to the other zone and the overall U-value of the TAB element as the insulation is generally located in the part separating the TAB element from zone j. So Eq. (4.14) can be approximated by:

$$\Delta = \frac{P_{AL \rightarrow j}}{P_{AL \rightarrow i}} Q_{pli,i} \quad (4.15)$$

As the part from the active layer to zone j contains insulation, while the part from the active layer to zone i is not insulated, the difference Δ will be small for a well built-up active building element. As an example the insulation thickness ($\lambda=0.04$ W/mK) has been determined to be 10 cm in order to achieve an error of 1.5% for a TAB element built up with 5 cm concrete plus 1 cm tiles above the active layer.

4.3 Testing the model's dynamic response

4.3.1 Emitter/absorber located in the zone.

To validate the dynamical response of the adapted formula, it should be compared to measurement data. Ham [8] describes such data when setting up a detailed model for different configurations of heat emission elements. The measurements show the dynamics of radiators and convectors for changes in supply water temperature and flow rate. However the detailed measurement data are not presented, formulas are given for calculation of the dynamical response of the water temperature and the emitted heat as a function of amongst others the current flow rate compared to the nominal flow rate. These formulas are shown to accurately agree with the

measurement data; the maximum deviation is 7% on the emitted flux and 4% on the water outlet temperature. The different configurations tested for that analysis all show a 'dead' time or a delay in response for the exit water temperature. That time is related to the water mass in the emission element and the flow rate used. This can be explained by the physical movement of the water; the 'old water' must be removed before the 'new water' arrives at the outlet.

To verify the implicit model, the above mentioned formulas are used to calculate the average temperature of the heat emitter/absorber element and the thermal flux input into the heat emission element. The data presented in [8] are for a narrow range around the nominal conditions and for relatively high values of the radiator exponent only. The effect of the improvements to the empirical formula is mainly on the radiant output, the difference between the non-improved and the improved formula is thus small for this case. The results will therefore be shown only for the improved formula, for a range of calculation timesteps.

The agreement between the results of Ham [8] and the single node adapted and non-adapted formulae is shown for the column radiator in Figure 4.21. In such a configuration, the element heats up almost uniformly, so the almost perfect agreement with the 1-node approach is thus to be expected.

The effect of increasing the simulation timestep to up to 3 minutes is shown in the figures below. For the column radiator, the maximum instantaneous deviation on the calculated thermal power output is limited to 5.5% for the 3-minute timestep. This deviation is an underestimation. Ham [8] mentions he achieved maximum deviations between measurements and calculations for a similar step change up to 7%, the calculated values then being an overestimation.

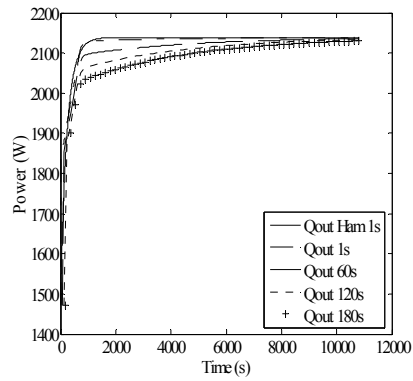


Figure 4.21: Dynamic response on a 70°C to 90°C water inlet temperature rise using the adapted and non-adapted empirically derived formula compared to empirically fitted functions by Ham [8]. The results are shown for a column radiator with n equal to 1.3, 14.2 kg metal casing and 44 kg of water content. $Q_{outHam\ 1\ s}$ refers to the calculated output using the Ham-model with a 1 second timestep, $Q_{out\ 1s}$, $Q_{out\ 60s}$, $Q_{out\ 120s}$ and $Q_{out\ 180s}$ refer to the calculated outputs using the implicit model with timesteps of 1 second, 60 seconds, 120 seconds and 180 seconds respectively.

There is a larger underestimation during start-up for the other configurations (shown in Figure 4.22 and Figure 4.23 for the panel radiator and the convector respectively), even up to 11%. For the panel radiator the reason is that there are dead ends with stagnating water. They are only indirectly activated. Consequently, there is a non-uniformity between the average temperature of the emission element and the mean average of water in- and outlet temperature: the average water temperature will be high compared to the single node implicit approach presented in this dissertation.

Such non-uniformity during heating up also appears in case of the convector. However, the fins of the convector are thin compared to the lamella of the panel radiator. The non-uniformity disappears faster, as can be seen comparing Figure 4.22 and Figure 4.23.

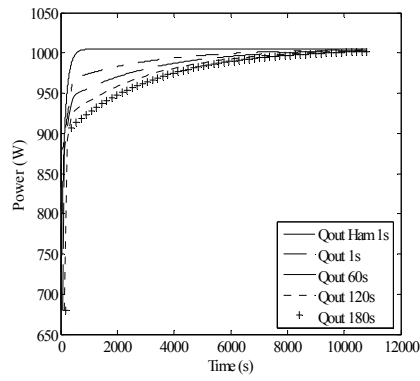


Figure 4.22: Dynamic response on a 70°C to 90°C water inlet temperature rise using the adapted and non-adapted empirically derived formula compared to empirically fitted functions by Ham [8]. The results are shown for a panel radiator with n equal to 1.3, 15,3 kg metal and 3.7 kg water. $Q_{outHam} 1 s$ refers to the calculated output using the Ham-model with a 1 second timestep, $Q_{out} 1s$, $Q_{out} 60s$, $Q_{out} 120s$ and $Q_{out} 180s$ refer to the calculated outputs using the implicit model with timesteps of 1 second, 60 seconds, 120 seconds and 180 seconds respectively.

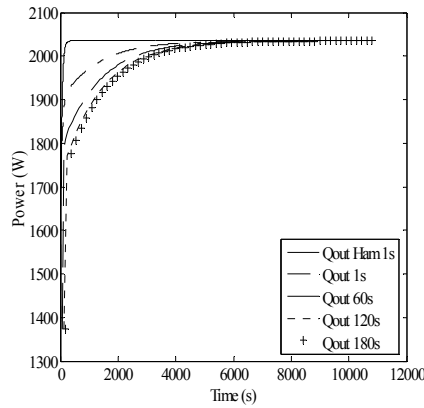


Figure 4.23: Dynamic response on a 70°C to 90°C water inlet temperature rise using the adapted and non-adapted empirically derived formula compared to empirically fitted functions by Ham [8]. The results are shown for a convector with n equal to 1.34, 1.4 kg of metal and 1.2 kg water. $Q_{outHam} 1 s$ refers to the calculated output using the Ham-model with a 1 second timestep, $Q_{out} 1s$, $Q_{out} 60s$, $Q_{out} 120s$ and $Q_{out} 180s$ refer to the calculated outputs using the implicit model with timesteps of 1 second, 60 seconds, 120 seconds and 180 seconds respectively.

Remark: the above shown dynamic comparison indicates that the effect of the timestep used is important. When focussing on emitter/absorber elements with a high fraction of convection, a small timestep might even be more important than the use of an improved calculation of the thermal output. However, this is no longer the case when the focus is on elements with a high fraction of radiant output. As indicated in chapter 3 (see amongst others Figure 3.10), the deviations between the empirical and the improved formula can then rise to higher values than those indicated above for timesteps of 180 seconds.

4.3.2 Dynamical verification of element embedded in the zonal enclosure.

The single node approach will here be compared to a 2-layer approach. The first layer, the lower layer, consists of the pipings and the concrete in between them, the second layer consists of the concrete and possible finishing above the piping. The 2-layer model is simplified assuming a thermal power flux in the direction of the zone of interest only. For the effect of losses to the zone on the other side of the TAB element the reader is referred to the steady state analysis presented before.

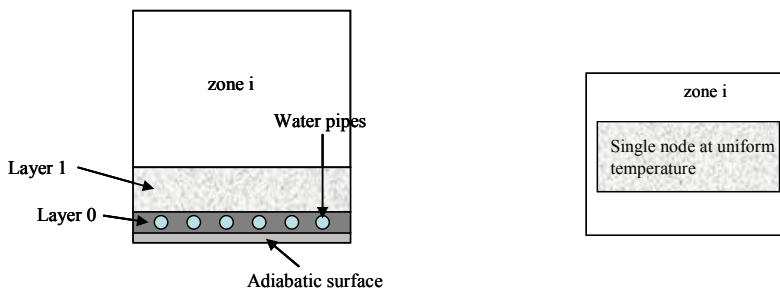


Figure 4.24: Schematic presentation of the two-layer approach on the left side and the single node implicit approach on the right side.

4.3.2.1 Two-layer approach

The heat balance of the lower layer is given by:

$$C_0 \frac{\partial T_0}{\partial t} = Q_{in} - P_{0 \rightarrow 1} A (T_0 - T_1) \quad (4.16)$$

where C_0 (J/K) denotes the heat capacity of the lower layer, T_0 (K) indicates the layer's average temperature, t (s) is the time, Q_{in} (W) the thermal power flux injected in the lower layer, P_{0i} (W/m²K) the thermal permeance for heat transfer from the lower to the upper layer and A (m²) is the surface area separating the two layers.

For the upper layer, the energy balance can be written as:

$$C_1 \frac{\partial T_1}{\partial t} = P_{0 \rightarrow 1} A (T_0 - T_1) - P_{1 \rightarrow i} A (T_1 - T_{op,i}) \quad (4.17)$$

where C_1 (J/K) denotes the heat capacity of the upper layer, T_1 (K) indicates the layer's average temperature, P_{1i} (W/m²K) the thermal permeance for heat transfer from the upper layer to the zone i , $T_{op,i}$ (K) the zonal operative temperature.

Equation (4.16) can be rearranged:

$$P_{0 \rightarrow 1} A (T_0 - T_1) = -C_0 \frac{\partial T_0}{\partial t} + Q_{in} \quad (4.18)$$

Combining Eqs. (4.17) and (4.18) results in:

$$C_1 \frac{\partial T_1}{\partial t} = -C_0 \frac{\partial T_0}{\partial t} + Q_{in} - P_{1 \rightarrow i} A (T_1 - T_{op,i}) \quad (4.19)$$

This can be written as a function of the average temperature of the upper layer, T_1 :

$$\frac{\partial T_1}{\partial t} = -\frac{C_0}{C_1} \frac{\partial T_0}{\partial t} + \frac{1}{C_1} Q_{in} - \frac{1}{C_1} P_{1 \rightarrow i} A (T_1 - T_{op,i}) \quad (4.20)$$

4.3.2.2 *Implicit single node approach*

The dynamic model of the implicit approach is given by:

$$(C_0 + C_1) \frac{\partial T_{emit,i}}{\partial t} = Q_{in} - P_{emit \rightarrow i} A (T_{emit,i} - T_{op,i}) \quad (4.21)$$

where the thermal permeance from the emitting/absorbing element to the zone is given by $P_{emit,i}$ (W/m^2K).

This can be rearranged as a function of the change in $T_{emit,i}$:

$$\frac{\partial T_{emit,i}}{\partial t} = \frac{1}{(C_0 + C_1)} Q_{in} - \frac{1}{(C_0 + C_1)} P_{emit \rightarrow i} A (T_{emit,i} - T_{op,i}) \quad (4.22)$$

4.3.2.3 Comparing the two approaches

When comparing the two approaches, the difference in temperature rise/fall of the single node approach is subtracted from the temperature rise/fall of the upper layer of the two-layer approach using Eqs. (4.20) and (4.22):

$$\begin{aligned} \frac{\partial T_1}{\partial t} - \frac{\partial T_{emit,i}}{\partial t} = & -\frac{C_0}{C_1} \frac{\partial T_0}{\partial t} + \left(\frac{1}{C_1} - \frac{1}{C_0 + C_1} \right) Q_{in} - \frac{1}{C_1} P_{1 \rightarrow i} A (T_1 - T_{op,i}) \\ & + \frac{1}{C_0 + C_1} P_{emit \rightarrow i} A (T_{emit,i} - T_{op,i}) \end{aligned} \quad (4.23)$$

As the value of the heat capacity is generally large compared to the value of the input thermal flux multiplied by the timestep and the value of the thermal permeance multiplied by the surface area⁴, Eq. (4.23) can be simplified to:

⁴ The order of magnitude of C_0 is typically in the range of 10^4 J/K, for C_1 it is typically in the range of 10^5 or even 10^6 J/K for common residential rooms, for the permeance of an uninsulated layer it is in the range of 2 to 4 W/m^2K and for the transmittance of an insulated layer it is in the range of 0.2 to 1.5 W/m^2K depending on the amount and type of insulation.

$$\frac{\partial T_1}{\partial t} - \frac{\partial T_{emit,i}}{\partial t} \approx - \frac{C_0}{C_1} \frac{\partial T_0}{\partial t} \quad (4.24)$$

It is generally accepted to take the thickness of the lower layer equal or slightly larger than the thickness of the water pipes embedded in it [15]. The upper layer consists of the concrete layer plus surface finishing above the piping, generally resulting in a large value for its heat capacity. The temperature change of the lower layer can only be large in case the heat capacity of this layer is limited. Water-based TAB elements, however, generally rely on the piping-in-concrete layer technique, with consequently large thermal capacity. For such a high capacity, the velocity of temperature change will be small. This effect limits the difference in dynamics between both approaches.

4.4 Summary and conclusions

In this chapter, the implicit model for the heat emission/absorption element has been verified. For the radiant heat transfer coefficient, it has been shown that the improved formula, as deduced in chapter 3, is more accurate over the temperature range of interest for water-based heating/cooling applications: the error is less than 0.6% for temperature differences between emitter/absorber and mean radiant temperature of -18°C to 50°C.

The simplified temperature-dependent correlation for the natural convection coefficient, used in both the non-improved and the improved formula (Eqs. (3.19) and (3.49)), results in minor deviations only when comparing with a more detailed theoretical formula for the case the emitting/absorbing element is heating the zone. For the cases considered the resulting average error is less than 0.3% for a vertical isothermal plate and 1.63% for an isothermal cylinder. Peak deviations of up to 3.9% for a vertical plate occur at small temperature differences. For the cylinder the highest deviation is observed for cooling cases with large temperature differences: 2.8% for a 12K temperature difference.

The assumption of an area-weighted mean radiant temperature as observed by the emitting/absorbing element showed deviations proportional to the ratio surface area over viewfactor. For the case of floor heating/cooling, the resulting deviation from

the viewfactor-weighted calculation is consequently the largest for changes to the ceiling's surface temperature. For the specific zone used as example deviations of up to 3% are shown for a 5K surface temperature change. Similar changes to the surface temperatures of a wall result in deviations of less than 1%. The case of a radiator shows deviations of less than 0.1% for changes of up to 5K in ceiling and wall surface temperatures. However, large deviations are shown for changes to the surface temperature of the floor: up to 7% for the case the floor temperature decreases by 5K.

Concerning the MRT as observed by an occupant of the zone, the use of an area-weighted calculation including the surface temperature of the thermally activated floor showed to result in less than 2% difference on the operative temperature compared to the more detailed viewfactor weighted calculation. This is, assuming the correct surface temperature is available. Using measurement data on a TAB, a model was set up to check on the accuracy of the use of the average temperature of the TAB element to represent the surface temperature. It was shown that for large layer thicknesses, the assumption is not correct. However, lack of correct convection coefficients for thermally active floors and ceilings does currently not allow modelling such elements in detail. Consequently, the model is not refined to account for the difference surface versus average element's temperature.

Further, it was shown that the deviation on the MRT calculation and the deviation on the surface temperature have an opposite influence in case of active floors. This will positively affect the overall deviation. For active ceilings the deviations are in the same direction and will thus enlarge the resulting deviation.

Concerning thermally active walls, the convective heat transfer is based on correlations for vertical elements. Those correlations are not subject to such large deviations as for horizontal elements. However, the deviation between viewfactor weighted and area weighted calculation might be small, depending on the zones geometry. That implies that a deviation between element's average and surface temperature will directly influence the operative temperature.

For the evaluation of the thermal comfort in case of a radiator, the deviation between the operative temperature calculated using a viewfactor weighted mean radiant temperature compared to a surface averaged is shown to go up to 3% for the case of a seated person and a 40°C temperature difference between emitter/absorber and zone. For the same conditions but for the case of a standing person, the deviation

equals 2%. In the case of a radiator, the emitter/absorber element's temperature is not used in the calculation of the mean radiant temperature, assuming its surface area is limited. The assumption of the average homogeneous temperature equal to the surface temperature is here accepted based on the limited thickness of the casing.

The steady state performance of the model for representing a radiator shows a convincing agreement with the results of a more detailed radiator model implemented in MATLAB. The latter model was calibrated using measurement data in the range 60°C to 80°C. Deviations showed to be within the error margin.

The dynamic response of the implicit heating/cooling element representing a radiator is compared to the model of Ham [8]. The latter model overestimates the thermal output with up to 7% compared to the measured values. The single node approach, as taken using the implicit heat emitter/absorber, shows good agreement with the model of Ham. The deviations, however, do increase when the element of interest has a configuration that heats up less uniformly.

The case of the implicit model representing a TAB element is verified theoretically. The steady state verification showed the implicit model to underestimate the losses to the surrounding zone by a factor equal to the ratio of the permeance of the layer(s) separating the water pipes and the surrounding zone versus the permeance of the layer(s) separating the water pipes and the zone to be heated/cooled. The former contain the insulation. The resulting ratio is thus small.

An analytical comparison is also used to verify the dynamics of an active solid building element. This shows a deviation that is proportional to the ratio of the heat capacity of the active layer containing the water pipes versus the layer separating this active layer from the zone of interest. Usually the latter value is higher compared to the active layer itself.

The verification has thus shown that the implicit emitter/absorber can be used to represent a wide range of heat emission/absorption systems. However, the application of the model to represent horizontal TAB elements should be done with care. As stated in chapter 3, more detailed correlations for convection coefficients are required in this case.

As now the strengths and weaknesses of the implicit formula have been verified, it can be used in the tool to determine the optimal characteristics of future heating/cooling elements, as will be shown in chapter 8.

In the next chapter, the model of the remaining component of the implicit plant structure, i.e. the production device, is presented.

References

- [1] S. Churchill, H. Chu, 1975, Correlating equations for laminar and turbulent free convection from a vertical plate, *International Journal of Heat and Mass Transfer*, vol. 18, pp. 1323-1329
- [2] F. Incropera, D. Dewitt, 1996, *Fundamentals of heat and mass transfer*, fourth edition, John Wiley and sons, Inc. New York, ISBN 0-471-30460-3
- [3] J. Howell, 2001, A catalogue of radiation heat transfer configuration factors, available online through: <http://www.me.utexas.edu/~howell/>
- [4] G. Cannistraro, G. Franzitta, C. Gianconia, 1992, Algorithms for the calculation of the viewfactors between human body and rectangular surfaces in parallelepiped environments, *Energy and Buildings*, vol. 19, pp. 51-60
- [5] R. De Herdt, T. Van Reet, N. Moenssens, M. Sourbron, W. Van Passel, 2008, *Handboek voor het verwarmen en natuurlijk koelen van thermisch actieve gebouwen*, W&K De Nayer instituut, Belgium
- [6] F. Khaldi, 2008, *Ontwikkeling en validatie van een RC-model voor betonkernactivering*, Master's thesis (coach: M. Sourbron, Promotor: L. Helsen), Department of Mechanical Engineering, University of Leuven (KUL), Belgium
- [7] M. Sourbron, 2009, *Dynamic behaviour of buildings with thermally activated building elements*, PHD (work in progress), Department of Mechanical engineering, University of Leuven (KUL), Belgium
- [8] P. Ham, 1988, *Dynamisch warmtegedrag van radiatoren en convectoren; Metingen en modelvorming*, *Verwarming en Ventilatie*, vol. 5, pp. 318-334
- [9] K. Chatziangelidis, D. Bouris, 2009, Calculation of the distribution of incoming solar radiation in enclosures, *Applied Thermal Engineering*, vol. 29, pp. 1096-1105
- [10] J. Van der Veken, E. Maes, 2008, *Verbeteren van de energie-efficiëntie van verwarmings-, koel- en ventilatieproducten d.m.v. gevalideerde dynamische modellen*, IWT-project of the Building Physics division the University of Leuven and Jaga, Belgium
- [11] H. Hens, 2003, *Bouwfysica 1: Warmte –en massatransport*, ACCO, Leuven, Belgium, ISBN 9 789033 454127
- [12] C. Bouthe, 2006, *Ontwikkeling van een theoretisch model voor de warmteafgifte van radiatoren*, Master's thesis (coach: V. De Meulenaere, Promotors: P. Van den Broeck, H. Hens), Katholieke Hogeschool Sint-Lieven, Gent
- [13] R. Fox, A. McDonald, P. Pritchard, 2003, *Introduction to fluid mechanics*, Wiley, New York, ISBN 0-471-73558-2
- [14] C. Underwood, F. Yik, 2003, *Modelling methods for energy in buildings*, Blackwell Publishing, Oxford, ISBN 0-632-05936-2
- [15] M. Gwerder, B. Lehmann, J. Todtli, V. Dorer, F. Renggli, 2008, Control of thermally activated building systems (TABS), *Applied Energy*, vol. 85, pp. 565-581

5 PRODUCING THE HOT/COLD WATER

The overall performance of the emission/absorption element is influenced by the hot/cold water production system¹ it is combined with. More specifically, the limitations in the operation of a certain production system might prevent the emission/absorption system from reaching an optimal performance, even if this last one is equipped with an ideal control. This has been a subject of research of the current author throughout the e²ep-project, the results of which have been published in several reports and presented at multiple conferences ([1] - [5]).

Based on that experience, in this chapter, a generic model for a heat/cold production system will be set up which allows the examination of the influences of real production systems on the performance of the overall heating/cooling

¹ In fact the production device does not ‘produce’ hot or cold water. It increases or decreases the internal energy, resulting in water at a higher or lower temperature respectively.

installation. The detailed modelling of the production systems itself, however, is not the aim of the current research.

5.1 Introduction

The e²ep-project has clearly shown that the overall performance of a heating installation cannot be determined solely based on the performance of the individual components [3]. It is a complicated interactive process between these components, the control and the building itself [6]. By way of example, floor heating has been shown to be the less energy efficient emission system in combination with non-condensing high efficiency boilers, whereas it can be one of the best options when producing the heat with a heat pump. Such ranking depends strongly on the circumstances, the ranking referred to here, was set up based on yearly simulations for an average insulated terraced house where set back was implemented. High-temperature radiators, on the other hand, showed to be perfectly combinable with high efficiency boilers but they should be replaced by low-temperature radiators in combination with a condensing boiler. Cogeneration systems, such as an internal combustion engine or the ‘first generation’ Stirling-boiler combinations, have been shown [5] insufficiently flexible to be directly coupled with low heat capacity emission/absorption systems. Besides the coupling of the different components of the heating system, also the building type and its insulation quality are factors of influence when evaluating the limitations of a production system [7].

Cooling was not considered in the e²ep project. However, it is obvious that the characteristics of the production element can influence the thermal comfort and energy consumption of a given heat emission/absorption element in a given context both for heating and cooling. This has been confirmed by Zogou and Stamatelos [8] by comparing the performances of different heating and/or cooling devices. To evaluate and optimise different combinations of emitters/absorbers and production systems in a given context, it is therefore important to take possibly limiting characteristics of the production device into account.

In this chapter a generic model is set up that allows accounting for such limitations in the performance evaluation of ideal and more realistic heating/cooling

installations. The detailed modelling of the production systems, however, is not the focus of the current research².

The control aspects of the production units will be treated in the next chapter.

5.2 The generic implicit production model

As described in chapter 2, the production model uses the facilities of the global controllers' structure. It is explained in that chapter that both the production control as well as the production model itself are embedded in this global structure. The overview, shown in Figure 2.14, indicates the sequence of the calculation steps: the implicit production controller first defines the thermal power to be produced, Q_{prod} (W), which is then used as an input for the implicit production model itself. Besides the power Q_{prod} , however, other information is shared as well. The two algorithms, representing the implicit production control and the implicit production model, are thus more strongly connected than suggested by the outline of Figure 2.14.

The interface of the implicit production simulation model allows the selection of the appropriate implicit production control. The inputs are thus mixed control and production element related. They will be listed and discussed below. However, the function of the inputs associated with the control aspects will be considered more in detail in chapter 6.

5.2.1 Schematic overview

In Figure 5.1 the scheme of the production device as given in chapter 2 is recalled and the allocation of the production-device-related input parameters is indicated. The thermal power, Q_{prod} (W) to be produced, is received from the production control. At that moment, it is already checked whether this amount can be produced based on the control-related parameters as given by Table 5-1. It thus concerns checks on lock-out times, off time between heating and cooling, and available heating/cooling capacity.

² For a detailed boiler modelling the reader is referred to [9]. For heat pump models reference [10] can be consulted. Models of CHP's can be found in [11].

As described in chapter 2, the calculated zonal thermal power fluxes are not directly allocated to the different zones. They first pass the distribution system routine, where some energy will be lost.

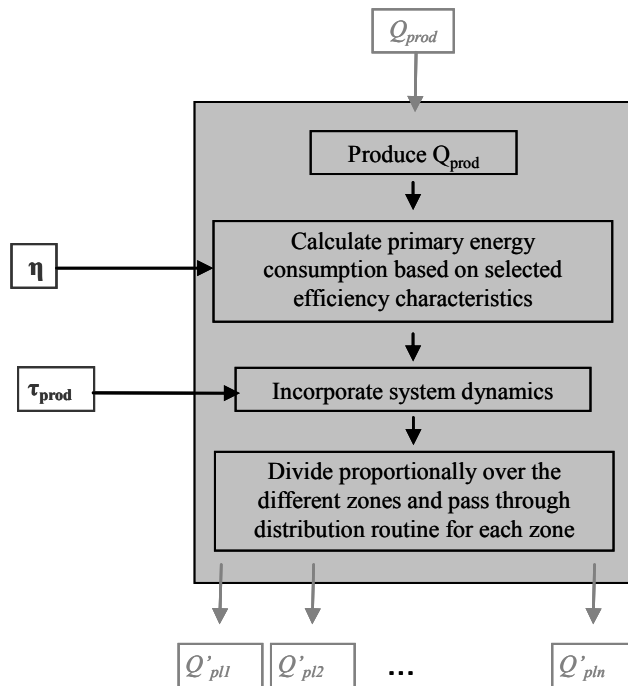


Figure 5.1: Schematic representation of the implicit production unit logic and allocation of input parameters. The grey box indicates the processing of information within the implicit production device model³. The required user-defined input parameters are indicated in bold, whereas the flow of information to and from the production device model is indicated in italic.

³ The logic of calculating the primary energy consumption first and consequently incorporating the system dynamics is purely related to model implementation.

5.2.2 The model parameters

5.2.2.1 *The parameters influencing the thermal power deliverance to the heat emitter/absorber*

The set of parameters describing the implicit production element must be suited to represent any production device and focus on the characteristics that could possibly influence the performance of the emission/absorption elements and thus the thermal comfort.

The most obvious parameter is the maximum heating/cooling capacity, i.e. the installed heating/cooling power the production unit can deliver, either for heating, for cooling or for both. For modulating systems also the lower limit needs to be specified. The impact of the thermal power limits is not negligible. The effect of an underestimation of the required capacity is self-evident. The effect of an overestimation of the capacity has been described by the current author in amongst others [12]. That work focused on boilers in combination with radiators with thermostatic radiator valves (TRV's). The detailed models of boiler and TRV's used for the simulations were developed by Van der Veken [13]. It was concluded that the thermal comfort was not affected by oversizing, thanks to the use of the radiator valves. The influence on the boiler efficiency, however, was negative; the efficiency showed a clear decrease as a function of the thermal capacity once over the required thermal capacity. The efficiency decreasing effect has been confirmed by additional simulations by Michiels and Smolders [14] and Zogou and Stamatelos [8].

The lock-out time is a parameter that is strongly related to the flexibility of the production system. It indicates the minimum time off between two operating periods. This parameter should be small, if the production system is directly coupled with the heat demand of the building [5].

The time off between heating and cooling indicates the minimum required time to change its system's cycle from heating into cooling mode and vice versa. It can also be used as a control parameter to prevent continuous switching between heating and cooling.

The dynamics of the production systems could be implemented using a power balance approach. Discussions with manufacturers on their measurements showed that the start-ups and shut-downs will have effects taking longer than 1 minute⁴. However, once through the start-up, the transition from a certain output to a lower or higher thermal power delivery has effects on a timescale that is smaller than 1 minute. This is confirmed for boilers by measurements performed in the framework of the before-mentioned el²ep-project [15]. Using a *time constant*⁵-approach for start-up and shut-down calculations only, enables a simplified dynamic modelling of the heat/cold production systems, while still incorporating all the necessary details. It avoids adding an iterative loop to solve the power balance equation.

Two additional input parameters are the maximum average production temperature and the efficiency characterisation. This maximum average production unit temperature limit can be required for devices such as heat pumps without electrical back up or booster. The *efficiency characterisation* parameter allows selecting a primary energy calculation method for the production system. So, it can indirectly represent an existing device. The currently implemented efficiency characterisation methods are described in detail in appendix C, the overview here will be limited to the main methodology.

All parameters described above are listed in Table 5-1. The maximum average production unit temperature is a parameter that is not treated on the production level, but passed on to the different emitter/absorber elements and it is accounted for on that level.

⁴ As the implicit approach is implemented in the structure of the building level, the standard minimum simulation timestep is 1 minute. This can be reduced, but negatively influences the simulation duration. As Kummert [16] mentions, the large capacity of the building itself will reduce the importance of small timestep effects.

⁵ The current model is based on a single time-constant. The model could be extended to an energy-balance model similar to the emitter model so that more detailed transient calculations could be performed. For the current analysis, however, such level of detail is not required.

Input parameter	Symbol
Maximum heating capacity (W)	$Q_{h_prod,max}$
Minimum heating capacity (W)	$Q_{h_prod,min}$
Maximum cooling capacity (W)	$Q_{c_prod,max}$
Minimum cooling capacity (W)	$Q_{c_prod,min}$
Lock out time (s)	t_{lock_out}
Time off between heating and cooling (s)	t_{heat_cool}
<i>Time constant (s)</i>	τ_{prod}
Control selection (-)	Control
<i>Efficiency characterisation (-)</i>	η
Maximum average production temperature (K)	$T_{prod,max}$

Table 5-1: Input parameters for generic implicit production model. The parameters indicated in italic are related to the production device model, the parameter in grey is passed on to the emitter/absorber model(s), and the other parameters are production control-related and will be discussed in chapter 5.

5.2.2.2 *The parameters related to the production system's primary energy consumption*

Efficiency data, measured by manufacturers, are available for a wide range of residential heating devices. The measurements are generally according to regional, national or international standards (e.g. [16] for Germany, [18] for The Netherlands or the European Standard En 14511 [19]), so as to serve as input values for building energy performance calculations (see e.g. Energieeinsparverordnung, EnEV, in Germany, National Calculation method, NCM, with the calculation tool Simplified Building Energy Model, SBEM, for the UK, Energieprestatiecertificaat, EPC, in the Netherlands and Energieprestatie en Binnenklimaat, EPB in Flanders).

The idea of the European Energy Performance Building Directive (EPBD) concerning cooling is that it should be avoided in residential buildings [20]. At present there is no legislation yet related to the EPBD concerning performance-measurements of domestic cooling installations. Information on cooling devices is thus not as widespread as it is for the heating devices. In the Flemish EPB-software, only a rough implementation of an active cooling installation exists. It is calculated based on the energy consumption for cooling during a warm summer. Ambient

temperatures and solar radiation are somewhat higher than the longtime average would be [21]. The area weighted average indoor temperature for the calculation of the cooling load is set to a constant value of 23°C. Comparing to the guidelines described in chapter 1, this is a rather low value. The efficiencies of the installation are fixed, non-user-supplied values, based on performance characteristics of less efficient devices. It can thus be stated that the EPW-calculation in general leads to an overestimation of the energy consumption related to the cooling load [22]. A similar approximate methodology, however with the average indoor cooling temperature set to 24°C, is found in the EPC implementation in the Netherlands [23].

The implicit production model aims to only give a rough estimation of the primary energy consumption related to a certain production device. It is thus obvious to use widely available data. However, the input should allow modelling a wide variety of devices. Therefore the test-data as defined by the German DIN 4701 and the European EN 14511, a.o., are used if possible. The currently implemented efficiency calculation methods are listed below. They allow modelling ideal devices, heat pumps, boilers and CHP's. It is up to the user to mark cooling being allowed/possible or not for each of these devices.

It should be noted that concerning efficiency calculations, the inputs can be related either to the energy source used (such as natural gas or electricity) or to primary energy.

Efficiency of an ideal production device

The efficiency of an ideal device is 100%. In that case the produced thermal power equals the primary power input. This is the only efficiency calculation for which the primary power input is calculated only after incorporating the dynamical effects.

Efficiency related to ambient temperature

This efficiency calculation is added mainly to model heat pumps. Where boilers have an efficiency that is only slightly affected by the outdoor temperature by means of the temperature of the combustion air, the influence of the outdoor temperature is of considerable impact for heat pumps with air as source [1]. Water- or ground-source heat pumps are subject to much smaller temperature variations at source side. Linking the variations at the source side to hourly averaged ambient temperatures

enables determining the performance of these types of heat pumps as a function of the outdoor temperature. The requested data for the efficiency calculation are based on the test data for air-to-water heat pumps in heating mode. As shown by [24] these data are sufficient to represent the performance of air-source heat pumps both in heating and in cooling mode.

It should be noted that such an approach is suited for on/off heat-pumps only. No data were available to determine the performance dependency for a modulating heat pump on both the part load ratio and the source temperature.

Efficiency related to part load ratio

Efficiency calculations related to the part load ratio⁶, PLR (%), are added to model boilers. The efficiency of boilers, however, is mainly related to both the part load ratio, PLR (%) and the water temperature. The latter parameter, the water temperature, is primarily an indicator for the occurrence of condensation.

The difference between condensing and non-condensing systems will here be made by correctly choosing the maximum average temperature of the production unit, T_{prod} , and providing the correct corresponding efficiencies at 10%, 30% and 100% part load ratio. It should be emphasized, though, that when the focus is on the detailed performance of a condensing boiler, the implicit approach cannot give a decisive answer on how much condensation appears.

Efficiency calculation for CHP devices

Different types of micro-cogeneration units are currently available [5], [11]. To characterise the performance of any combined heat and power (CHP) unit, data is necessary on both the thermal and the electrical output. The electrical output E (W) of the CHP device is calculated based on Eq. (5.1) as a function of the instantaneous part load ratio and the user supplied data on minimum and maximum electricity production, i.e. E_{min} (W) and E_{max} (W) respectively. The efficiency of the CHP is

⁶ The part load ratio is the ratio of the capacity of the device at a certain time interval versus the maximum capacity it could deliver during that interval.

then defined by the fuel utilisation ratio⁷, FUR (-), as given by Eq. (5.2), where PP is the input primary power.

$$E = \max(PLR \cdot E_{\max}, E_{\min}) \quad (5.1)$$

$$FUR = \frac{Q_{\text{prod}} + E}{PP} \quad (5.2)$$

Transient effects in the efficiency calculation

Except for the ideal efficiency, the calculation of the primary energy is done before dynamical effects are taken into account. This approach presumes that the fuel/electricity use of the device is at its steady state input directly. As the output of the device is subject to transient effects as described below, while the primary power input is not, this results in a lower efficiency during start up. For shut-down calculations, no primary power input is considered, while the remaining device output is still distributed amongst the different zones.

This approach is not as far from reality as it might seem at first sight. That is confirmed for heat pumps by Vargas and Parise [26] through simulations, through measurements for internal combustion engines by Voorspools and D'haeseleer [27] and similarly through measurements for boilers by Michiels et al. [14].

5.2.3 The production system dynamics

To incorporate the dynamics, the statistics on heating and cooling have to be retained and adapted at each simulation timestep. It involves:

- Total time heating on since last off
- Total time heating off since last on
- Total time cooling on since last off

⁷ The fuel utilisation ratio, sometimes called Energy Utilisation Factor, is often erroneously called total efficiency. This last term, although formally correct in the sense of the first law of thermodynamics, is meaningless in the philosophy of the second law which encompasses the concept of exergy, clearly distinguishing between electricity and heat [25].

- Total time cooling off since last on.

These data are defined in the implicit production control and passed on to the algorithm representing the production device. Based on these statistics and the timeconstant τ_{prod} of the system, start up and shut down factors, SU (-) and SD (-) respectively, can be calculated.

$$SU = 1 - \exp\left(-\frac{\text{time on}}{\tau_{\text{prod}}}\right) \quad (5.3)$$

$$SD = \exp\left(-\frac{\text{time off}}{\tau_{\text{prod}}}\right) \quad (5.4)$$

Whether to calculate the device's output with the start-up factor SU for heating or for cooling, or the shut down factor SD for heating or for cooling, depends on the value of the thermal power requested by the device's control, Q_{prod} . The finally selected factor is then referred to as DF (-), i.e. the dynamical factor.

5.2.4 The overview of the production system algorithm

Figure 5.2 gives the schematic overview of the algorithm implemented to represent the implicit production unit.

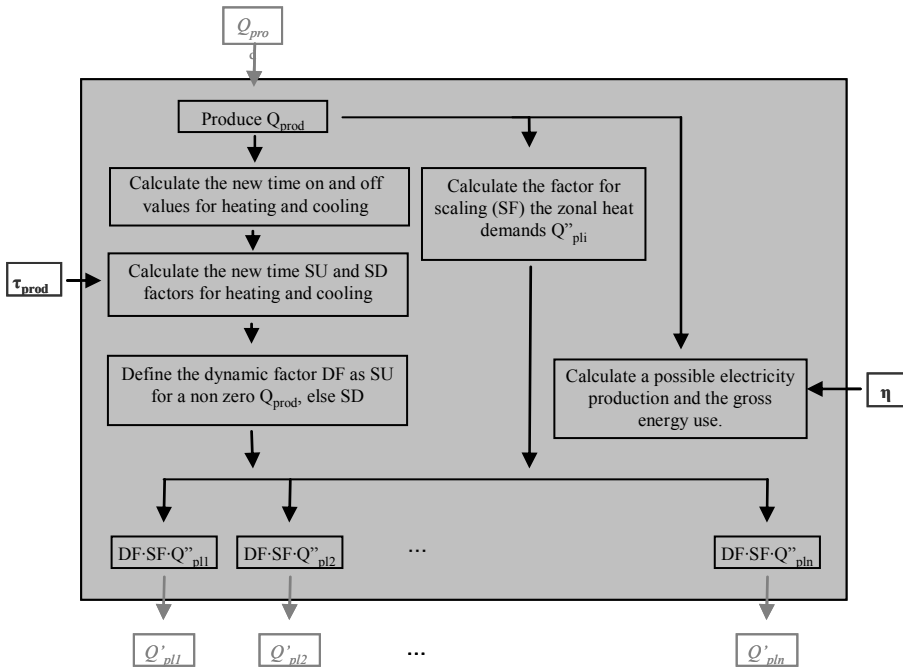


Figure 5.2: Schematic representation of the implicit production unit calculation methodology and allocation of input parameters. The grey box indicates the calculations within the implicit production device model. The required user-defined input parameters are indicated in bold, whereas the flow of information to and from the production device model is indicated in *italics*.

5.3 Summary and conclusions

In this chapter a generic model has been described for simulation of heating/cooling production devices. It is a rather rough model, mainly focussing on parameters that could influence the output of the device.

A rudimentary efficiency calculation methodology is presented enabling to observe major performance differences between different devices.

All hardware components of the implicit heating/cooling device have now been modelled. The next step to complete the implicit plant level is to define the controls for these hardware components. This issue will be tackled in the next chapter.

How the model is embedded in *ESP-r* and how it interacts with the other structures is schematically shown in appendix B.

References

- [1] L. Peeters, W. D'haeseleer, 2007, WKK en warmtepomp voor woningverwarming, report TME/WDH/2007/TR04, Division of applied mechanics and energy, University of Leuven (KULeuven), Belgium (In Dutch)
- [2] J. Van der Veken, L. Peeters, L. Helsen, H. Hens, W. D'haeseleer, 2005, Economy, energy and ecology based comparison of heating systems in dwellings, 9th IBPSA, Montreal, August 15-18, electronic proceedings.
- [3] L. Peeters, J. Van der Veken, H. Hens, L. Helsen, W. D'haeseleer, 2006, Economic, energetic and ecologic comparison of CHP and heat pumps with high efficiency gas boilers in domestic dwellings, 3rd International Building Physics Conference, Montreal, August 27-31, electronic proceedings.
- [4] L. Peeters, J. Van der Veken, L. Helsen, H. Hens, W. D'haeseleer, 2006, The performance of different heating systems in buildings with varying insulation quality. 4th Esim Conference, Toronto, May 3-5.
- [5] L. Peeters, D. Haeseldonckx, W. D'haeseleer, 2006, Onderzoek Stirling-ketel combinatie voor WKK, report TME/WDH/06-01/PRL, Applied Mechanics and Energy, University of Leuven (KULeuven), Belgium (In Dutch)
- [6] L. Peeters, J. van der Veken, H. Hens, L. Helsen, W. D'haeseleer, 2008, Control of heating systems in residential buildings: current practice, *Energy and Buildings*, Volume 40, pp. 1446-1455
- [7] G. Verbeeck, 2007, Optimisation of extremely low energy residential buildings, PhD-thesis, Civil Engineering. Laboratory of Building Physics, University of Leuven (KULeuven), Belgium
- [8] O.Zogou, A. Stamatelos, 2007, Optimisation of the thermal performance of a building with ground source heat pump system, *Energy Conversion and Management*, vol. 48, pp. 2853-2863
- [9] J. Van der Veken, 2008-2009, Overall efficiency of heating systems in low energy buildings PhD-dissertation, Civil Engineering. Laboratory of Building Physics, University of Leuven (KULeuven), Belgium, (Work in progress)
- [10] ECBCS-IEA, Annex 48; heat pumping and reversibel airconditioning, operating agents, J. Lebrun, P. Andre, Universite de Liege, Belgium
- [11] WP IEA, 2008, annex 42 subtask B report, Experimental Investigation of Residential Cogeneration Devices and Calibration of Annex 42 Models, operating agent I. Beausoleil-Morisson, Carlton University, Montreal, Canada.
- [12] L. Peeters, J. Van der Veken, L. Helsen, H. Hens, W. D'haeseleer, 2007, Sizing of boilers for residential buildings, 9th REHVA World Congress, Clima 2007, Helsinki, Finland, June 10-14, electronic proceedings
- [13] J. Van der Veken, V. De Meulenaer, H. Hens, 2007. Optimisation of extremely low energy residential buildings, el²ep final report: heating system, Civil Engineering. Laboratory of Building Physics, University of Leuven (KULeuven), Belgium (in Dutch)

- [14] S. Michiels, N. Smolders, 2008, Micro-WKK: Dimensionering voor residentiële gebouwen, Applied Mechanics and Energy, Masters thesis, University of Leuven (KULeuven), Belgium (In Dutch)
- [15] J. Van der Veken, V. De Meulenaer, H. Hens, 2007. Optimisation of extremely low energy residential buildings, el²ep final report: meetcampagne studentenresidentie Vesuvius. K.U.Leuven, Civil Engineering. Laboratory of Building Physics, University of Leuven (KULeuven), Belgium (in Dutch)
- [16] M. Kummert, 2000, Contribution to the application of modern control techniques to solar buildings; Simulation-based approach and experimental validation, PhD thesis, Fondation Universitaire Luxembourgeoise, Belgium
- [17] DIN, 2003, DIN V 4701: Energy efficiency of heating and ventilation systems in buildings - Part 10: Heating, domestic hot water supply, ventilation, Germany
- [18] NEN, 2003, NEN-EN 304:1993/A2:2003; Verwarmingsketels - Beproevingvoorschriften voor verwarmingsketels met verstuivingsbranders, The Netherlands (in Dutch)
- [19] NBN, 2008, NBN-EN 14511-2: Luchtbehandelingsapparatuur, koeleenheden met vloeastof en warmtepompen met elektrisch aangedreven compressoren voor ruimteverwarming en -koeling - Deel 2: Beproevingomstandigheden, Belgium (in Dutch)
- [20] European commission, 2002, Directive 2002/91/EC of the European Parliament and of the Council on the energy performance of buildings, <http://eur-lex.europa.eu/LexUriServ/LexUriServ.do?uri=CELEX:32002L0091:EN:NOT>
- [21] Vlaamse Overheid, 2005, Bijlage 1 bij de EPW: Bepalingsmethode van het peil van primair energieverbruik van woongebouwen, <http://www.energiesparen.be/epb/bijlagen> (in Dutch)
- [22] VEA, 2006, EPW. Lespakket module 3: Oververhitting en koeling, <http://www2.vlaanderen.be/economie/energiesparen/epb/doc/module36.pdf> (In Dutch)
- [23] NEN, 2004, NEN 5198:2004: Energieprestatie van woonfuncties in woongebouwen - Bepalingsmethode, The Netherlands (In Dutch)
- [24] NRCAN, 2005, Information on "Air-Source Heat Pumps", National Resources Canada, Office of Energy Efficiency, available at: <http://www.oeec.nrcan.gc.ca/publications/infosource/pub/home/heating-heat-pump/asheatpumps.cfm>; Last consulted September 2008 (General web site NRCAN: www.nrcan.gc.ca)
- [25] J. Horlock, 1997, Cogeneration, combined heat and power (CHP), Krieger, Malabar FL, USA, ISBN 0-89464-928-0
- [26] J. Vargas, J. Parise, 1995, Simulation in transient regime of a heat pump with closed-loop and on-off control, International Journal of Refrigeration, vol. 18, pp. 235-243
- [27] K. Voorspools, W. D'haeseleer, 2001, Mini- en micro-WKK; Electrabel CO₂-project fase 3, report TME/WDH/01-01.2/FIN, Applied Mechanics and Energy Conversion, University of Leuven (KUL), Belgium (In Dutch)

6 CONTROLS FOR HEAT EMISSION/ABSORPTION AND HEAT/COLD PRODUCTION SYSTEMS

As now all the hardware plant components have been defined, the implicit plant level is completed with controllers for both the emission/absorption elements and the production system. In order to optimise the emitters/absorbers and define the requirements for a suitable production system, an ideal control for both plant components is essential. To improve the usefulness of the implicit plant modelling level, however, more realistic controllers are implemented as well. These controls will be discussed in this chapter.

6.1 Introduction

A controller is an element that senses a certain physical quantity and reacts to it based on a certain logic. For most heat emitters/absorbers in a residential setting, the sensed quantity will be an indoor temperature. The reaction of the actuator will be

on the thermal power flux. The way this flux is affected, is determined by the logic of the controller itself.

The control of the production system, however, allows sensing a variable out of a much broader range of possible physical quantities. It might be the water temperature in the production system, the temperature in a specific zone or the ambient temperature, an increased water flow rate or a time. The reaction is an effect on the production of hot/cold water. This can be through increasing or decreasing the gas supply to the burner in a boiler, or the speed of a compressor in case of a heat pump.

A wide variety of controllers for both emitters/absorbers and production systems currently exists. However, perfect control in a residential building is utopian due to the unpredictability of the context. It has been shown that the internal gains due to inhabitants and the use of appliances as well as the sun have a large impact [1]. The large impact of the sun is also confirmed by simulation results of Persson et al. [2]. The effect of the control strategy chosen for both the emission/absorption and the production can result in a major difference in primary energy consumption for a given setting. This has been proven by the current author throughout the eL²ep-project [3] and [4]. It is confirmed with simulations by Fraisse et al. [5] and with experiments by both Cho et al. [6] and Liao and Dexter [7].

The emphasis in the current dissertation is on determining the optimal characteristics of the heat emission/absorption. Controllers are necessary so as to determine when, where and how much energy injection is required. But to focus on the performance of the installation components, the controller should be ideal. Therefore, idealised controllers, for both the emission/absorption and production system, have been set up and are described below. The implicit plant level is further extended with more realistic controllers for both levels.

This chapter will focus on the controllers implemented and the way they interact with the different installation components. The main focus is on the idealised controls used for the optimisation of the emitter/absorber elements. A brief description of the other controls implemented is given in this chapter; more details on those controls are given in appendix D.

6.2 Controllers for the emission/absorption of heat

6.2.1 Desired indoor temperatures

Before the calculation of the necessary amount of heat can start, the comfort temperatures must be selected. In chapter 1, thermal comfort algorithms have been defined specifically for the 3 different zones in a residential building. Within the implicit plant level, the user can select one of those three comfort algorithms, opt for the adaptive algorithm as defined by Tuohy et al.[8], or select a constant value.

Table 6-1 shows inputs associated to the control of the emitter/absorber. The parameters indicated in *italic* are related to setting the desired indoor temperatures. The parameters in *grey* are more related to the settings of the controllers that will react to these temperatures. Specific additional inputs for the different emission/absorption controls will be indicated in *grey* throughout the description of these controls.

Input parameter	Symbol
<i>Comfort algorithm (-)</i>	<i>Comf</i>
<i>Required deadband¹ (K)</i>	<i>DB</i>
<i>Number of set back periods (-)</i>	<i>NSB</i>
<i>Start of each set back (h)</i>	<i>STA_j</i>
<i>Stop of each set back (h)</i>	<i>STO_j</i>
<i>Maximum temperature in set back</i>	<i>SBT_{max}</i>
<i>Minimum temperature in set back</i>	<i>SBT_{min}</i>
<i>Control selection (-)</i>	<i>Control</i>
Maximum average emitter temperature (K)	$T_{\text{emit},i,\text{max}}$
Minimum average emitter temperature (K)	$T_{\text{emit},i,\text{min}}$

Table 6-1: Input parameters for control of implicit heat emission/absorption model

6.2.2 The different control strategies

6.2.2.1 The ideal control

Restart after set-back

Defining an ideal control is, as stated before, essential in case the focus is on the performance of the installation components. When comparing different installations, the boundary condition obviously is that the required thermal comfort must be achieved during occupancy. This last aspect introduces the concept of intermittent heating and cooling and consequently the issue of restarting on time.

The calculation of the reheat/recool time in case of intermittent heating and cooling has been the subject of many researches. Different approaches have been proposed, simulated and validated. The most basic control, which in the residential context is

¹ This is only valid for the selection of the adaptive algorithm of Tuohy et al. [8] or when a constant indoor temperature has been defined. In case of the residential adaptive comfort, as described in chapter 1, the deadband is as determined there.

still often applied, is the use of a fixed restart time. Seem et al. [9] describe more advanced self-learning polynomial functions of the indoor and outdoor temperature. Their performance is compared to more sophisticated algorithms by Fraisse et al. [10], [11] and [12], which apply fuzzy logic principles to the restart problem, as well as a basic model predictive control. Although the latter is a rather rough 2-time constant building model, results are close to the performances achieved by applying fuzzy principles.

The use of building models to predict the restart time is common. As part of his PhD work MacQueen [13] described the Britles and John equation, implemented in *ESP-r*. That model uses the building's thermal mass and a delay factor to estimate the reheat time. Liao and Dexter [7], [14] model the building using an electrical network analogy to estimate the indoor air temperature. They, however, do not give the full details of their controller. Zaheeruddin [15] applies energy balances to both the building and the installation and builds up the interconnections between all building and installation aspects. He uses this approach to estimate performance augmentation of different heating and cooling installations. Improvements of his model involve incorporating forecast and load data ([16], [17] and [18]) and even energy prices [19] to end up with extended building energy management systems [20]. The results are promising, but the method is not easily generalised and requires detailed information on both the building and the installation. In these publications, Zaheeruddin shows only seldom the accuracy of estimating start-ups. In the oldest publication [15], he simply applies a trial and error strategy. More recent work [19] shows gradient search based optimisation of operating strategies with constraints that determine the desired temperature range after set back.

For the implicit modelling approach as developed in the framework of the current dissertation, the most suitable technique with proven accuracy therefore seems the 2-time constant approach described by Fraisse et al. [10]. They applied the technique to a heating case, but the physical principles it relies on are valid for cooling as well. For the calculation of the restart time, the technique assumes the ambient temperature and the energy flux to be constant during recovery. These are reasonable assumptions for the context of residential buildings with relatively small temperature difference between set-back periods and occupied periods [3]. The method calculates the zone control temperature $T_i(t)$ (K) at time t (s) based on the current zone temperature $T_i(0)$ (K) and the maximum zonal temperature $T_{\max,i}$ (K) that would be achieved at time t when injecting the maximum heating or cooling flux constantly between time 0 and time t .

$$T_i(t) = T_i(o) + (T_{\max,i} - T_i(o)) \left[1 - \left(K_1 \exp\left(\frac{-t}{\tau_1}\right) \right) - \left((1 - K_1) \exp\left(\frac{-t}{\tau_2}\right) \right) \right] \quad (6.1)$$

where the zone temperature in the current context is a mix of mean radiant and air temperature, K_1 (-) is a weighing factor between 0 and 1, τ_1 (s) and τ_2 (s) are time constants.

The timeconstant τ_1 used in Eq. (6. 1) is calculated for each zone at the start of the simulation. This is done taking into account the thermo-physical properties of the solid inner layer of the zonal enclosure and half of the second solid layer. The calculation itself is based on the method of Mackey and Wright as described by Clarke [21]. The **weighing factor K_1** and the second **timeconstant τ_2** (s) are user-defined values. For current research, they will be determined through the optimisation process².

Within *ESP-r*, the control temperature reached at the next simulation-timestep when injecting an amount of thermal power $Q_{\text{pli},i}$ (W), can be calculated using the relation given by Eq. (2.19). That equation can be rewritten in the format given by Eq. (6. 2), using previous timestep data for defining the coefficients A, B and C:

$$T_i(t + \Delta t) = \frac{C - B \cdot Q_{\text{pli},i}(t + \Delta t)}{A} \quad (6.2)$$

As explained in chapter 2, this relation is the result of a reduction process of a matrix containing all energy balance equations related to the zone of interest. Throughout the reduction process all coefficients and variables are reduced, apart from the control point temperature T_i (K) and the plant thermal power flux $Q_{\text{pii},i}$.

The estimation can be refined if the coefficients A, B and C are ‘updated’ taking into account their change due to the thermal power injection. That can be done by

² The weighing factor K_1 and the timeconstant τ_2 are additional parameters when the emission/absorption element is to be optimised for a case with set backs.

allocating the energy flux according to the defined actuator and consequently reduce the zonal matrix to calculate the updated coefficients A, B and C³.

Based on these formulae, (6. 1) and (6. 2), the logic has been set up to determine whether or not the system is in restart mode, as schematically presented in Figure 6.1.

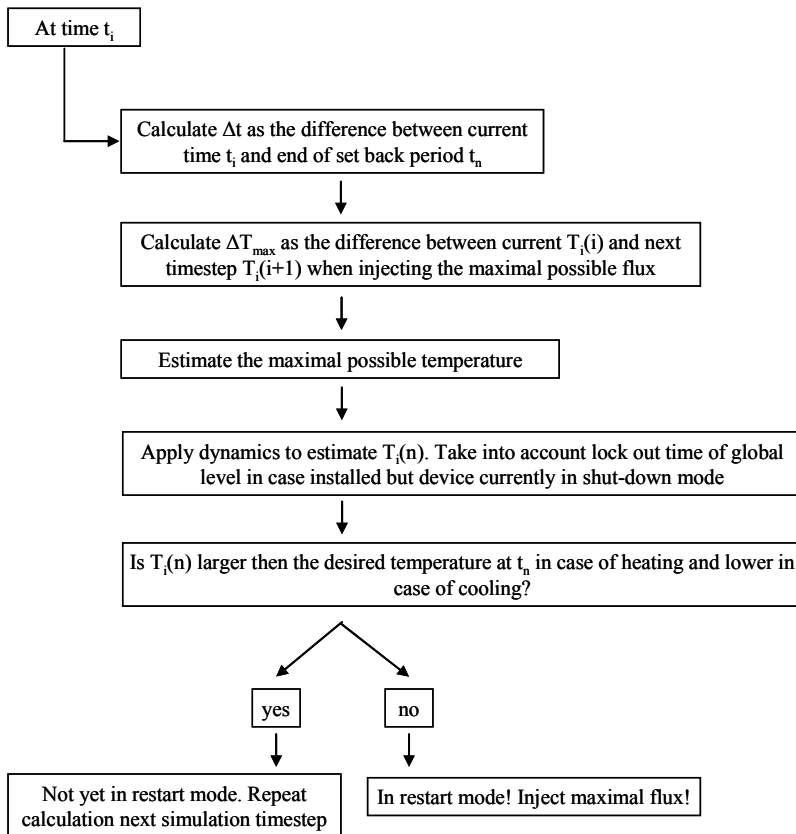


Figure 6.1: Decision logic for ideal restart calculation.

³ For this updating of the coefficients within the iterative procedure, a part of the *mzrcpl*-routine, located in *esrubld/bcfunc.F* of the *ESP-r* software is called (appendix A).

The maximum heating and cooling fluxes are calculated based on the improved empirical formula, as described in chapter 3. The maximum heating flux is calculated based on the lowest value of the user-defined values for the maximal average production unit temperature $T_{\text{prod,max}}$ and the maximum average emitter/absorber temperature of the element in the specific zone $T_{\text{emit,i,max}}$. The maximum cooling capacity takes into account a condensation safety measure. This is done by calling a subroutine that calculates the instantaneous relative humidity of the zone. Based on that instantaneous value, the dewpoint is calculated. The average of this dewpoint and the zone air temperature is then the lower limit to avoid condensation⁴. If the user provided minimum average emitter temperature, $T_{\text{emit,i,min}}$, is higher, the latter temperature is considered as lower limit.

The simulation result of the restart calculation for a single zone building is given in Figure 6.2 for a cold January afternoon in Brussels.

⁴ The reason to not take the dewpoint is that for the implicit approach average emitter/absorber temperatures are used.

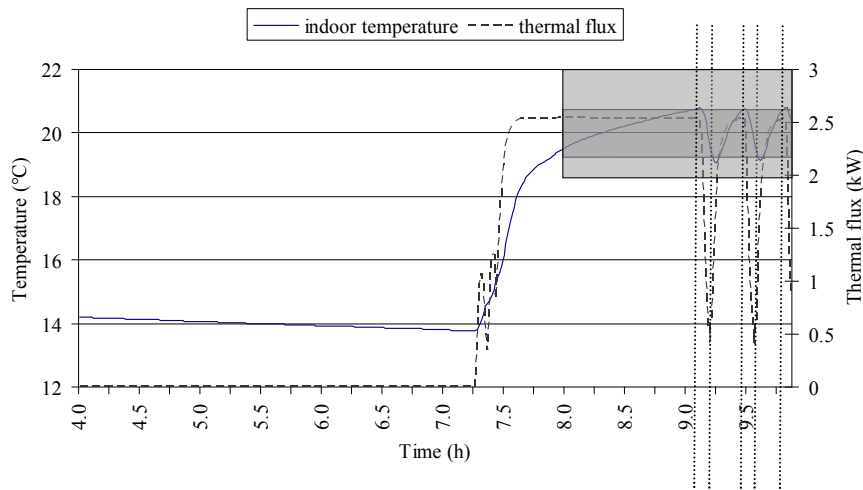


Figure 6.2: Ideal restart in heating mode for a single zone building during an 8 to 10 o'clock occupancy. The comfort temperature is set to 20 °C, the 1.5 K deadband for the controller is indicated in dark grey. The thermal comfort band has been indicated in lighter grey. The dotted vertical lines emphasize the action of the controller to stop or restart injecting heat into the emission/absorption element once the indoor temperature drops below the lower limit of the 1.5 K band. Due to the inertia of the emission element, a further decrease in indoor temperature appears. The effect is here limited as the inertia of the simulated emitter/absorber is set to 2.5 kJ/K only.

Maintaining the comfort temperature

To maintain a comfort temperature once within the occupied period, some of the above techniques could be applied. The method developed by Liao and Dexter [7] (briefly described in the beginning of this paragraph) has been shown to decrease variations of the indoor temperature. Zaheeruddin [15], [17] (see page 186 as well) achieved temperature variations as low as 0.1K, but does not give details on the circumstances it was tested for. Al-Assadi et al. [22] apply sophisticated optimisation methods to reduce the fluctuation of the indoor temperature to even less than 0.05 K when applied to similar, but not well described cases.

As discussed in chapter 1, steady state thermal comfort is one aspect but also temperature fluctuations influence the evaluation or sensation of an indoor environment. The ASHRAE 55 standard [23], for non-residential settings, puts the limit on the maximum amplitude to 0.55 K. Hensen [24] judges the latter to be too conservative for dwellings. Although, as mentioned in chapter 1, the 1.1 K limit for 2 cycles an hour is accepted for the current model.

The ideal controller⁵ is developed to maintain a certain temperature within a 1.1 K band⁶, asymmetrically spread around the neutral temperature. This asymmetry is in agreement with the finding that people are more sensitive to cold than to heat. The same 70%-30% split, as mentioned in chapter 1, is applied here. Temperature variations within that band are not considered in the control algorithm⁷; the control mainly affects the amplitude of the temperature fluctuations. This can be seen in Figure 6.2 for a heating case.

Once within the band, the aim is to maintain a temperature that is as close as possible to the neutral temperature. The required heating/cooling flux to do so can be calculated based on the same Eq. (6. 3) after rearranging:

$$Q_{pi,i}(t + \Delta t) = \frac{C - A \cdot T_{n,i}(t + \Delta t)}{B} \quad (6. 3)$$

where $T_{n,i}$ (K) is the neutral or comfort temperature of zone i . Through an iterative process, the value of $Q_{pi,i}(t+\Delta t)$ is determined so that a zonal temperature $T_i(t+\Delta t)$ is achieved that is close to the desired comfort temperature. This estimation does not account for the dynamics of the heat emitter/absorber. That effect, however, is accounted for in the internal emitter/absorber model as described in chapter 3.

The desired flux is compared to what can be delivered based on the limits due to the maximum and minimum average emitter/absorber element's temperatures. In case of TAB's a simplified relation⁸ between average and surface temperature is used in order to account for the surface temperature limits as imposed by thermal comfort standards.

⁵ The term 'ideal controller' is here used as the controller estimates as good as possible what the thermal flux should be based on the actual thermal state of the building and the effect of the heat emission/absorption. Such strategy does not ensure that the exact desired operative temperature is reached due to the non-ideal hardware components of the plant.

⁶ Unless the user-defined deadband for a fixed indoor temperature or for the adaptive comfort theory is stricter. In that case, this user-defined value is decisive.

⁷ This effect is taken into account when evaluating the thermal comfort within the optimisation routine, as described in chapter 7.

⁸ When more accurate measurement data on a wide range of TAB elements is available, this simplified relation can be refined.

The scheme of this logic is presented in Figure 6.3.

It should be noted that successive injection of hot/cold water into the emission/absorption element is prevented. This implies that undercooling and overheating can occur. How large the undercooling or overheating is and how long it lasts, depends to a large extent on the thermal capacity of the emitting/absorbing element and the characteristics of the building structure. The overheating/undercooling will cause thermal discomfort⁹.

⁹ In the next chapter the weight of thermal discomfort in the judgement on the performance of a certain emission/absorption element will be discussed.

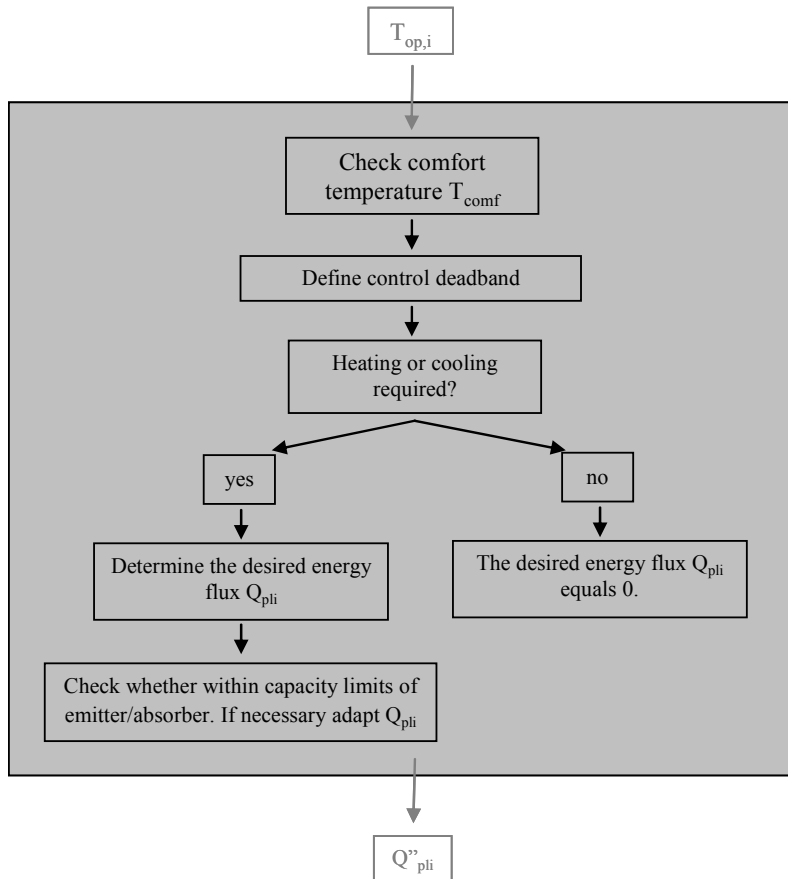


Figure 6.3: Decision logic of the ideal controller.

The ideal control for the implicit heat emission/absorption element has now been defined. As stated in the introduction of this chapter, other emitter/absorber controls are implemented as well so as to increase the usefulness of the implicit plant level. These non-ideal controls are briefly described below, a more extended description can be found in appendix D.

6.2.2.2 *The on/off room thermostat*

The start-up time of an on/off controller is a fixed user-defined reheat/recool time. Once in the start-up period, the controller requests the maximum possible energy flux, whether it is for heating or for cooling, until the upper limit of the comfortband around the desired temperature is reached. When it comes to maintaining the comfort temperature, the logic of an on/off controller is simple: take action if the temperature is not within the comfortband. The action to be taken is to ask for the maximum heating power in case the temperature is below the lower limit of the comfortband. The maximum cooling power is asked for in case the temperature is above the upper limit of the comfortband.

6.2.2.3 *The modulating room thermostat*

The start-up of a modulating controller is a linear function of the temperature difference between current and desired temperature. If in the start-up period, the controller requests for the maximum possible energy flux, whether it is for heating or for cooling.

To maintain the comfort temperature, if not in a start-up regime, this controller is developed to start heating once below the lower limit of the comfortband and then continue heating till the upper limit. For cooling it is the other way around: start cooling once above the upper limit and continue till the lower limit. The required heating/cooling flux is calculated using the iterative procedure based on the above given Eq. (6. 3). Once again the maximum thermal power fluxes must be respected in all cases.

6.2.2.4 *The thermostatic radiator valve*

The thermostatic radiator valve implemented in the framework of the current dissertation is a non-programmable one. Consequently, it is not combined with any restart control.

In the literature several models for thermostatic radiator valves TRV's have been developed, for example [24]-[28]. These TRV-models rely on actions on flow rates. In the implicit modelling no flow rate data are available. Therefore, the implicit TRV is modelled using its basic working mechanism; a proportional control action with hysteresis.

6.3 Controllers for the production of hot/cold water

6.3.1 Production controls in general

As described in chapter 2, the models for the production devices and their controls are strongly connected. The inputs to the control part are indicated in italic in Table 6-2.

Similar to before, the parameter indicated in grey is indirectly related to the emitter/absorber controls. It's value is passed on to that level, to ensure that the maximum capacity is calculated based on a temperature that is as low as, or lower than, the maximal average temperature of the production unit , $T_{\text{prod,max}}$ (K).

Input parameter	Symbol
<i>Maximum heating capacity (W)</i>	$Q_{h_prod,max}$
<i>Minimum heating capacity (W)</i>	$Q_{h_prod,min}$
<i>Maximum cooling capacity (W)</i>	$Q_{c_prod,max}$
<i>Minimum cooling capacity (W)</i>	$Q_{c_prod,min}$
<i>Lock out time (s)</i>	t_{lock_out}
<i>Time off between heating and cooling (s)</i>	t_{heat_cool}
Time constant (s)	τ_{prod}
<i>Control selection (-)</i>	<i>Control</i>
Efficiency characterisation (-)	η
Maximum average production temperature (K)	$T_{\text{prod,max}}$

Table 6-2: Input parameters for the implicit control of the production model.

To take into account the constraints on the lock out time $t_{\text{lock_out}}$ and time off between heating and cooling $t_{\text{heat_cool}}$, the statistics on heating and cooling have to be saved and adapted at each simulation timestep. This is done after the desired flux

has been defined. The statistics are saved so as to be accessible by the production system logic for calculation of start-up and shut-down effects.

The scheme as given by Figure 2.13 is recalled in Figure 6.4 below, with indication of the input of the control-related parameters.

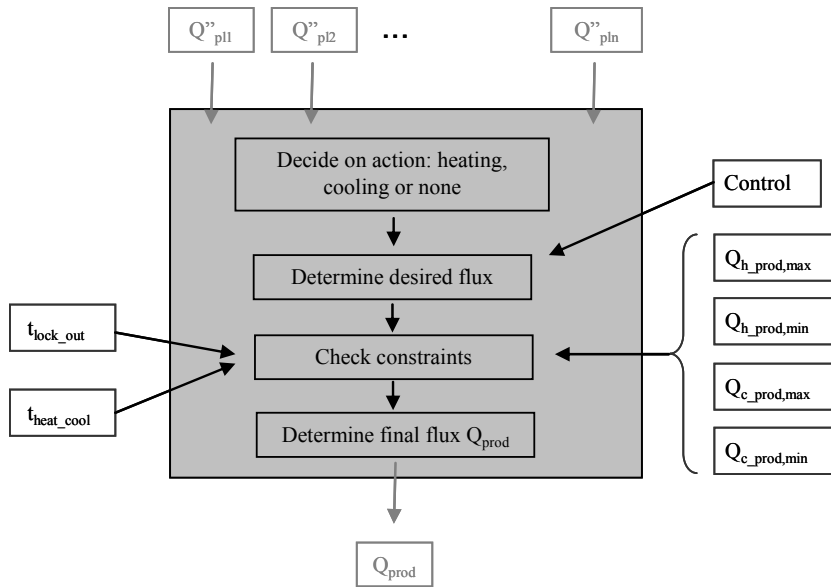


Figure 6.4: Schematic representation of the controller of the implicit production device.

6.3.2 The ideal control

The ideal control is a modulating control. It allows the production system to produce any thermal power flux requested by the zones as long as it is not in conflict with other parameters such as maximum and minimum capacities, lock off times and dynamical effects due to start up and shut down cycles. If there is a restricted thermal power flux produced compared to the required total power flux, the different zonal fluxes are rescaled.

The decision on working either in heating, or in cooling mode is determined by the maximum of the total heating and total cooling demand summed over all zones. Only those zones requiring a flux conform the active mode are served. This thus

assumes that there might be zones that do not achieve the flux they desire. This approach is based on the assumption of 1 circuit only with one production device only.

Figure 6.5 shows the result of a combination of the ideal global controller with an ideal zone controller, applied to a 3-room building. Room 1 has large windows at the south side and higher internal gains compared to the other rooms. The global heating capacity is for this example limited to 0.5 kW so as to show that the instantaneous total output, summed over the three rooms, is constantly equal to the maximum global capacity, less the distribution losses and divided proportional to the heat demand of the different rooms¹⁰.

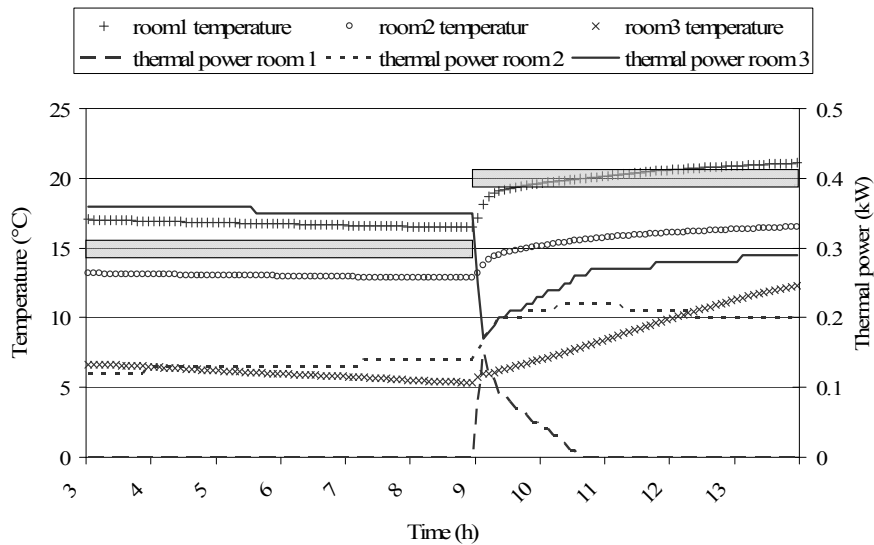


Figure 6.5: Result of an ideal global controller in heating mode. The global capacity is limited to 0.5 kW. The desired comfort band for all zones is indicated in semi-transparent grey¹¹.

¹⁰ Using a larger more realistic heat capacity of say 10kW, would result in achieving the comfort temperature in all zones and hence would not demonstrate that the control actually works.

¹¹ The unsmooth behaviour in the thermal fluxes has to do with the accuracy of the saved results compared to the scale of the right vertical axis.

As for the heat emitter/absorber element, also for the implicit production device a more realistic control strategy has been implemented. The modulating central room thermostat is briefly described below and more in detail in appendix D.

6.3.3 The central room thermostat with modulating production control

The central room thermostat works as the ideal/modulating control, where its decision on either heating or cooling mode is based on a sensed temperature in 1 specific room. This control algorithm can also be used to simulate on/off central room thermostats simply by setting the minimum heating or cooling capacity equal to the maximum heating or cooling capacity.

6.4 Summary and conclusions

The controllers of both heat emission/absorption elements and production systems have been described. The first set of controllers includes a detailed ideal control as required for the purpose of defining optimal emission/absorption elements.

Additional emitter/absorber controllers have been implemented so as to extend the implicit approach and improve its usefulness. According to the implicit modelling logic, all controllers determine the desired energy flux and will pass that on to the production level. For most controllers the flux estimation is based on a relation between desired temperature and required thermal flux as available within *ESP-r* (Eq. (2.19)). The exception is the TRV, where the flux calculation is based on the logic of a proportional control with hysteresis.

The structure of the production controllers allows simulating the effects of the most common real control strategies for domestic dwellings.

As now all components and the necessary ideal controls have been described, the next step is the coupling with an optimisation code. That is described in the next chapter, where it is demonstrated for a wide range of building settings. How the model is embedded in *ESP-r* and how it interacts with the other structures is schematically shown in appendix B.

References

- [1] L. Peeters, L. Helsen, W. D'haeseleer, 2005, Prediction of heat demand to minimise heat-pump heating costs, *Clima 2005*, Lausanne, Switzerland, electronic proceedings
- [2] M. Persson, A. Roos, M. Wall, 2006, Influence of window size on the energy balance of low energy houses, *Energy and Buildings*, vol. 38, pp. 181-188
- [3] L. Peeters, L. Helsen, W. D'haeseleer, 2007, Advanced control strategies, TME/WDH/2007/TR05, Applied Mechanics and Energy, University of Leuven (KUL), Belgium
- [4] L. Peeters, J. van der Veken, H. Hens, L. Helsen, W. D'haeseleer, 2008, Control of heating systems in residential buildings: current practice, *Energy and Buildings*, vol. 40, pp. 1446-1455
- [5] G. Fraisse, J. Virgone, C. Menezo, 2000, Proposal for a highly intermittent heating law for discontinuously occupied buildings, *Proceedings Institution of Mechanical Engineers*, vol. 214, pp. 29-39
- [6] S. Cho, M. Zaheeruddin, 2003, Predictive control of intermittently operated radiant floor heating systems, *Energy Conversion and Management*, vol. 44, pp. 1333-1342
- [7] Z. Liao, A. Dexter, 2003, An inferential control scheme for optimizing the operation of boilers in multi-zone heating systems, *Buildings Service Engineering Research and Technologies*, vol. 24, pp. 245-256
- [8] P. Tuohy, H. Rijal, M. Humpreys, J. Nicol, A. Samuel, J. Clarke, 2007, Comfort driven adaptive window opening behaviour and the influence of building design, *Building Simulation Conference 2007*, Beijing, China, electronic proceedings
- [9] J. Seem, P. Armstrong, C. Hancock, 1989, Algorithms for predicting recovery time from night set back, *ASHRAE transactions*, vol. 95, pp. 439-446
- [10] G. Fraisse, J. Virgone, R. Yezou, 1999, A numerical comparison of different methods for optimizing heating-restart time in intermittently occupied buildings, *Applied energy*, vol. 62, pp. 125-140
- [11] G. Fraisse, J. Virgone, J. Roux, Thermal control of discontinuously occupied buildings using a classical and a fuzzy-logic approach, vol. 26, pp. 303-316
- [12] G. Fraisse, J. Virgome, 1996, Commande floue et thermique du bâtiment. Proposition d'une loi de chauffe adaptee a la régulation des bâtiment de type tertiaire a occupation discontinue, *Rev. Gen. Therm.* Vol 35, pp. 359-372
- [13] J. MacQueen, 1997, The modelling and simulation of energy management control systems, PhD dissertation, ESRU, University of Strathclyde, Glasgow, UK
- [14] Z. Liao, A. Dexter, 2004, A simplified physical model for estimating the average air temperature in multi-zone heating systems, *Building and Environment*, vol. 39, pp. 1013-1022

- [15] M. Zaheeruddin, 1993, Energy start-stop and fluid flow regulated control of multizone HVAC systems, *Energy*, vol. 18, pp. 289-302
- [16] M. Zaheeruddin, 1994, Intelligent control strategies for HVAC processes in buildings, *Energy*, vol.19, pp. 67-79
- [17] M. Zaheeruddin, 1994, Temperature control of multizone indoor spaces based on forecast and actual loads, *Building and Environment*, vol. 29, pp. 486-493
- [18] G. Singh, M. Zaheeruddin, R. Patel, 2000, Adaptive control of multivariable thermal processes in HVAC systems, *Energy Conversion and Management*, vol. 41, pp. 1674-1685
- [19] M. Zaheeruddin, G. Zheng, Optimal control of time-scheduled heating, ventilation and air conditioning processes in buildings, *Energy Conversion and Management*, vol. 41, pp. 49-60
- [20] N. Nassif, S. Moujaes, M. Zaheeruddin, 2008, Self-tuning dynamic models of HVAC system components, *Energy and Buildings*, vol. 40, pp. 1709-1720
- [21] J. Clarke, 2001, *Energy simulation in building design*, Butterworth-Heinemann, ISBN 0-7506-5082-6
- [22] S. Al-assadi, R. Patel, M. Zaheeruddin, M. Verma, J. Breitingner, 2004, Robust decentralised control of HVAC systems using H_{∞} -performance measures, *Journal of the Franklin Institute*, vol. 341, pp. 543-567
- [23] ANSI/ASHRAE standard 55-2004, 2004, Thermal Environment conditions for Human Occupancy, American Society of Heating, Refrigerating and Air-conditioning engineers, Inc. Atlanta, USA
- [24] J. Hensen, 1991, On the thermal interaction of building structure and heating and ventilating system, PhD dissertation, Technical University of Eindhoven, The Netherlands
- [25] H. Ast, 1988, IEA annex 10, System simulation, thermostatic valve, University of Stuttgart, Germany
- [26] ESRU, 2002, The ESP-r system for building energy simulation; User guide version 10 series, University of Strathclyde, Glasgow, UK
- [27] J. Van der Veken, V. de Meulenaer, H. Hens, 2007, Eindrapport GBOU-project 020212, Analyse per systeem: verwarmingsinstallaties, Department of Building Physics, University of Leuven (KUL), Belgium
- [28] B. Xu, L. Fu, H. Di, 2008, Dynamic simulation of space heating systems with radiators controlled by TRV's, *Energy and Buildings*, vol. 40, pp. 1755-1764

7 OPTIMAL HEAT EMITTER/ABSORBER

Optimisation strategy

Determining the optimal set of characteristics of a potential future heat emitter/absorber is a multiple parameter optimisation problem. It requires a well-managed solution technique. Therefore ESP-r has been coupled with GenOpt [1] enabling the use of an intelligent optimisation strategy. In this chapter, the optimisation problem and the further applied solution strategy is described.

7.1 Introduction

Any heat emitter/absorber is installed to realise a certain indoor thermal comfort. For residential buildings, the comfort settings have been defined in Chapter 1. The use of the implicit heat emitter/absorber as developed in Chapter 3 allows to set up a model that can cover a wide range of potential heat emitters/absorbers simply by varying the model input parameters.

Evaluating this model for a wide range of parameters then allows sorting out the set of parameters for the heat emitter/absorber that is best suited to achieve that predefined comfort in a given context, with minimum energy consumption. To handle this selection of parameter sets and their resulting performance, an intelligent management technique is required. Therefore, *GenOpt* is used. It is an optimisation program for minimisation of an objective function¹ which is calculated by an external simulation program. It is developed for computationally intensive programs with unpredictable effect of changes in the parameters of interest [1].

GenOpt has been used in a building heating/cooling context before. Thornton et al. [2] coupled *TRNSYS* and *GenOpt* to calibrate geothermal heat pump models, while Ferguson [3] coupled *ESP-r* with *GenOpt* to calibrate cogeneration models. Hassan et al. [4] coupled *IDA ICE* and *GenOpt* to optimise building envelope characteristics to minimise the life cycle cost of a residential building. Liu et al. [5] used a *GenOpt* - *Energy Plus* coupling to calibrate control parameters for a HVAC-installation. Similarly Wetter [6] combined *GenOpt* with *Energy Plus* to optimise the energy consumption of heating, cooling and lighting in an office building for variations in window sizes and shading transmittance. Wetter and Wright [7] describe the optimisation of similar parameters for a more complicated *Energy Plus* building model using climate data of different US cities. Also Djuric et al. [8] coupled *GenOpt* with *Energy Plus*. They optimised a range of parameters influencing the energy consumption of a school building. They concentrated on hydronic heating systems aiming to achieve a certain thermal comfort with minimum energy consumption. They focussed mainly on the control and evaluated radiators only.

In this dissertation, the aim is to develop a tool to define which characteristics would result in an optimal emission/absorption element for a given context. The optimisation strategy is explained in the current chapter. To demonstrate the possibilities of this tool, it is applied to a number of case studies which will be discussed in the next chapter. The tool is general, in the sense that it can be applied to a wide range of problems. However, to set up general results one would need to perform a range of optimisations varying amongst others building type, geometry of the zone, building envelope and climate characteristics. Therefore, the results given in the next chapter are examples on what information can be extrapolated from the

¹ An objective function is an evaluation function that weighs the factors that are of importance when it comes to a model's performance to be optimized.

optimisation results more than general guidelines on what the exact parameter values for an optimal emitter/absorber should be.

7.2 Optimisation process

Solving an optimisation problem requires modifying a set of independent variables to find a minimum of a function, which is called the objective function. The objective function to be minimised here, incorporates the evaluation of the energy consumption and the thermal comfort. What the determining factor is or how energy and comfort relate to each other can be decided based on a Pareto-front, as will be discussed later in this chapter.

The optimisation problem considered here is characterised by a relatively large number of independent parameters, especially as in this dissertation a generic model is set up that allows extending the optimisation process to multiple zone problems. The course of the energy consumption curve as a function of the combined effect of variations of these parameters is difficult to predict [9].

The user-selected parameters may vary continuously or in discrete steps. For practical reasons, these parameters may be constrained such that they vary over a limited range. Constraints may be handled directly by the optimization algorithms, such as for the simple case of lower and upper bounds of independent parameters. More complex constraints may be implemented by embedding a penalty function in the objective function.

The objective and possible constraint functions are evaluated by the building simulation software, i.e. in this case *ESP-r*. The set of parameters for which the objective function needs to be evaluated, is prepared by *GenOpt*. The selection of these parameter values is done based on the logic of the selected optimisation algorithm. Several optimisation algorithms are currently available in *GenOpt's* library. Wetter [1] provides an extended summary of the different optimisation algorithms, including a mathematical description.

For the optimisation of a heat emitter/absorber, many parameters need to be evaluated. When first applying an optimisation technique that roughly ‘maps’ the results of the whole range of possibilities, the global minimum can be situated. A more refined method can subsequently be used to determine the exact ‘location’ of

that global minimum in the n-dimensional exploration space of possible solutions (where n indicates the number of parameters). Applying such a combination of optimisation algorithms strongly reduces the required optimisation time.

7.2.1 The rough mapping technique

The rough mapping technique applied here is the particle swarm optimisation technique (PSO). The PSO algorithm randomly generates a set of initial points to be evaluated. Each point is called a particle and a set of points is called a population. The next populations are computed using a particle update equation. This equation is modelled based on the social behaviour of bird flocks or fish schools [1]. The particle update equation attracts particles towards the best known iterate in a way that moves the whole population towards regions where the objective function is expected to be decreasing. It also contains a term that leads to a global exploration of the search space in order to increase the chance of finding a global minimum.

In general, the PSO algorithms are well-suited for exploring large parts of the parameter space and quickly identify potential optimal solutions. But because they are inherently stochastic, they require many iterations to refine the solution and consequently they consume a lot of computation time. Therefore, they are here combined with another optimisation strategy.

7.2.2 The more refined detailed search technique

The algorithm that is combined with the PSO, is a Generalised Pattern Search (GPS) algorithm. It is invoked once the range of possibilities of all parameters is reduced by the PSO.

GPS algorithms systematically explore small regions of the parameter space. The parameters for the next generation are based on the gradient computed for the current iteration. This approach allows the algorithm to quickly converge to a (local) minimum within the reduced exploration space.

It is to be expected that, applying a GPS on a too large space would include the risk of ending up with a local minimum instead of a global minimum. This risk is reduced by first calling a PSO algorithm and consequently applying a GPS algorithm to a limited exploration space around the global minimum located by the

PSO. To further increase the chance to find the global minimum, the same optimisation problem can be solved starting from different initial parameter values.

7.2.3 The parameter space considered

The parameter range of all n variables to be optimised defines the parameter space, i.e. the n -dimensional polytope, for the optimisation algorithm. It incorporates all combinations of the different variables. Some of these combinations might be physically impossible. Extracting these impossible combinations from the polytope beforehand prevents ending up with a physically unfeasible solution.

The polytope is first defined by determining the range of possible values for the different parameters.

The emitter's/absorber's *nominal power*², $Q_{emit,N}$ (W) and *heat capacity* C_{emit} (J/K) are in theory unlimited. However, narrowing their range will limit the n -dimensional space and thus speed up the optimisation process. The element's nominal power will therefore be limited to a range around the steady state heat demand Q_{ss} ³ (W) that is determined by the transmission and ventilation losses as given in the European standard EN 12831 [10]:

$$Q_{ss} = U_{average} A_{envelope} (T_{Comf} - T_{surroundings}) + 0.34V_i (T_{Comf} - T_{source}) \quad (7.1)$$

In this equation, $U_{average}$ (W/m²K) is the average U-value of the zonal building envelope, $A_{envelope}$ (m²) is the surface area of that envelope, T_{Comf} (K) is the zonal desired indoor temperature and $T_{surroundings}$ (K) is the envelope surface weighted temperature of the surrounding zones or the exterior for a cold winter day in case the heating load is expected to be higher than the cooling load, V_i (m³) is the volume of air in the zone and T_{source} (K) is the temperature of the air supplied to the zone.

² For a climate where cooling dominates the thermal energy demand, Eq. (7.1) should be replaced in order to account for the higher cooling load.

³ This could be refined taking into account the element's heat capacity, but the aim is only to give an indication.

The maximum heat capacity is determined by the capacity that could be considered for TAB elements, i.e. the heat capacity of the layers containing the imaginary water pipes in the building structure and the ones from that layer up to the zonal air. The value is here set to 6 000 kJ/K for the 32 m² zone. The lower limit is taken equal to 10 kJ/K, which corresponds to the use of small heat exchangers with low water content.

As shown in chapter 4, care should be taken when evaluating thermally active ceilings or walls with high capacity. To prevent that such elements are given too much weight in the optimisation, they are extracted from the polytope. This is done by the use of a penalty function as will be described in the next paragraph.

Considering the generic emitter/absorber model, the remaining parameters are the *selection of TAB element or no TAB element* indicated by β (-), the *radiator exponent*, n (-) and the *nominal fraction of convection*, α_N (-). The first parameter is only limited by the range of elements it indicates; whether or not it is a TAB element and its possible location. The parameter α_N has a lower limit $\alpha_{N,\min}$ that is a function of the difference between nominal zonal temperature and nominal average emitter temperature, and of the radiant heat output. A general formula as determined by Alamdari and Hammond [11] is applied to determine $\alpha_{N,\min}$. That formula gives the convective output for a range of emission elements. Selecting the configuration that results in the lowest value for this convective output and combining it with the maximum possible linear radiant heat transfer coefficient, the minimum value of the fraction of convection can be determined. The maximum value, $\alpha_{N,\max}$, is here set to 0.95. The reason is that any emitter will have some surface area and thus an amount of radiation. The fraction of radiation depends on the emissivity of the material and can thus be small, but not zero.

As the fraction of convection is limited, the radiator exponent n is limited: values lower than n_{\min} as defined by Eq. (7.2) are physically impossible.

$$n_{\min} = (1 - \alpha_{N,\min}) + \alpha_{N,\min} (b_{\min} + 1) \quad (7.2)$$

where b_{\min} is the minimum value of the power coefficient b for which examples are listed in Table 3-1.

The maximum value of the radiator exponent, n_{\max} (-), is determined by the maximum nominal fraction of convection and the maximum possible power coefficient for natural convection, b_{\max} (-):

$$n_{\max} = (1 - \alpha_{N,\max}) + \alpha_{N,\max} (b_{\max} + 1) \quad (7.3)$$

Figure 7.1 shows the effect of extracting the impossible values of the radiator exponent, n , and the percentage of convection for the nominal case, α_N , as a function of the maximum average emitter's/absorber's temperature. Only solutions for α_N and n falling inside the polytope make physically sense.

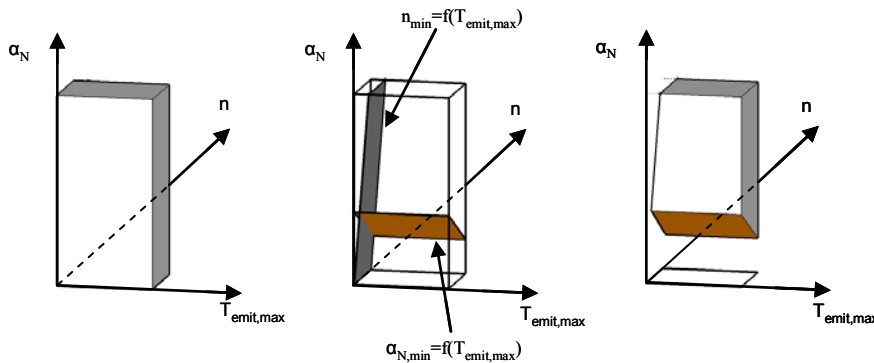


Figure 7.1: The possible values of n and α_N as a function of the maximum average temperature of the heat emitter/absorber. The left figure shows the whole range of possible n - α_N combinations. The figure in the middle shows the surfaces $\alpha_{N,\min}$ and n_{\min} as a function of $T_{\text{emit,max}}$. The right figure shows the so determined limited area.

The parameters α_N and n are discretised. The reason is that for the scope of this research a detailed value of those parameters is not required. The aim is to show that tendencies can be determined. When afterwards ‘translating’ such tendencies into real product designs, an additional optimisation might be performed with accurate approximations for the configuration-dependent parameters.

7.3 The objective function

7.3.1 The function terms

The optimisation tool developed has the aim to determine the most suitable potential heat emitter/absorber for a given context. So, it means determining those parameters resulting in a minimal energy use while satisfying the predefined thermal comfort as good as possible for the given setting. However, the energy consumption, *Energy* (Wh), must be minimised, the thermal comfort obviously not. Consequently not achieving the required comfort should increase the value of the objective function. It thus should be penalised.

As the thermal comfort sensation does not suddenly change when exceeding the limits of the comfortband, a penalty function linearly increasing from the neutral temperature to the borders of the comfortband has been implemented. Outside this comfortband, a second power of the temperature deviation from the comfortzone determines the value of the penalty function. This is a reasonable approach in accordance with [12], [13] and [14].

The penalty is further linked to the duration of the discomfort by multiplying the value with the length of the simulation timestep Δt (h). The penalty function, called *Penalty₁* (K²h), is evaluated only during periods of occupancy.

In case of an indoor operative temperature T_{op} below the neutral temperature T_n , Eq. (7.4) is applied. For indoor operative temperatures above the neutral temperature Eq. (7.5) applies.

$$\begin{cases} T_{op} \geq T_{ll} \ \& \ T_{op} < T_n & \Rightarrow \text{Penalty}_1 = c_1 (T_n - T_{op}) \Delta t \\ T_{op} < T_{ll} & \Rightarrow \text{Penalty}_1 = c_1 (T_n - T_{ll}) \Delta t + c_2 (T_{ll} - T_{op})^2 \Delta t \end{cases} \quad (7.4)$$

$$\begin{cases} T_{op} \leq T_{ul} \ \& \ T_{op} > T_n & \Rightarrow \text{Penalty}_1 = c_3 (T_{op} - T_n) \Delta t \\ T_{op} > T_{ul} & \Rightarrow \text{Penalty}_1 = c_3 (T_{ul} - T_n) \Delta t + c_2 (T_{op} - T_{ul})^2 \Delta t \end{cases} \quad (7.5)$$

where T_{ll} (K) indicates the lower limit of the comfortband for the zone of interest and T_{ul} (K) the upper limit. c_1 (K) and c_3 (K) are constants selected in order to end up with identical values for the penalty for operative temperatures equal to T_{ll} or T_{ul} , i.e. 0.4 K for c_1 and 0.17 K for c_3 . The constant c_2 (-) is dimensionless and has been chosen equal to 1.

As discussed in Chapter 1, besides discomfort due to the temperature being outside the comfortband, thermal discomfort also occurs due to temperature fluctuations. To evaluate these temperature variations, a small fixed timestep is used⁴. Based on the analysis of Hensen [15] and on the details given in the ASHRAE 55-standard [16], it can be concluded that small (i.e. 1.1 K) peak to peak variations will not result in discomfort. For larger temperature fluctuations, the maximum temperature variation ΔT_{max} (K) is determined as a function of the time period tP (h) considered:

$$\Delta T_{max} = 410 \exp\left(-5.26 / tP^{0.07}\right) \quad (7.6)$$

The function is fitted through the maximum temperature variation given by [16]. It does not fully agree with the shape shown by Hensen [15] based on his literature overview. However, this formula shows good agreement with the limits of [16] for a 0.5h to 4h timespan: the maximum deviation is shown to be 4.8% only.

Discomfort then occurs for higher peak to peak operative temperature variations within the time period tP . Such discomfort should be penalised.

Furthermore, ASHRAE [16] indicates a limit on the rate of temperature change for temperature variations. The limits are given as a function of the duration of the period considered. As an example: the standard suggest a 2.2K/h limit for a 1 hour period.

The discomfort due to transient temperature effects, either due to exceeding the amplitude limit during a given period or due to exceeding the given limit on the rate

⁴ Variable timesteps could be used. But the determination of those should be done with care as both the transients of the heating/cooling installation as well as the change in indoor temperature (due to any possible cause) must be reflected in the results in order to correctly evaluate the thermal comfort.

of temperature change, is quantified by $Penalty_2$ (-). This penalty is set to a constant (currently equal to 1⁵). The reason is that little information is available on transient temperature conditions in residential buildings. Hensen [15] concludes that the ASHRAE standard 55 indications might be somewhat conservative for a residential case. It is thus clear that there is discomfort, but not to what extent it causes a change in PPD. Therefore, for the current analysis, the ASHRAE 55 values are accepted to set the limits for a simple fixed penalty-value.

The above mentioned inaccuracy for thermally active walls and ceilings is handled by an additional penalty. That penalty is set when the capacity of these elements exceeds a certain limit. This limit is proportional to the surface area A_{TAB} (m²) and is lower for ceiling TAB elements than for wall TAB elements. The reason is the higher error on the MRT calculation in case of ceiling heating/cooling elements and the effect of the use of the average element's temperature. The resulting penalty, $Penalty_3$, is a fixed constant value, a_3 (-). It is set high enough to prevent optimising to such elements:

$$Penalty_3 = a_3 \quad (7.7)$$

The objective function, further referred to as O (-), can thus be formulated as:

$$O = a_0 Energy + a_1 Penalty_1 + a_2 Penalty_2 + Penalty_3 \quad (7.8)$$

where a_0 (1/Wh), a_1 (1/ K²h) and a_2 (-) are constants.

7.3.2 The function coefficients

The value of coefficients a_0 , a_1 and a_2 determines the weight of the energy and thermal comfort-factors. Different values of those coefficients thus indicate different priorities and will consequently result in other optima [13], [14]. Therefore, a 3D-Pareto front has been determined, comparing the thermal discomfort indicators,

⁵ The final value of this constant is determined based on the Pareto-front as will be discussed later in this chapter.

quantified by $Penalty_1$ (Eqs. (7.4) and (7.5)) and $Penalty_2$, to each other and to the consumed energy, $Energy$.

As an example, a Pareto-front has been set up based on the results of a full scale optimisation problem with focus on the ground zone of a 3-zone heavyweight averagely insulated building (see description in appendix E), located in Brussels. An indoor temperature was selected, according to the ‘other zones’ neutral temperature as defined in chapter 1. The two other zones of the 3-zone building are equipped with standard $ESP-r$ ideal controls. The thermal comfort evaluation for the objective function is focused on the zone of interest. The energy consumption is related to the whole building. The simulation period was set from January 2nd to July 2nd, the simulation timestep was 3 minutes. The resulting 3D Pareto front is shown in Figure 7.2. The 2D-views are given in Figure 7.3, Figure 7.4 and Figure 7.5.

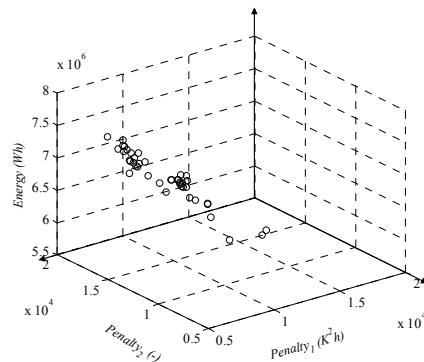


Figure 7.2: 3D-view of the Pareto front, resulting from a variation of the parameters a_1 and a_2 for a given a_0 , applied to the problem of optimising a heat emission absorption element in 1 zone of a 3-zones building. The plot shows the resulting values for energy consumption, $Energy$, and the evaluation of steady and transient thermal comfort, $Penalty_1$ and $Penalty_2$ respectively.

The Pareto front is set up based on 48 optimisation runs. Each of the optima is the result of the evaluation of around 560 parameter combinations. Due to the possible unsmoothness and discontinuity, some of the values shown might be local instead of global minima. One of such is indicated by the grey square, pointed to by the grey arrow, in Figure 7.3, Figure 7.4 and Figure 7.5; for a similar value of $Penalty_1$ other optimisation runs converged to better results for both $Energy$ and $Penalty_2$. However, when analysing the results, such local minima were observed to be exceptional.

General tendencies indicate that a lower weight to thermal comfort results in lower energy consumptions: energy savings are to be paid by a decrease in thermal comfort. The effect on the steady thermal comfort evaluation, i.e. $Penalty_1$, is shown in Figure 7.3. It is clear that there is a decisive influence: high ratios of a_0/a_1 cause high values of $Penalty_1$. There is a smaller influence observed for an increasing value of a_2 compared to a_1 .

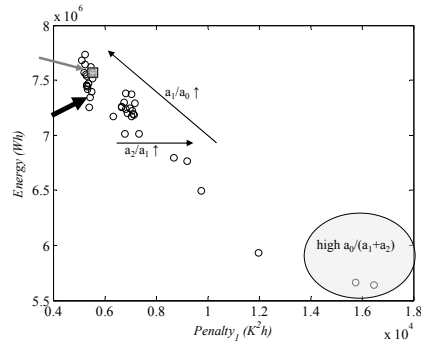


Figure 7.3: 2D-view of the Pareto front, resulting from a variation of the parameters a_1 and a_2 for a given a_0 , applied to the problem of optimising a heat emission absorption element in 1 zone of a 3-zones building. The plot shows the resulting values for energy consumption, $Energy$, and steady thermal comfort, $Penalty_1$. The grey square indicates a local minimum, the thick black arrow indicates the point that corresponds to the selected values for a_1 and a_2 .

Comparing $Energy$ and $Penalty_2$ (Figure 7.4), it is shown that the relation between these terms of the objective function is weaker. There is no clear link observed between $Energy$ and $Penalty_2$.

The effect of an increasing weight for $Penalty_1$ compared to $Penalty_2$, results in an obvious decrease in transient thermal comfort, i.e. a higher value of $Penalty_2$. This is shown in Figure 7.4 and Figure 7.5. Those figures further indicate the wide spread in values of $Penalty_2$ for high ratio's of a_1 over a_0 . Such spread is not observed in the values of $Penalty_1$ for a given value of $Penalty_2$. This emphasizes the dominating importance of the value of a_1 compared to the one for a_2 for a given value of a_0 .

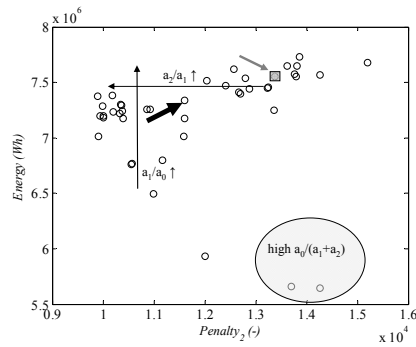


Figure 7.4: 2D-view of the Pareto front, resulting from a variation of the parameters a_1 and a_2 for a given a_0 , applied to the problem of optimising a heat emission absorption element in 1 zone of a 3-zones building. The plot shows the resulting values for energy consumption, Energy, and transient thermal comfort, Penalty₂. The grey square indicates a local minimum, the thick black arrow indicates the point that corresponds to the selected values for a_1 and a_2 .

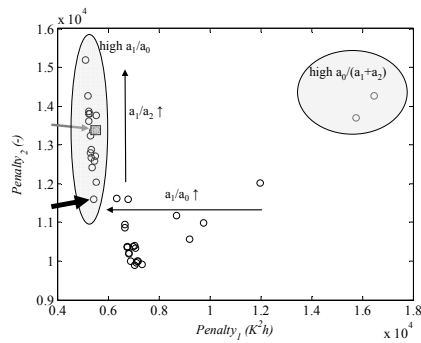


Figure 7.5: 2D-view of the Pareto front, resulting from a variation of the parameters a_1 and a_2 for a given a_0 , applied to the problem of optimising a heat emission absorption element in 1 zone of a 3-zones building. The plot shows the resulting values for steady thermal comfort, Penalty₁, and transient thermal comfort, Penalty₂. The grey square indicates a local minimum, the thick black arrow indicates the point that corresponds to the selected values for a_1 and a_2 .

The selection of the coefficients for the objective function determines the weight of each of the terms in the equation: energy consumption, steady and transient thermal comfort. As shown by the above described analysis of the Pareto front, giving a too high weight to one of the terms could result in significant effects on the others. It is

therefore important to select the coefficients with care, so the optimum shows acceptable values⁶ for all terms. A good choice for a_1 and a_2 in that sense is the one indicated by the thick black arrow in the 2D-graphs above. This corresponds to a value of $4000/K^2h$ for coefficient a_1 and 1000 for coefficient a_2 . This combination results in good comfort evaluations for a reasonable energy consumption.

7.4 The optimum and its neighbourhood

The selected algorithm combination, PSO and GPS, within *GenOpt* should converge to a minimum value of the objective function. It should thus be checked whether the necessary conditions for a minimum are fulfilled. Additionally, it should be known what information is to be found on this minimum and how sensitive it is to changes in the heat emission/absorption element's parameters.

7.4.1 The optimum itself

To check the conditions for a minimum, it is assumed that in the neighbourhood of a so-found potential minimum, the objective function $O(-)$ can be approximated using a second degree Taylor's expansion⁷:

$$O(p^* + \Delta p) = O(p^*) + \nabla O(p^*)^T \Delta p + \frac{1}{2} \Delta p^T \nabla^2 O(p^* + \Delta p) \Delta p + R(p) \quad (7.9)$$

where p^* is the vector containing the optimal set of parameters, and Δp is the difference of another set of parameters versus the optimal set. $R(p)$ is a remainder, that is proportional to the third order gradient of the objective function.

If p^* is a minimum, the first order gradient of the objective function evaluated for that optimal set, $\nabla O(p^*)$, is equal to zero. Furthermore, if the second order

⁶ What exactly 'acceptable' means, will depend on the scope of the research.

⁷ Generally, the objective function will not be smooth [17] when it concerns problems solved by BES. However, the assumption of a quadratic course in a close neighbourhood around the minimum is a commonly encountered efficient technique applicable for nonlinear and even non-differentiable cost functions ([18], [19]).

gradient, $\nabla^2 O$, exists and is continuous in the neighbourhood of the optimum, then $\nabla^2 O(p^*)$ should be positive semidefinite, i.e. it should have positive eigenvalues [18], [19].

These conditions characterise a minimum. However, they do not give any information on whether it concerns a local or a global minimum. In fact, for a non-convex and possibly discontinuous objective function, it is difficult to prove that the minimum found is the global minimum. A technique that gives a good indication, but not a proof, is to perform the same optimisation starting from different locations in the n -dimensional polytope. When the results converge to the same solution, this is a strong indication that the so-found minimum is the global minimum within the polytope⁸.

7.4.2 Interpretation of the optimum and its neighbourhood

The Hessian matrix, containing the second order information of the Taylor expansion, can be split by an eigenvalue decomposition. The so-determined matrices give information on the eigenvalues and the corresponding linearly independent eigenvectors. They thus indicate the sensitivity of the optimum to changes in specific parameters, or combinations of parameters⁹. A high positive eigenvalue indicates that changes in the direction of the corresponding eigenvector have a high impact. For low positive eigenvalues, the sensitivity of the optimum to changes in the direction of the corresponding eigenvector is much more limited. This is shown in Figure 7.6 for a fictitious 2-parameter optimisation problem. The value of the objective function is given as the difference compared to the value of the objective function in the minimum. It is further referred to as $\Delta O (-)$.

As stated above, to have an optimal solution, the eigenvalues should be positive. However, negative eigenvalues can appear for eigenvectors containing parameters

⁸ All cases discussed in the next chapter are optimised starting from at least 4 different initial points in the n -dimensional polytope. In the results discussion, the occurrence of multiple local minima is pointed out when relevant.

⁹ More on this type of mathematical analysis on optimum search can be found e.g. in Nocedal and Wright [18] and Boyd and Vandenberghe [19].

that can vary over a limited interval only. The optimal solution could in that case be outside the possible n-dimensional polytope.

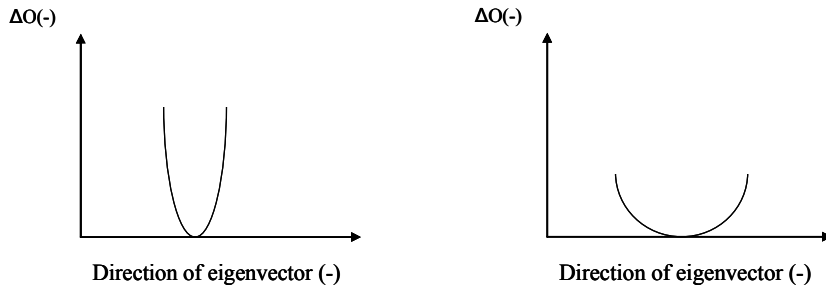


Figure 7.6: The effect of the eigenvalues as a function of parameter changes in the direction of the corresponding eigenvector. The left hand graph shows the result of changes in the direction of the eigenvector with a high eigenvalue. The right hand graph gives the same for a low eigenvalue.

Considering the fictitious 2-parameter problem, the ratio between the two eigenvalues gives information on the shape of the optimum. A combination of two eigenvalues with the same order of magnitude shows a spherical shape of the objective function. For a high first eigenvalue combined with a low second eigenvalue, the shape becomes elliptical. This is shown in Figure 7.7 for the fictitious 2-parameter optimisation problem.

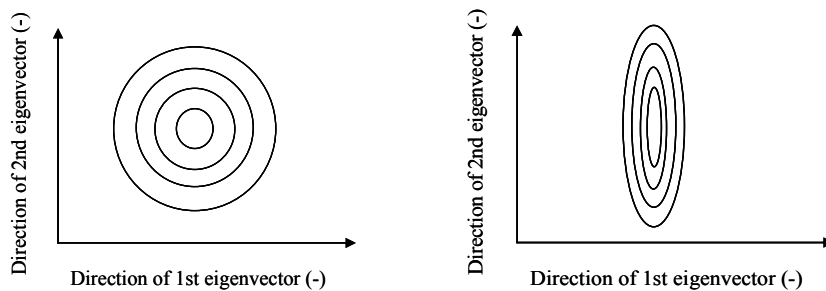


Figure 7.7: The sensitivity of the optimum as a function of changes in the direction of the two eigenvectors. The left hand graph shows the result of changes in the direction of the first and second eigenvector for two similar eigenvalues. The right hand graph gives the same for a high first eigenvalue and a much lower second eigenvalue.

The eigenvectors contain a specific combination of the parameters of the optimisation problem. These combinations indicate the sensitivities of the optima to changes in the parameters. A parameter that is given a high weight in the composition of the eigenvector will have a high influence compared to a parameter that has been indicated a low weight. When two parameters are given an equal weight but a different sign, this implies that a decrease in the value of one parameter can be compensated by an increase in the value of the other parameter. The resulting eigenvector has the same value. This denotes the possibilities of multiple parameters corresponding to the same value for the objective function. That implies that an optimum can be composed of multiple parameter combinations. Care should thus be taken when showing the value of the objective function of a multiple parameter optimisation problem as a function of a single parameter only.

Based on a combination of the eigenvectors and the corresponding eigenvalues it is thus possible to indicate the sensitivity of the optimum to changes in the different parameters of the optimisation problem. The Hessian matrix is determined in a small open neighbourhood of the minimum. The exact eigenvalues and corresponding eigenvectors depend on the set of data considered. Enlarging or reducing the neighbourhood influences the eigenvalues and consequently also the eigenvectors. However, the tendencies shown are similar. It is thus important to give the tendencies, more than showing the exact eigenvalues and the exact composition of the corresponding eigenvectors.

Throughout the discussion of the optimisation results these tendencies will be described. They are often illustrated showing the impact of changes to one parameter on the objective function. As mentioned before, such figures need to be interpreted with care.

It should be noted that all parameters should be scaled in order to show the sensitivity of the objective function to parameter value variations.

7.5 Summary and conclusions

This chapter describes the optimisation strategy for the selection of the optimal heat emission/absorption element. The optimisation algorithm is proposed and the n-dimensional parameter space is deduced. The objective function has been set up taking into account the energy consumption for heating/cooling as well as the

quality of the indoor thermal environment. Physically impossible elements are eliminated from the parameter space on beforehand or avoided by a constraint. Such constraint is here implemented as a high penalty, to avoid its resulting objective function value would be in the neighbourhood of the optimum.

Furthermore a Pareto-front has been set up to determine the weight of energy compared to steady and to dynamic thermal comfort. These coefficients of the objective function will be used in the next chapter to demonstrate the possibilities and limitations of the tool.

The overall optimisation problem can thus be described by:

$$\min_x O = \frac{1}{Wh} \text{Energy} + \frac{4000}{K^2 h} \text{Penalty}_1 + 1000 \text{Penalty}_2 + \text{Penalty}_3$$

$$\text{where : } X = \begin{bmatrix} Q_{emit,N} \\ C_{emit} \\ n \\ \alpha_N \\ \beta \end{bmatrix}$$

$$Q_{emit,N} \in [0.3Q_{ss}, 6Q_{ss}]$$

$$C_{emit} \in [10000 J/K, 6000000 J/K]$$

$$\text{with: } n \in \{1.10, 1.15, \dots, 1.45, 1.48\}$$

$$\alpha_N \in \{0.35, 0.40, \dots, 0.95\}$$

$$\beta \in \{0, 1, 2, 3\}$$

Furthermore, a general theoretical description on what information is embedded in the optimisation results is given. This will be applied in the analysis of the case studies in the next chapter.

References

- [1] M. Wetter, 2008, GenOpt: Generic Optimisation Program, User Manual Version 2.1.0, Ernest Orlando Lawrence Berkeley National Laboratory, University of California, US
- [2] J. Thornton, 2008, TESS, Madison-Wisconsin, US, personal communication
- [3] I. Beausoleil-Morisson, A. Ferguson, 2007, Inter-model comparative testing and empirical validation of Annex 42 models for residential cogeneration devices. A report of Subtask B of FC+COGEN-SIM the simulation of building-integrated fuel cell and other cogeneration systems. Annex 42 of the International Energy Agency Conservation in Buildings and Community systems Programme
- [4] A. Hassan, M. Vuole, K. Siren, 2008, Minimisation of life cycle cost of a detached house using combined simulation and optimisation, *Building and Environment*, IN PRESS
- [5] S. Liu, G. Henze, 2005, Calibration of building models for supervisory control of commercial buildings, *Proceedings of 9th international IBPSA Conference*, Montreal, Canada, pp. 641-648
- [6] M. Wetter, 2000, Design Optimisation with GenOpt, *Building Energy Simulation, User News*, Lawrence Berkeley National Laboratory, vol. 21
- [7] M. Wetter, J. Wright, 2003, Comparison of a generalized pattern search and a genetic algorithm optimization method, *Proceedings of the 8th International IBPSA Conference*, Eindhoven, The Netherlands, pp. 1401-1408
- [8] N. Djuric, V. Novakovic, J. Holst, Z. Mitrovic, 2007, Optimisation of energy consumption in buildings with hydronic heating systems considering thermal comfort by use of computer-based tools, *Energy and Buildings*, vol. 39, pp. 471-477
- [9] M. Wetter, E. Polak, 2003, A convergent optimization method using pattern search algorithms with adaptive precision simulation, *8th International Building Performance Simulation Association Conference*, Eindhoven, The Netherlands, August 11-14
- [10] CEN, 2000, EN 12831: Heating systems in buildings: method for calculation of the design heat load, *European Committee for Standardisation*, Brussels, Belgium
- [11] F. Alamdari, G. Hammond, 1983, Improved data correlations for buoyancy-driven convection in rooms, *Building Services Engineering Research & Technology*, vol. 4, pp. 106-112
- [12] M. Kummert, 2001, Contribution to the application of modern control techniques to solar buildings: simulation-based approach and experimental validation, PhD thesis, *Fondation Universitaire Luxembourgeoise*, Belgium
- [13] T. Van Oevelen, 2008, Regeling van warmtepompsystemen in woningen: implementatie van Modelgebaseerde Predictieve Controle, *Department of Mechanical Engineering, Applied Mechanics and Energy Conversion*,

- Masters thesis (Promotors L. Helsen and J. Swevers, coach C. Verhelst), University of Leuven (KULeuven), Belgium (In Dutch)
- [14] R. Wimmer, 2004, Regelung einer Wärmepumpenanlage mit Model Predictive Control, PhD dissertation, ETH Siwtzerland
 - [15] J. Hensen, 1990, Literature review on thermal comfort in transient conditions, *Building and Environment*, vol. 25, pp. 309-316
 - [16] ANSI/ASHRAE 55-2004, Thermal Environmental Conditions for Human Occupancy, American Society of Heating, Refridgerating and Air-conditioning Engineers, Inc. Atlanta, USA
 - [17] M. Wetter, 2008, Lawrence Berkeley National Laboratory, US, personal communication
 - [18] J. Nocedal, S. Wright, 2000, Numerical optimization, Springer, New York, ISBN 0-387-30303-0
 - [19] S. Boyd, L. Vandenberghe, 2004, Convex optimization, Cambridge University Press, Cambridge, ISBN 0-521-83378-7

8 CASE STUDIES

Single zone optimal heat emitter/absorber¹

The tool for optimisation of emission/absorption elements, as developed in the framework of this dissertation, is here applied to a range of case studies. The aim is to demonstrate what the possibilities are, more than to determine general guidelines.

The focus here is on the optimal emitter/absorber element of a single zone in a specific setting (climate, construction details and operational details). The settings are varied and the optima are discussed.

¹ As the focus is here on the optimisation of a single heat emission/absorption element in a specific zone, the subscript *i* has been dropped for the sake of clarity.

8.1 Introduction

A 3-zone building model has been set up and the emitter/absorber characteristics are optimised for a variety of conditions: variation of outdoor conditions, variation of building envelope, changes in indoor temperature settings, restrictions linked to the production device, etc.

The case studies are meant to demonstrate the possibilities of the tool. The results are to be seen in the context given. They are determined for the specific objective function coefficients as selected in the previous chapter, the control as proposed in chapter 6 and for the specific building considered. Furthermore, the uncertainty on the convection coefficients for especially horizontal TAB elements, as discussed in chapter 3, implies that the results related to such elements should be interpreted with care.

There is also a strong dependency of heating and cooling loads on amongst others internal gains [1], [2], building structure [3], [4], and glazing surface and type [5], [6], [7]. However, certain tendencies can be indicated based on the case studies described in this chapter.

8.2 Description of the simulated building

A detailed description of the building used for this analysis (shown in Figure 8.1) is given in appendix E. A brief summary of the relevant parameters will be given here.

8.2.1 The building

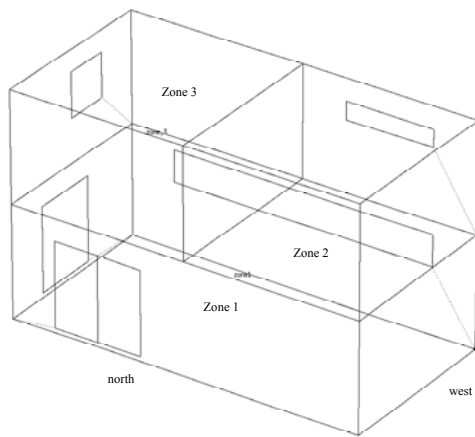


Figure 8.1: The 3-zone building used for current analysis, north-west view.

The building's dimensions are given in Table 8.1. The average U-value of the building envelope is given in Table 8.2. The heavyweight construction is a typical brick construction, while the term lightweight refers to a wood-frame construction.

<i>Element</i>	<i>Surface area (m²)</i>
Floor area	8m·4m
Height per floor	2.5m

Table 8.1: Dimensions of the building.

	<i>Heavyweight</i>			<i>Lightweight</i>		
	U_{avg} (W/m ² K)	U_{good} (W/m ² K)	U_{well} (W/m ² K)	U_{avg} (W/m ² K)	U_{good} (W/m ² K)	U_{well} (W/m ² K)
Average U-value	0.55	0.45	0.35	0.55	0.45	0.35

Table 8.2: Average U-values of the building envelope, for the different construction types and insulation qualities. The indices avg, good and well refer to an average, good and well insulated building respectively.

The effect of furniture is modelled by implementing a ‘floating’ volume with capacity in each zone.

8.2.2 The internal gains

The internal gains are set according to guidelines as given by ASHRAE [8]. The heat gains in the ground zone are estimated based on a 2-person occupancy. Lighting is on in the morning and evening only, while appliances are given a lower heat emission during set back. Zone 2 is given the same occupancy time schedule as zone 1, but gains are related to a 1-person occupancy. Zone 3 is given a profile of a bedroom with 2-persons at night, no gains due to appliances and lights only in the evening hours. A more detailed overview is given in appendix E.

The ventilation rate is set to 0.3 AC/h constantly.

8.2.3 Simulation details

The simulation time is set from January 2nd to July 2nd. The simulation timestep is set to 3 minutes. If not stated otherwise, the climate file selected is related to Brussels and based on measurements of the year 2001. To avoid ending up in a local minimum, each case is optimised in at least 3 optimisation runs, starting from different initial locations in the n-dimensional parameter space as discussed in the previous chapter.

The optimisation involves the 5 parameters characterising the emitter/absorber elements: the nominal power, the heat capacity, the radiator exponent, the nominal fraction of convection and the indication whether it involves a TAB element. Besides these characteristics, the control parameters related to the start-up calculation are optimised as well. They will not be discussed in the analysis given below, as the focus is here on the parameters characterizing the emitter/absorber element itself. The maximum and minimum average emitter/absorber element’s temperatures are kept constant. However, a simplified correlation between these variables and the capacity is applied in case of TAB elements in order to prevent uncomfortable surface temperatures and discomfort due to radiant asymmetry. The limits for those temperatures are according to ISO 7730 [9]. The correlation could be refined when more measurement data in dynamic situations are available for TAB elements.

8.3 Case studies

The case studies considered below are selected due to the difference in heating/cooling load. The first cases involve the optimisation of the emitter/absorber element itself, without any influence of other plant components. First, the influence of variations in the outdoor conditions is discussed, i.e. the effect of different climates. Secondly, the effect of changes to the building envelope is evaluated. Subsequently the impact of variations in temperature settings is checked. Finally, the last case discusses the effect of the emitter/absorber being coupled to a non-ideal production device.

The exact numbers for eigenvalues and the exact coefficients of the eigenvectors will not be given. The reason is that they depend on the number of parameter combinations considered for the determination of the Hessian. The tendency shown by these eigenvectors and eigenvalues is not that sensitive to the number of data considered. Therefore, the discussion might contain less precise descriptions as 'larger than' or 'almost equal'.

As mentioned in the previous chapter the value of the objective function is given as the difference compared to the value of the objective function in the minimum, ΔO (-). The energy consumption is related to the whole building. The thermal discomfort due to excess indoor temperatures in the zone that is focused on, being either over- or undershoots, is given by $Penalty_1$. $Penalty_2$ quantifies the discomfort due to temperature variations in that zone. For the cases without global production element, the other zones are equipped with standard *ESP-r* ideal controls. Their resulting thermal comfort will thus hardly be influenced by the heat emitter/absorber characteristics. The objective function will consequently evaluate the discomfort in the zone of interest. This is different for the case with a global production device, where actions due to the demand for thermal power of 1 zone will affect the thermal output in the remaining zones. In that case, the possible thermal discomfort ($Penalty_1$ and $Penalty_2$) of all zones is incorporated in the objective function.

8.3.1 Location of the building

Brussels shows a climate with relatively cold winters, long midseasons and average summers (Figure 8.2). Temperature variations are rather limited, both in amplitude and frequency. Montreal, in contrast, has very cold winters, a short midseason and

warm summers (Figure 8.3). It shows large temperature variations in short periods. Finally, as a third case, Pisa has a Mediterranean climate with moderate short winters and long warm summers (Figure 8.4). Temperature variations show smaller amplitudes compared to the climate data of Brussels and Montreal².

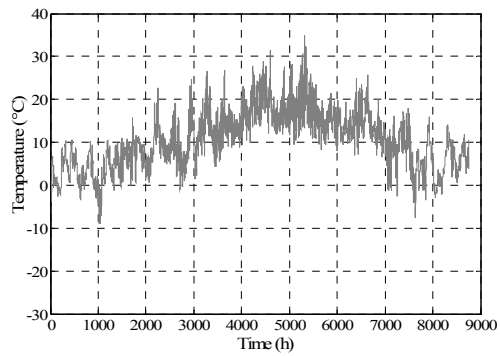


Figure 8.2: Dry bulb temperature of Brussels, Belgium (2001) as available through the ESP-r standard climate database.

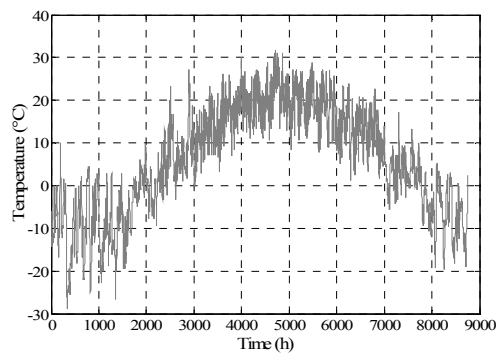


Figure 8.3: Dry bulb temperature of Montreal, Canada (1965) as available through the ESP-r standard climate database.

² The climate data shown are as standard available in ESP-r.

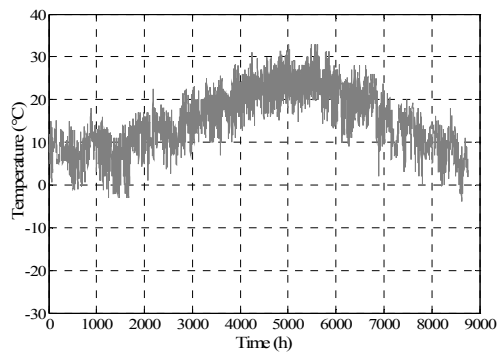


Figure 8.4: Dry bulb temperature of Pisa, Italy (1982) as available through the ESP-r standard climate database.

The optimisation involved the emitter/absorber in zone 1 of the heavyweight averagely insulated 3-zone building. The focus was on the ground zone with 'other zones'-temperature profile and no set backs. The temperature plots given above indicate a very different demand for heating and cooling for the three locations. The building has the lowest heating and the highest cooling load when located in Pisa (Figure 8.5).

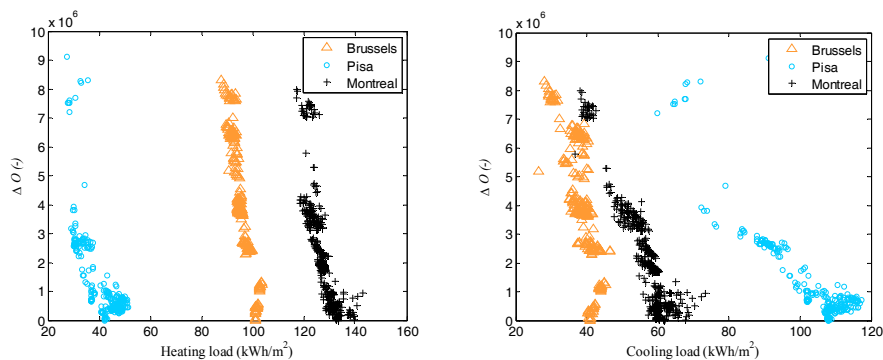


Figure 8.5: Optimisation results for the yearly heating and cooling load per square meter floor area for zone 1 of the averagely insulated brick house located in Brussels, Pisa or Montreal. The left hand graph shows the results for the heating load. The right hand graph shows the results for the cooling load.

The highest heating load is obviously for Montreal, which shows a climate with warm summers as well. The heat demand for the same building located in Brussel will be in between, while it will experience a lower cooling load. This is shown in Figure 8.5.

The heating and cooling loads of Brussels and Montreal clearly differ from one another. However, the ratios of cooling over heating load are not that different; 2.5 for Brussels and 2.2 for Montreal. For Pisa this ratio equals 0.5. It is to be expected that the optimisation results show different tendencies, especially for Montreal and Brussels versus Pisa. This is confirmed when comparing the composition of the first eigenvectors for the different locations:

$$\text{Brussels:} \quad a_B Q_N - \frac{a_B}{2} C + \frac{a_B}{4} n + \frac{a_B}{8} \alpha_N + 0\beta$$

$$\text{Montreal:} \quad a_M Q_N - a_M C + a_M n + \frac{a_M}{4.5} \alpha_N + 0\beta$$

$$\text{Pisa:} \quad a_P Q_N + \frac{a_P}{4} C - \frac{2}{3} a_P n - \frac{a_P}{4} \alpha_N + \frac{a_P}{40} \beta$$

where a_B , a_M and a_P are the dimensionless coefficients of the nominal power in the eigenvectors of the Brussels, Montreal and Pisa case respectively.

These eigenvectors show similar signs for all parameters in case of Montreal and Brussels. The weights are different, but the parameters cooperate in similar directions. The dominating weight of the nominal power in the case of Brussels implies that the other parameters need to change substantially in order to be able to compensate for changes in the nominal power. That effect is further enforced by a large difference between the first and second eigenvalue for this climate case. The more evenly distributed weight for the Montreal case will result in a wider spread of possible variations in parameter values for the same value of the objective function, at least in the neighbourhood of the optimum. These effects are shown in the different graphs of Figure 8.6.

Pisa is the only case with a small difference between the first and second eigenvector, i.e. a factor 0.25. That implies that, besides the dominating parameters in the above given first eigenvector, also those of the second eigenvector will strongly influence the course of the parameters in the neighbourhood of the optimum. That second eigenvector is dominated by the nominal fraction of

convection with a smaller weight with opposite sign for the radiator exponent. This effect reduces the impact of the nominal power and results in a wide spread in the neighbourhood of the optimum for all parameters with a reasonable weight in the first and/or the second eigenvector. The course of the objective function in the neighbourhood of the optimum is as shown by the left hand scheme of Figure 7.7.

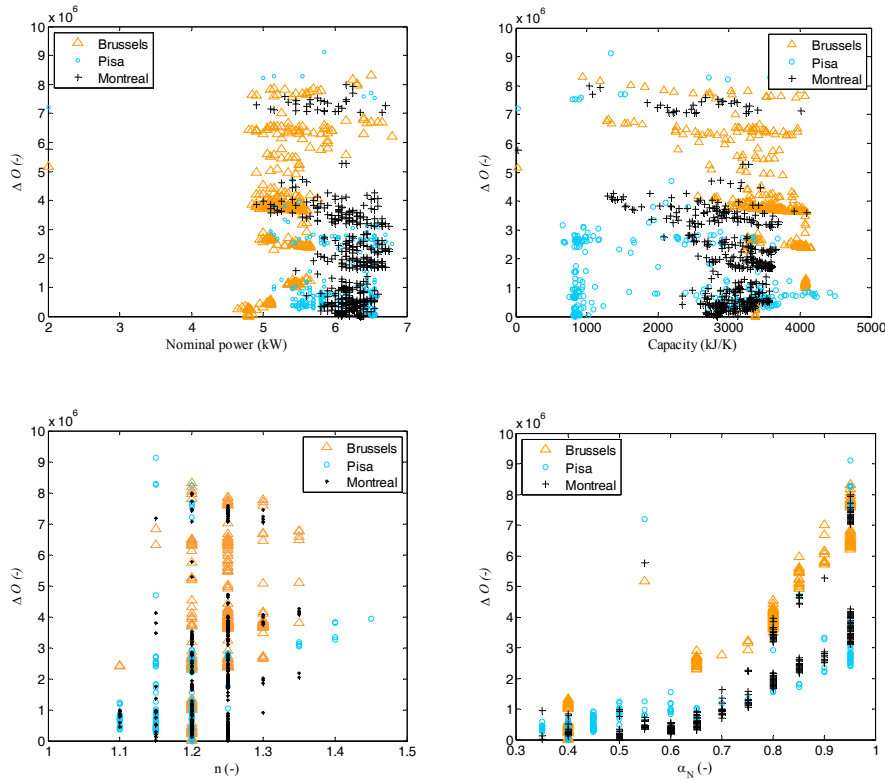


Figure 8.6: Optimisation results for zone 1 of the averagedly insulated brick house located in Brussels, Pisa or Montreal. The left hand upper graph shows the results for the nominal power, the right hand upper graph shows the results for the element's heat capacity, the left hand lower graph shows the results for the radiator exponent and the right hand lower graph those for the nominal fraction of convection.

Furthermore, the above given graphs indicate the need for a high nominal power when the cooling load dominates the heating load as for the climate of Pisa. This high nominal power is combined with a moderate radiator exponent of 1.2, a nominal fraction of convection around 0.4 and a relatively high heat capacity. The reason is that such values for the two first parameters listed allow realising a high

cooling power. The optimal heat capacity of around 1000 kJ/K for Pisa is much lower than the same optimal value for that parameter in case of Brussels or Montreal. However, a value of 1000 kJ/K is rather high. To give an idea, it corresponds to a 0.66 m³ concrete. Such heat capacity is a way of storing heat/cold and avoiding a too fluctuating output. Combined with the lower value for the fraction of convection the fluctuations of the surface temperatures can be tempered. In this warm and sunny climate, solar radiation will cause such fluctuations on the mean radiant temperature. If not tempered, this causes excessive fluctuations of the operative temperature. As can be seen in Figure 8.7 the strategy results in a good thermal comfort: low values are observed for both the steady state and the transient thermal comfort, expressed by $Penalty_1$ and $Penalty_2$ respectively.

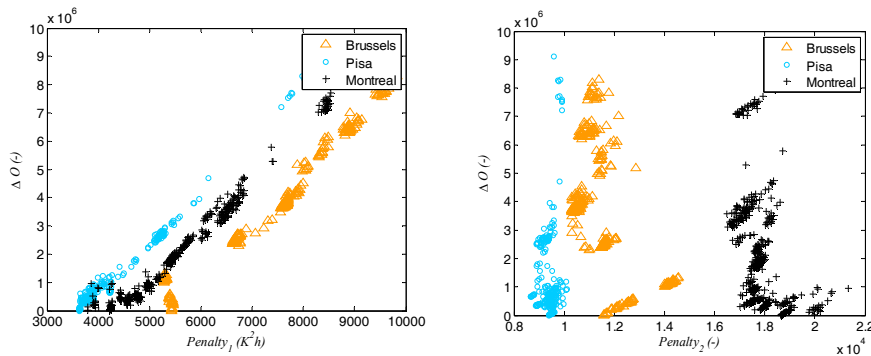


Figure 8.7: Optimisation results for the yearly heating and cooling load per square meter floor area for zone 1 of the averaged insulated brick house located in Brussels, Pisa or Montreal. The left hand graph shows the results for the $Penalty_1$. The right hand graph shows the results for $Penalty_2$.

Also the optimal heat emitter/absorber for Montreal shows the need to flatten indoor operative temperature variations with a combination of a high heat capacity and a small fraction of convection. The nominal power is high and it is even enlarged by the maximum radiator exponent that is still physically possible for the optimum fraction of convection of 0.5. As for the case of Pisa, this combination could deliver a high thermal power. However, as shown in Figure 8.7, it is not as effective for the Montreal climate as it is for the climate of Pisa. The reason is the much higher velocity of temperature changes for Montreal compared to Pisa. This can be seen when comparing Figure 8.3 and Figure 8.4.

For the climate of Brussels no excessive outdoor temperature fluctuations are to be tempered. The required nominal power is consequently lower. To be able to still

achieve a reasonable indoor temperature during warm summer days, the low fraction of convection is combined with a high heat capacity for the emitter/absorber. This combination cannot react fast, with a consequent impact on the thermal comfort.

The climate of Pisa shows results for low capacity floor heating (i.e. a heat capacity equivalent to 1.5 cm of concrete) that are close to the optimum. Compared to the results for the optimum itself, which is not a thermally active building element, a rise in energy consumption of 2% only, combined with an increase of 7% in the value of $Penalty_1$ and a reduction of over 5% in the value of $Penalty_2$. The moderate to low fraction of convection of around 50% is necessary in order to compensate for the fixed, relatively low, constant convection coefficient. The high heating and high cooling loads for Montreal prevent the selection of TAB elements. The average emitter/absorber element's temperature is limited throughout the simulation in order to prevent uncomfortable surface temperatures. Also for Brussels such systems were not observed in the neighbourhood of the optimum.

Radiators are for none of the climates in the neighbourhood of the optimum, as they are inadequate to fulfil the cooling need without causing uncomfortable indoor temperature fluctuations.

8.3.2 Heavyweight versus lightweight building structures

High (thermal) mass structures are often used in low-energy applications. One of the benefits is that due to the inertia peak loads are reduced [3], [10] and [11]. Fraisse et al. [12] conclude, based on an extended simulation study for summer comfort in moderate climates that the thermal comfort in lightweight timber frame constructions benefits from increased thermal mass. Cheng et al. [13] investigate the impact of thermal mass in more detail for hot humid climates and conclude that thermal mass cuts down indoor maximum temperatures and brings up indoor minima. The effect on the maxima, however, is more pronounced than the impact on the minima. Gregory et al. [4] describe a simulation study where the effect of thermal mass is examined for various construction systems in Australian residential buildings. They focus on summer behaviour and observed a clearly higher energy consumption for lightweight constructions compared to heavyweight types. Depending on the construction type and orientation of the windows, they mention cooling loads of up to 28% higher for the lightweight variants. This increased energy consumption, however, is not sufficient to improve the thermal comfort of the lightweight construction up to the level of the heavyweight buildings.

Feng [14] emphasizes the importance of the coupling between the heat transfer coefficient of the building envelope and its thermal inertia. The thermal inertia is given as the ratio of the building's thermal capacitance over the steady state heat loss coefficient of the building. The latter includes the transmission heat loss coefficient and a ventilation heat loss coefficient. Feng describes the physical phenomenon of the coupling as follows: *'If the thermal resistance of two exterior walls is the same, but the walls are made of different materials, the temperature distribution will differ in response to intensive solar heat on the outer wall of the building envelope. Here the heat transfer process will be transient. The decrease in mean temperature results from the thermal resistance (heat transfer coefficient) of the wall, but the decrease in the amplitude of the temperature fluctuation is affected by the index of thermal inertia'*. Catalina et al. [15] focus on temperate climates (e.g. France) and set up a simplified model to determine building heating loads. The model was subject to an extended validation study and showed limited deviations compared to more detailed TRNSYS-simulations. Catalina et al. confirm the conclusion of Feng on the importance of the building thermal inertia. They describe higher thermal mass to result in a lower heating demand, with a decreasing effect for increasing inertia. They nevertheless emphasize that the results are sensitive to climate and building U-values. Noren and Akander [16] simulated 3 different building types in a northern European climate. They observed that for the heating system high thermal inertia mainly located at the inner side of the wall reduces the energy consumption. But they indicate the effect to be decreasing for increasing insulation quality and for thin inner layers.

In the literature [17], [18] describing the dynamic effects of ambient conditions on heat transfer through building structures it is emphasized that thermal storage capacity of the materials and direct solar radiation can not be neglected. The actual rate of heat flow through typical massive brick walls can be up to 60 % lower in transient conditions compared to steady state cases, while the effect for lightweight constructions can be an increase of 20 to 60% [17].

The effect of the building envelope dynamics obviously plays a role when performing dynamic building energy simulations. The increased energy consumption for heating, as mentioned by Catalina et al. [15] and Noren and Akander [16], is confirmed by the optimisation runs performed in the framework of the current dissertation. The left hand graph of Figure 8.8 shows an increase of 15% in the yearly heating load per m² floor area for zone 1 of the intermittently heated/cooled building located in Brussels for the lightweight variant compared to

the heavyweight one. Both have an average U-value of $0.55 \text{ W/m}^2\text{K}$ for their building envelope. During the set back implemented, the temperature was allowed to drop to 15°C or rise to 32°C . Set back periods were scheduled from 10 a.m. to 6 p.m. and from 10 p.m. till 8 a.m..

The increased energy consumption for cooling, as indicated by Gregory et al. [4], is confirmed by the results of the optimisation runs performed in the framework of the current dissertation. An increased energy consumption of around 30% is observed for the lightweight building with low thermal mass at the inner side compared to the heavyweight case (right hand graph of Figure 8.8). As the U-value of the building envelope is similar and the glazing is identical, this difference is due to the above described impact of dynamics.

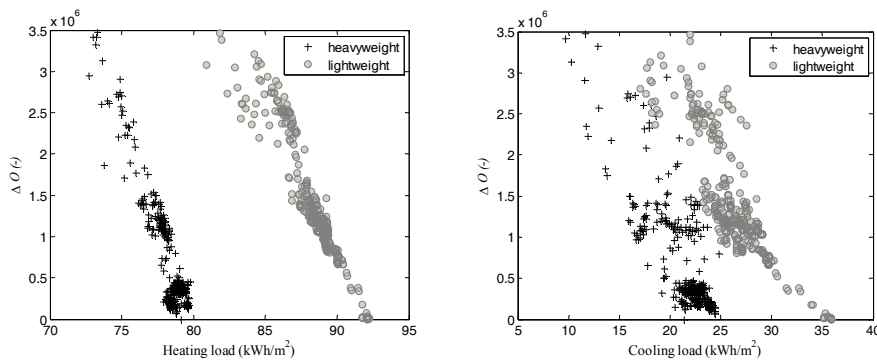


Figure 8.8: Optimisation results for the yearly heating and cooling load per square meter floor area for zone 1 of the averagely insulated house located in Brussels, for both the heavyweight and the lightweight construction. The left hand graph shows the results for the heating load. The right hand graph shows the results for the cooling load.

The reduced thermal comfort as described by the above mentioned authors [4], [12], [13] is partly encountered when analysing the results of the optimisation runs. Figure 8.9 shows $Penalty_1$ and $Penalty_2$, the Over-temperature hours and the Under-temperature hours for zone 1 in both the heavyweight and the lightweight averagely insulated building. The ‘Over-temperature hours’ is introduced to quantify the discomfort due to uncomfortably high indoor temperatures. It is calculated as the height of the temperature excess, compared to the upper value of the comfortband, multiplied by the duration of the discomfort and is evaluated during occupancy only. It is given in Kh. Similarly, discomfort due to a too low temperature can be expressed by ‘Under-temperature hours’.

Figure 8.9 shows these thermal comfort indicators for both the heavyweight and lightweight building.

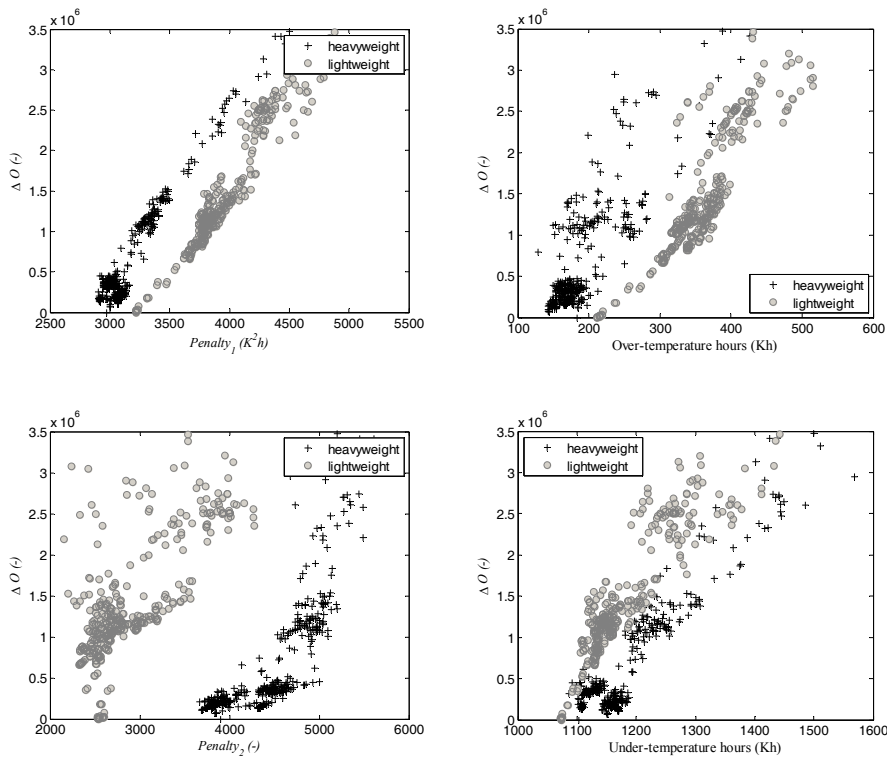


Figure 8.9: Optimisation results showing the value of $Penalty_1$ (left hand upper graph), the Over-temperature hours (right hand upper graph), $Penalty_2$ (bottom left) and the Under-temperature hours (bottom right) for the heavyweight versus lightweight case for zone 1 of the intermittently heated/cooled averagely insulated house located in Brussels.

There is an obvious agreement between the course of the results for $Penalty_1$ and the Over-temperature hours for the lightweight building. It is clear that $Penalty_1$ will mainly be higher for the lightweight building due to too high indoor temperatures. There is less agreement between the course of the results for the Under-temperature hours and $Penalty_1$ for this building type. This confirms the findings described in the literature on peak indoor maxima. That high thermal mass, mainly at the inner side of the building envelope, can reduce excessive indoor temperature peaks is confirmed by the lower value of both $Penalty_1$ and the Over-temperature hours for the heavyweight building.

The results for $Penalty_2$ show a remarkable difference in transient thermal comfort between the heavyweight and lightweight building. The lightweight building shows a lower value for $Penalty_2$ which means less temperature fluctuations. This suggests that the optimal emitter/absorber element is selected in order to reduce indoor temperature swings. Such indoor temperature variations will strongly be affected by the building envelope with low buffering capacity. So, it is expected that the optimal emitter/absorber will have a high nominal power combined with a low fraction of convection and a high heat capacity (Figure 8.10). In warm summer conditions the latter prevents that during set back excessive peaks in indoor temperature would occur. Less outdoor temperature variations occur in winter, with also a less intense solar radiation on the building. Consequently, there are fewer variations in zonal indoor surface temperatures. The low fraction of convection, optimally around 0.35, combined with the high heat capacity and high nominal power of the emitter/absorber shows to be insufficient to realise fast temperature rises during winter. This is confirmed by the high value for the Under-temperature hours for the lightweight building (right hand lower graph of Figure 8.9).

The dominant effect of these parameters, the nominal power, the heat capacity and the nominal fraction of convection of the emitter/absorber, is confirmed by their weights in the first and second eigenvector. Furthermore, there is a negative fifth eigenvalue, which is dominated by the nominal fraction of convection. This indicates that the optimal value for this parameter would even be lower. However that is physically impossible and such low value was extracted from the n-dimensional polytope on beforehand.

The results further show to not prefer TAB-elements. The reason is the limitation of the actual thermal output and storage due to preventing excessive surface temperatures.

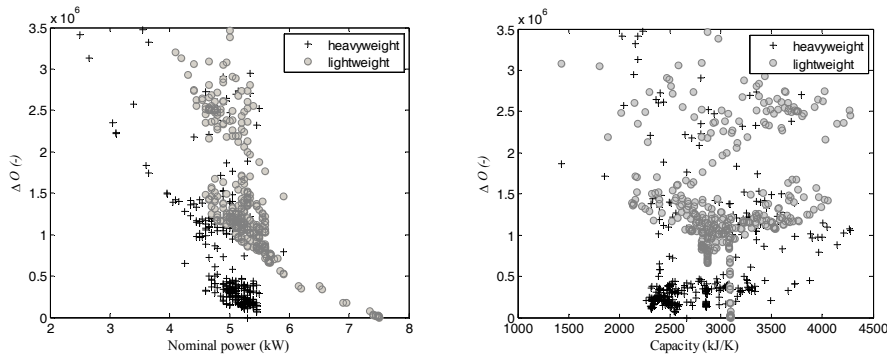


Figure 8.10: Optimisation results for zone 1 of the averagely insulated house located in Brussels, for both the heavyweight and the lightweight construction. The left hand graph shows the results for the nominal power. The right hand graph shows the results for the heat capacity.

The high value for the Under-temperature hours of the heavyweight building, combined with the high value for $Penalty_2$, suggest that the start-up control does not work properly. The low value of the Over-temperature hours compared to the value of the Under-temperature hours indicates that the main problem occurs in winter and that for summer conditions it works properly. That suggests that the start up control could be improved using two separate sets of inputs for winter and summer³.

The lower nominal power for the heavyweight building combined with an almost similar value for the radiator exponent (1.1 to 1.2) and the nominal fraction of convection (0.35-0.4) indicate that less variation in thermal output is required. That is due to the ambient fluctuations being flattened out by the high thermal mass of the heavyweight building.

Again, low capacity elements as radiators and convectors do not appear in the neighbourhood of the optimum. Also TAB elements show not to be optimal as they

³ It should be noted that the set of parameter inputs for the start-up time calculation is determined throughout the optimisation as well. There is a higher weight to steady thermal comfort compared to transient thermal comfort in the objective function. Consequently a reduction of $\times K^2h$ on the value of $Penalty_1$ may 'cost' up to an additional 4x on the value of $Penalty_2$ to still cause a similar value of the objective function. With another weight-distribution in the objective function, the result would have been different.

have insufficient thermal power for this case with 2 set backs per day due to limitations on the surface temperatures.

8.3.3 Variations in insulation quality

Kaynaki [19] optimises the thickness of the insulation for a heating-only case with constant heavyweight wall configuration. He considers residential buildings in Burma, Turkey. He shows that the relationship between heating demand and optimal insulation thickness is non-linear. This non-linearity is confirmed by Yu et al. [20] in their evaluation of different heavyweight building envelope designs for hot summer/cold winter zones in China. They show the heating load to decrease with increasing insulation thickness. While during warm summer months, the effect on the cooling load is not obvious. Increasing the insulation thickness lowers the cooling load during the day. At night, for an insulation thickness above a value of 25 mm the cooling load could even increase. The results given in the paper show the savings to strongly depend on the placement of the insulation within the wall.

Feng [14] describes this conflict between heating and cooling as the consequence of the transient bidirectional heat transfers between the indoor and outdoor. He emphasizes it to be much more difficult to determine the ideal building envelope configuration when considering both heating and cooling.

These trends of increasing cooling load and decreasing heating load as a function of insulation thickness are confirmed with the optimisation runs performed in the framework of the current dissertation. Figure 8.11 shows the heating and cooling loads for both building types. The optimisation was performed for the emission/absorption element of the ground zone of the 3-zone building located in Brussels. During the 2 set backs implemented, the temperature was allowed to drop to 15°C or rise to 32°C. Set back periods were scheduled from 10 a.m. to 6 p.m. and from 10 p.m. till 8 a.m..

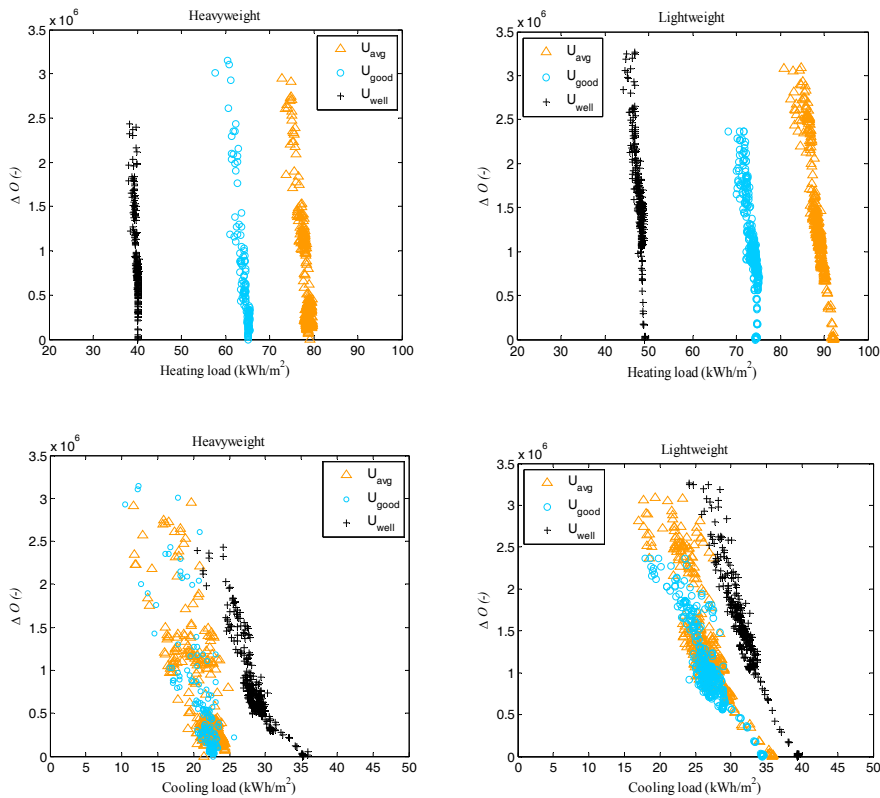


Figure 8.11: Optimisation results showing the heating load for zone 1 of the heavyweight (lefthand upper graph) and lightweight (right hand upper graph) and the cooling load for the heavyweight (bottom left) and lightweight (bottom right) house for varying insulation qualities (see Table 8.2). The house is located in Brussels and set backs are implemented.

The above mentioned non-linearity is clearly shown for both the heating and cooling loads for the lightweight and the heavyweight building. The heating load shows an expected decrease for increasing insulation quality. The cooling load, however, shows an almost equal value for both the averagely and the good insulated buildings, with a clear increase for the well insulated building. Comparing the course encountered in the graphs for the cooling load (bottom graphs in Figure 8.11), with the course for the Over-temperature hours (Figure 8.12), there is an obvious agreement.

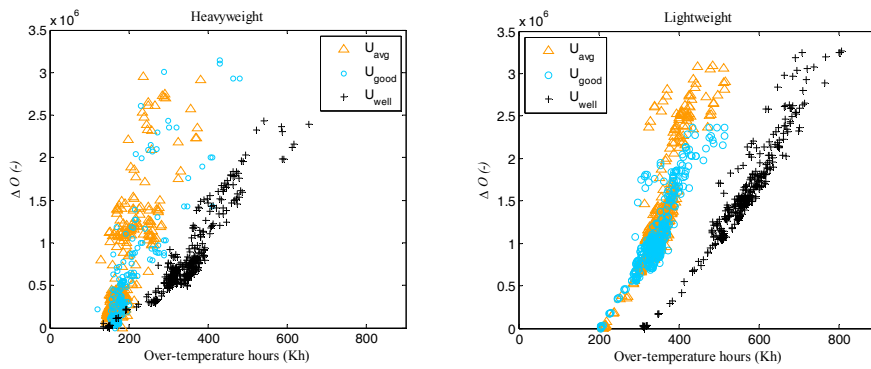


Figure 8.12: Optimisation results showing the Over-temperature hours for zone 1 of the heavyweight (left graph) and lightweight (right graph) house for varying insulation qualities (see Table 8.2). The house is located in Brussels and set backs are implemented.

The Over-temperature hours in the heavyweight variant all converge to a similar value. However, the course of the well insulated building shows a lower slope close to the optimum. Such lower slope is also found in the course of the cooling load for that building. The difference between the slope close to the optimum and the slope for parameter combinations further away from the optimum is much higher for the cooling load compared to the Over-temperature hours. This indicates that these last thermal comfort improvements are to be paid by a relatively high increase in cooling load.

The above quoted almost equal cooling load for the averagely and the good insulated buildings, both heavyweight and lightweight, combined with the almost equal course of the Over-temperature hours of these variants, indicates that the reason for the cooling load is the solar radiation entering the zone through the windows. Adding more insulation increases the inertia of the building. As mentioned before, the thermal inertia is given as the ratio of the building's thermal capacitance over the steady state heat loss [14] and [15]. And an increased inertia slows down the positive effect of a decrease in ambient temperature at night.

For high thermal mass buildings, analysing the simulation results shows the optimal nominal power to be significantly lower compared to the lightweight variant (upper graphs in Figure 8.13). However, there is one remarkable exception. The best insulated variant shows a deviating course in the neighbourhood of the optimum. Such deviating course is also observed in the results for the heat capacity of the

emitter/absorber. In the neighbourhood of the optimum, both other insulation qualities show a wider spread for this parameter. This is again related to the attempt to further reduce the Over-temperature hours (bottom graphs in Figure 8.13), which is confirmed by a lower value for $Penalty_1$ and a similar value for $Penalty_2$ for the well insulated heavyweight variant compared to the averagely and good insulated heavyweight building.

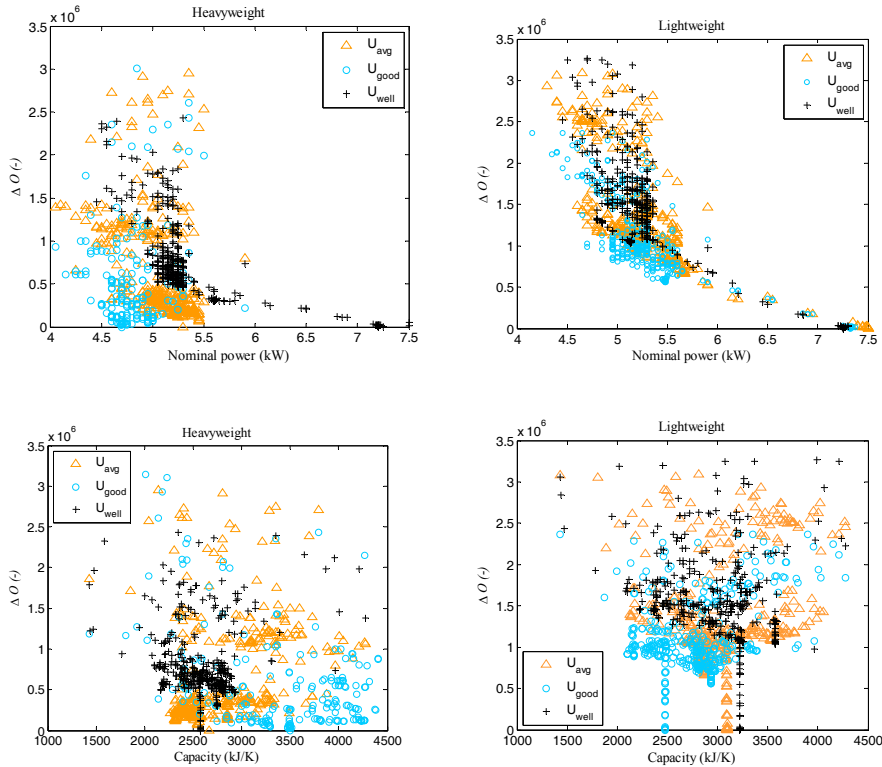


Figure 8.13: Optimisation results showing the nominal power for zone 1 of the heavyweight (left hand upper graph) and lightweight (right hand upper graph) and the emitter/absorber element's heat capacity for the heavyweight (bottom left) and lightweight (bottom right) house for varying insulation qualities (see Table 8.2). The house is located in Brussels and set backs are implemented.

The lightweight buildings show some similarity with the heavyweight well insulated building. There is the attempt to further reduce the Over-temperature hours by an increase in nominal power, however without changing the element's heat capacity. And again this is confirmed to be an effective strategy as the value of $Penalty_2$ remains almost constant, while the value of $Penalty_1$ decreases.

Figure 8.13 further indicates a similar, but opposite effect for the heat capacity of the lightweight compared to the heavyweight buildings. The optimal heat capacity of the averagely and well insulated buildings is similar, while the heat capacity for the good insulated buildings shows to diverge. The reason is that such buildings are less sensitive to temperature falls in winter, when compared to the less insulated variant, while they still benefit from the effect of outdoor temperature reductions in summer. So they need less buffering capacity in winter and are subject to a lower cooling load in summer.

For the heavyweight well insulated building and the lightweight buildings, the objective function shows to be more sensitive to changes in the values of the radiator exponent and the fraction of convection compared to the less insulated heavyweight variants. The heavyweight well insulated building and the lightweight buildings all tend towards low n-values of around 1.1 and a fraction of convection of around 0.4. The low value for the radiator exponent is necessary so as to reduce the temperature dependency of the thermal output. Combined with the relatively high thermal capacity, this is a strategy to emit/absorb a constant and high amount of thermal energy. The low fraction of convection is to temper surface temperature variations.

These low n-values and low fractions of convection, combined with a reasonable heat capacity for the well insulated heavyweight and all lightweight variants agree well with the characteristics of thermally active elements. However, the optimal value of β shows to not prefer TAB elements. For active walls and ceilings, this is due to the penalty when such elements are modelled with high capacities. For floor heating/cooling, the reason can be twofold: a reduction in effective thermal output which is due to the measure to prevent uncomfortable surface temperatures and/or the use of a constant convection coefficient.

8.3.4 Constant indoor temperature versus intermittent heating/cooling

The possible decrease in energy consumption due to implementing set backs has been discussed widely in the literature. Mathews et al. [21] mention savings of up to 60% on the HVAC consumption when applying set back control to an air conditioned 22-floor building in Pretoria, South Africa. The building considered comprises lecture halls and offices. The authors describe an additional 6%-points savings when implementing an improved start-stop time algorithm. The savings reported in that study are high as the set backs in offices are relatively long and incorporate weekends and public holidays as well. The importance of the duration of

the set backs on the potential savings has also been reported by Manning et al. [22]. These authors describe a range of experiments performed on a test house in Ottawa, Canada. The authors show that savings are not to be generalized; they not only depend on the time-settings. Climate, building design and specifications of the heating/cooling installation might influence the achievable savings.

Comparing the case of no set backs in zone 1 with the case of implementing 2 set back periods per day in that zone for the optimisation runs performed within the framework of the current dissertation, savings in the range of 30% can be achieved on the heating/cooling load for zone 1 of the averagely insulated building (Figure 8.14). During the set back implemented in zone 1, the temperature was allowed to drop to 15°C or rise to 32°C. Set back periods were scheduled from 10 a.m. to 6 p.m. and from 10 p.m. till 8 a.m.. The two other zones were given temperature profiles as described in appendix E.

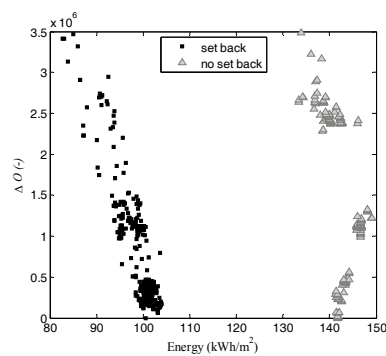


Figure 8.14: Optimisation results showing the yearly total thermal load per square meter floor area for the no set back versus set back case for zone 1 of the averagely insulated brick house located in Brussels. The graph shows the results of a range of optimisation runs with different initial parameter values.

The savings for the heating consumption of zone 1, for which the heat emitter/absorber was optimised, equal 22% (left hand graph of Figure 8.15) and those for the cooling load almost 50% (right hand graph of Figure 8.15). The effect on the total load of the surrounding zones is limited: their temperature settings were kept constant and their absolute consumption remains the same.

The data show a wide spread. Consequently a large variation in potential savings is possible depending on the selected emitter/absorber elements. This confirms the

finding of Manning et al. [22] to not generalise the potential savings due to the implementation of set backs.

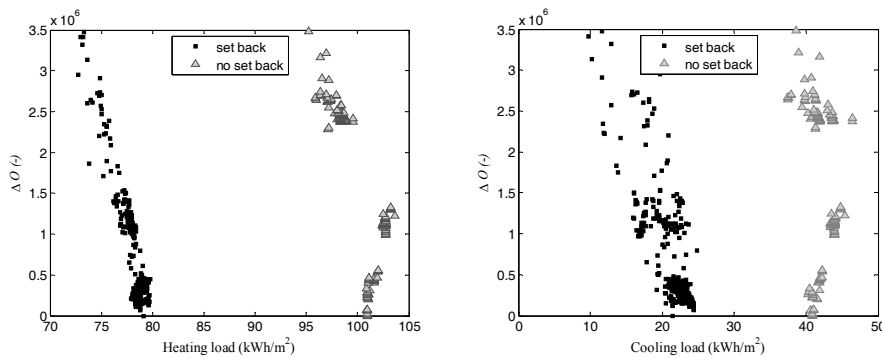


Figure 8.15: Optimisation results for the yearly heating and cooling load per square meter floor area for zone 1 of the averagely insulated brick house located in Brussels. The left hand graph shows the results for the heating load. The right hand graph shows the results for the cooling load.

There are two aspects which determine the optimal nominal power of the emitter/absorber. The first aspect is that due to a more constant indoor temperature profile in the absence of set backs, peaks in heating/cooling load are flattened out. Based on this phenomenon, it is to be expected that the nominal power of the heat emitter/absorber is smaller in the absence of set backs. The second aspect is related to the ratio of cooling load versus heating load for the ground zone. For the case without set backs this ratio is 40%, for the case with set backs the value is 27%. To be able to deliver enough cooling power, the nominal power should be high enough. Both aspects will have an opposite effect on the optimal nominal power which reduces the difference between the set back and the no set back case. As can be seen in Figure 8.16, the impact of the first aspect of flattened peaks is slightly dominant and results in a lower nominal power for the case without set backs compared to the case with set backs.

It is to be expected that the optimal heat capacity of the emitter/absorber is smaller in case of set backs, as it is related to the timeconstant of the element. In that sense, one could expect the capacity to be as low as possible. However, also in this case there is a countereffect related to tempering indoor temperature variations. A high heat capacity for the emitter/absorber results in a smooth emission/absorption of heat. The effect is important due to the high weight of transient thermal comfort in

the objective function. As can be seen in Figure 8.16, the resulting capacity is high but remains smaller than the heat capacity for the case without set backs.

The importance of those two parameters, nominal power and heat capacity, is confirmed by their weight in the first eigenvector for both the set back case and the case without set backs. The heat capacity for the case without set backs further shows limited variations in the neighbourhood of the optimum. The reason is that the first eigenvector gives a high weight with opposite sign to both the nominal power and the heat capacity, while the second eigenvector gives the same sign, but a much higher weight to the heat capacity. Such difference in proportion is not encountered in the set back case.

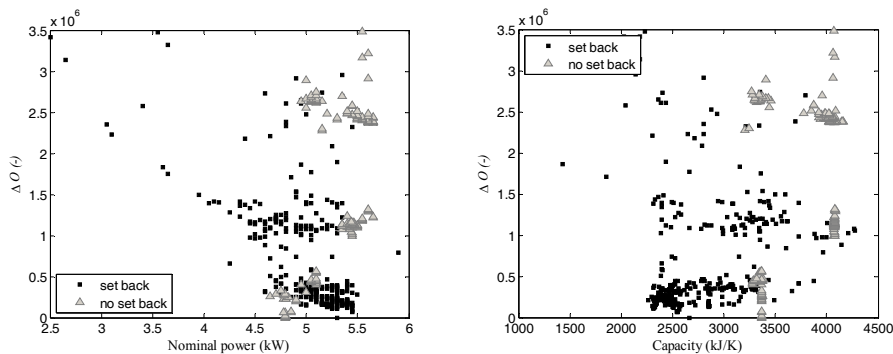


Figure 8.16: Optimisation results showing the results for the emitter/absorber of zone 1 of the averagely insulated brick house located in Brussels. The left hand graph shows the results for the nominal power. The right hand graph shows the results for the emitter/absorber element's heat capacity.

However, as can be seen in Figure 8.16, especially for the case without set backs, there is a third parameter that affects the relation between capacity and nominal power. If not, there would have been confirmity in the course of the two parameters in the neighbourhood of the optimum. The eigenvector for both cases, set back and no set back, indicates the third important parameter to be the radiator exponent. That is to be expected as this parameter determines the temperature dependency of the emitted/absorbed thermal power; a higher n -value will result in more power to be available when the absolute value of the temperature difference between element and zone exceeds the nominal temperature difference.

The eigenvector indicates the possibility to compensate a decrease of the element's heat capacity by a decrease in the values of both the nominal power and the radiator exponent. That is due to the attempt to temper the velocity of temperature changes as they will be penalised ($Penalty_2$). If the element's heat capacity decreases, the inertia decreases. In order to prevent the velocity of temperature changes to increase and cause uncomfortable fluctuations, the thermal output must be reduced. That can be done by lowering the nominal power and/or reducing the temperature dependency by lowering the radiator exponent.

The optimal value of that radiator exponent is for both cases, set backs and no set backs, around 1.2. More variation is observed in the neighbourhood of the optimal value in case of set backs (indicated by ellipse in left hand graph of Figure 8.17). This is due to a fourth parameter with a relatively high weight in the eigenvector for the case with set backs, i.e. the nominal fraction of convection. Also this parameter shows a wide variation in the neighbourhood of the optimum in the case with set backs (ellipse in right hand graph of Figure 8.17). Both variables have a similar weight with opposite sign in the first eigenvector. A reduction in one can thus be compensated by a similar reduction in the other.

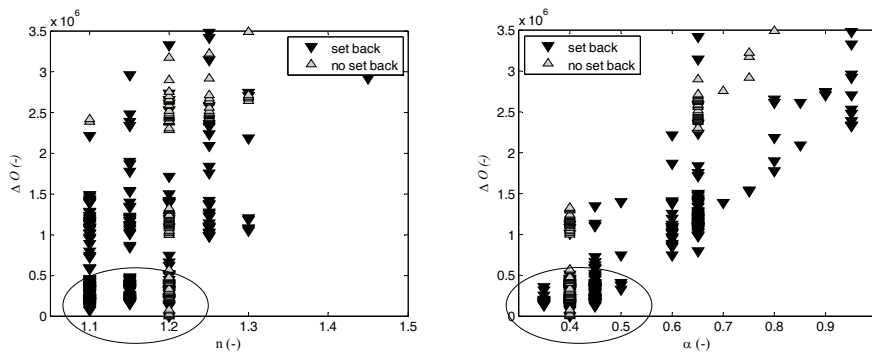


Figure 8.17: Optimisation results showing the results for the emitter/absorber of zone 1 of the averagely insulated brick house located in Brussels. The left hand graph shows the results for the radiator exponent. The right hand graph shows the results for the nominal fraction of convection.

The weight of this fraction of convection is much lower in the first eigenvector in the absence of set backs. As is shown in the neighbourhood of the optima of the nominal power, the element's heat capacity (Figure 8.16) and the radiator exponent (left hand graph of Figure 8.17), less variation in parameter values is encountered in the absence of set backs.

The fraction of convection is low, 0.4 for both the case with and without set backs. This low fraction is again the result of the two opposing aspects. The first one is the activation of extra thermal mass and the consequent tempering of variations in surface temperatures especially in summer. The second aspect is the attempt to react fast and the increased controllability of directly activating no other but the element's thermal mass. It is clear that especially the first aspect is important in the absence of set backs due to the higher cooling load over heating load ratio.

For the no set back case the optimum indicates the element's heat capacity to agree well with the capacity of real thermally active floors. In this case the optimum heat capacity would result in a concrete layer thickness of around 6 cm. Also the preference for a lower fraction of convection agrees with the real active floor systems. However, the optimal n-value is slightly higher, 1.2 versus 1.1 for real floor heating cases. In the ranking, active floors do not appear in the neighbourhood of the optimum. The reason is that insufficient fast cooling power is available due to the constant convection coefficient implemented for floor cooling. This results in overheating in summer, with a consequently high value for thermal discomfort. The latter also results in a lower ranking for active building elements in case of set backs. However the heat capacity, fraction of convection and n-value of floor heating show to be closer to the optimum for this set back-case.

Conventional radiators show higher n-values (in the range of 1.3) and consequently also higher fractions of convection (around 0.75). Furthermore, the heat capacity for radiators, commonly of an order of magnitude of 10 kJ/K to 30 kJ/K, is far from what has been shown the optimal value.

In the absence of cooling, the optima tend towards the characteristics of real floor heating systems for a case without set backs. Increasing the deadband of the controller (1.5K instead of 1.1K) for a heating and cooling case without set backs, results in higher heating and cooling energy consumptions; 9% and 4% respectively. That is combined with a preference for even more heat capacity (increase with 15%) in order to reduce the thermal discomfort due to temperature fluctuations. Changes to the desired indoor temperature, i.e. using the bathroom neutral temperatures in the ground zone, results in an increase of 24% in optimal heat capacity for a case without set backs. The reason is the larger impact of the steady state thermal comfort evaluation on the objective function. The high inertia, however, prevents to react fast to temperature changes due to casual gains or changes in outdoor conditions. The preferred nominal power is reduced by 15%. The reason is the reduced cooling

load as the bathroom-profiles shows a preference for higher neutral temperatures, also in summer. The optima for the other parameters remain the same as in the case the temperature profile was set to the ‘other zones’-profile.

8.3.5 Limitations to production device: increased lock out time

Little literature is available on the effect of limitations of the production device that delay the energy production. However it is well-known that less flexible production devices should be coupled to a storage tank or another system that could temporarily store the thermal energy [23], [24].

When increasing the lock out time of a production device, the thermal energy deliverance to the zonal emission/absorption elements is delayed. To be able to account for a possible delay, it is important that enough inertia is available to avoid high temperature drops in the heating season or strong temperature rises during the cooling season.

The simulations for this case study involve the averagely insulated heavyweight house, located in Brussels. No set backs were implemented and the temperature profile is set to the ‘other zones’. All zones have an emitter/absorber according to the implicit model, the lock out time of the production device is set to 0.5h. However, the optimisation here focuses on the characteristics of the element in the ground zone only. The objective function now minimises both the energy consumption and the thermal comfort penalties of the whole building. It is compared to the same case without limitations of the production device and where the surrounding zones are equipped with a standard ideal *ESP-r* zone control and will consequently achieve an almost perfect thermal comfort. Due to the differences in objective function it is hard to show the absolute influence of the parameter changes on the objective function. Care should thus be taken when comparing the course shown by the graphs giving the objective function as a function of a certain parameter.

The first eigenvector for the lock-out case exhibits a high weight of the heat capacity:

$$\text{Lock out time: } \frac{a_G}{4} Q_N + a_G C - \frac{a_G}{20} n - \frac{a_G}{20} \alpha_N + 0\beta$$

No lock out time:
$$a_B Q_N - \frac{a_B}{2} C + \frac{a_B}{4} n + \frac{a_B}{8} \alpha_N + 0\beta$$

where a_G and a_B are the dimensionless coefficients of the dominating parameter in the first eigenvector for the case with lock out and without lock out times respectively.

The high importance of the heat capacity is to be expected as it is a way of storing thermal energy to overcome shortage of deliverance by the heat production device. Based on the above given eigenvector, one could expect that a decrease in heat capacity could be compensated by an increase in nominal power. That is prevented by the opposite sign for the nominal power and the element's heat capacity in the second eigenvector. The ratio between the two first eigenvalues is of the order of magnitude of 40.

Figure 8.18 shows an almost constant heat capacity in the neighbourhood of the optimum. Higher variations are observed for the nominal power. This is due to a smaller effect of the latter variable in the first eigenvector. Furthermore, the influence in the direction of the second eigenvector can be compensated by a change in either the radiator exponent or the nominal fraction of convection. Those two last ones have a limited impact in the direction of the first eigenvector.

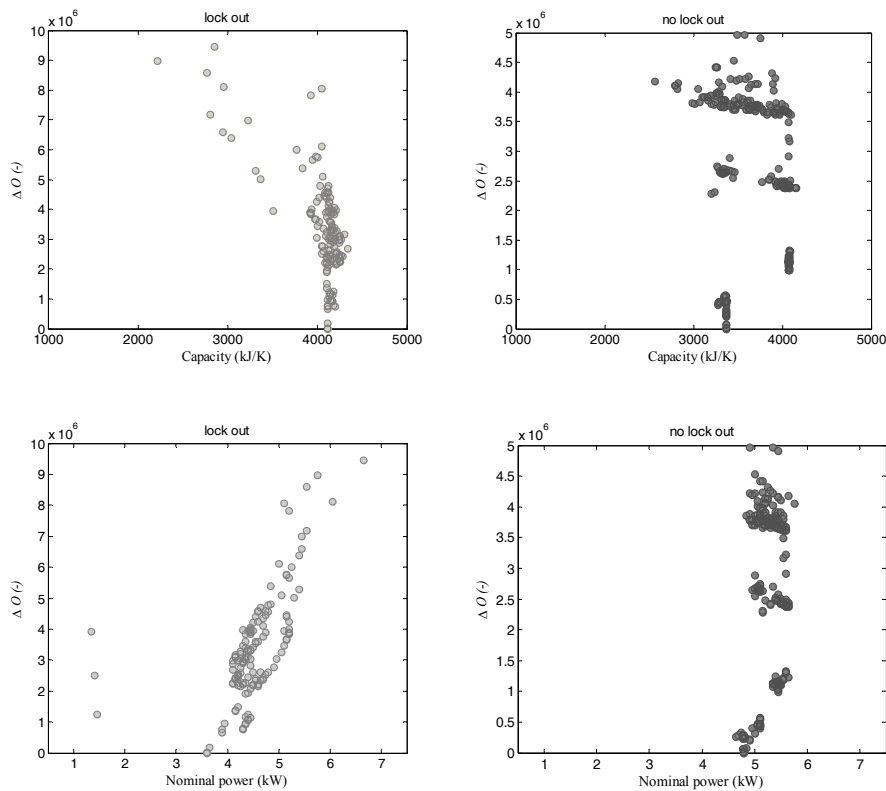


Figure 8.18: Optimisation results showing the optima as a function of the heat capacity for the lock out-case and the no lock out-case (upper left and right hand graphs respectively) and the nominal power for both cases (lower left and right hand graphs respectively). The results are for zone 1 of the averagely insulated heavyweight building, without set back once with a 0.5h lock out time of the production device and once without lock out time.

The radiator exponent shows an optimal value of 1.25. For the nominal fraction of convection, the optimum is around 0.7. Those two parameters, mainly influencing the second eigenvector, indicate that for a given value of the heat capacity and for a given nominal power, there is an attempt to emit/absorb the heat in a fast way that directly influences the operative temperature: a direct effect on the thermal output for any change in average emitter/absorber element's temperature and no extra thermal mass activation that slows down the reaction due to the highly convective output.

Compared to the case without limitations of the production device the heat capacity for the case with lock out time is indeed higher. This is combined with a lower value of the nominal power and a similar radiator exponent for the case with lock out time. That again, as a way to prevent the buffer is 'empty' too soon. Based on that reasoning, one could expect an even higher heat capacity, in order to be able to store even more thermal energy and be able to emit/absorb faster. However a too high capacity would reduce the velocity of changes in the element's average temperature and thus slow down possible fluctuations in thermal output.

The thermal comfort of the ground zone has a lower weight in the overall objective function in the case with lock out. The changes in the values of $Penalty_1$ and $Penalty_2$ for the two other zones are limited, but their values are high. Consequently, the weight of the thermal (dis-)comfort of the ground zone is reduced. The Over-temperature hours for the ground zone are 4.5 times higher when implementing a 0.5h lock out time. The Under-temperature hours are even 7 times higher. This is directly translated in an increase of a factor 8 for the value of $Penalty_1$ in that zone. The value of $Penalty_2$, however, benefits from a much higher element's heat capacity. The decrease in that value is a factor 3 for the lock out case compared to the case without lock out time.

The heat capacity for the lock out case agrees well with that of conventional thermally active floors. However, in order to slightly increase the effect of the thermal output on the operative temperature, the fraction of convection is high in the optimal case. It is reduced when moving away from the optimum, but remains accompanied by a radiator exponent of around 1.25, which is high compared to the value of 1.1 common for thermally active floors.

The reader should remind, however, that the conclusions are based on the results for the specific case considered here with the coefficients of the objective function as selected in the previous chapter. The tendencies given should thus not be generalised.

8.4 Summary and conclusions

The cases described in this chapter, all indicate the importance of the eigenvalues and eigenvectors when analysing a multiple-dimensional optimisation problem. Through such analysis, it is shown how sensitive the minimum is to changes in certain parameters or parameter-combinations. The examples show that both the sensitivity and the dominating parameters are context-dependent and can not be generalised. It should be emphasized that the results given are valid for the cases considered, the selected control settings and the chosen objective function. The tool developed allows changing both these control settings and the objective function.

For the settings described in this thesis, there are some effects that have been shown repeatedly throughout the results discussion. It is shown that for high outdoor temperature variations, there is lower optimal emitter/absorber element's heat capacity with a higher nominal power compared to a case with more constant outdoor conditions. When the cooling load is reduced, also the nominal power can be reduced in heavyweight buildings. The expected reduction in optimal nominal power and increase in optimal heat capacity for a more constant indoor temperature setting was confirmed by the results.

In none of the cases thermally active walls or ceilings appeared close to the optimum. This is due to the inaccuracy of the model for highly capacitive active walls and ceilings, such combinations were penalised.

Through this chapter, the use of the optimisation framework has been shown. Results are in line with findings of several authors, confirming the accuracy of the developed tool. In contrast to results presented in state of the art publications, which are either based on measurements, ad-hoc methods or case-studies, the tool developed in the framework of this dissertation allows a complete exploration of the solution space.

References

- [1] L. Peeters, L. Helsen, W. D'haeseleer, 2005, Prediction of heat-demand to minimize heat-pump heating costs, 8th Rehva World Congress, CLIMA, Lausanne, Switzerland, October 9-12
- [2] P. Hoes, J. Hensen, M. Loomans, B. de Vries, D. Bourgeois, 2009, User behaviour in whole building simulation, vol. 41, pp. 295-302
- [3] E. Kossecka, J. Kosny, 2002, Influence of insulation configuration on heating and cooling loads in a continuously used building, *Energy and Buildings*, vol. 34, pp. 321-331
- [4] K. Gregory, B. Moghtaderi, H. Sugo, A. Page, 2008, Effect of thermal mass on the thermal performance of various Australian residential construction systems, *Energy and buildings*, vol. 40, pp. 459-465
- [5] E. McPherson, L. Herrington, G. Heisler, Impacts of vegetation on residential heating and cooling, *Energy and Buildings*, vol. 12, pp. 41-51
- [6] B. Andersson, W. Place, R. Kammerud, 1985, The impact of building orientation on residential heating and cooling, *Energy and Buildings*, vol. 8, pp. 205-224
- [7] M. Persson, A. Roos, M. Wall, 2006, Influence of window size on the energy balance of low energy houses, *Energy and Buildings*, vol. 38, pp. 181-188
- [8] ASHRAE, 2005, *Fundamentals*, American Society for Heating, Refrigerating and Air conditioning Engineers, Atlanta
- [9] ISO, 2005, ISO 7730; Ergonomics of the thermal environment – Analytical determination and interpretation of thermal comfort using the PMV and PPD indices and local thermal comfort criteria, International Organisation for Standardization, Switzerland
- [10] P. Tuohy, L. Mc Elroy, C. Johnstone, 2005, Thermal mass, insulation and ventilation in sustainable housing – an investigation across climate and occupancy, *Proceedings of the 9th IBPSA Conference*, pp. 1253-1260
- [11] J. Hacker, T. De Saullles, A. Minson, M. Holmes, 2008, Embodied and operational carbon dioxide emissions from housing: a case study on the effects of thermal mass and climate change, *Energy and Buildings*, vol. 40, pp. 375-384
- [12] G. Fraisse, V. Trillad-Berdal, B. Soury, 2005, Improvement of summer comfort in wood frame buildings, *International Conference Passive and Low Energy Cooling for the built-environment*, Santorini, Greece, May 19-21
- [13] V. Cheng, E. Ng, B. Givoni, 2005, Effect of envelope colour and thermal mass on indoor temperatures in hot-humid climate, *Solar energy*, vol. 78, pp. 528-534
- [14] Y. Feng, 2003, Thermal design standards for energy efficiency of residential buildings in hot summer/cold winter zones, *Energy and Buildings*, vol. 36, pp. 1309-1312

-
- [15] T. Catalina, J. Virgone, E. Blanco, 2008, Development and validation of regression models to predict monthly heating demand for residential buildings, *Energy and Buildings*, IN PRESS
- [16] A. Noren, J. Akander, 1999, The effect of thermal inertia on the energy requirement in a Swedish building: Results obtained with three calculation models, *International Journal of Low Energy and Sustainable Buildings*, vol. 1, pp. 1-16
- [17] The Brick Industry Association, 1997, Technical notes on brick constructions; Technical note 4-Heat transfer coefficients of brick masonry walls, Reston, US
- [18] J. Kosny, E. Kossecka, A. Desjarlais, J. Christian, 2001, Dynamic thermal performance and energy benefits of using massive walls in residential buildings, in roofs and walls, Oak Ridge National Laboratory and Institute of Fundamental Technological Research, Polish academy of Sciences
- [19] O. Kaynakli, 2008, A study on residential heating energy requirement and optimum insulation thickness, *Renewable energy*, vol. 33, pp. 1164-1172
- [20] J. Yu, C. Yang, L. Tian, 2008, Low-energy envelope design of residential building in hot summer and cold winter zone in China, *Energy and Building*, vol. 40, pp. 1536-1546
- [21] E. Mathews, C. Botha, D. Arndt, A. Malan, 2001, HVAC control strategies to enhance comfort and minimize energy usage, *Energy and Buildings*, vol. 33, pp. 853-863
- [22] M. Manning, M. Swinton, F. Szadkowski, J. Gusdorf, K. Ruest, 2007, The effects of thermostat setback and setup on seasonal energy consumption, surface temperatures and recovery times at the CCHT twin house research facility, *ASHRAE Transactions* 2007, pp. 630-641
- [23] D. Tanton, R. Cohen, S. Probert, 1987, Improving the effectiveness of a domestic central-heating boiler by the use of heat storage, *Applied energy*, vol. 27, pp. 53-82
- [24] L. Peeters, D. Haeseldonckx, W. D'haeseleer, 2006, Onderzoek Stirling-ketel combinatie voor WKK, Division of Applied Mechanics and Energy Conversion, TME/WDH/06-01/PLRK.

9 CONCLUSIONS AND SUGGESTIONS FOR FUTURE RESEARCH

Heat emission/absorption elements have not received the attention they deserve in recent research on energy savings in residential buildings. Therefore, in this dissertation a tool has been developed that allows optimising the characteristics of an emission/absorption element in a given context.

In the following, the general conclusions of the present dissertation are summarised. These are followed by some recommendations for future research in the area of heat emission/absorption in residential buildings.

9.1 Conclusions

When evaluating the thermal environment in a residential building, one should keep in mind the specific characteristics of such a setting. Comparing existing standards on thermal comfort with measurement data described in the literature, the standards showed to be rather conservative. The main reason is a range of adaptive options

available to the inhabitants of a residential dwelling which is not accounted for by the conventional standards.

The indoor comfort temperatures are strongly determined by and linked to the ambient temperature. Additionally, different comfort values need to be defined for each thermal zone in a dwelling due to a different clothing insulation and activity level in each of these zones. The range of acceptable indoor temperatures is further asymmetrically spread around the neutral or comfort temperature, as people are more sensitive to cold than to heat.

This thermal comfort should be satisfied by a potential heating/cooling installation. To evaluate potential installation components, the different aspects influencing the thermal state of a building, should be taken into account. Therefore, the thermal comfort requirements for a residential building have been implemented in an existing building energy simulation program, *ESP-r*. This program has been extended with an implicit plant modelling structure. This implicit level allows simulating the behaviour of the different components of a water-based heating/cooling installation based on energy flows only, by assuming isothermal single node installation components.

The main focus of the current dissertation is on the heat emission/absorption elements. Therefore, a widely used formula for calculation of heat output of most existing emitters has been improved so as to represent any heat emitter/absorber in the implicit level. This improved formula has been validated showing good agreement with both measurement data and analytical multiple node-models.

To determine the optimal set of characteristics of a heat emission/absorption element, *ESP-r* has been coupled with the optimisation tool *GenOpt*. The so-determined optima can be evaluated to show their sensitivity to a certain parameter or a combination of parameters. Through a range of case studies, it was concluded that the ideal water-based heat emitter/absorber strongly depends on the building, the temperature requirements and the climate. Through these case studies, the use of the optimisation framework has been shown. Results are in line with findings described in the literature, confirming the accuracy of the developed tool. In contrast to results presented in state of the art, the tool developed in the framework of this dissertation allows a complete exploration of the solution space.

9.2 Suggestions for future research

When it comes to modelling buildings, there is always something that can be improved or modelled in more detail. At the moment of finishing this dissertation, there is already a list of things answering the question ‘What next?’

The major inaccuracy was encountered when examining current convection coefficients for a range of emission/absorption elements. This emphasizes the need for more research in order to improve these correlations and estimate the effect of furniture, ventilation and indoor activity on the convective heat transfer.

Concerning the use of the results, once these convection coefficient correlations have been improved, it would be meaningful to select a range of ‘typical zones’, including their specific gain patterns. This allows determining optimal heat emission/absorption elements that will suit such typical zones. Once this kind of analysis is performed, the next step is to translate the optimal characteristics into a realistic configuration and determine its optimal location. For such translation into reality and optimisation of configuration and location, a computational fluid dynamics program should be used.

To improve the usefulness of the implicit plant level, a more user-friendly interface could be implemented. The option to model a plant implicitly should be listed in the main interface next to the option to model the plant explicitly. Furthermore, the implicit level could be extended with an option to select more accurate correlations for more precise emitter/absorber configurations, both for the convective heat transfer coefficient as well as for the correlation between average element’s temperature and surface temperature in case of TAB elements. Solar gains could also be incorporated in the element’s energy balance for such more precise configurations.

As the current dissertation has focussed on water-based heating and cooling, this could be extended to air-based systems as well. In that sense it would be suitable to evaluate techniques commonly applied in passive housing in Europe or more generally in the US.

NEDERLANDSTALIGE SAMENVATTING

Water-gebaseerde verwarming/koeling in
residentiële gebouwen

Naar optimale warmte emissie-/absorptie-elementen

Inleiding

Het verminderen van het energieverbruik in gebouwen is een veelvuldig besproken onderwerp. Verschillende onderzoekers [1], [2] stelden lijstjes op om aan te geven welke maatregelen eerst zouden genomen moeten worden wanneer men een woning energiezuiniger wil maken. Vele daarvan duiden het verbeteren van de bouwschil aan als eerste maatregel. Pas daarna komen aanpassingen aan de verwarmings- en koelinstallatie. Toch toont literatuuronderzoek aan dat de besparingen die door installatieverbeteringen kunnen worden behaald aanzienlijk kunnen zijn [3], [4], [5], [6]. Het meest voor de hand liggende onderdeel van een installatie is de component die instaat van de bereiding van het koude of warme water. Die component krijgt dan ook erg veel aandacht in de literatuur [3], [4] and [5]. Toch wordt ook wel eens beschreven wat de impact is van mogelijke verbeteringen aan bestaande afgifte-/absorptie-elementen [6], [7].

De efficiëntieverbeteringen die in dergelijke publicaties worden gemeld voor veranderingen aan de afgifte-/absorptiesystemen duiden het belang aan van een goed ontwerp en een correcte dimensionering. Toch werd tot op heden niet onderzocht wat de optimale karakteristieken zijn van een afgifte-/absorptiesysteem in gegeven omstandigheden. Het zoeken naar die optimale kenmerken is het onderwerp van voorliggend doctoraat.

Om die optimale karakteristieken te bepalen wordt in eerste instantie onderzocht wat dient gerealiseerd te worden door die elementen, ofwel het beoogde thermisch comfort. Voor kantoren en commerciële gebouwen bestaat daarover behoorlijk wat literatuur. Voor woongebouwen is er geen eensluidende onderbouwde richtlijn. Het opstellen daarvan is dus de eerste stap in de bepaling van de optimale installatie.

Eens is vastgelegd wat dient gerealiseerd te worden, is de volgende stap de bepaling van het afgifte-/absorptiesysteem. Dat afgifte-/absorptiesysteem moet zo goed mogelijk het opgelegde binnenklimaat kunnen realiseren op een energie-efficiënte manier.

De volgende stap in de installatie is het distributiesysteem. Zodra geweten is wat er aan de verschillende afgifte-/absorptiesystemen dient geleverd te worden, is het mogelijk te bepalen wat aan het distributiesysteem moet worden geleverd.

Wat aan het distributiesysteem moet worden geleverd is uiteindelijk wat geproduceerd dient te worden. De optimale karakteristieken van de component die instaat voor de bereiding van het koude of warme water kunnen bepaald worden voor die gegeven vraag.

Door die stapsgewijze aanpak kan een aangenaam binnenklimaat met een zo efficiënt mogelijke installatie worden bepaald. De nadruk ligt hierbij op de 'hardware'. Dat betekent niet dat de regeling, de 'software', minder belangrijk is. Een slechte regeling kan een goede installatie inefficiënt maken, een goede regeling kan met een slechte installatie echter geen goede rendementen halen.

Dit doctoraat tracht dan ook een methodiek op te stellen die toelaat de optimale installatie te bepalen voor een gegeven gebouw. Door gebruik te maken van wiskundige technieken, wordt de impact van de regeling geminimaliseerd.

Thermisch comfort

The meeste softwarepakketten voor gebouwensimulatie gebruiken vandaag de dag de conventionele criteria voor de beoordeling van het thermisch binnenklimaat. Die evaluatiecriteria werden ontwikkeld op basis van gegevens voor constante omgevingen [8] en werden gebruikt voor het opstellen van internationale normen [9], [10]. Nochtans toont een uitgebreid literatuuronderzoek [11], [12], [13], [14] en [15] aan dat dergelijke theorieën niet zonder meer toepasbaar zijn in woningen. De reden daarvoor is dat sommige aspecten niet te vatten zijn in zuivere energiebalansen of in wiskundige formuleringen. Deze aspecten worden vaak samengevat onder de noemer 'adaptatie'. Adaptatie heeft onder meer te maken met ervaringen, verwachtingen en aanpassingen op korte en op lange termijn.

Thermisch comfort in woningen blijkt sterk gerelateerd te zijn aan de buitentemperatuur. Daarom geven de correlaties die in dit werk werden opgezet een verband tussen binnen- en buitentemperatuur. Verder werd de woning verdeeld in 3

zones met een merkbaar verschillende vraag: de badkamer, de slaapkamer en de overige zones. Voor die eerste werd een evenwicht gezocht tussen het comfort voor een natte naakte persoon en dat voor een geklede persoon met beperkt activiteitsniveau. Voor de slaapkamers en overige zones werden meetdata van Belgische woningen gekoppeld met bevindingen beschreven in de literatuur. Naast met de buitentemperatuur variërende neutrale binnentemperaturen werden ook maximale en minimale binnentemperaturen gedefinieerd. Vooral voor slaapkamers zijn deze belangrijk: bij te koude binnentemperaturen zal het gevaar voor infecties aan luchtwegen toenemen, bij te hoge binnentemperaturen vermindert de slaapkwaliteit.

Naast neutrale temperaturen voor elk van die zones werd verder ook een band van temperaturen aangeduid die een zone met gelijkaardig comfort aangeeft. Die band werd hier asymmetrisch verdeeld rond de neutrale temperatuur. De reden daarvoor is dat mensen gevoeliger zijn voor koude dan voor warmte.

Het dient echter benadrukt dat momenteel erg weinig gegevens beschikbaar zijn over thermisch comfort of thermisch neutrale condities in woningen. Het zou dus kunnen dat de hier voorgestelde correlaties ietwat conservatief zijn. Wanneer in de toekomst meer data beschikbaar zouden zijn, kunnen de correlaties aangepast worden.

Modellering van energiesystemen in gebouwen

Om te evalueren of nieuwe ontwikkelingen nodig zijn voor de verwarming/koeling van woongebouwen werd de code *ESP-r* [16] voor gebouwensimulatie uitgebreid met een vrij abstracte structuur. De hierboven besproken correlaties voor binnentemperaturen werden in deze structuur ingebed.

ESP-r is een onderzoeksgerichte simulatiecode. Het is gebaseerd op energiebalansen van controlevolumes. Op die basis worden fysieke grootheden berekend voor thermische zones, gebouwstructuur en installatiecomponenten. Het is daarom een bijna perfecte basis voor de modellering van abstracte, theoretisch en zelfs niet bestaande systemen.

Daarom werd in deze code, naast de reeds bestaande expliciete structuur voor de simulatie van installaties, ook een impliciete structuur geïmplementeerd. Het grote voordeel van die aanpak is de mogelijkheid om fictieve componenten te simuleren op basis van energiestromen en gemiddelde temperaturen alleen: dit wil zeggen zonder het vastleggen van exacte aanvoer- en retourtemperaturen en bijhorend debiet. Dat laat toe de nadruk te leggen op de componenten zelf, zonder het resultaat te laten domineren door de gekozen controle. De aanpak heeft echter ook een aantal nadelen. Zo kan geen gedetailleerde temperatuursverdeling van het afgifte-/absorptiesysteem worden gemodelleerd. In dynamische omstandigheden zou dat verschillen kunnen geven voor ongelijkmatig opwarmende elementen. Ook verhindert een niet-gedetailleerde modellering van de temperaturen het correct begroten van de extra warmtewinst door condensatie.

Elementen voor warmte afgifte/absorptie

De afgifte of absorptie van warmte door eender welk afgifte-/absorptie-element gebeurt door straling en convectie. Om een generisch 1-puntsmodel op te stellen voor de modellering van een configuratie- en locatieonafhankelijk element voor warmte-afgifte-/absorptie werd van een veelvuldig gebruikte empirische correlatie uitgegaan. Er werd aangetoond dat die formule inderdaad kan worden gebruikt voor elementen met een voornamelijk convectieve afgifte/absorptie, zoals conventionele radiatoren en convectoren. Aangetoond werd dat door het gebruik van deze formule de hoeveelheid straling wordt overschat. Dat is te wijten aan het gebruik van een gelineariseerde warmte-overdrachtscoëfficiënt voor straling gedefinieerd bij relatief hoge nominale temperaturen.

De formule werd gecorrigeerd om die overschatting te vermijden. Door gebruik te maken van de in dit werk voorgestelde gecorrigeerde formule wordt de gelineariseerde stralingscoëfficiënt voor nieuwe situatie herberekend.

Verder werd een duidelijke discrepantie ondervonden tussen verschillende bestaande correlaties voor convectieve warmteoverdracht van horizontale thermisch actieve bouwdelen naar de zone [17], [18]. Deze discrepantie was vooral erg groot wanneer dergelijke warmteoverdracht ook gepaard gaat met stratificatie. Er werd benadrukt dat dergelijke correlaties verder ook geen rekening houden met reële

omstandigheden in woningen. Daarom werd voor de dergelijke overdracht met stratificatie het gebruik van constante, vereenvoudigde convectiecoëfficiënten voorgesteld.

Het is dan deze gecorrigeerde generische formule die werd geïmplementeerd in de impliciete structuur in *ESP-r*.

Modelverificatie

Verschillende deelaspecten van het model voor elementen van afgifte en absorptie van warmte werden nagekeken. Wat betreft de coëfficiënten voor warmte overdracht door straling en door convectie werd aangetoond dat de gemiddelde fout tussen de aannames van de gecorrigeerde formule en de meer exacte theoretische berekeningen beperkt was tot maximum 1.63%.

Verder werd de aanname van een oppervlakte-gewogen gemiddelde stralingstemperatuur onderzocht. Wat de stralingstemperatuur betreft zoals het afgifte-/absorptie-element deze ervaart, bleken de afwijkingen beperkt, behalve voor het geval een radiator in een kamer geplaatst werd waar de vloer een temperatuur heeft die meer dan 5K afwijkt van de temperatuur van de wanden en het plafond. Er dient echter benadrukt dat een dergelijke afwijking weinig realistisch is. De stralingstemperatuur zoals die door een gebruiker van de zone wordt ervaren bleek sterk af te wijken wanneer de oppervlaktetemperaturen van thermisch actieve bouwdeelen niet in rekening werd gebracht. Omdat in de 1-knoopsmodellering deze oppervlaktetemperaturen niet beschikbaar zijn, werd verder nagegaan hoe groot de afwijking is tussen de gemiddelde temperatuur van het actieve bouwdeel en zijn oppervlaktetemperatuur. Voor elementen met een grote dikte bleek die aanname sterk af te wijken. Echter, in het geval van thermische actieve vloeren reageerde ze als een correctie op de afwijking door het gebruik van een oppervlakte-gewogen temperatuur. In het geval van actieve plafonds en muren werd benadrukt dat de fout onaanvaardbaar groot werd bij elementen met een grote warmtecapaciteit. Daarom werd voor dergelijke elementen het gebruik van de formule enkel voorgesteld bij beperkte warmtecapaciteit.

Het generieke model vertoonde verder goede overeenkomsten met meer gedetailleerde modellen en meetdata [19] en [20]. Zowel voor de berekening van het thermisch vermogen in niet-variërende omstandigheden, als voor dynamische situaties.

Productie van warm en koud water

Ook voor dit onderdeel van de gehele verwarmings- en koelinstallatie in een woning werd een generisch model opgesteld. Het is een vrij ruw model, waarbij vooral de nadruk ligt op de simulatie van de effecten van mogelijke beperkingen door niet-ideale productiesystemen. De efficiëntieberekeningen zijn derhalve ook enkel bedoeld om een eerste idee te geven, meer dan de basis te willen vormen voor een gedetailleerde vergelijking.

Controlestrategieën voor de afgifte/absorptie van warmte en de productie van warm of koud water

De belangrijkste controlestrategie voor de afgifte/absorptie van warmte is gebaseerd op een verband tussen de gewenste binnentemperatuur, de huidige toestand van het gebouw en de benodigde energie. Dat verband is lineair, de coëfficiënten ervan worden in *ESP-r* bepaald door matrixreductie en hebben geen fysische betekenis. Naast deze abstracte, irreële controlestrategie werden ook bestaande controlestrategieën geïmplementeerd.

Ook voor de productie-elementen werden verscheidene controlestrategieën uitgewerkt. Die laten toe zowel geïdealiseerde structuren als bestaande strategieën te modelleren.

Optimale elementen voor afgifte/absorptie van warmte.

De optimale elementen worden bepaald door *ESP-r* met de impliciete modelstructuur te koppelen met een externe optimalisatiecode. Deze code, *GenOpt* [21] werd speciaal ontworpen voor koppeling met codes voor simulatie van gebouwen. De objectieffuncties daarbij kennen vaak een ongelijkmatig verloop en zijn geregeld discontinu. Voor het voorliggend optimalisatieprobleem werd uit de databank van algoritmes beschikbaar in *GenOpt* geselecteerd voor een combinatie van Particle Swarm algoritme en Generalised Pattern Search algoritme. De eerste techniek laat toe een ruw beeld te vormen van de waarden van de objectieffunctie in de n-dimensionele parameter ruimte en het minimum benaderend te lokaliseren. De tweede techniek zoekt dan verder in deze afgebakende ruimte. Deze techniek berekent de gradiënt van de objectieffunctie in de afgebakende ruimte en gaat zo op zoek naar de exacte lokatie van het minimum. Door het onvoorspelbare en soms discontinuë karakter van het optimalisatieprobleem kan niet worden gegarandeerd dat het gevonden minimum ook het globale minimum is. Om de kans te verkleinen dat geëindigd wordt in een lokaal minimum werd in de voorbeelden die hierna worden besproken telkens hetzelfde optimalisatieprobleem gestart vanuit verschillende initiële parametercombinaties in de n-dimensionele ruimte.

De objectieffunctie maakt een afweging tussen het energieverbruik, het momentane thermisch comfort en het transiënte thermisch comfort. Door het opstellen van een Pareto-front kon een weloverwogen keuze worden gemaakt voor het gewicht van elk van de termen in de objectieffunctie. Naast de aan energieverbruik en thermisch comfort gerelateerde termen werden in de objectieffunctie eveneens beperkingen ingevoerd om te vermijden dat de optimalisatie convergeerde naar fysisch onmogelijke parametercombinaties.

Voorbeelden

Verskillende variaties van een eenvoudig 3-zone model werden bekeken. Het emissie/absorptie -element werd geoptimaliseerd voor variaties in buitencondities,

variaties in gebouwschil en temperatuurstellingen en er werd gekeken naar de invloed van beperkingen van een mogelijk productiesysteem. De voorbeelden toonden duidelijk het belang aan van een analyse van de optima op basis van de eigenwaarden-eigenvectoren ontbinding van de 2^{de} graads benadering van de objectieffunctie in de buurt van het optimum.

De voorbeelden bevestigen verder dat de optimale parameterwaarden, alsook de sensitiviteit van het optimum voor variaties in de parameters, context-afhankelijk zijn. Het is dus van belang te duiden op de specifieke gewichten van de verschillende termen in de objectieffunctie en de gekozen instellingen van de controle.

Voor de beschreven instellingen van de optimalisatietool toonden de voorbeelden enkele effecten die meermaals voorkwamen. Zo is er een voorkeur voor een iets lagere warmtecapaciteit en een hoger nominal vermogen bij sterk fluctuerende buitentemperaturen. In het geval van een daling van de koellast kan in massiefbouw ook het nominale vermogen worden gereduceerd. Voor een meer constante instelling van de binnentemperatuur werd het vermoeden van een lager optimaal vermogen en een hogere warmtecapaciteit bevestigd. Het gewicht van het transient thermisch comfort in de objectieffunctie resulteerde in de selectie van elementen met een hoge capaciteit met bij voorkeur een beperkte convectieve afgifte.

Conclusie en suggesties voor verder onderzoek

Het is belangrijk de specifieke karakteristieken van woningen in het oog te houden wanneer men er het thermisch comfort van bekijkt. Wanneer bestaande normen worden vergeleken met meetdata van temperaturen in woningen, dan blijken de normen meestal vrij conservatief te zijn. De belangrijkste redenen daarvoor blijken verschillende vormen van adaptatie te zijn.

Daarom werden in het kader van voorliggend doctoraat correlaties opgesteld die neutrale binnentemperaturen geven als functie van de buitentemperatuur en dit voor de verschillende zones in een woning.

Dit thermisch comfort dient te worden behaald door een verwarmings-/koelinstallatie. Om de nadruk te leggen op de componenten van de installatie en de invloed van de controle zoveel mogelijk te beperken, werd een impliciete modelleringsstructuur geïmplementeerd in een bestaande code voor gebouwensimulatie. Deze aanpak maakt gebruik van energiestromen en gemiddelde temperaturen.

De nadruk in voorliggend werk ligt op de elementen voor afgifte en/of absorptie van warmte. Daarom werd een bestaande correlatie onderzocht en verbeterd. De verificatie van het model dat gebaseerd is op die formule toonde goede resultaten voor alle elementen, behalve voor thermisch actieve plafonds en muren met grote warmtecapaciteiten.

Om voor deze elementen de optimale karakteristieken te bepalen, werd *ESP-r* met de impliciete structuur gekoppeld aan de optimalisatiecode *GenOpt*. Een studie van de eigenwaarden en eigenvectoren van de parametercombinaties in de buurt van de optima levert dan informatie over de gevoeligheid van het optimum voor veranderingen van de parameterwaarden.

Deze methodiek werd toegepast op een aantal voorbeelden. De resultaten bleken in de lijn te liggen van wat in de literatuur wordt beschreven. In tegenstelling tot die referenties laat de huidige methodiek echter een volledige exploratie van de n -dimensionele parameterruimte toe.

Toch werd in de loop van het onderzoek duidelijk dat er nog een aantal aspecten zijn die verduidelijkt moeten worden vooraleer generische resultaten toelaten algemene tendensen voor ontwikkeling aan te geven. Het belangrijkste aspect heeft te maken met de convectieve warmte-overdracht van de elementen.

Referenties

- [1] C Balaras, A. Gaglia, E. Georgopoulou, S. Mirasgedis, Y. Sarafidis, D. Lalas, 2007, European residential buildings and empirical assessment of the Hellenic building stock, energy consumption, emissions and potential savings, *Building and environment*, vol. 42, pp. 1298-1314
- [2] G. Verbeeck, H. Hens, 2005, Energy savings in retrofitted dwellings: economically viable?, *Energy and Buildings*, vol. 37, pp. 747-754
- [3] O. Zogou, A. Stamatelos, 1998, Effect of climatic conditions on the design optimization of heat pumps for space heating and cooling, *Energy Conservation and Management*, vol. 39, pp. 609-622
- [4] O. Ozgener, A. Hepbasli, 2007, Modelling and performance evaluation of ground source (geothermal) heat pump systems, *Energy and Buildings*, vol. 39, pp. 66-75
- [5] V. Kuhn, J. Klemes, I. Bulatov, 2008, MicroCHO: Overview of selected Technologies, products and field test results, *Applied Thermal Engineering*, vol. 28, pp. 2039-2048
- [6] S. Beck, S. Grinsted, S. Blakey, K. Worden, 2004, A novel design for panel radiators, *Applied Thermal Engineering*, vol. 24, pp. 1291-1300
- [7] Y. Chen, A. Athienitis, 1995, A three-dimensional numerical investigation of the effect of cover materials on heat transfer in floor heating systems, *ASHRAE Transactions* 1995, part 2, pp. 1350-1355
- [8] P. Fanger, 1970, *Thermal Comfort: Analysis and applications in environmental engineering*, McGraw-Hill Book Company, United States, ISBN 0-07-019915-9
- [9] ASHRAE, 2004, *ANSI/ASHRAE 55: Thermal Environmental Conditions for Human Occupancy*, American Society of Heating, Refrigerating and Air-conditioning Engineers, Inc. Atlanta, USA
- [10] ISO, 2005, *ISO 7730: Ergonomics of the thermal environment – Analytical determination and interpretation of thermal comfort using PMV and PPD indices and local thermal comfort criteria*, International Organisation for standardization, Switzerland
- [11] B. Jones, 2000, *Capabilities and limitations of thermal models*, Smart Controls and Thermal Comfort Project, Final Report (Confidential), Oxford Brookes University
- [12] M. Humphreys, J. Nicol, 2002, The validity of ISO-PMV for predicting comfort votes for everyday thermal environments, *Energy and Buildings*, vol. 34, pp. 667-684
- [13] M. Jokl, K. Kabele, 2007, The substitution of comfort PMV values by a new experimental operative temperature, *Electronic proceedings of Clima 2007, WellBeing Indoors*, Helsinki, Finland
- [14] G. Brager, R. De Dear, 1998, Thermal adaptation in the built environment: a literature overview, *Energy and Buildings*, vol. 27, pp. 83-96

-
- [15] D. Fiala, K. Lomas, 2001, The dynamic effect of adaptive human responses in the sensation of thermal comfort, Moving thermal Comfort standards into the 21st century, Windsor, UK, Conference Proceedings, pp. 147-157
- [16] J. Clarke, 2001, Energy Simulation in Building Design, Butterworth Heinemann, Oxford, ISBN 0-7506 -082
- [17] T. Min, L. Schutrum, G. Parmelee, J.Vouris, 1956, Natural convection and radiation in a panel-heated room, Heat Piping and Air Conditioning, May, pp. 153-160
- [18] H. Awbi, A. Hatton, 1999, Natural convection from heated room surfaces, Energy and Buildings, vol. 30, pp. 233-244
- [19] J. Van der Veken, E. Maes, 2008, Verbeteren van de energie-efficiëntie van verwarmings-, koel- en ventilatieproducten d. m. v. gevalideerde dynamische modellen, IWT-project van de afdeling Bouwfysica van de K.U.Leuven en JAGA, België
- [20] P. Ham, 1998, Dynamische warmtegedrag van radiatoren en convectoren; Metingen en modelvorming, Verwarming en Ventilatie, vol. 5, pp. 318-334
- [21] M. Wetter, 2008, GenOpt; Generic Optimisation Program, User Manual Version 2.1.0, Ernest Orlando Lawrence Berkeley National Laboratory, University of California, US

Appendices

APPENDIX A EXPRESSIONS FOR MIXED CONVECTION AND FOR SURFACE TEMPERATURES OF TAB ELEMENTS

A.1 Mixed convection

As stated in chapter 3, the overall surface averaged convection coefficient for mixed convection, \bar{h}_c^k (W/m²K), is given by:

$$\bar{h}_c^k = \bar{h}_{c,n}^k + \bar{h}_{c,f}^k \quad (A. 1)$$

where $\bar{h}_{c,n}$ (W/m²K) is the surface averaged convection coefficient for natural convection and $\bar{h}_{c,f}$ (W/m²K) is the surface averaged convection coefficient for forced convection.

As $\bar{h}_{c,n}$ can be written as a function of the temperature difference between emission/absorption element and zone, the above given equation can be rewritten as:

$$\bar{h}_c^k = (a\Delta T^b)^k + \bar{h}_{c,f}^k \quad (A. 2)$$

where a (-) and b (-) are the coefficients as summarized in Table 3-1.

Taking into account the surface area for convection A_c (m²) the results in:

$$A_c^k \bar{h}_c^k = (aA_c \Delta T^b)^k + A_c^k \bar{h}_{c,f}^k \quad (A. 3)$$

This is further generalized by introducing the coefficients C_2 (W/K^{b+1}) and C_3 (W/K):

$$A_c^k \bar{h}_c^k = (C_2 \Delta T^b)^k + C_3^k \quad (A. 4)$$

Similarly, for radiation a coefficient C_1 (W/K) is introduced:

$$A_r \bar{h}_r = C_1 \quad (A. 5)$$

The general equation for the heat emission/absorption in nominal conditions, Q_N (W), is given by:

$$Q_N = A_r \bar{h}_r \Delta T_N + \left(A_c^k \bar{h}_{c,n}^k \Delta T_N^{bk} + A_c^k \bar{h}_{c,r}^k \right)^{1/k} \Delta T_N \quad (A. 6)$$

Combining with Eqs. (A. 4) and (A. 5) results in:

$$Q_N = C_1 \Delta T_N + \left(C_2^k \Delta T_N^{bk} + C_3^k \right)^{1/k} \Delta T_N \quad (A. 7)$$

As $\alpha_N (-)$ indicates the fraction of convection, the fraction of radiation is given by:

$$(1 - \alpha_N) Q_N = C_1 \Delta T_N \quad (A. 8)$$

Rewriting as an expression for C_1 :

$$C_1 = \frac{(1 - \alpha_N) Q_N}{\Delta T_N} \quad (A. 9)$$

The fraction of forced convection to overall convection, $\gamma_N (-)$, can, for the nominal case, be given by the following expression:

$$\gamma_N = \frac{C_3 \Delta T_N}{\alpha_N Q_N} \quad (A. 10)$$

Rewriting as an expression for C_3 :

$$C_3 = \frac{\alpha_N Q_N \gamma_N}{\Delta T_N} \quad (A. 11)$$

The amount of convection in the nominal case is given by:

$$\alpha_N Q_N = \left(C_2^k \Delta T_N^{bk} + C_3^k \right)^{1/k} \Delta T_N \quad (A. 12)$$

Combined with Eq. (A. 11) this results in an expression for C_2 :

$$C_2^k \Delta T_N^{bk} = \left(\frac{\alpha_N Q_N}{\Delta T_N} \right)^k (1 - \gamma_N^k) \quad (A. 13)$$

As for the non-mixed convection case, it is now also assumed that in the neighbourhood of the nominal conditions the derivative of the well established formula for the thermal output of a radiator/convector equals the derivative of the theoretically set-up right hand side of Eq. (A. 7):

$$\frac{nQ_N}{\Delta T_N} = C_1 + \Delta T_N \frac{1}{k} \left(C_2^k \Delta T_N^{bk} + C_3^k \right)^{\left(\frac{1}{k}\right)-1} \left(bk C_2^k \Delta T_N^{bk-1} \right) + \left(C_2^k \Delta T_N^{bk} + C_3^k \right)^{\frac{1}{k}} \quad (A. 14)$$

Replacing the constants C_1 , C_2 and C_3 by the above given expressions (Eqs. (A. 9), (A. 13) and (A. 11) respectively) results in:

$$\begin{aligned} \frac{nQ_N}{\Delta T_N} = \frac{Q_N}{\Delta T_N} (1 - \alpha_N) + & \left(\left(\frac{\alpha_N Q_N}{\Delta T_N} \right)^k (1 - \gamma_N^k) + \left(\frac{\alpha_N Q_N \gamma_N}{\Delta T_N} \right)^k \right)^{\left(\frac{1}{k}\right)-1} \\ & \left(\left(\frac{\alpha_N Q_N}{\Delta T_N} \right)^k (1 - \gamma_N^k) (1 + b) + \left(\frac{\alpha_N Q_N \gamma_N}{\Delta T_N} \right)^k \right) \end{aligned} \quad (A. 15)$$

This can be solved to find an expression that links the radiator exponent n , the fraction of convection α_N , the power coefficient b , the fraction of forced convection γ_N and the coefficient k .

$$n - 1 = \alpha_N b (1 - \gamma_N^k) \quad (A. 16)$$

A.2 Surface temperatures for TAB elements

A.2.1 Steady state conditions

The transient analysis is based on the simple 4-node resistance model as presented in chapter 4.

In a transient situation the injected flux q_{in} (W/m^2), either positive or negative, equals the emitted/absorbed flux q_{out} (W/m^2). The flux is therefore further referred to as q (W/m^2):

$$q_{in} = q_{out} = q \quad (A.17)$$

This thermal flux is also passed from water node with average temperature \bar{T}_{water} (K) to surface node of the main material composing the TAB element T_{cs} (K):

$$q = \frac{1}{\left(R_0 + \frac{d_1}{\lambda_1} + \frac{d_2}{\lambda_2} \right)} \left(\bar{T}_{water} - T_{surface} \right) \quad (A.18)$$

where R_0 (W/m^2K) is the resistance related to the convective heat transfer from water to plastic, d_1 (m) is the equivalent thickness of the tube casing layer, i.e. the volume of this material per square meter of TAB element surface, equally divided over $1 m^2$ of TAB element. d_2 (m) is the equivalent thickness of the material of the main layer. λ_1 (W/mK) and λ_2 (W/mK) the thermal conductivity of the tube casing and main layer respectively. The above given equation can be rewritten as:

$$\bar{T}_{water} = \left(R_0 + \frac{d_1}{\lambda_1} + \frac{d_2}{\lambda_2} \right) q + T_{surface} \quad (A.19)$$

In a steady state case, assuming the thickness of the tube casing layer to be negligible, the average temperature of the TAB element, T_{emit} (K), can be written as:

$$\frac{\bar{T}_{water} + T_{surface}}{2} = T_{emit} \quad (A.20)$$

Combining Eqs. (A.19) and (A.20) results in:

$$T_{emit} = T_{surface} + \frac{1}{2} \left(R_0 + \frac{d_1}{\lambda_1} + \frac{d_2}{\lambda_2} \right) q \quad (A.21)$$

Assuming the capacity of the water and tube casing layer to be negligible, the thickness d_2 can be approximated by:

$$d_2 = \frac{C}{A\rho_2c_2} \quad (A.22)$$

where C (J/K) is the total capacity of the TAB element, A (m^2) is the surface area of the TAB element. ρ_2 (kg/m^3) is the density of the main composing material and c_2 is the heat capacity of that material.

Combining Eqs. (A.21) and (A.22) and assuming the resistance of the water node and tube casing layer to be negligible compared to the resistance of the concrete layer, this results in:

$$T_{emit} = T_{surface} + \frac{1}{2} \frac{C}{A\rho_2c_2\lambda_2} q \quad (A.23)$$

Further refinements of this formula can be made when the details on pipe diameters, material used and average distance between pipes are known.

A.2.2 Dynamic conditions

The simple 4-nodes resistance model is no longer valid due to the effect of the storage of heat in the layers composing the TAB element. The governing equations for this situation are given below.

For the water:

$$q_{in} - \frac{1}{\left(R_0 + \frac{\lambda_1}{d_1}\right)} \left(\bar{T}_{water} - T_1\right) = C_{water} \frac{\partial \bar{T}_{water}}{\partial t} \quad (A.24)$$

For the tube casing layer:

$$\frac{\lambda_1}{d_1} \left(\bar{T}_{water} - T_1\right) - \frac{\lambda_2}{d_2} (T_1 - T_2) = C_2 \frac{\partial \left(\frac{\bar{T}_{water} - T_1}{2}\right)}{\partial t} \quad (A.25)$$

For the main layer:

$$\begin{aligned} \frac{\lambda_2}{d_2} (T_1 - T_2) - Q_{emit,N} \left(\frac{T_2 - (\alpha_N T_a + (1 - \alpha_N) MRT)}{T_{2,N} - (\alpha_N T_{a,N} + (1 - \alpha_N) MRT_N)} \right) \\ \left[\left(\frac{|T_2 - (\alpha_N T_a + (1 - \alpha_N) MRT)|}{T_{2,N} - (\alpha_N T_{a,N} + (1 - \alpha_N) MRT_N)} \right)^{n-1} \right] \\ - (1 - \alpha_N) \left[1 - \left(\frac{T_2 + MRT}{T_{2,N} + MRT_N} \right)^3 \right] = C_2 \frac{\partial \left(\frac{T_2 - T_1}{2}\right)}{\partial t} \end{aligned} \quad (A.26)$$

where it should be emphasized that T_1 and T_2 indicate the upper surface layers of the tube casing and main layers respectively.

APPENDIX B CODING

B.1 Relevant routines: state at project commencement

The main simulation controller is called *MZNUMA*. Within this controller, a series of routines is looped through for each zone in order to define amongst others plant-zone interactions. One of the main routines within this series is called *MTXCTL*. The subroutine coordinating the actions for the mixed air/mean radiant controller is called *MZMRX4*, located in *esrubld/matsv.F*. This subroutine reduces the zonal matrices to define the coefficients of the linear relationship between desired temperature and required heating load. The call to the different plant controls is coordinated from this routine (Figure B.1).

At project commencement, the sequence of calls was as summarised in Figure B.2.

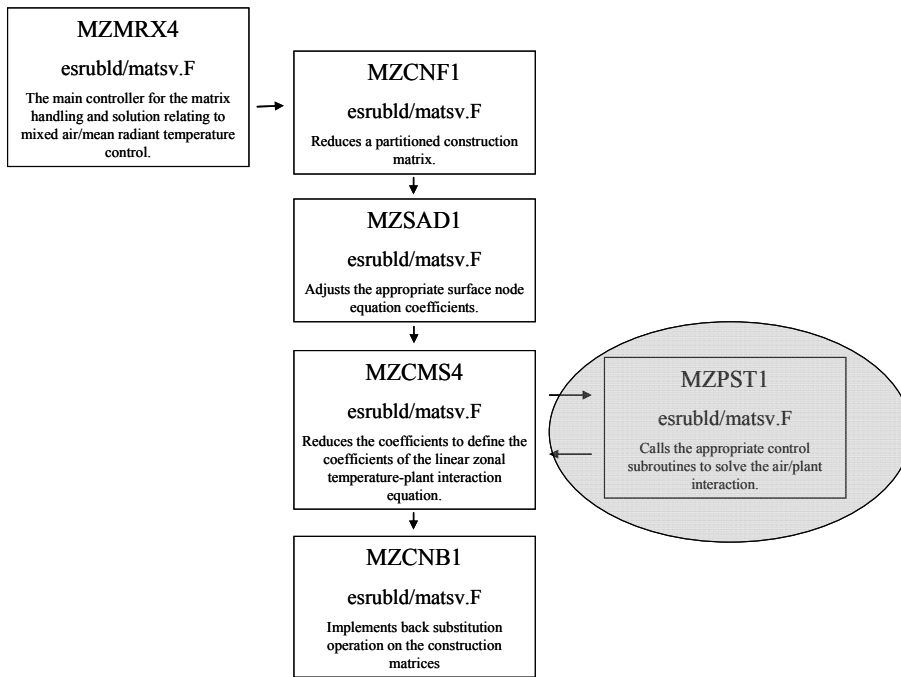


Figure B.1: General overview of the sequence of processing zonal-plant interactions. The series of routines shown is looped through for each zone. The routine in the grey oval is the one that is affected by the implicit plant modelling approach.

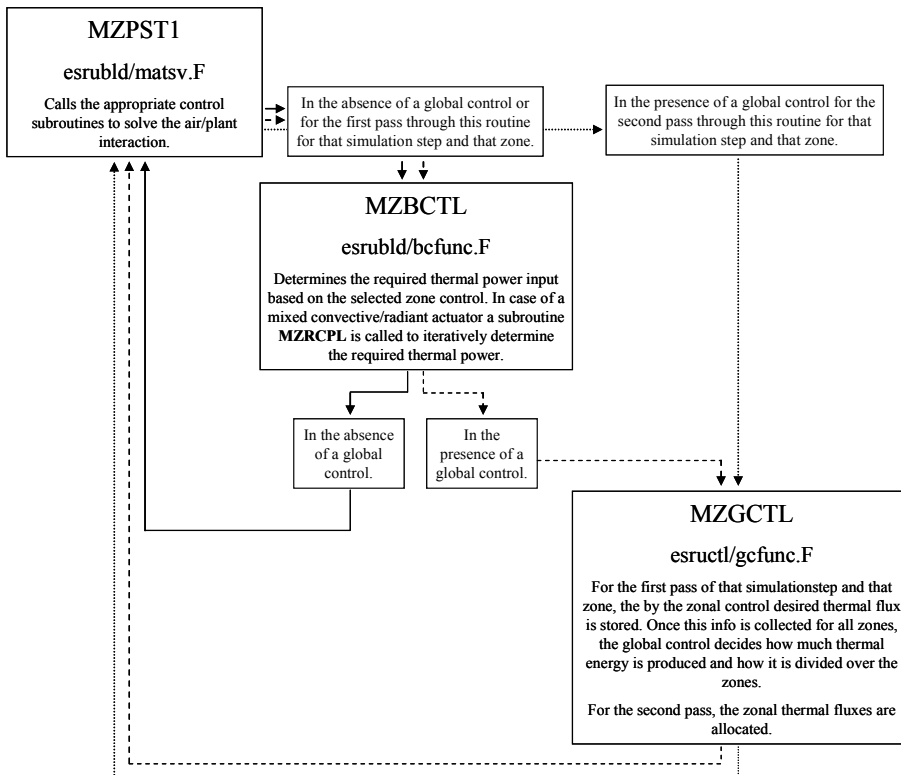


Figure B.2: Overview of the sequence of gathering data on thermal power fluxes in case of zonal and/or global controls. The solid line indicates the sequence of calculations in the absence of a global level, the dashed line is for the first pass in the presence of a global level, the dotted line for the second pass.

B.2 Changes to the software structure for the implementation of the implicit plant level

As explained in chapter 2, the implicit plant modelling structure is embedded within the above shown structure. However, it holds the emission/absorption elements and the production device as well as the corresponding controls. In order to correctly account for the transient effects of these implicit plant components, the above shown structure has been adapted (Figure B.3)

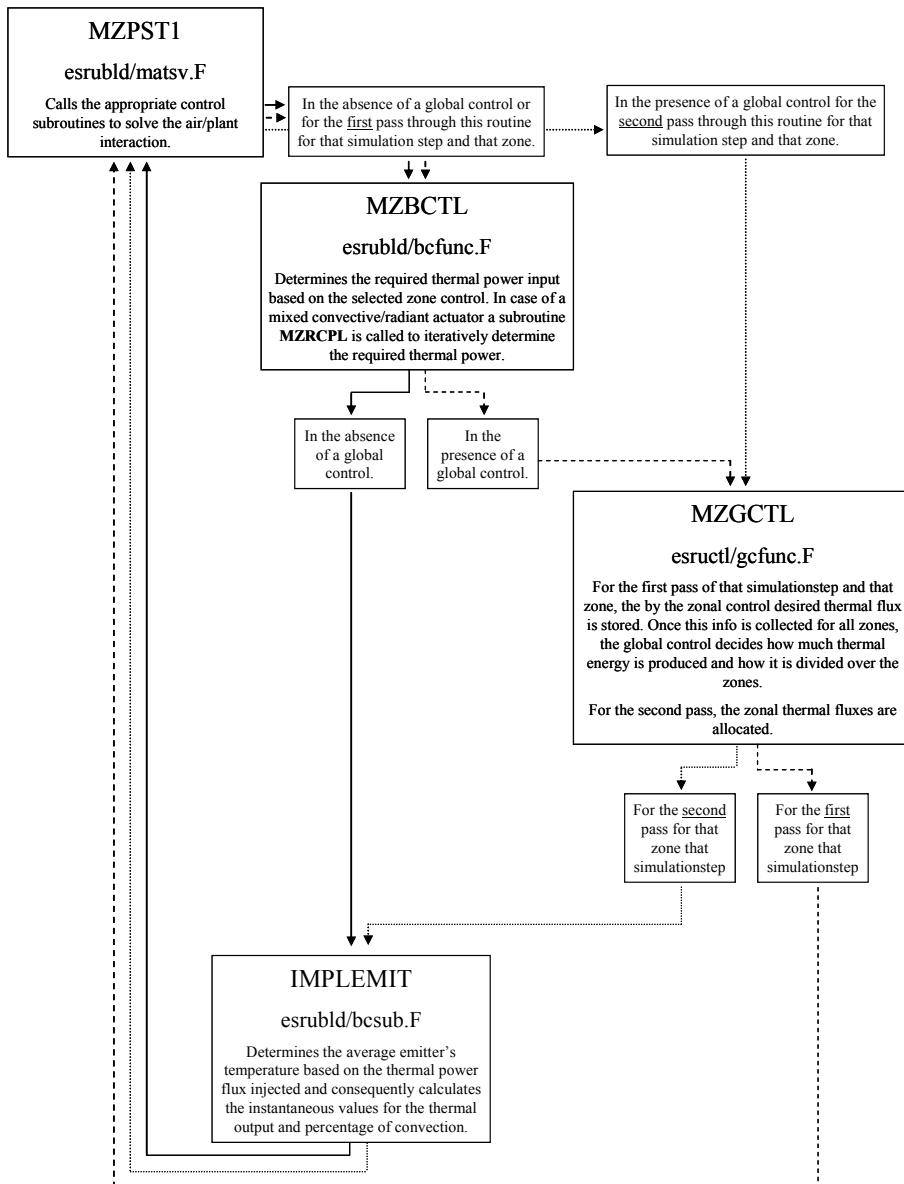


Figure B.3: Overview of the sequence of gathering data on thermal fluxes in case of the implicit plant model. The solid line indicates the sequence of calculations in the absence of a global level, the dashed line is for the first pass in the presence of a global level, the dotted line for the second pass.

The *MZBCTL*-routine was extended to hold the main structure of the implicit emission/absorption element. For the different subroutines related to the indoor temperature, amongst others the calculation of comfort temperature and the check for set-backs, a separate file was created. This file, called *bcsub.F*, stored in *esrubld*, also holds the subroutine for the calculation of the emission/absorption element itself. The controls related to this element are stored in another newly added file, i.e. *esrubld/implcont.F*. The changes to the *matsv.F* file were limited to adaptations to calculation sequences and calls to newly added subroutines.

The file holding the global structure was strongly affected. After resolving some problems with the already existing subroutines, the global control *gc104* was added. This global control is the production device representing control. It is combined with several subroutines for calculation of dynamical effects and efficiency calculations. The structure also holds the subroutine for the distribution system.

The interface adaptations and the data for the ‘*help*’ and ‘*info*’ are, as for the other zonal and global controls, located in the *esruprj/bpfcontrl.F* and *esrucom/econtrol.F* file.

In the above given scheme, only the major information flows are shown. Calls such as for the calculation of the building timeconstant for start-up calculations are not indicated.

In total some 4500 lines were required to extend *ESP-r* with the implicit plant level.

APPENDIX C EFFICIENCY CALCULATIONS FOR THE IMPLICIT PRODUCTION DEVICE

C.1 Input parameters

The currently implemented efficiency characterisation methods for the production device are listed in Table C.1, showing the additionally required parameters as well.

Efficiency characterisation	Additional parameters	Symbol
Ideal	-	-
Linear relation with ambient temperature	Performance ¹ for -7°C (-)	P_{-7}
	Performance for 2°C (-)	P_2
	Performance for 10°C (-)	P_{10}
Linear relation with part load ratio (PLR)	Efficiency for 10% PLR (%)	$\eta_{10\text{PLR}}$
	Efficiency for 30% PLR (%)	$\eta_{30\text{PLR}}$
	Efficiency for 100% PLR (%)	$\eta_{100\text{PLR}}$
CHP	Fuel utilisation ratio for 10% PLR (%)	$\text{FUR}_{10\text{PLR}}$
	Fuel utilisation ratio for 30% PLR (%)	$\text{FUR}_{30\text{PLR}}$
	Fuel utilisation ratio for 100% PLR (%)	$\text{FUR}_{100\text{PLR}}$
	Minimal electrical output (W)	E_{min}
	Maximal electrical output (W)	E_{max}

Table C.1: Input parameters related to efficiency calculations for generic production model.

C.1.1 Efficiency of an ideal production device

The efficiency of an ideal device is 100%. In that case the produced thermal power equals the primary power input.

¹ When modelling heat pumps, the *performance* can be related to either the COP, or the SPF, depending on the modeller's preferences.

C.1.2 Efficiency related to ambient temperature

The implemented performance curve of the heat pumps is a combination of two linear functions; one for low outdoor temperatures and one for average to high outdoor temperatures. This is as given by Eq. (C.1) where P is the performance (-) at a given ambient temperature T_{amb} (K). Equation (C.2) can then be applied to calculate the primary energy PE (J) based on the simulation timestep Δt (s).

$$\begin{cases} P = P_{-7} + \frac{P_2 - P_{-7}}{9}(T_{amb} + 266) & \text{for } T_{amb} \leq 275K \\ P = P_2 + \frac{P_{10} - P_2}{8}(T_{amb} - 275) & \text{for } T_{amb} > 275K \end{cases} \quad (C.1)$$

$$PE = \frac{Q_{prod}}{P} \cdot \Delta t \quad (C.2)$$

C.1.3 Efficiency related to part load ratio

A linear interpolation based on the user-defined PLR-efficiencies can be applied to determine the efficiency η (%) at any part load ratio (Eq. (C.3)). Equation (C.4) can then be used to calculate the primary energy consumption.

$$\begin{cases} \eta = \eta_{10PLR} + \frac{\eta_{30PLR} - \eta_{10PLR}}{20}(PLR - 10) & \text{for } PLR \leq 30\% \\ \eta = \eta_{30PLR} + \frac{\eta_{100PLR} - \eta_{30PLR}}{70}(PLR - 30) & \text{for } PLR > 30\% \end{cases} \quad (C.3)$$

$$PE = \frac{Q_{prod}}{\eta} 100\Delta t \quad (C.4)$$

C.1.4 Efficiency calculation for CHP devices

The efficiency of a CHP is defined by the fuel utilisation ratio FUR (-), which can be calculated through interpolation as given by Eq. (C.5) below. In case of a non-modulating device, the FUR is a constant.

$$\begin{cases} FUR = FUR_{10PLR} + \frac{FUR_{30PLR} - FUR_{10PLR}}{20} \cdot (PLR - 10) & \text{for } PLR \leq 30\% \\ FUR = FUR_{30PLR} + \frac{FUR_{100PLR} - FUR_{30PLR}}{70} \cdot (PLR - 30) & \text{for } PLR > 30\% \end{cases} \quad (C.5)$$

The FUR incorporates both the thermal and the electrical output of the CHP-device. Equation (C.6) can thus be used to calculate the primary energy based on the calculated electrical and thermal output.

$$PE = \left(\frac{Q_{prod} + E}{FUR} \right) \Delta t \quad (C.6)$$

APPENDIX D NON-IDEAL IMPLICIT EMISSION/ABSORPTION AND PRODUCTION CONTROLS

D.1 Emitter/absorber controls

D.1.1 The on/off room thermostat

Restart after set-back

This control uses a fixed start-up time. Once in that start-up period, the maximum possible thermal power flux is supplied to the emission/absorption element until the upper limit of the comfortband is reached in case of heating and the lower limit in case of cooling..

In accordance with the logic of the ideal control, the maximum cooling flux is calculated using the maximum of a condensation-preventing lower limit and a user-

defined lower limit. The maximum heating capacity is calculated taking into account current air and mean radiant temperatures and the maximum average emitter/absorber or production unit temperature.

The result is shown in Figure D.1 for a heating case. A two hours restart up has been selected for a 7 to 10 o' clock occupancy. It is shown in the graph that the heating consequently turns on at 5 o' clock.

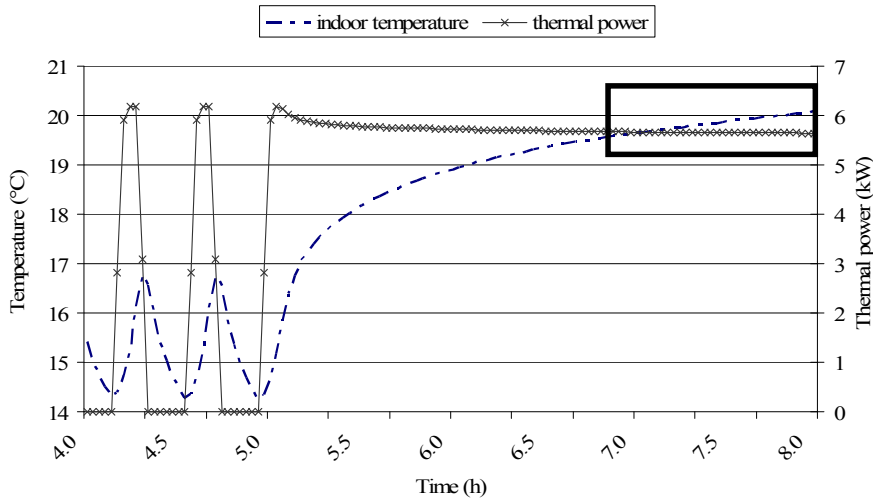


Figure D.1: Fixed 2-hour restart in heating mode for a single zone building. The rectangle indicates the 1.5K comfort zone during the 7 to 10 o'clock occupancy. Night set back temperature is set to 15.5°C with a 2K deadband.

Maintaining the comfort temperature

The logic of an on/off controller is simple: take action if the temperature is not within the comfortband. The action to be taken is to ask for the maximum heating power in case the temperature is below the lower limit of the comfortband. The maximum cooling power is asked for in case the temperature is above the upper limit of the comfortband.

D.1.2 The modulating room thermostat

Restart after set-back

The start-up of a modulating controller is a linear function of the temperature difference between the current and the desired temperature. The user is therefore asked to provide a **start-up time for a 3 K temperature difference** and a **start-up time for a 5 K difference**. This allows to set-up the linear function that can be used to determine the restart time for all other temperature differences. In the start-up period, the controller requests the maximum possible energy flux, whether it is for heating or for cooling. As can be seen in Figure D.2 showing the results for a heating case, the start up period calculation is redone each timestep and might thus be interrupted and restarted depending on the temperature difference to be bridged.

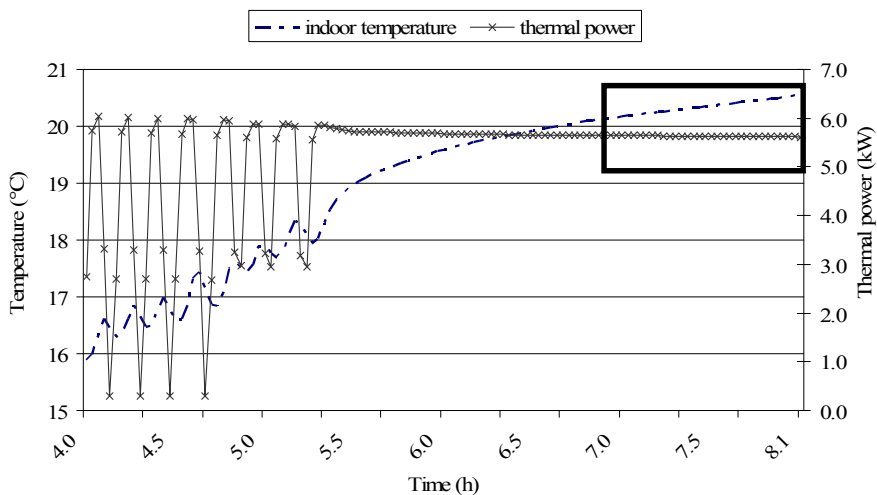


Figure D.2: Linear restart (4 h for 5K, 2 h for 3K difference) in heating mode for a single zone building. The rectangle indicates the 1.5K comfort zone during the 7 to 10 o'clock occupancy. The heating is turned on just before 4 o'clock, as the temperature difference to be bridged is just above 4K.

Again the maximum cooling flux is calculated using the maximum of a condensation-preventing lower limit and a user-defined lower limit. The maximum heating capacity is calculated taking into account the current air and mean radiant temperatures.

Maintaining the comfort temperature

This controller is developed to start heating once below the lower limit of the comfortband and then continue heating till the upper limit. For cooling it is the other way around: start cooling once above the upper limit and continue till the lower limit. The required heating/cooling flux is calculated using the iterative procedure based on Eq. (2.19), where once again the maximum and minimum thermal power values must in all cases be respected.

D.1.3 The thermostatic radiator valve

Restart after set-back

The thermostatic radiator valve implemented is a non-programmable one. Consequently, it is not combined with any restart control.

Maintaining the comfort temperature

In the implicit modelling approach, no flow rate data are available. The TRV is thus modelled using its basic working mechanism; a proportional control action with hysteresis.

The first parameter, required to define any proportional controller, is the **throttling range** TR (K). It defines the width of the band wherein the proportional control defines its desired output as a linear function of the error signal.

As any other implicit heat emitter/absorber control, the TRV reacts to a sensed temperature. This temperature is not equal to the zonal operative temperature. Therefore a distorted sensed temperature, T'_i (K) is used (Eq.(D.1)), which is in a format that is in agreement with [1]. This distorted temperature is a function of the current indoor air temperature T_{ai} (K) and the zonal mean radiant temperature MRT_i . In addition, as for real TRV's, it is influenced by the water temperature of the heat emission/absorption element, $T_{emit,i}$ (K).

$$T'_i = (l - k)T_{ai} + (1 - l - k)MRT_i + kT_{emit,i} \quad (D.1)$$

The values of the **coefficients l (-) and k (-)** are user supplied data.

To account for the valve's inertia, a third **weighing factor**, w_{TRV} (-), is required. It indicates the weight of the newly calculated energy flux $Q''_{pli_new}(t)$ compared to the value $Q''_{pli}(t-\Delta t)$ calculated the last timestep when defining the desired energy flux Q''_{pli} :

$$Q''_{pli}(t) = w_{TRV} Q''_{pli_new}(t) + (1 - w_{TRV}) Q''_{pli}(t - \Delta t) \quad (D.2)$$

The last aspect included in the logic of the TRV-model is the hysteresis. The user is therefore asked for a **hysteresis temperature difference**, T_{hyst} (K). The actuating signal of the TRV is then allowed to change from an increasing energy output to a decreasing one, or vice versa, after the indoor temperature has changed with a temperature difference T_{hyst} . As long as this condition is not fulfilled, the output remains the same as the point of the desired change in energy flux.

Figure D.3 shows the results of a simulation of a single zone building using the implicit emitter/absorber in combination with a TRV. The constants k , l and w_{TRV} are here arbitrarily set to 0.05, 0.60 and 0.95 respectively. The valve's throttling range is set to 2 K, the hysteresis temperature difference is 0.6 K.

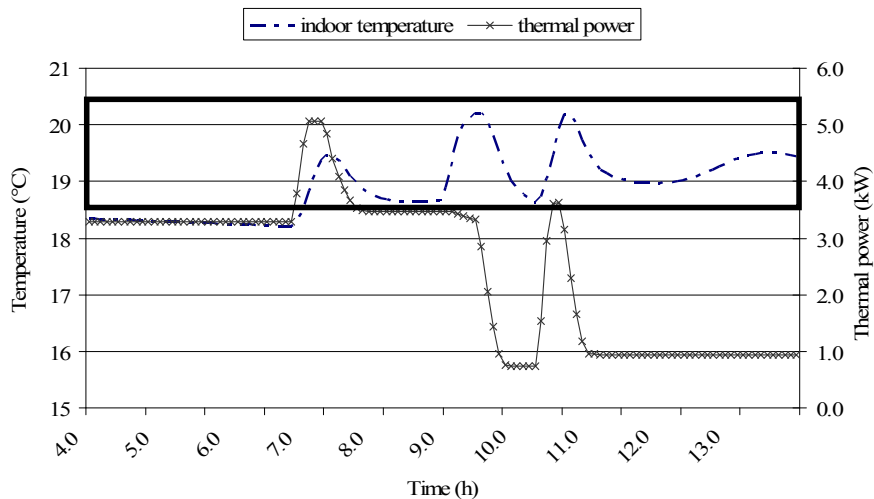


Figure D.3: Result for a TRV in heating mode in the single zone building. The rectangle indicates the comfort zone around the 19.5 °C comfort temperature. No set back has been implemented for this case. The maximum energy flux in nominal conditions is set to 7 kW. Solar radiation causes the indoor temperature rise around 9 o' clock.

D.2 Production controls

D.2.1 The central room thermostat

This control reacts to a sensed indoor temperature in a user-selected zone. If this zone requires no thermal power flux, no hot/cold water will be prepared. This is shown in Figure D.4 for a room thermostat located in room 1. It can be seen that the production of heat is limited to the period room 1 requires a thermal flux.

To see the effect of the global control, the production device is undersized. Room 1 is further subject to more internal and solar gains compared to the other 2 rooms.

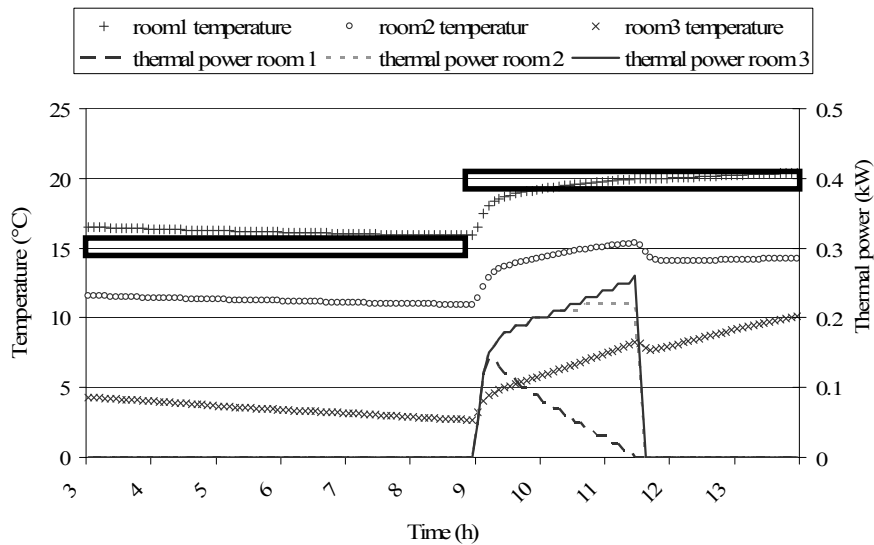


Figure D.4: Result of an ideal global controller in heating mode. The heat emitter in room 3 is undersized. The global capacity is limited to 0.5 kW. The desired comfort band for all zones is indicated by the rectangles with thick black lines.

References

- [1] J. Van der Veken, V. De Meulenaer, H. Hens, 2007, Eindrapport GBOU-project 020212, Analyse per system: verwarmingsinstallaties, Department of Building physics, University of Leuven (KUL), Belgium

APPENDIX E BUILDING MODEL DESCRIPTION

E.1 Dimensions of the building

The building, as shown in Figure E.1, consists of 3 zones; zone 1 is a large zone at the ground floor, and zones 2 and 3 are smaller zones at the first floor.

In Table E.1 the geometrical details of the building are listed.

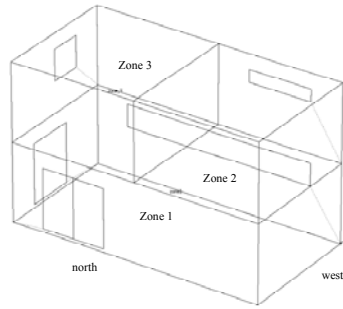


Figure E.1: The 3-zone building used in current dissertation.

element	size
Surface area ground floor	8 m · 4 m
Height per floor	2.5 m
Surface area zone 2	4 m · 4 m
Surface area zone 3	4 m · 4 m
Window north zone 1	2 m · 1.9 m
Window east zone 1	1.5 m · 1.9 m
Window south zone 1	6 m · 0.7 m
Window south zone 2	3 m · 0.4 m
Window east zone 3	1 m · 1 m

Table E.1: Geometrical details of the 3-zone building

E.2 Thermo-physical properties

E.2.1 Heavyweight construction

The heavyweight construction is a typical brick construction, as shown in Figure E.2.

The U-values of the different building elements are summarized in Table E.2 for the different insulation qualities simulated. U_{avg} ($\text{W}/\text{m}^2\text{K}$) stands for the U-value of the average insulated building U_{good} ($\text{W}/\text{m}^2\text{K}$) and U_{well} ($\text{W}/\text{m}^2\text{K}$) for the good and very good insulated building respectively. The average U-values are given as well. The g-value of the glass is 0.65 for all insulation qualities.

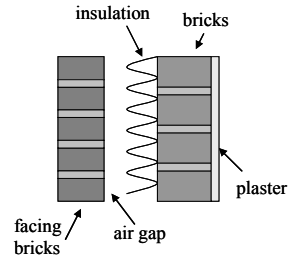


Figure E.2: Typical brick construction.

Element	U_{avg} ($\text{W}/\text{m}^2\text{K}$)	U_{good} ($\text{W}/\text{m}^2\text{K}$)	U_{well} ($\text{W}/\text{m}^2\text{K}$)
External wall	0.60	0.50	0.40
Roof \uparrow	0.40	0.30	0.20
Roof \downarrow	0.39	0.29	0.20
Window	1.59	1.32	1.00
Ground floor \uparrow	0.35	0.30	0.20
Ground floor \downarrow	0.34	0.30	0.20
Internal wall	1.17	1.06	0.98
Ceiling \uparrow	0.48	0.36	0.27
Ceiling \downarrow	0.46	0.36	0.27
Door	0.52	0.44	0.38
Average U-value	0.55	0.45	0.35

Table E.2: U-values for the different building elements in the heavyweight construction for the average ($_{\text{avg}}$), good ($_{\text{good}}$) and well ($_{\text{well}}$) insulated building.

E.2.2 Lightweight construction

The lightweight construction is a wooden construction, as shown in Figure E.3. The U-values of the different building elements are summarized in Table E.3 for the different insulation qualities of the lightweight building simulated. The g-value of the glass is 0.65 for all insulation qualities.

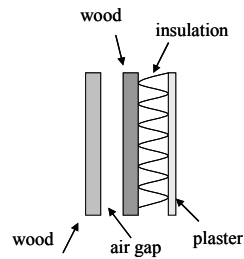


Figure E.3: Lightweight wooden construction.

element	U_{avg} (W/m ² K)	U_{good} (W/m ² K)	U_{well} (W/m ² K)
External wall	0.60	0.50	0.40
Roof ↑	0.40	0.30	0.20
Roof ↓	0.39	0.30	0.20
Window	1.59	1.32	1.00
Ground floor ↑	0.35	0.30	0.20
Ground floor ↓	0.34	0.30	0.20
Internal wall	1.20	1.04	0.92
Ceiling ↑	0.48	0.37	0.27
Ceiling ↓	0.46	0.36	0.26
Door	0.52	0.44	0.38
Average U-value	0.55	0.45	0.35

Table E.3: U-values for the different building elements in the lightweight construction for the average (*avg*), good (*good*) and well (*well*) insulated building.

E.2.3 Additional capacity

To model the effect of furniture and decoration, a floating volume has been added. For the ground zone, zone1, this volume has a capacity of 672 kJ/K. For the two remaining zones, zone 2 and zone 3, the capacity is 336 kJ/K. This agrees with the same capacity increase as resulting from multiplying the specific heat of the air in the zone by a factor 6.

E.3 Ventilation/infiltration

No internal air flows are modelled. The infiltration rate has been set to a constant value of 0.3 AC/h for all zones in the building.

E.4 Internal gains

The internal gains are dictated by the periods indicated in Table E.4 below.

zone 1 and zone 2	zone 3
8h-10h	0h-8h
18h-22h	22h-24h

Table E.4: Periods of non-zero internal gains for each of the zones.

The values of the sensible and latent gains due to occupants are summarized in Table E.5. The fractions of radiation and convection are given as well.

	Gains (W)	Latent	Sensible	Radiation	Convection
Zone 1	240	30%	70%	50%	50%
Zone 2	120				
Zone 3	190				

Table E.5: The heat gains related to occupants for the 3zone-building considered.

Table E.6 summarized the gains due to lighting and the corresponding fractions of radiation and convection. Similarly, gains and corresponding fractions of radiation and convection for appliances are given in Table E.7.

Gains (W)

	Occupied	Not occupied	Radiation	Convection
Zone 1	100	0	10%	90%
Zone 2	60	0		
	22h-24h	else		
Zone 3	20	0		

Table E.6: The heat gains related to lighting for the 3zone-building considered.

Gains (W/m²)

	Occupied	Not occupied	Radiation	Convection
Zone 1	5.4	1	30%	70%
Zone 2	2.7	1		
Zone 3	0	0		

Table E.7: The heat gains related to appliances for the 3zone-building considered.

Curriculum Vitae

Leen Peeters was born in Geel (Belgium) on May 20th, 1977. In 2001 she graduated as Burgerlijk Bouwkundig Ingenieur, optie gebouwen (Civil Engineer) at the Katholieke Universiteit Leuven.

After graduating, she has gained industrial experience at Transport and Mobility Leuven, a consultancy company for traffic related issues and at CEI, a large building contractor. After an interim at the Hogeschool Limburg in 2003, teaching amongst other building physics and stability, she decided to pursue a PhD degree.

She started December 2003 at the Department of Mechanics, division of Applied Mechanics and Energy Conversion. She was hired on the el²ep-project till February 2007. Meanwhile she worked on a study on the feasibility of Stirling CHP's for the Belgian residential sector and joined the IEA ECBCS annex 42 on modelling CHP's.

After the el²ep-project, she started focusing on her PhD, for which she spent 2 months at Eindhoven University during the summer of 2007 and 4 months at Strathclyde University, Glasgow in the first half of 2008.

Articles in journals with review

1. D. Haeseldonckx, L. Peeters, L. Helsen, W. D'Haeseleer, 2007, The impact of thermal storage on the operational behaviour of residential CHP facilities and the overall CO₂-emissions, *Sustainable and Renewable Energy Reviews*, vol. 11, 2007, pp. 1227-1243
2. P. Luickx, L. Peeters, W. D'Haeseleer, 2007, Influence of massive heat-pump introduction on the electricity-generation mix and the GHG effect. Belgian Case study, *International Journal of Energy Research*, vol. 32, pp. 57-67
3. L. Peeters, J. Van der Veken, H. Hens, L. Helsen, W. D'Haeseleer, Control of heating systems in residential buildings: current practice, *Energy and Buildings*, vol. 40, 2008, pp. 1446-1455
4. L. Peeters, R. De Dear, J. Hensen, W. D'Haeseleer, 2008, Thermal comfort in residential buildings: comfort values and scales for building energy simulation, *Applied Energy*, vol. 86, pp. 772-780

Articles in other journals

5. L. Peeters, L. Helsen, W. D'Haeseleer, 2005, Voorspelling van warmtevraag, *Atic Newsletter*, oktober 2005
6. L. Peeters, 2006, WhisperGen en Senertec, *Nieuwsbrief Cogen Vlaanderen*, vol 6
7. G. Verbeeck, L. Peeters, 2008, Een lage-energie woning: hoe begin je eraan?, *Ik ga Bouwen en Renoveren*, Speciale editie nr 1, P509555

Symposia and conference contributions

8. L. Peeters, L. Helsen, W. D'Haeseleer, 2005, Prediction of next day's heat demand to minimize heat pump heating costs, 8th Rehva World Congress, Clima, Lausanne, Switzerland, October 9-12
9. J. Van der Veken, H. Hens, L. Peeters, L. Helsen, W. D'Haeseleer, 2006, Economy, energy and ecology based comparison of heating systems in dwellings, 3rd International Building Physics Conference, Montreal, Canada, August 27-31

10. L. Peeters, L. Helsen, W. D'haeseleer, 2006, Comparison of heating systems in a residential building, 9th International Building Performance Simulation Association Conference, Montreal, Canada, August 15-18,
11. L. Peeters, J. Van der Veken, L. Helsen, W. D'haeseleer, H. Hens, 2006, The performance of different heating systems in buildings with varying insulation quality, 4th ESIM, national building simulation conference, Toronto, Canada, May 3-5
12. L. Peeters, J. Van der Veken, H. Hens, L. Helsen, W. D'haeseleer, 2007, Sizing of boilers for residential buildings, 9th Rehva World Congress, Clima, Helsinki, June 10-14
13. L. Peeters, N. Kelly, W. D'haeseleer, 2008, Thermal comfort in residential buildings with water-based heating systems: a tool for selecting appropriate heat emitters when using μ -cogeneration, 1st Microcogen conference, Montreal, Canada, April 29-May 1
14. L. Peeters, W. D'haeseleer, 2008, Implicit modelling of water-based heating/cooling installations in residential buildings, Buildings Physics Symposium in honour of Hugo Hens, Leuven, October 29-31

International Reports

15. I. Beausoleil-Morrison, et al., 2008, Experimental Investigation of Residential Cogeneration Devices and Calibration of Annex 42 Models: Subtask B of FC+COGEN-SIM: The Simulation of Building-Integrated Fuel Cell and Other Cogeneration Systems, Natural Resources Canada, ISBN 978-0-662-47923-1
16. I. Beausoleil-Morrisson et al., 2008, An Experimental and simulation based investigation of the performance of small-scale fuel cell and combustion-based cogeneration devices serving residential buildings, final report of IEA ECBCS annex 42, Natural Resources Canada, ISBN 978-0-662-47924-6

National Reports

17. L. Peeters, D. Haeseldonckx, W. D'haeseleer, 2006, Onderzoek Stirling-ketel combinatie voor WKK, Division of Applied Mechanics and Energy Conversion, TME/WDH/06-01/PRL
18. A. Janssens, E. Van Londersele, L. Willems, L. Peeters, W. D'haeseleer, 2007, Deel 5: Implementatie van resultaten in EPB: Eindrapport GBOU-project 020212: Ontwikkeling via levenscyclus-optimalisatie van extreem lage energie- en pollutiewoningen, Katholieke Universiteit Leuven, Tech. Rep. 2007R07

19. L. Peeters, W. D'haeseleer, 2007, Deel 3c: Optimalisatie van installaties; meetcampagne WisperGen WKK: Eindrapport GBOU-project 020212: Ontwikkeling via levenscyclusoptimalisatie van extreem lage energie- en pollutiewoningen, Katholieke Universiteit Leuven, Tech. Rep. 2007R05
20. L. Peeters, W. D'haeseleer, 2007, Deel 3b: Optimalisatie van installaties; analyse per systeem: WP en WKK voor woningverwarming: Eindrapport GBOU-project 020212: Ontwikkeling via levenscyclusoptimalisatie van extreem lage energie- en pollutiewoningen, Katholieke Universiteit Leuven, Tech. Rep. 2007R04
21. L. Peeters, W. D'haeseleer, 2007, Deel 3b: optimalisatie van installaties: analyse per systeem: afstandsverwarming met WKK: Eindrapport GBOU-project 020212: Ontwikkeling via levenscyclusoptimalisatie van extreem lage energie- en pollutiewoningen, Katholieke Universiteit Leuven, Tech. Rep. 2007R03
22. L. Peeters, L. Helsen, W. D'haeseleer, 2007, Deel 3b: Optimalisatie van installaties; analyse per systeem: controlestrategieën: Eindrapport GBOU-project 020212: Ontwikkeling via levenscyclus-optimalisatie van extreem lage energie- en pollutiewoningen, Katholieke Universiteit Leuven, Tech. Rep. 2007R02
23. G. Verbeeck, G. Van der Veken, V. De Meulenaer, H. Hens, L. Peeters, W. D'haeseleer, A. Janssens, E. Van Londersele, L. Willems, P. Vermeyen, 2007, Valoriseringsrapport: Eindrapport GBOU-project 020212: Ontwikkeling via levenscyclusoptimalisatie van extreem lage energie- en pollutiewoningen, Katholieke Universiteit Leuven, Tech. Rep. 2007R08.